Universidad Nacional Autónoma de México

Facultad de Química

Regulación del cotransportador $Na^+/K^+/2Cl^-$ NKCC2 por la concentración de cloruro intracelular

T E S I S

P R E S E N T A D A P O R:

JOSE PONCE CORIA

PARA OBTENER EL GRADO A:

DOCTOR EN CIENCIAS BIOQUÍMICAS

FACULTAD DE QUÍMICA

Ciudad Universitaria, octubre del 2010.

Vanderbilt University Medical Center

Eric Delpire, Ph.D.
Professor of Anesthesiology
and Molecular Physiology & Biophysics

1161 21st Avenue South
T-4202 MCN
Nashville, TN 37232-2520
(615) 343-7409
Fax: (615) 343-3916

March 29, 2010

Jose Ponce Coria
Molecular Physiology Unit,
Instituto Nacional de Ciencias Médicas y Nutrición Salvador Zubirán
Instituto de Investigaciones Biomédicas,
Universidad Nacional Autónoma de México, Tlalpan,
14000 Mexico City,
Mexico

Dear Jose,

I am delighted to be able to offer you a Postdoctoral Fellowship position in my laboratory in the Department of Anesthesiology at Vanderbilt Medical Center. This will be contingent upon successful completion and defense of your PhD. We can agree on a starting date of May1, 2010, pending that your defense of your Ph.D. thesis is completed and the necessary visas can be obtained in time. There will be no problem moving the date forward if necessary. Your initial salary will be $37,000 plus standard fringe benefits. Assuming satisfactory performance and available funding, I anticipate that your contract will be renewed annually and your salary reviewed for increases along NIH guidelines.

As discussed during your visit, the major focus of your work will be on to study the different modes of kinase activation and their roles in regulating ion transport in sensory neurons. Your responsibilities will include the planning, performance, and analysis of experiments, and presentation of data at lab meetings, National conferences, and in manuscripts. I will work closely with you in this regard.

Please note that this offer is also contingent upon the successful completion of the background screen and education verification, and nothing contained in this letter should be construed to create an employment contract or to otherwise alter your status as an employee at will.

I am looking forward to you joining the lab. For our records, please confirm your acceptance of this offer by signing and returning one copy of this letter. You will then be contacted in due course to begin the process of obtaining the necessary visa and work authorization.

Cordially,

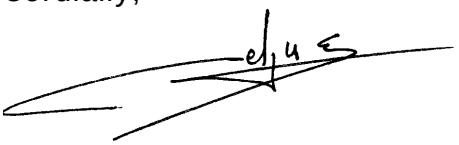

Eric Delpire, Ph.D.

_____

Jose Ponce-Coria Date

Ciencias Bioquímicas

FQ IFC IBT IIBM

UNAM POSGRADO Ciencias Bioquímicas

PROGRAMA DE MAESTRÍA Y DOCTORADO EN CIENCIAS BIOQUÍMICAS

A LOS MIEMBROS DE
JURADO DE EXAMEN

Por medio del presente manifiesto que he revisado el texto que será sometido a su consideración del (a) alumno (a) de Doctorado en Ciencias Bioquímicas **LIBB. JOSE PONCE CORIA** *titulado:*

"Regulación de la actividad del cotransportador $Na^+/K^+/2Cl^-$ por el cloruro intracelular"

ATENTAMENTE

DR. GERARDO GAMBA AYALA
Tutor

Ciencias Bioquímicas

FQ IFC IBT IIBM

UNAM POSGRADO Ciencias Bioquímicas

PROGRAMA DE MAESTRÍA Y DOCTORADO EN CIENCIAS BIOQUÍMICAS

ENTIDADES CAMPUS CIUDAD DE MÉXICO

PMDCB/031/2010

LIBB. JOSÉ PONCE CORIA
Alumno del Doctorado en Ciencias Bioquímicas
P r e s e n t e

Los miembros del Subcomité Académico en reunión ordinaria del día 18 de enero del presente, conocieron su solicitud de asignación de JURADO DE EXAMEN para optar por el grado de DOCTOR EN CIENCIAS (BIOQUIMICAS), con la réplica de la tesis "Regulación de la actividad del cotransportador $Na^+/K^+/2Cl^-$ por el cloruro intracelular", dirigida por el Dr. Gerardo Gamba Ayala.

De su análisis se acordó nombrar el siguiente jurado:

PRESIDENTE	Dr. José Pedraza Chaverri
VOCAL	Dra. Laura Escobar Pérez
SECRETARIO	Dr. Fernando López Casillas
SUPLENTE	Dr. Alejandro Zentella Dehesa
SUPLENTE	Dr. José de Jesús García Valdés

Sin otro particular por el momento, aprovecho la ocasión para enviarle un cordial saludo.

A t e n t a m e n t e
"POR MI RAZA HABLARÁ EL ESPÍRITU"
Cd. Universitaria, D.F., a 26 de enero de 2010.
EL COORDINADOR DE LA ENTIDAD ACADÉMICA-FQ

DR. ROGELIO RODRÍGUEZ SOTRES

C.c.p. Archivo

RRS*lgg

PROGRAMA DE MAESTRÍA Y DOCTORADO EN CIENCIAS BIOQUÍMICAS

Ciudad Universitaria a 10 deagosto de 2010

Dr. Isidro Ávila Martínez
Director General de Administración Escolar
UNAM
P R E S E N T E

Me es grato comunicarle que después de revisar cuidadosamente y de discutir mis sugerencias y correcciones al documento de tesis titulado

Regulación del cotransportador $Na^+/K^+/2Cl^-$ NKCC2 por la concentración de cloruro intracelular

que para obtener el grado presenta el (la) alumno **José Ponce Coria** con número de cuenta 099236469, inscrito(a) en la Maestría ( ) el Doctorado (x) en Ciencias Bioquímicas, considero que la Tesis reúne los requisitos establecidos y por ello emito mi **VOTO APROBATORIO** para que realice la réplica oral.

Agradezco de antemano la atención que se sirva prestar a la presente.

Atentamente,

Dr. José Pedraza Chaverri
Nombre y firma

PROGRAMA DE MAESTRÍA Y DOCTORADO EN CIENCIAS BIOQUÍMICAS

Ciudad Universitaria a 10 de agosto de 2010

Dr. Isidro Ávila Martínez
Director General de Administración Escolar
UNAM
P R E S E N T E

Me es grato comunicarle que después de revisar cuidadosamente y de discutir mis sugerencias y correcciones al documento de tesis titulado

Regulación del cotransportador $Na^+/K^+/2Cl^-$ NKCC2 por la concentración de cloruro intracelular

que para obtener el grado presenta el (la) alumno **José Ponce Coria** con número de cuenta 099236469, inscrito(a) en la Maestría ( ) el Doctorado (x) en Ciencias Bioquímicas, considero que la Tesis reúne los requisitos establecidos y por ello emito mi **VOTO APROBATORIO** para que realice la réplica oral.

Agradezco de antemano la atención que se sirva prestar a la presente.

Atentamente,

Dr. Fernando López Casillas
Nombre y firma

PROGRAMA DE MAESTRÍA Y DOCTORADO EN CIENCIAS BIOQUÍMICAS

Ciudad Universitaria a 10 de agosto de 2010

Dr. Isidro Ávila Martínez
Director General de Administración Escolar
UNAM
P R E S E N T E

Me es grato comunicarle que después de revisar cuidadosamente y de discutir mis sugerencias y correcciones al documento de tesis titulado

Regulación del cotransportador $Na^+/K^+/2Cl^-$ NKCC2 por la concentración de cloruro intracelular

que para obtener el grado presenta el (la) alumno **José Ponce Coria** con número de cuenta 099236469, inscrito(a) en la Maestría ( ) el Doctorado (x) en Ciencias Bioquímicas, considero que la Tesis reúne los requisitos establecidos y por ello emito mi **VOTO APROBATORIO** para que realice la réplica oral.

Agradezco de antemano la atención que se sirva prestar a la presente.

Atentamente,

Dra. Laura Escobar Pérez
Nombre y firma

PROGRAMA DE MAESTRÍA Y DOCTORADO EN CIENCIAS BIOQUÍMICAS

Ciudad Universitaria a 26 de Agosto de 2010

Dr. Isidro Ávila Martínez
Director General de Administración Escolar
UNAM
P R E S E N T E

Me es grato comunicarle que después de revisar cuidadosamente y de discutir mis sugerencias y correcciones al documento de tesis titulado

Regulación del cotransportador $Na^+/K^+/2Cl^-$ NKCC2 por la concentración de cloruro intracelular

que para obtener el grado presenta el (la) alumno(a)

José Ponce Coria

con número de cuenta 099236469, inscrito(a) en la Maestría ( ) el Doctorado (X) en Ciencias Bioquímicas , considero que la Tesis reúne los requisitos establecidos y por ello emito mi **VOTO APROBATORIO** para que realice la réplica oral.

Agradezco de antemano la atención que se sirva prestar a la presente.

Atentamente,

Dr. Alejandro Zentella Dehesa
Nombre y firma

PROGRAMA DE MAESTRÍA Y DOCTORADO EN CIENCIAS BIOQUÍMICAS

Ciudad Universitaria a 10 de agosto de 2010

Dr. Isidro Ávila Martínez
Director General de Administración Escolar
UNAM
P R E S E N T E

Me es grato comunicarle que después de revisar cuidadosamente y de discutir mis sugerencias y correcciones al documento de tesis titulado

Regulación del cotransportador $Na^+/K^+/2Cl^-$ NKCC2 por la concentración de cloruro intracelular

que para obtener el grado presenta el (la) alumno **José Ponce Coria** con número de cuenta 099236469, inscrito(a) en la Maestría ( ) el Doctorado (x) en Ciencias Bioquímicas, considero que la Tesis reúne los requisitos establecidos y por ello emito mi **VOTO APROBATORIO** para que realice la réplica oral.

Agradezco de antemano la atención que se sirva prestar a la presente.

Atentamente,

Dr. José de Jesús García Valdés
Nombre y firma

“Regulación del cotransportador $Na^+/K^+/2Cl^-$ NKCC2 por la concentración de cloruro intracelular”

R E C O N O C I M I E N T O S

A mi tutor y maestro, el Dr. Gerardo Gamba Ayala por sus enseñanzas y permitirme realizar el presente trabajo en el Instituto Nacional de Nutrición Salvador Zubirán dentro del departamento de Nefrología y Metabolismo Mineral, el cual es una unidad periférica del Instituto de Investigaciones Biomédicas de la Universidad Nacional Autónoma de México.

A la Dra. Norma A. Bobadilla Sandoval por su colaboración y asesoría académica al formar parte del comité tutoral a lo largo de mis estudios de posgrado.

R E C O N O C I M I E N T O S

Al Dr. José de Jesús García Valdés por su colaboración y asesoría académica al formar parte del comité tutoral a lo largo de mis estudios de posgrado.

A la Q.F.B. Norma Vázquez por su asesoría académica-técnica y colaboración experimental.

A los ex miembros y miembros actuales de la Unidad por sus comentarios y colaboración académica-experimental:

A los ex miembrios del laboratorio del Dr. Gamba: Myrlene Rodiguez Brito, Tomas Garzon Muvdi, Jetzabeh Rivera, Penélope Ortal Vite, Lilia Martínez de la Maza, Patricia Juárez Camacho, Pedro San Cristóbal Zepeda, Paola de los Heros Ríos

A los miembrios del laboratorio del Dr. Gamba: Consuelo Plata, Damián Hernández de Santiago, Rocío Acuña, Juan Pablo Arroyo, Erika Moreno, Diana Pacheco Álvarez, Maria Castañeda Bueno, ZeSergio Melo y Silvia Cruz Rangel.

A los ex miembrios del laboratorio de la Dra. Bobadilla: Alondra Díaz, Victoria Ramírez, Juan Manuel Mejia Vilet, Juan Garzon Muvdi, Rafael Valdez,

A los miembrios del laboratorio de la Dra. Bobadilla: Joyce Trujillo Silva, Silvia Karina Rodríguez, Jonatan Barrera, Rosalba Pérez, Cristino Cruz, Marcos Ojeda, Cesar Cortes, Katy Sánchez Pozos.

R E C O N O C I M I E N T O S

Al Consejo Nacional de Ciencia y Tecnología que me otorgó a lo largo de mis estudios de Doctorado una beca con número de registro 205063.

A los miembros del jurado designado por el Comité Académico del Programa de Maestría y Doctorado en Ciencias Bioquímicas UNAM para la evaluación del examen de candidatura al grado de doctor:

Presidente Dr. Fernando López Casillas
Dr. Omar Pantoja Ayala.
Dra. Norma Bobadilla Sandoval
Dr. José de Jesús García Valdés
Dra. Laura Escobar Pérez

A los miembros del jurado designado por el Comité Académico del Programa de Maestría y Doctorado en Ciencias Bioquímicas UNAM para la revisión y evaluación de la presente tesis:

Presidente: Dr. José Pedraza Chaverri
Vocal: Dra. Laura Escobar Pérez
Secretario: Dr. Fernando López Casillas
Suplente: Dr. Alejandro Zentella Dehesa
Suplente: Dr. José de Jesús García Valdés

Dedicatorias

A mi alma mater:

La Universidad Nacional Autónoma de México
"Por mi raza hablará el espíritu"

A mis amados padres:

José Ponce Guerrero y Paulina Coria Figueroa

Dedicatorias

A mis hermanos:

Tanya Ponce Coria, Emma C Ponce Coria y Ruy Ponce Coria

A mi sobrino:

José Xavier Melchor Ponce

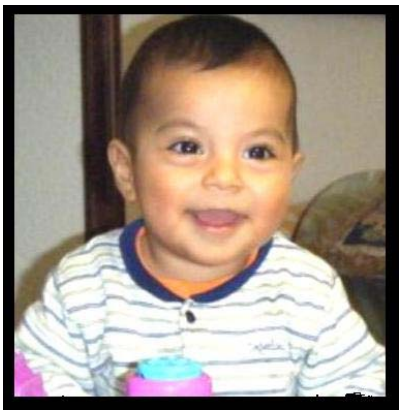

VNIVERSIDAD NACIONAL
AVTNOMA DE
MEXICO

"No creo que haya en este país una institución que haya sido más generosa que la nuestra. El conocimiento que aquí se genera, que aquí se cultiva, desde aquí se comparte. Ésta es una casa que siempre ha estado y estará abierta a todo aquel universitario o no, que tenga el genuino deseo de conocerla y acercarse a sus hombres y sus mujeres, de venir a debatir sus ideas y a defender sus verdades."

Dr. Juan Ramón de la Fuente

RESUMEN

Mantener en rangos normales los niveles de presión sanguínea es fundamental para sostener la salud de un organismo. Un determinante muy importante sobre los niveles de presión sanguínea es la reabsorción renal de sodio (Na^+). En la nefrona, a lo largo de la rama ascendente gruesa del asa de Henle (RAGAH), la participación directa y coordinada de al menos cinco proteínas es necesaria para una adecuada reabsorción transcelular de Na^+. Además de ser necesaria para sostener los niveles de presión sanguínea, dicha reabsorción de Na^+ en la RAGAH es fundamental para una correcta concentración-dilución urinaria, el metabolismo acido base y la reabsorción renal de iones divalentes. El cotransportador apical de $Na^+/K^+/2Cl^-$ conocido NKCC2 es el responsable del primer paso durante la reabsorción transcelular de Na^+ a lo largo de la RAGAH. Para continuar con la reabsorción de Na^+ en este segmento de la nefrona se requiere de: a) la recirculación de K^+ hacia la luz tubular mediada por el canal apical de K^+ conocido como ROMK, b) el paso de Cl^- hacia el espacio intersticial por el canal basolateral de Cl^- constituido por las proteinas CLC-Kb y Barttina y c) el correcto funcionamiento del sensor de calcio conocido como CaSR. Mutaciones en NKCC2, ROMK, CLC-Kb, Barttina y CaSR son responsables del desarrollo del Síndrome de Barrter tipo I, II, III, IV y V respectivamente. Dicho síndrome es una enfermedad monogénica y heterogénea de herencia autosómica recesiva, donde debido a una disminución en los niveles de reabsorción de Na^+ en la RAGAH se presenta: a) depleción de volumen, activación del sistema renina angiotensina aldosterona, hipokalemia, alcalósis metabólica e hipercalciuria. El mecanismo molecular por el cual mutaciones en CLC-Kb o la Barttina conducen a una disminución en la reabsorción de Na^+ es desconocido, sugiriendo que las concentraciones intracelulares de Cl^- juegan un papel importante sobre la actividad de NKCC2. En el presente trabajo, se utilizó como sistema de expresión funcional heteróloga, ovocitos de rana *Xenopus laevis*, donde se demostró que mediante maniobras de depleción de Cl^- intracelular, se favorece un incremento significativo en la actividad de NKCC2 asociado a la fosforilación de los residuos de treonina 96, 101 y 113 presentes en la región amino terminal. De manera consistente, la sustitución dichos residuos por el aminoácido alanina previno la activación de NKCC2 durante una depleción de cloruro intracelular.

En conclusión, nuestros datos indican que NKCC2 se activa al disminuir las concentraciones intracelulares de Cl^-, por un mecanismo que involucra a las serina treonina cinasas WNK3 y SPAK. WNK3 posiblemente es la cinasa sensora de Cl^-, la cual mediante su interacción física con la cinasa SPAK, favorece la fosforilación de NKCC2 en los residuos de treonina 96, 101 y 113, lo cual se traduce en un incremento en la actividad de NKCC2. Con lo anterior, probablemente en el síndrome de Bartter tipo III y IV donde se afecta la reabsorción de Cl^- por mutaciones en CLC-Kb y Barttina respectivamente, un aumento en la concentración intracelular de Cl^- resulta en la ausencia de fosforilación de las treoninas 96, 101 y 113 y por tanto a una reabsorción alterada de Na^+ mediada por NKCC2.

ABSTRACT

Blood pressure levels must be kept within narrow normal levels in order to sustain health. An important determinant of blood pressure levels is the renal Na^+ reabsorption. In the nephron, along the thick ascending limb of Henle (TALH), a direct and coordinate function of at least five different proteins is necessary for an adequate Na^+ reabsorption. Besides being crucial to maintain normal blood pressure levels, such Na^+ reabsorption along the TALH is critical for the urine concentration-dilution mechanism, acid-base metabolism and the reabsorption of divalent ions. The apical $Na^+/K^+/2Cl^-$ cotransporter known as NKCC2 is the responsible for the first step in the reabsorption of Na^+ along the TALH. In order to continue with the Na^+ reabsorption along the TALH it is necessary: a) the K^+ secretion mediated by the K^+ channel known as ROMK, b) Cl^- reabsorption through the basolateral Cl^- channel composed of two subunits (CLC-Kb and Barttin) and c) the proper functioning of the calcium sensing receptor known as CaSR.Mutations in the genes encoding for NKCC2, ROMK, CLC-Kb, Barttin and CaSR are the cause of Bartter syndrome type I, II, III, IV and V respectively. The Bartter syndrome is a recessive monogenic and heterogenic disease in which patients have a decreased Na^+ reabsortion along the TALH, volume depletion, activation of the renin angiotensin system, hipokalemia, metabolic alkalosis and hipercalciuria. The molecular mechanism by which mutations in either CLC-Kb or Barttin lead to a deacreased Na^+ reabsortion remains unknown, suggesting that intracellular chloride concentrations might play a role upon NKCC2 activity.In the present work, using *Xenopus laevis* oocytes as heterologous expression system, we showed that during chloride depletion maneuveurs, the activity of NKCC2 is increased. NKCC2 activation is associated with the phosphorylation of amino terminal trenonines 96, 101 and 113. Consistently, the substitution by alanine of such residues rendered NKCC2 unable to respond to chloride depletion maneuveurs and with lower basal activity. In conclusion our results show that NKCC2 is activated during intracellular chloride depletion by a mechanism that involves the serine-treonine kinases WNK3 and SPAK. WNK3 could be the “chloride sensitive kinase” which by physical interaction with SPAK phosphorylates the amino terminal residuos 96, 101 and 113 of NKCC2.

Abreviaciones utilizadas en la escritura de esta tesis:

$[Cl^-]_i$	Concentraciones intracelulares de ion cloruro
A	Aminoácido de alanina
AC	Proteína adenilato ciclasa transmembranal
ACTH	Hormona adrenocorticotropa
ADH	Hormona antidiurética
ADN	Acido desoxiribonucleico
Ala	Aminoácido de alanina
AMPc	Adenosin monofosfato-3',5'cíclico
AQP1	Canal de agua acuaporina tipo 1
AQP2	Canal de agua acuaporina tipo 2
ARG	Aldosteronismo remediable con glucocorticoides
Arg	Aminoácido de arginina
ARN	Acido ribonucleico
ARNc	Acido ribonucleico complementario
Asn	Aminoácido de asparagina
Asp	Aminoácido aspártico
ATP	Adenosina trifosfato
C	Aminoácido de cisteina
Ca^{++}	Ion de calcio
CaSR	Sensor de calcio
CCT	Domino carboxilo terminal conservado
Cl^-	Ion de cloruro
CLC-Kb	Canal basolateral de cloruro tibo b
CRH	Hormona liberadora de corticotropina
Cys	Aminoácido de cisteina
D	Aminoácido aspártico
DAG	1,2-diacilglicerol
DIC	Diabetes insipida central
EAM	Exceso Aparente de Mineralocorticoides
ECA	Enzima convertidora de angiotensina
F	Aminoácido de fenilalanina
FC	Frecuencia cardiaca
Fig	Figura
GC	Gasto cardiaco
Gln	Aminoácido de glutamina
Gly	Aminoácido de glicina
H	Aminoácido de histidina
HAC	Hiperplasia adrenal congenita
Hg	Mercurio
His	Aminoácido de histidina
HTA	Hipertensión arterial
Ile	Aminoácido de isoleucina
IMH	Intersticio medular hiperosmótico
IP3	Inositol 1,4,5-trifosfato
K	Aminoácido de lisina
K^+	Ion de potasio
KCC2	Cotransportador de potasio y cloruro tipo dos

L	Aminoácido de leucina
Leu	Aminoácido de leucina
Lys	Aminoácido de lisina
MAP4K	MAPK cinasa cinasa cinasa cinasa
MAPK	Cinasa activada por mitógenos
Met	Aminoácido de metionina
Mg^{++}	Ion de magnesio
MPC	Mecanismo multiplicación por contracorriente
N	Aminoácido de asparagina
Na^{+}	Ion de sodio
NaCl	Cloruro de sodio
NCC	Cotransportador renal de sodio y cloruro sensible a diuréticos tipo tiazida
ND96	Solucion tipo ringer para ovocitos de *Xenopus laevis*
Nedd4-2	E3 ubiquitina ligasa de la familia de las HECT
NH_4^{+}	Ion de amonio
NKCC1	Cotransportador ubicuo de sodio potasio dos cloruro
NKCC2	Cotransportador renal de sodio potasio dos cloruro
NKCC2-TM	NKCC2 triple mutante debido a las susticiones: T96A T101A y T113A
NO	Óxido nítrico
OMIM	Base de datos Online Mendelian Inheritance in Man http://www.ncbi.nlm.nih.gov/omim/
OSR1	Serina treonina cinasa tipo 1 de respuesta a estrés oxidativo
P	Aminoácido de prolina
P13K	Fosfatidil inositol 3-cinasa
PAK	Cinasas activadas por p21
PAM	Presión arterial media
PDK1	Proteína cinasa tipo 1 dependiente de IP3
PDK2	Proteína cinasa tipo 2 dependiente de IP3
PHAII	Pseudohipoaldosteronismo tipo dos ó síndrome de Gordon
PHAII-A	Pseudohipoaldosteronismo tpo II clase A
PHAII-B	Pseudohipoaldosteronismo tipo II clase B
PHAII-C	Pseudohipoaldosteronismo tipo II clase C
Phe	Aminoácido de fenilalanina
PIP2	Fosfatidil inositol 4,5-bifosfato
PKA	Proteína cinasa A
PKB	Proteina cinsa B
PKC	Proteína cinasa C
PLC	Fosfolipasa C
PLC-β	Fosfolipasa C tipo beta
Pro	Aminoácido de prolina
P_s	Presión sanguínea
R	Aminoácido de arginina
RAAS	Sistema renina angiotensina aldosterona
RAGAH	Rama ascendente gruesa del asa de Henle de la nefrona
Rb^{+}	Ion de rubidio
RG	Receptor a glucocorticoides
RGF	Resistencia a Glucocorticoides Familiar
RM	Receptor a mineralocorticoides
ROMK	Canal apical de ion potasio
R_{vp}	Resistencia de la vasculatura periférica

S	Aminoácido de serina
SDS	Dododecil sulfato de sodio
SG	Síndrome de Geller
SGK1	Cinasa inducible por suero y por glucocortIcoides tipo 1
SIADH	Síndrome de la secreción inadecuada de la ADH
SL	Síndrome de Liddle
SLC12	Familia de cotransportadores electroneutros tipo 12
SO_4^{-2}	Sulfato
SPAK	Serina treonina cinasa relacionada a Ste20 abundante en aminoácidos de prolina y alanina
Ste20p	Proteina cinasa estéril 20
T	Aminoácido de treonina
TC	Túbulo colector de la nefrona
TC-ME	Túbulo colector de la medula externa
TC-MI	Túbulo colector de la médula interna
TD	Túbulo distal de la nefrona
Tyr	Aminoácido de tirosina
UT-A1	Cotransportador de urea tipo A1
UT-A2	Cotransportador de urea tipo A2
UT-A3	Cotransportador de urea tipo A3
V	Aminoácido de valina
Val	Aminoácido de valina
VCE	Volumen circulante efectivo
VI	Volumen Intravascular
VS_E	Volumen sistólico de eyección
WNK	Serina treonina cinasa ausente de lisina (se pronuncia “uink”)
WNK1	Serina treonina cinasa ausente de lisina tipo 1
WNK2	Serina treonina cinasa ausente de lisina tipo 2
WNK3	Serina treonina cinasa ausente de lisina tipo 3
WNK4	Serina treonina cinasa ausente de lisina tipo 4
Xaa	Cualquier aminoácido
Y	Aminoácido de tirosina
11−βHSD2	Enzima 11-beta hidroxiesteroide deshidrogenada tipo 2
Δ	Mutación tipo deleción

INDICE

INTRODUCCIÓN Y ANTECEDENTES

Presión sanguínea

Los niveles de presión sanguínea (P_s) deben ser regulados de manera precisa para permitir la perfusión constante y adecuada de oxígeno y nutrientes, así como la remoción de productos de desecho en todos los órganos y tejidos que constituyen a un organismo (1). La disminucion ó el incremento no controlado sobre los niveles de P_s puede resultar en daño a diversos órganos dentro de un ser vivo. Por ejemplo, la interrupción temporal en el flujo sanguíneo al cerebro puede ocasionar desde cefalea hasta perdida de la conciencia, mientras que interrupciones más prolongadas y por lo tanto, disminuciones drásticas en los niveles de P_s, pueden conducir inclusive a la muerte del organismo (1).

En términos fisiológicos, la P_s ha sido definida como el producto del gasto cardiaco (GC) y la resistencia que opone la vasculatura periférica (R_{vp}) (2).

$$P_s = GC * R_{vp}$$

El GC se define como el volumen de sangre que abandona los ventrículos por minuto (alrededor de 5 L/min), y sus valores se modifican por factores que alteren la frecuencia cardiaca (FC), así como aquellos que cambien el volumen intravascular (VI) y por lo tanto, el volumen sistólico de eyección (VS_E), que comprende el volumen de sangre expulsado por el corazón hacia la aorta durante el periodo de contracción ó sístole (alrededor de 75 mL) (1).

$$GC = VS_E * FC$$

$$GC = (75 \text{ mL/latido}) * (70 \text{ latidos/min}) = 5.25 \text{ L/min}$$

Por su parte, la R_{vp} está determinada principalmente por la contracción de las células de músculo liso que recubren las paredes de las arteriolas y se modifica por diversos factores entre los que se encuentran: a) el tono simpático, b) el óxido nítrico y c) las hormonas circulantes endotelina y angiotensina II (2).

Regulación de los niveles de presión sanguínea

Hoy en día se conocen una gran variedad de sistemas fisiológicos complejos que en conjunto modulan los niveles de la P_s, entre los que se encuentran: a) baroreceptores arteriales, encargados de sensar cambios de presión en los vasos sanguíneos (3), b) péptidos natriuréticos, liberados por el corazón y el cerebro en respuesta a incrementos en la P_s en estos órganos (4,5), c) el sistema adrenérgico, que modifica el tono vascular, la frecuencia y contracción cardiaca (2), d) el sistema cinina-calicreina, con la bradicinina y lisilbradicinina que promueven la vasodilatación arterial (6,7), e) el óxido nítrico (NO) (8-10) y la endotelina (11,12) producidos por los vasos sanguíneos para favorecer su vasodilatación y vasoconstricción respectivamente y f) el sistema renina angiotensina aldosterona (SRAA), encargado de controlar los niveles de P_s mediante alteraciones en la R_{vp} y en los niveles de reabsorción renal del ión sodio (Na^+) y agua (H_2O) (2;13-15).

Dado que los niveles de P_s se encuentran en gran medida determinados por la composición-volumen de los líquidos corporales, a lo largo de las secciones siguientes se describirá el control del volumen y la osmolalidad de los líquidos corporales, así como la reabsorción renal de Na^+ y H_2O haciendo énfasis en el papel del SRAA.

El riñón en el proceso del control del volumen, composición y osmolalidad de los líquidos corporales

A pesar de las variaciones diarias en la ingesta de solutos y H_2O, los riñones desempeñan una función muy importante al mantener relativamente constante la composición y volumen de los líquidos corporales. Los riñones son los encargados de la regulación del balance hídrico y electrolítico, así como la principal vía regulada para la eliminación de H_2O y la eliminación de productos finales del metabolismo o de desecho del organismo (urea, ácido úrico y creatinina) (1).

Aunque la cantidad de H_2O en un ser vivo depende de la edad, el sexo y la cantidad de tejido adiposo, en general, el H_2O constituye alrededor de un 60% del peso corporal (42

L en un hombre de 70kg) y se distribuye principalmente entre dos compartimientos: el líquido intracelular (LIC) y el líquido extracelular (LEC) (16,17) (**Fig. A**).

El LIC es el más grande de estos compartimientos y está compuesto por aproximadamente dos terceras partes del total de H_2O del organismo (28 L en un hombre de 70 kg), mientras que el tercio restante (14 L en un hombre de 70 kg) lo conforma el LEC que se subdivide en el líquido intersticial (LI) y el plasma sanguíneo, también conocido como VI (1) (**Fig. A**).

El LI es el volumen que rodea a las células en los diversos tejidos del ser vivo y representa tres cuartas partes del LEC (alrededor de 10.5 L). La cuarta parte restante del LEC (alrededor de 3.5 L) la constituye el VI, el cuál comprende la fracción líquida y acelular de la sangre. El volumen sanguíneo (VS), que constituye de 70 a 80 mL/kg en un adulto sano, está conformado por la suma del VI y el hematocrito (1).

Para sostener el metabolismo celular es fundamental una perfusión tisular adecuada. A la fracción del LEC presente en el sistema arterial que se encuentra efectivamente perfundiendo a los tejidos se le conoce como volumen circulante efectivo (VCE) (700 mL en un hombre de 70 kg). Este volumen se regula principalmente mediante modificaciones en la reabsorción-excreción renal de H_2O y Na^+ a través del SRAA (2) (**Fig. 1**).

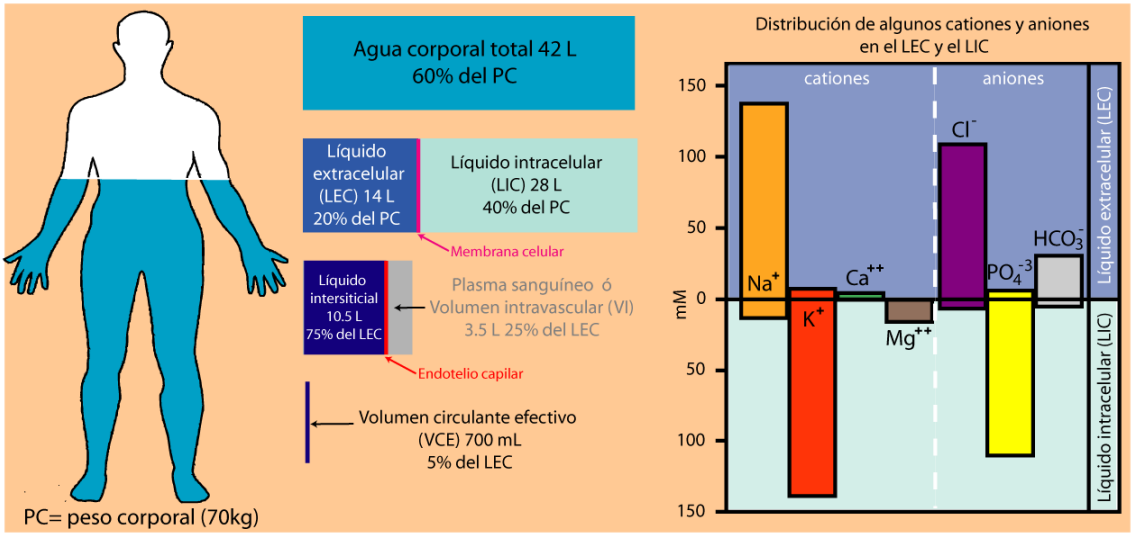

Figura 1. Líquidos corporales y distribución de los principales cationes y aniones en el LEC y LIC.

El volumen del LEC depende de manera muy importante de la cantidad total de solutos con actividad osmótica. Ya que el Na^+, el cloruro (Cl^-) y el bicarbonato (HCO_3^-) son por mucho los solutos con actividad osmótica más abundantes del LEC, y como los cambios en el Cl^- y HCO_3^- son en gran medida secundarios a las variaciones en la concentración de Na^+ (debido a su presencia en forma de bicarbonato de sodio $NaHCO_3$ y cloruro de sodio NaCl), la cantidad de Na^+ en el LEC es la determinante más importante de su volumen y osmolalidad. Por consiguiente, se puede obtener una estimación de la osmolalidad plasmática normal, que oscila entre unos 285 y 295 mOsm/kg H_2O, simplemente duplicando la concentración plasmática del Na^+.

Una estimación más precisa del valor de la osmolalidad plasmática (Osm_p) se obtiene tomando también en cuenta la contribución de la urea y la glucosa. En la práctica clínica se puede calcular la osmolalidad plasmática de la manera siguiente:

$$Osm_p = 2(\text{Plasma } [Na^+ \text{ mmol/L}]) + \frac{[\text{glucosa mg/dL}]}{18} + \frac{[\text{urea mg/dL}]}{2.8}$$

Al utilizar la ecuación anterior, se deben utilizar las concentraciones de glucosa y urea expresadas en miligramos por decilitro para que la división por 18 de la glucosa y por 2.8 de la urea, que se mide como el nitrógeno existente en su molécula, permita la conversión de las unidades de miligramos por decilitro a milimoles por litro y por lo tanto a miliosmoles por kilogramo de H_2O.

Esta estimación de la Osm_p es especialmente útil en pacientes con insuficiencia renal crónica, cuya concentración plasmática de urea se encuentra elevada y en aquellos pacientes con concentraciones plasmáticas de glucosa elevadas y secundarias a la presencia de diabetes mellitus (1).

Contrario a lo que sucede en el LEC, la concentración de Na^+ en el LIC es menor (14 mM) y el ión potasio (K^+) es el cation intracelular más abundante (120 mM). Esta distribución asimétrica entre el Na^+ y el K^+ se mantiene por la acción de la bomba Na^+/K^+/ATPasa que se expresa de manera ubicua en las células de todos los organismos vivos (1).

La composición aniónica del LIC difiere también mucho de la presente en el LEC, con concentraciones intracelulares bajas de Cl^- (5 mM) y HCO_3^- (12 mM) en comparación con las presentes en el LEC (Cl^- 105 mM y HCO_3^- 25 mM) (**Tabla 1**).

ión	LEC (mM)	LIC (mM)
Na^+ sodio	140	14
K^+ potasio	10	120
Ca^{++} calcio	5	.001
Cl^- cloruro	105	5
HCO_3^- bicarbonato	25	12
PO_4^{-3} fosfato	25	100
pH	7.4	7.1

Tabla 1. pH y concentración de algunos cationes y aniones en el LEC y el LIC.

La función principal de los riñones es regular el volumen y la composición del LEC. Para lograrlo, filtran grandes volúmenes de plasma y reabsorben de manera selectiva compuestos necesarios para el organismo y secretan a la orina productos de desecho (2).

Los procesos de filtración, reabsorción y secreción renal se regulan de manera precisa para minimizar cambios en la composición del LEC. Por lo tanto, en condiciones normales se produce un volúmen y composición de orina adecuado para la homeostasis del LEC (2).

Estructura y función de los riñones

Los riñones son dos organos, de color rojizo, con forma de “frijol” que se localizan en la cavidad abdominal detrás del peritoneo, a los costados de la columna vertebral. En relación con la columna vertebral, los riñones se encuentran ubicados entre la última vértebra torácica y la tercera lumbar y se encuentran parcialmente protegidos por las costillas 11 y 12 (2).

En promedio, un riñón humano pesa 150 g y mide unos 11 cm de alto, por 6 cm de ancho y 2.5 cm de grueso. El riñón izquierdo suele ubicarse ligeramente dos centímetros

más abajo que el derecho debido a que éste último está presionado hacia arriba por el hígado.

Los riñones se encuentran envueltos por una cápsula translucida, delgada y fibrosa la cual los protege de infecciones, mantiene su volumen al prevenir su hinchamiento y les confiere cierta protección en conjunto con una capa más externa de tejido adiposo perinéfrico (1) (**Fig. 2**).

Los riñones desempeñan diversas funciones en un organismo entre las que se encuentran regular: a) la osmolalidad, composición electrolítica, volumen y pH de los líquidos corporales, b) la excreción de productos metabólicos y sustancias extrañas y c) la producción y secreción de diversas hormonas (1).

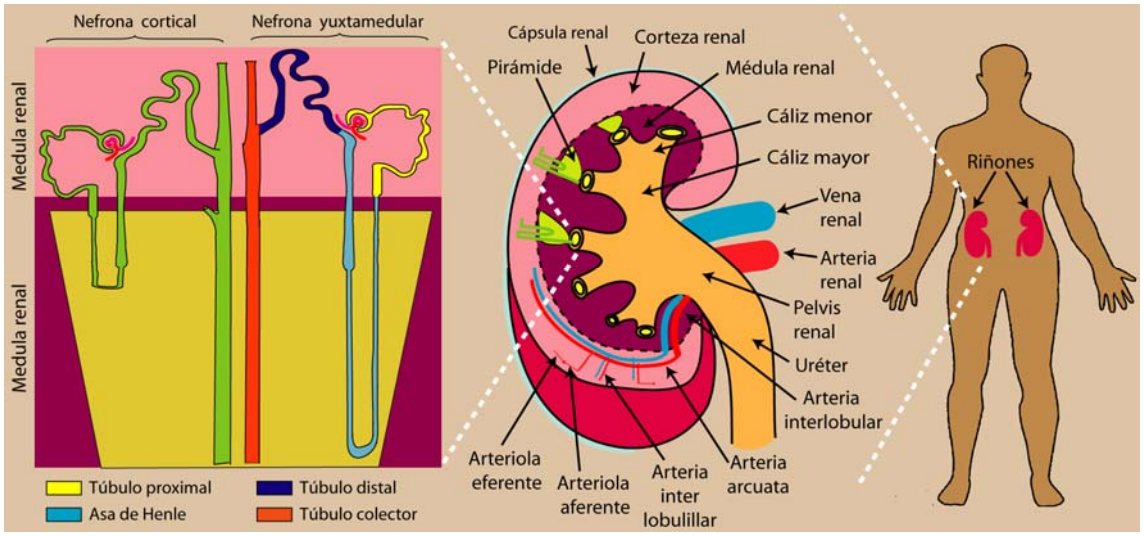

Figura 2. Estructura de los riñones y su unidad funcional, la nefrona.

Los riñones controlan la osmolalidad de los líquidos corporales la cual es importante para el mantenimiento del volumen celular normal y regulan la homeostasis de los líquidos corporales la cual es necesaria para el adecuado funcionamiento del sistema cardiovascular y sostener los niveles de P_s. Los riñones también son fundamentales en la regulación de varios iones inorgánicos importantes para el organismo, como el Na^+, K^+, Cl^-, HCO_3^-, calcio (Ca^{++}), magnesio (Mg^{++}) y fosfato (PO_4^{-3}) (1).

Muchas de las funciones metabólicas del organismo son extraordinariamente sensibles a cambios en el pH. Gracias a la acción coordinada de los pulmones, el hígado y los

riñones, se regula el equilibrio ácido-base para mantener dentro de límites muy estrechos el pH de los líquidos corporales y por lo tanto, una adecuada función celular (1).

Los riñónes excretan numerosos productos finales del metabolismo. Estos productos de desecho son: la urea (que permite eliminar el nitrógeno procedente de los aminoácidos), el ácido úrico (derivado de los ácidos nucleicos), la creatinina (a partir de la creatina muscular), los productos terminales del metabolismo de la hemoglobina y las hormonas. Los riñones representan además una vía importante para la eliminación de sustancias extrañas del organismo, como son los fármacos y otros productos químicos (2).

Finalmente, los riñones son organos endócrinos importantes, que producen y secretan las hormonas: renina, el calcitriol (1,25-dihidroxivitamina D_3) y la eritropoyetina. La renina activa al SRAA, importante para regular los niveles de P_s, así como el equilibrio del Na^+ y del K^+. El calcitriol producido por los riñones en respuesta a la estimulación por la hormona paratiroidea (PTH) regula la correcta reabsorción renal e intestinal de Ca^{++}, mientras que la eritropoyetina estimul la formación de glóbulos rojos en la medula ósea (1:18,19).

Cuando se secciona un riñón por la mitad, se pueden distinguir dos regiones: una región externa, denominada corteza y una región interna denominada médula. La medula del riñón se divide en segmentos cónicos denominados “pirámides renales”. La base de cada pirámide se sitúa en el borde entre la corteza y la médula y su punta termina en la papila, situada dentro de una estructura denominada “cáliz menor”. Los cálices menores recogen la orina de cada papila y se fusionan dando origen a dos o tres cavidades denominadas cálices mayores, que a su vez desembocan en la pelvis renal. La pelvis renal constituye la región superior ensanchada del uréter, que se encarga de transportar la orina desde la pelvis renal hasta la vejiga urinaria (2) (**Fig. 2**).

A pesar de que los riñones constituyen menos del 0.5% del peso corporal total, el flujo sanguíneo de ambos riñones equivale aproximadamente al 25% del GC en resposo. La arteria renal se ramifica dando lugar sucesivamente a las arterias interlobulares, arcuatas, interlobulillares y a las arteriolas aferentes que acaban en los capilares glomerulares. Estos capilares confluyen para formar la arteriola eferente que da origen a

una segunda red capilar, los capilares peritubulares, que irriga a la nefrona y a los vasos rectos. Los vasos del sistema venoso se distribuyen de manera paralela a los arteriales y forman progresivamente las venas interlobulillares, arcuatas, interlobulares y la vena renal cuyo trayecto se extiende junto al uréter (2).

Estructura de la nefrona

Cada riñón humano contiene alrededor de 1.2 millones de nefronas, que son tubos huecos delineados por una única capa celular. La nefrona es la unidad estructural básica y funcional del riñon y consta de un corpúsculo renal, un túbulo proximal (TP), una asa de Henle (AH), un túbulo distal (TD) y un sistema de conductos ó túbulos colectores (TC). El corpúsculo renal está constituido por los capilares glomerulares y la cápsula de Bowman. El TP da inicialmente varias vueltas (túbulo contorneado proximal) y luego presenta una porción recta que desciende hacia la médula. El siguiente segmento es la AH, formada por la rama delgada descendente (RDDAH), la rama delgada ascendente (RDAAH) y la rama ascendente gruesa (RAGAH) (2) (**Fig. 2**).

Cerca del final de la AH, ésta pasa entre las arteriolas aferente y eferente correspondientes a esa misma nefrona. Este corto tramo de la RAGAH se denomina mácula densa. El TD comienza poco después de la mácula densa y se extiende hasta el punto de la corteza donde dos o más nefronas se reúnen para formar un TC cortical. EL TC penetra en la médula y se convierte en el túbulo colector medular externo (TC-ME) y después en el túbulo colector medular interno (TC-MI) (**Fig. 2**) (2).

Las nefronas pueden subdividirse en corticales y yuxtamedulares. El corpúsculo renal de cada nefrona cortical se localiza en la zona externa de la corteza. Su asa de Henle es corta y su arteriola eferente se ramifica para dar lugar a los capilares peritubulares que rodean a los segmentos tubulares de su propia nefrona y de las adyacentes. Esta red capilar aporta oxígeno y nutrientes importantes a los segmentos tubulares, transporta sustancias a los túbulos para su secreción y sirve de vía para la recuperación de H_2O y los solutos reabsorbidos (**Fig. 2**) (2).

El corpúsculo renal de las nefronas yuxtamedulares se localiza en la zona de la corteza renal adyacente a la médula. En comparación con las nefronas corticales, las

yuxtamedulares se diferencian estructuralmente en dos aspectos importantes: el AH es más larga y penetra profundamente en la médula renal y la arteriola eferente no solo forma una red de capilares peritubulares, sino también una serie de asas vasculares denominadas vasos rectos (**Fig. 2**).

Los vasos rectos descienden hacia la médula, donde forman redes capilares que rodean a los TC y a las dos ramas de la AH. Aunque menos del 1% del flujo sanguíneo renal circula por los vasos rectos, estos vasos desempeñan funciones muy importantes como: a) aporte de oxígeno y nutrientes b) transporte de sustancias a la nefrona para su secreción, c) una vía de regreso hacia el sistema circulatorio para el H_2O y solutos reabsorbidos y d) la concentración y dilución de la orina.

Reabsorción renal de Na^+ y niveles de presión sanguínea

El riñón es el regulador más importante del balance del VI y del Na^+, el principal catión determinante del volumen del LEC y la Osm_p (20). Como se discutirá en parrafos posteriores, la reabsorción de Na^+ a lo largo de la nefrona, constituye un determinante crítico sobre la regulación de la P_s.

En condiciones normales, los riñones filtran diario alrededor de 175 litros de plasma o VI que contiene ~24.5 moles de cloruro de sodio (NaCl), de los cuales se reabsorbe el 99.5% a través de diversas rutas coordinadas de transporte transcelular (por medio de canales, intercambiadores y transportadores) y paracelular (a través de las uniones estrechas de las células) (20).

Los mecanismos de transporte transcelular de Na^+ son heterogéneos dependiendo del segmento de la nefrona en cuestión, no obstante en todos los segmentos existe un transporte activo de Na^+ en la membrana basolateral regulado por la bomba Na^+/K^+/ATPasa que se encarga de mantener una concentración baja de Na^+ (14 mM) en el interior de las células tubulares y de esa manera generar un gradiente de concentración favorable para el Na^+ y promover su reabsorción desde la luz tubular a través de diversas proteínas de transporte presentes en la membrana apical (20,21).

Alrededor del 60% del Na^+ filtrado por el corpúsculo renal, componente de filtración inicial de una nefrona, es reabsorbido principalmente de manera transcelular en el TP por: el intercambiador Na^+/protón (H^+) conocido como NHE3, el cotransportador de Na^+/PO_4^{-3} conocido como NaPi2, tres cotransportadores de Na^+/glucosa SGLT1-3, cotransportadores de Na^+/aminoácidos y el cotransportador de Na^+/sulfato (SO_4^{-2}) conocido como NaSi-1 (22-25) (**Fig. 3**).

A lo largo de la RAGAH donde se reabsorbe el 30% del Na^+ filtrado, el principal responsable del movimiento transcelular de Na^+ es el cotransportador de $Na^+/K^+/2Cl^-$, inhibido por diuréticos tipo asa como bumetanida y furosemida, conocido como NKCC2 (26-29) (**Fig. 3**).

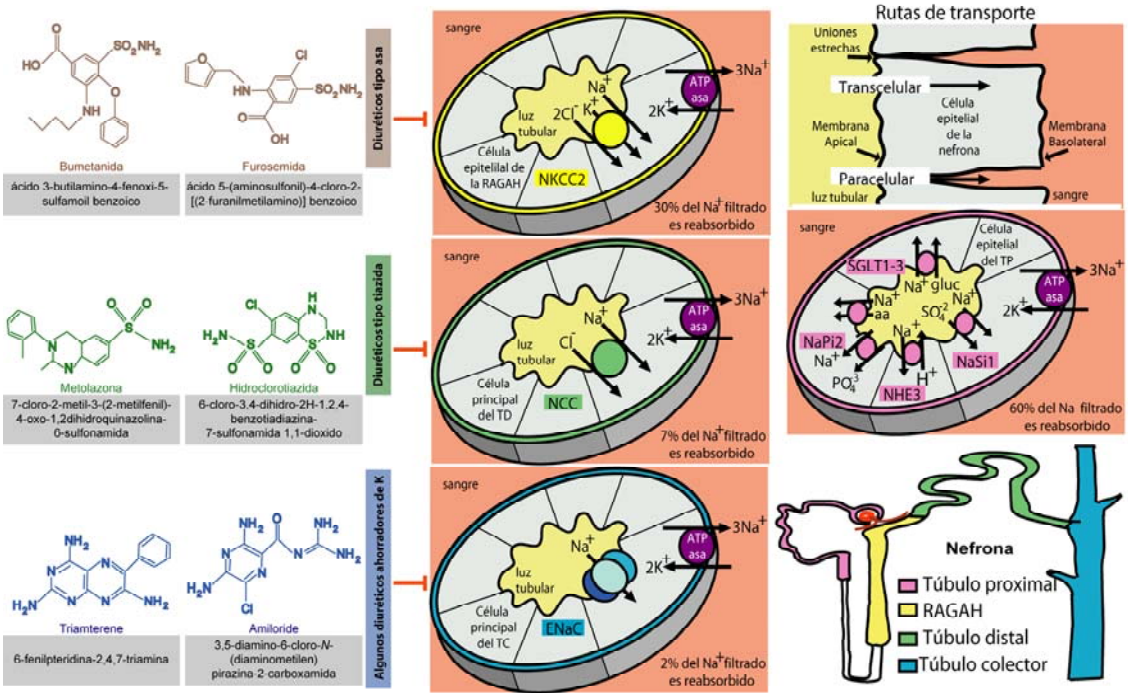

Figura 3. Esquema general de la reabsorción renal de Na^+ y sus inhibidores.

En la nefrona distal, que comprende al TD y al TC, se reabsorben el 7% y el 2% del Na^+ filtrado respectivamente. En el TD, el encargado de la reabsorción transcelular de Na^+ es el cotransportador de Na^+/Cl^- conocido como NCC (30), inhibido por diuréticos tipo tiazida como metolazona e hidroclorotiazida. A lo largo del TC, el responsable del transporte de Na^+ es el canal epitelial de Na^+ conocido como ENaC (31), inhibido por

algunos diuréticos ahorradores de ion potasio (K^+) como la amiloride y triamterene (**Fig. 3**).

Desde los años 60, gracias a los trabajos del Dr. Arthur Clifton Guyton y colaboradores, hoy sabemos que eventos que favorezcan la reabsorción renal de Na^+ elevarán la P_s, mientras que aquellos que la desfavorezcan, resultarán en una disminución en los niveles de P_s (32,33).

La relación fisiopatológica entre la reabsorción renal de Na^+ y P_s es predecible a partir de la homeostasis del LEC (32;34-36). Una elevada reabsorción renal de Na^+ necesitará estar acompañada de un incremento en la reabsorción renal de H_2O mediada por la hormona antidiurética (ver más adelante) para mantener constante la Osm_p (~290 mOsm/Kg H_2O) y la concentración plasmática del Na^+ (140 mM), quien además de ser el principal catión extracelular, se encuentra de manera muy importante involucrado en la regulación de la presión osmótica celular (37).

A través de una elevada reabsorción renal de Na^+ y H_2O, se favorecerá un aumento del VI, lo cual se traducirá en un incremento en el GC. Al recordar que los niveles de P_s están directamente relacionados con los niveles de GC (P_s = GC * R_{vp}), resulta fácil entender como un incremento en el GC provoca de manera directa un aumento en la P_s. Cambios tan pequeños en el GC de tan solo 5 al 10% pueden resultar en incrementos de la presión arterial media (PAM) normal que oscila alrededor de 100mm de mercurio (Hg) a niveles de hasta 150 mm de Hg (1) (**Fig. 4**).

$$\text{PAM= Presión Diastólica} + \frac{\text{Presión sistolica - Presión diastólica}}{3}$$

De manera indirecta, el aumento en los niveles de GC también contribuye a un incremento en los niveles de la P_s debido al fenómeno conocido como “autorregulación del flujo sanguíneo por la vasculatura” mediante el cual, la vasculatura normaliza el aumento del flujo sanguíneo y el suministro de oxígeno y nutrientes mediante favorecer la vasoconstricción, y por lo tanto incrementos en los niveles de la R_{vp} (**Fig. 4**).

Debido a lo anterior, un incremento en el GC y el indirecto aumento en la R_{vp} por la autorregulación del flujo sanguíneo por la vasculatura contribuyen de manera

simultánea al incremento en los niveles de la P_s (38). Por el proceso inverso descrito en líneas anteriores, al existir una disminución en los niveles de reabsorción renal de Na^+, se promoverá una disminución en los niveles de la P_s (**Fig. 4**).

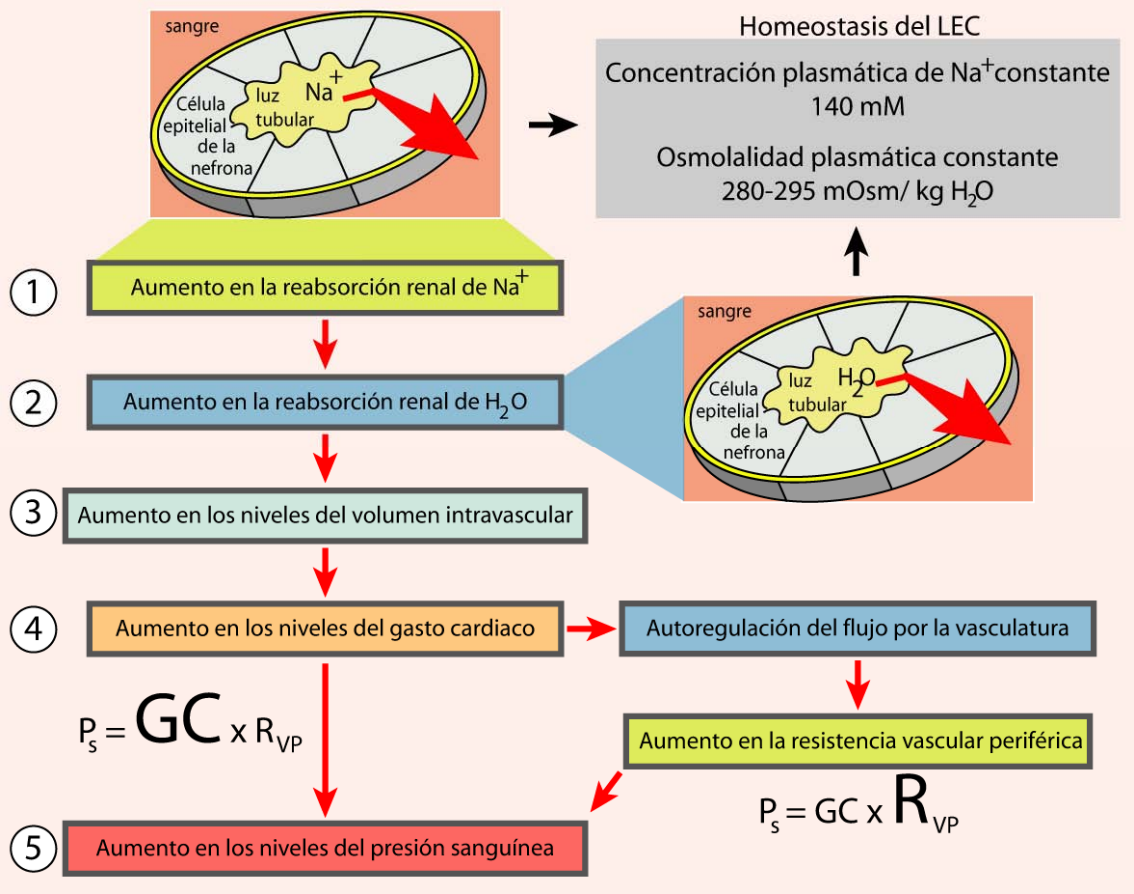

Figura 4. Relación fisiopatológica entre reabsorción renal de Na^+ y niveles de presión sanguínea.

En resumen, mantener la homeostasis del Na^+ y por lo tanto del volumen del LEC, requiere un complejo sistema de sensores y señales efectoras que actúan principalmente sobre los riñones, para regular la reabsorción-excreción de Na^+ y H_2O. En una persona normal, cambios en el volumen del LEC originan cambios paralelos en VI, el GC y la P_s. Estos tres factores son los principales reguladores de la reabsorción-excreción de Na^+ y H_2O. Así pues, el descenso en la reabsorción renal de Na^+ conduce a una situación denominada "contracción de volumen" debido a la disminución del VI, GC y la P_s. Por el contrario, el ascenso en la reabsorción renal de Na^+ conduce a una situación denominada "expansión de volumen", donde existe un aumento en el VI, GC y la P_s. Cuando el volumen del LEC disminuye, la excreción de Na^+ se reduce. Por el contrario,

la elevación en el volumen del LEC conduce a un incremento en los niveles de excreción de Na^+. A dicho mecanismo también se le conoce como natriuresis por presión y se describirá en los parrafos siguientes (2).

Natriuresis por presión

Uno de los mecanismos más importantes para la homeostasis del VS, y del LEC es el efecto de la P_s sobre la excreción renal de Na^+ y H_2O. A dicho mecanismo se le conoce como diuresis-natriuresis por presión.

En general, una elevación en los niveles de la P_s resultará en un incremento en el volumen urinario (diuresis por presión) y de manera similar, una elevación crónica o aguda en los niveles de la P_s conducirá a un incremento en los niveles de excreción renal de Na^+ (natriuresis por presión). Dado que la diuresis y natriuresis por presión se presentan de manera simultánea, al hablar de natriuresis por presión se da por hecho que existe también pérdida renal de H_2O (diuresis) ó la generación de un mayor volumen urinario (**Fig. 5**) (2).

Mediante el mecanismo de natriuresis por presión se puede reducir notablemente el volumen del LEC y los niveles de la P_s al favorecer la eliminación de Na^+ y H_2O. Lo anterior es muy importante ya que durante una adecuada funcion renal, a través del mecanismo de natriuresis por presión, grandes cambios en la ingesta de electrolitos (Na^+) y H_2O pueden ser tolerados en el organismo mediante ajustes en la P_s, y por lo tanto de la excreción de Na^+ y H_2O (**Fig. 5**).

Un incremento en la ingesta de Na^+ por arriba de su excreción renal ocasionaría un incremento temporal del LEC y la P_s. Sin embargo, gracias al mecanismo de natriuresis por presión, estos cambios en el LEC o VS son imperceptibles debido principalmente a que el mismo aumento en los niveles de la P_s, favorece una mayor excreción de volumen urinario y de Na^+.

La eficacia del mecanismo de natriuresis por presión para prevenir grandes cambios en el VS se puede observar en la figura E, la cual muestra que cambios en el VS son

prácticamente imperceptibles a pesar de grandes variaciones en la ingesta de H_2O y de Na^+ (2).

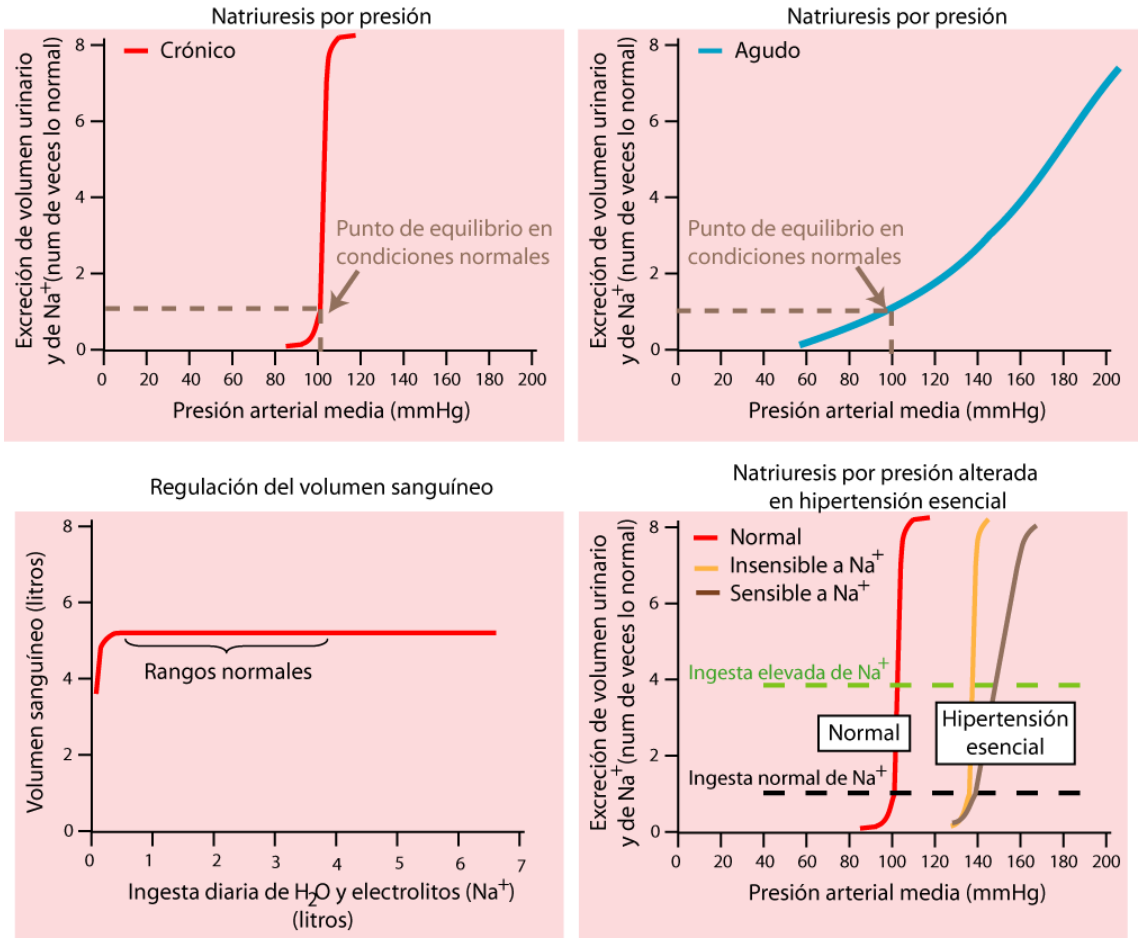

Figura 5. Natriuresis por presión y regulación de los niveles de presión sanguínea.

A lo largo de la evolución, multiples refinamientos se han añadido al sistema de natriuresis por presión para hacerlo más exacto en el control de la reabsorción-excreción de Na^+ y H_2O. Un refinamiento importante y que se discutirá en los parrafos siguientes es lo que conocemos como el SRAA.

Sistema Renina Angiotensina Aldosterona (SRAA)

Se le considera el regulador maestro de los niveles de la P_s a mediano y a largo plazo por varias razones (13-15), una muy importante es la basada en los elegantes trabajos realizados por el grupo del Dr. Richard Lifton en la Universidad de Yale, donde ha demostrado que todos los desordenes mendelianos con un impacto sobre la homeostasis

de los niveles de la P_s, son ocasionados por mutaciones que afectan la reabsorción renal de Na^+ y H_2O mediada por el SRAA (ver más adelante) (39-44).

Diversos estímulos pueden favorecer la función y activación del SRAA para regular los niveles de la P_s como por ejemplo: a) disminución de los niveles de la P_s (2), b) una menor perfusión del glomérulo (2), c) disminución en la cantidad de Na^+ que llega a las células de la mácula densa (dieta baja en NaCl) (3) ó d) estimulación del sistema nervioso simpático a través de los receptores β1 adrenérgicos (45,46).

En presencia de alguno de los estímulos mencionados, se favorece la secreción de la aspartil proteasa renina desde células modificadas del músculo liso de la arteriola aferente glomerular, conocidas como células granulares del aparato yuxtaglomerular (47) (**Fig. 6**).

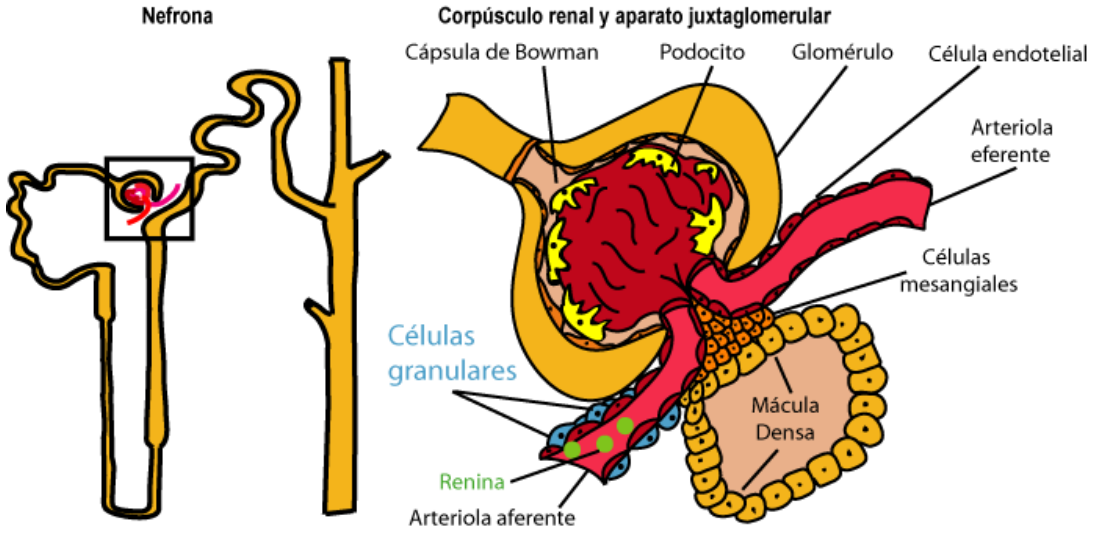

Figura 6. Corpúsculo renal, aparato juxtaglomerular y secreción de renina.

La renina liberada llevará a cabo la proteólisis del angiotensinógeno secretado por el hígado para favorecer la formación del deca-péptido angiotensina I (Asp-Arg-Val-Tyr-Ile-His-Pro-Phe-His-Leu) (**Fig. 8**).

Una vez formada la angiotensina I, esta sufrirá una hidrólisis que ocurre principalmente en los pulmones, por la enzima convertidora de angiotensina (ECA), resultando en la producción del octa-péptido angiotensina II (Asp-Arg-Val-Tyr-Ile-His-Pro-Phe) (**Fig. 8**).

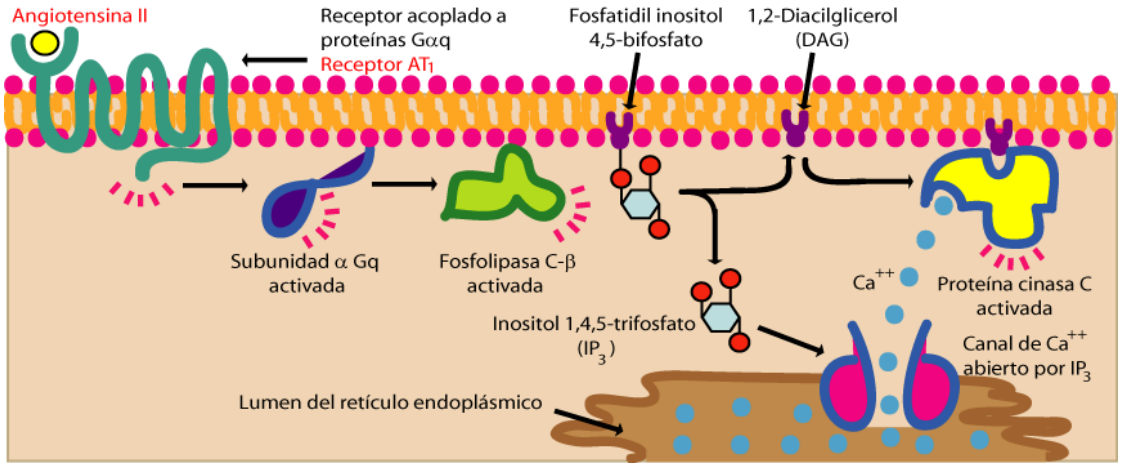

Figura 7. Angiotensina II y generación de IP_3 y DAG**.**

La angiotensina II, a través de sus receptores AT_1 acoplados a proteínas Gαq, favorecerá la activación de fosfolipasa C tipo beta (PLC-β), hidrólisis de fosfatidil inositol 4,5-bifosfato (PIP2) y la generación de segundos mensajeros como inositol 1,4,5-trifosfato (IP_3) y 1,2-diacilglicerol (DAG) (48) (**Figs. 7 y 8**).

La formación de DAG e IP_3 favorece la activación de la proteína cinasa C (PKC) y el incremento en las concentraciones citoplásmicas del ion calcio (Ca^{++}) (49). Con lo anterior, se promueven diversos efectos entre los que se encuentran: a) vasoconstricción sobre la vasculatura periférica (50) b) secreción desde la neurohipófisis de la hormona antidiurética (ADH) (51,52) y c) la secreción desde la glomerulosa adrenal de la hormona mineralocorticoide aldosterona (1;53) (**Figs. 7 y 8**).

Al activar al SRAA y favorecer: a) el incremento en la R_{vp} al promover la vasoconstricción arterial mediada por angiotensina II y b) elevar el VI y VCE al promover la reabsorción renal de H_2O y Na^+ mediada por ADH y aldosterona, se elevan y restauran a su normalidad los niveles de la P_s (48).

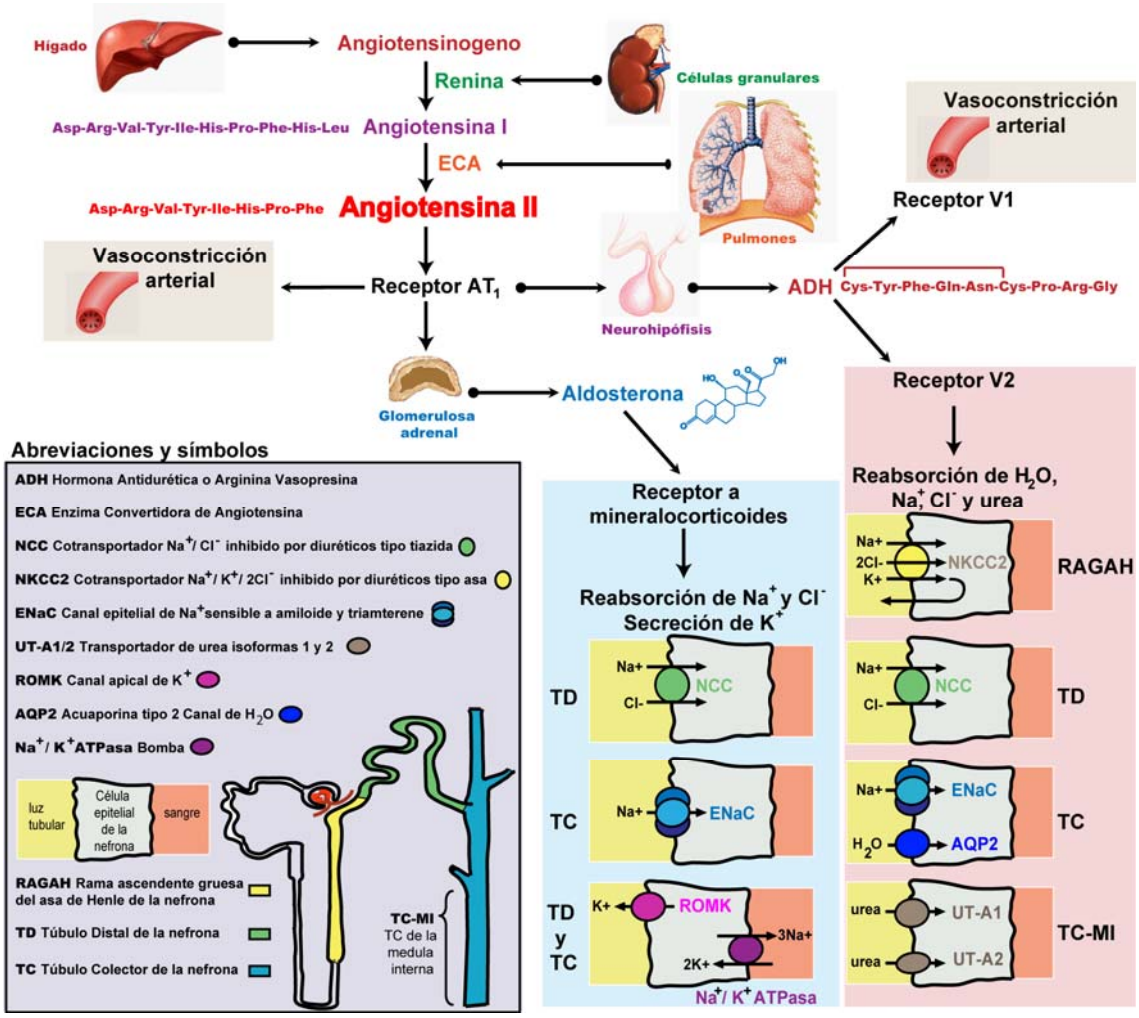

Figura 8. Esquema general de acciones del sistema renina angiotensina aldosterona.

Hormona antidiurética

La ADH es una hormona de nueve aminoácidos (Cys-Tyr-Phe-Gln-Asn-Cys-Pro-Arg-Gly), con un puente disufuro entre las dos cisteinas de su secuencia, que se sintetiza en las células neuroendócrinas localizadas en los núcleos supraóptico y paraventricular del hipotálamo. Una vez sintetizada, la ADH se almacena en gránulos que se transportan a lo largo de los axones neuronales y se acumulan en las terminaciones nerviosas situadas en la neurohipófisis desde donde se lleva acabo su secreción (2) (**Fig. 9**).

La ADH a través de sus receptores V1 acoplados a proteinas Gαq promueve el incremento en la R_{vp} al favorecer la vasoconstricción arterial. Por otro lado, la ADH a menores concentraciones plasmáticas, a través de sus receptores V2 acoplados a proteínas Gαs actúa sobre los riñones con el fin de regular: a) la reabsorción de urea en

la el TC-MI y la RDDAH, b) la reabsorción de Na^+ a lo largo de la RAGAH, TD y TC así como c) la reabsorción de H_2O en el TC. Con lo anterior la ADH regula los niveles del LEC, P_s, el volumen y la concentración urinaria. Cuando las concentraciones plasmáticas de la ADH son bajas, se excreta un gran volumen urinario (diuresis acuosa) y la orina está diluida. Cuando sus valores plasmáticos están elevados, se excreta una pequeña cantidad de orina concentrada o hiperósmótica con respecto al plasma (antidiuresis) (**Fig. 11**) (2).

Existen dos mecanismos que regulan de manera importante la secreción de la ADH: a) el osmótico y b) el hemodinámio (2). Dentro de estos dos mecanismos, el osmótico es el más importante ya que cambios en la Osm_p de tan solo 1% son suficientes para modificar de manera dramática la secreción de la ADH (**Fig. 9**).

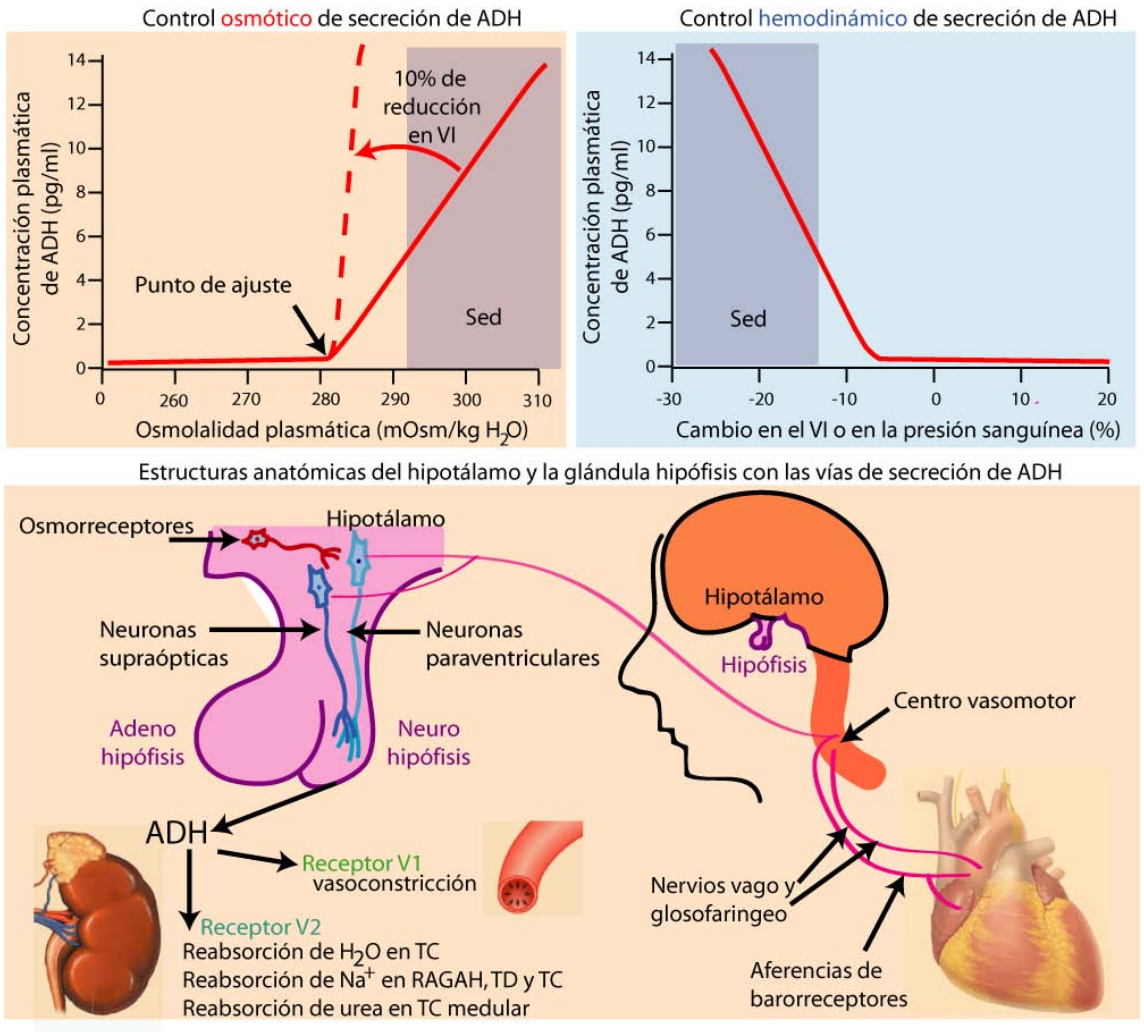

Figura 9. Mecanismos que regulan la secreción de la hormona antidiurética.

Otros factores que pueden modificar la secreción de la ADH son las nauseas, el péptido natriurético auricular y la angiotensina II. Diversos productos tambien influyen sobre la secreción de la ADH. Por ejemplo la nicotina la estimula, mientras que el etanol la inhibe (2) (**Fig. 9**).

Control osmótico de la secreción de ADH

El principal factor que determina los niveles de secreción de la ADH es la variación en la Osm_p. Cuando la Osm_p aumenta, los osmorreceptores hipotalámicos envían señales a las neuronas sintetizadoras de la ADH situadas en los núcleos supraóptico y paraventricular para estimular su secreción. Por el contrario, cuando disminuye la Osm_p se inhibe la secreción de la ADH (2) (**Fig. 9**). ´

En la figura 9 se representa el efecto de los cambios en la Osm_p sobre las concentraciones circulantes de la ADH. El punto de ajuste del sistema es el valor de la Osm_p desde el cual comienza la secreción de ADH. En individuos sanos dicho punto de ajuste oscila entre 280 y 295 mOsm/kg H_2O. Por debajo de esta cifra, prácticamente no existe secreción mesurable de esta hormona. Sin embargo, a medida que aumenta la Osm_p, la secreción de ADH es notoria y refleja la sensibilidad de este sistema para favorecer la reabsorción renal de H_2O y Na^+ y el reestablecimiento de los niveles normales de la Osm_p.

Control hemodinámico de la secreción de la ADH

La disminución drástica del VS (hipovolemia) o de los niveles de la P_s favorecen la secreción de la ADH. Los barorreceptores responsables de esta respuesta son sensibles al estiramiento de la pared de su estructura y se localizan tanto en la aurícula izquierda cardiaca y vasos pulmonares (zona de baja presión), asi como en el seno carotídeo y cayado aórtico del sistema circulatorio (zona de alta presión). Los barorreceptores de baja presión responden a cambios en el VS, mientras que los de alta presión lo hacen frente a modificaciones en los niveles de la P_s (2) (**Fig. 9**).

Las señales desde estos barorrecpetores se transmiten a través de las fibras aferentes de los nervios glosofaringeo y vago hasta los centros vasomotores del tronco del encéfalo

encargados de la regulación de la FC y la P_s. Posteriormente, las señales se transmiten desde estas estructuras hacia las células secretoras de la ADH de los núcleos hipotalámicos supraóptico y paraventricular. La sensibilidad de este sistema barorreceptor es menor que la de los osmorreceptores ya que se necesita un descenso del 5 al 10% en el VS o en la P_s para que se estimule la secreción de la ADH (2) (**Fig. 9**).

Las modificaciones del VS y de la P_s también influyen sobre la respuesta ante cambios en la Osm_p. Cuando se disminuye drásticamente los niveles del VS y de la P_s, el punto de ajuste osmótico se desplaza hacia cifras menores y la pendiente de la curva es mayor. Cuanso la P_s o el VS aumentan ocurre lo contrario, el punto de ajuste osmótico se desplaza a cifras mayores y la pendiente de la curva disminuye (2) (**Fig. 9**).

Transtornos relacionados a la secreción o efectos de ADH

En pacientes donde existe una disminución en los niveles de secreción de la ADH se presenta una elevada excreción de volumen urinario el cual se encuentra diluido (poliuria hipotónica). Para compensar esta pérdida excesiva de H_2O, se promueve su ingesta (polidipsia o sed severa) con el fin de mantener constante la Osm_p. Sin embargo, si el paciente carece de H_2O se presenta una severa deshidratación, disminución de los niveles de la P_s y la Osm_p aumenta. Esta situación se denomina diabetes insipida hipofisaria o diabetes insipida central (DIC). La DIC puede ser hereditaria y con frecuencia aparece tras un traumatismo craneoencefálico, en neoplasias o infecciones cerebrales. Los pacientes con DIC presentan un defecto en la concentración de la orina que se puede corregir con la administración de ADH exógena (2).

Cuando se presenta una correcta secreción de la ADH, pero no se pueden ejercer sus acciones, los individuos no son capaces de concentrar su orina al máximo. En general los pacientes no responden normalmente a la ADH debido a mutaciones que afectan al receptor V2 de la ADH o su vía de señalización mediante impedir la incorporación de canales de H_2O conocidos como acuapirna 2 (AQP2) en el TC de la nefrona (ver más adelante). Por consiguiente cursan con una elevada excreción de volumen urinario (poliuria) y un aumento anormal de la sed (polidpsia) debido a la severa deshidatación. Al cuadro clínico mencionado se le denomina diabetes insípida nefrógena. Aunque existen formas hereditarias, la mayoría de los casos son secundarios a trastornos

metabólicos o ciertos fármacos. Por ejemplo, aproximadamente el 35% de las personas que toman litio frente a un trastorno bipolar contraen una diabetes insípida nefrógena (2).

El síndrome de la secreción inadecuada de la ADH (SIADH) es un transtorno que se caracteriza por concentraciones plasmáticas de la ADH superiores a las normales que se puede ocasionar por infecciones, el uso de antineoplásicos y neuropatías. En pacientes con SIADH la excreción renal de H_2O se encuentra disminuida y por lo tanto, existe una elevada concentración urinaria. Debido a la acumulación de H_2O, una característica clínica importante en pacientes con SIADH es la marcada disminución en los niveles de la Osm_p (2).

<u>Mecanismos moleculares de acción natriurética y antidiurética de la ADH</u>

Las principales acciónes de la ADH sobre los riñones son: a) incrementar la reabsorción de Na^+ en la RAGAH y la nefrona distal al favorecer la actividad de NKCC2, NCC y ENaC, b) incrementar la permeabilidad de la RDFAH y del TC al H_2O al favorecer la actividad de los canales de agua AQPl y AQP2 y c) favorecer la permeabilidad a la urea en el TC-MI y en la RDFAH al promover la actividad de los cotransportadores de urea UT-A1, UT-A2 y UTA-3.

La ADH incrementa la permeabilidad al H_2O de las células principales del TC de la nefrona al unirse a su receptor V2 acoplado a proteínas Gαs y promover la activación de la adenilato ciclasa transmembranal (AC), la cual favorecerá la formación de adenosín monofosfato-3',5' cíclico (AMPc) y activación de la proteína cinasa A (PKA) (**Fig. 10**) (54). La PKA es un complejo tetramérico compuesto por dos subunidades catalíticas y dos subunidads reguladoras. En presencia de AMPc la inhibición sobre las subunidades catalíticas ejercida por las subunidades reguladoras se interrumpe. Con lo anterior, las subunidades catalíticas de PKA se liberan y son capaces de fosforilar a proteínas sustratos en residuos de serina y/o treonina. La fosforilación mediada por PKA altera la actividad de proteínas blanco para coordinarla con la respuesta a estímulos extracelulares como la presencia de ADH.

La PKA lleva a cabo la fosforilación de la serina 256 presente en el canal de H_2O conocido como acuaporina 2 (AQP2) y dicha fosforilación promueve la traslocación de AQP2 desde vesículas citoplásmicas hasta la membrana apical de las células principales del TC y el papel antidiurético de ADH (55-57) (**Fig. 10**). De manera similar, la PKA favorecerá la llegada a membrana de AQP1 a lo largo de la RDFAH para favorecer la reabsorción de H_2O en este segmento de la nefrona necesario para la concentración-dilución urinaria.

De manera paralela, la ADH tendrá efectos antinatriuréticos al favorecer la reabsorción renal de Na^+ en la RAGAH, el TD y a lo largo del TC de la nefrona, al promover la actividad de NKCC2, NCC y ENaC (58) (**Fig. 10**).

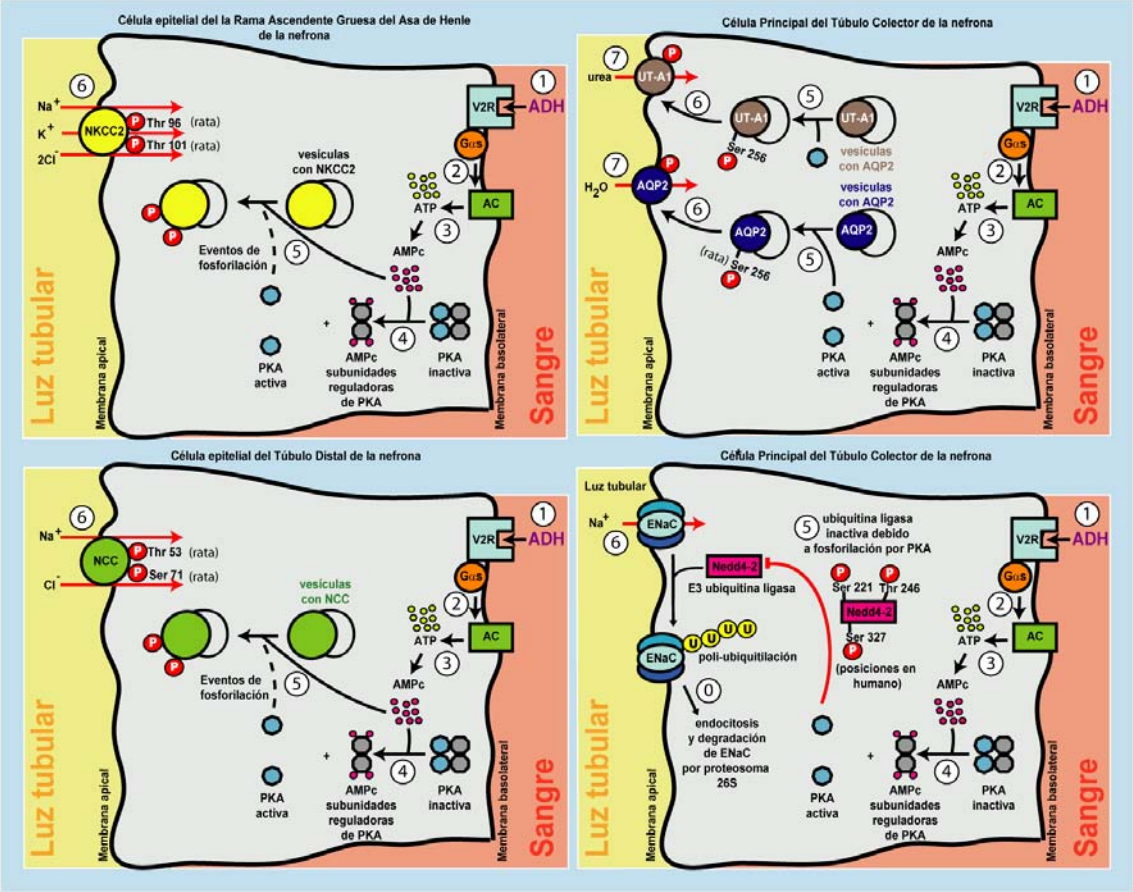

Figura 10. Mecanismos moleculares de acción antidiurética de ADH en el TC y antinatriurética en la RAGAH, TD y TC de la nefrona. (Los números indican el orden de eventos)

En la RAGAH, la ADH promoverá la actividad de NKCC2 mediante incrementos intracelulares de AMPc y eventos de fosforilación por PKA que resultarán en la fosforilación de los residuos de treonina 96 y 101 y la inserción de NKCC2 en la membrana apical de las células epiteliales de la RAGAH (59,60) (**Fig. 10**).

De manera similar, en el TD de la nefrona, la ADH favorecerá una mayor actividad y llegada a membrana de NCC al promover la fosforilación de NCC en los residuos de treonina 53 y serina 71 (61), mientras que a lo largo del TC, mediante la activación de PKA, se favorecerá la fosforilación de la E3 ubiquitina ligasa de la familia de las HECT conocida como Nedd4-2 (neural precursor cell expressed, developmentally down-regulated 4-2) en los residuos de serina 221, treonina 246 y serina 327. La fosforilación en estos aminoácidos presentes en Nedd4-2 impedirá la interacción entre Nedd4-2 y ENaC favorecida por los dominios WW (regiónes ricas en aminoácidos de triptofano) presentes en Nedd4-2 y el dominio PY (Pro-Pro-Xaa-Tyr) localizado en cada una de las tres subunidades (α-alfa, β-beta y γ̃-gamma) que constituyen a ENaC (62). Al impedir la interacción entre Nedd4-2 y ENaC, se prevendrá la poli-ubiquitilación de ENaC, su endocitosis, degradación proteosomal y lisosomal y por lo tanto: se aumentará la expresión de ENaC a nivel de la membrana apical de las células principales del TC y una mayor reabsorción de Na^+ en este segmento de la nefrona (63) (**Fig. 10**).

La activación mediada por ADH del cotransportador NKCC2 en la RAGAH y de los transportadores de urea UT-A1 y UTA-3 en el TC-MI asi como de UT-A2 en la RDDAH, son procesos críticos para sostener el mecanismo conocido como multiplicación por contracorriente (MPC). Mediante el MPC y la acción coordinada de la ADH se puede llevar a cabo el proceso de concentración y dilución de la orina.

Mecanismo de multplicación por contracorriente y concentración-dilución urinaria

Los riñones pueden excretar orina diluida o hipo-osmótica con respecto al plasma (proceso conocido como diuresis acuosa) o excretar orina concentrada o hiperosmótica con respecto al plasma (proceso conocido como antidiuresis). Para lograr lo anterior, se requiere que el H_2O de la orina sea separada de los solutos (2) (**Fig. 11**).

La orina hipo-osmótica se forma al reabsorber solutos desde la luz tubular de la nefrona sin permitir que el agua los siga. Mientras que para la formación de orina hiperosmótica, el H_2O debe ser removida de la luz tubular sin la remoción de solutos.

Debido a que el movimiento pasivo del H_2O solo puede ocurrir desde una región de baja presión osmótica a una de elevada presión osmótica (proceso conocido como ósmosis). Para generar una orina hiperosmótica y remover H_2O desde la luz tubular de la nefrona, los riñones deben ser capacer de generar una zona de eleveda presión osmótica alrededor de la nefrona (2).

Alrededor de la AH, debido a la alta concentración de Na^+ y de urea se encuentra la zona de elevada presión osmótica. Debido a su localización se le conoce como instersticio medular hiperosmótico (IMH).

A lo largo de la AH y especialmente en la RAGAH es donde se separa el H_2O de los solutos. Por lo tanto, para la formación de una orina hipo-osmótica o hiper-osmótica se requiere del adecuado funcionamiento de la AH y de la generación del IMH alrededor de ella.

Para la comprensión del mecanismo de producción de una orina concentrada o diluida se deben tener presente diversos aspectos entre los que se encuentran los siguientes:

La reabsorción de Na^+ mediada por NKCC2 a lo largo de la RAGAH diluye el líquido tubular y el Na^+ reabsorbido se acumula en el intersticio medular elevando su osmolalidad (IMH).

La acumulación de Na^+ en el intersticio medular es decisiva para la producción de orina hiper-osmótica con respecto al plasma ya que proporciona la energía osmótica para la reabsorción de H_2O por medio de AQP2 a lo largo del TC en presencia de la ADH.

Al proceso global de generación del gradiente hiperosmótico en el intersticio medular por parte de la RAGAH, se denomina multiplicación por contracorriente (MPC). Este término se debe tanto a la forma, así como a la función del AH. Dicho segemento de la nefrona está formado por dos ramas paralelas con un flujo del líquido tubular en

sentidos opuestos (flujo por contracorriente, el líquido fluye hacia la médula por la rama descendente y desde la médula por la rama ascendente) (**Fig. 11**).

La RAGAH es impermeable al agua y reabsorbe Na^+ desde el líquido tubular gracias a las acciones de NKCC2. Por lo tanto, el líquido se va diluyendo en su interior. A esta separación de Na^+ y H_2O por la RAGAH se denomina "efecto único" del proceso de MPC (2).

Como se ha mencionado, el Na^+ extraido desde el líquido tubular de la RAGAH se acumula en el intersticio medular circundante aumentando su osmolalidad. Dado que la RDFAH es muy permeable al H_2O debido a la presencia del canal de agua conocido como acuaporina 1 (AQP1), entre mayor sea la osmolalidad del intesticio medular generada por NKCC2, mayor cantidad de H_2O se reabsorberá en la RDDAH y se concentrara el líquido tubular en este segmento de la nefrona. El flujo por contracorriente en las ramas descendente y ascendente del AH amplía o "multiplica" el gradiente osmótico entre el fluido tubular de ambas ramas (**Fig. 11**).

En primer lugar, se describirá como se excreta una orina hipo-osmótica, cuando los valores plasmáticos de ADH son bajos.

Debido a que la reabsorción de solutos en el TP de la nefrona está siempre acompañada de la reabsorción de una cantidad proporcional de H_2O. En el TP no se produce la separación entre solutos y H_2O y el fluido que entra a la RDDAH tiene una concentración osmótica similar al plasma (aproximadamente 300 mOsm/kg H_2O) (2).

Gracias a la presencia de AQP1 a lo largo de la RDDAH, ésta es muy permeable al H_2O y mucho menos a los solutos como el Na^+ y la urea. En consecuencia, al ir profundizando el fluido tubular por la rama fina descendente hacía la médula hiperosmótica, el agua se reabsorbe debido al gradiente osmótico (mayor osmolaridad en el intersticio medular) creado por la constante reabsorción de Na^+ mediada por NKCC2 a lo largo de la RAGAH para generar el IMH (**Fig. 11**).

Aunque la osmolalidad del fluido tubular y del intersticio medular tienden a igualarse debido a la salida de H_2O por AQP1 desde la RDDAH, sus composiciones son

diferentes. La concentración de Na^+ en el líquido tubular de la rama fina descendente es mayor que en el líquido intersticial circundante. Sin embargo, el de la urea es menor en el líquido tubular que en el líquido intesticial (2).

La RDDAH es impermeable al H_2O pero permeable al Na^+ y la urea. En consecuencia, al ascender el fluido tubular por esta rama, se reabsorbe pasivamente Na^+, mientras la urea difunde también pasivamente hacia el fluido tubular (la concentración luminal de urea es menor que la intersticial). El efecto neto es que el volumen del líquido tubular permanece fijo a lo largo de la RDAAH, pero la concentración de Na^+ disminuye y la de urea aumenta. En conjunto, la salida de Na^+ desde la luz de la rama fina ascendente supera a la entrada de urea y el fluido tubular se diluye (**Fig. 11**).

Como se puede observar, para lograr la concentración o dilución urinaria se emplean las diferencias en las propiedades de transporte a todo lo largo de la AH (**Tabla 2**). La RAGAH es impermeable al H_2O y a la urea y a lo largo de este segmento de la nefrona se reabsorbe activamente Na^+ desde el líquido tubular por medio de NKCC2 y por tanto, el líquido tubular se diluye. La dilución llega a tal punto, que esta porción se denomina a menudo "segmento de dilución del riñón". El fluido tubular que sale de la RAGAH es hiposmótico con respecto al plasma (aproximadamente 150 mOsm/kg H_2O) (2).

		Permeabilidad en ausencia de ADH para			Permeabilidad en presencia de ADH para		
Nefrona	Segmento tubular	Na^+	urea	H_2O	Na^+	urea	H_2O
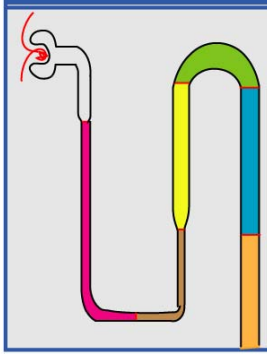	Rama delgada descendente del asa de Henle	✓	✓	✓✓✓	✓	✓	✓✓✓✓
	Rama delgada ascendente del asa de Henle	✓✓	✓	–	✓✓✓	✓✓	–
	Rama ascendente gruesa del asa de Henle	✓✓	–	–	✓✓✓	–	–
	Túbulo distal	✓	–	–	✓✓	–	–
	Túbulo colector cortical	✓	–	–	✓✓	–	–
	Túbulo colector de la medula interna	✓	✓	✓	✓✓	✓✓✓	✓✓✓

Tabla 2. Propiedades de transporte o permeabilidad de los segmentos de la nefrona que participan en la concentración-dilución urinaria.

Gracias a las acciones de NCC y de ENaC, a lo largo del TD y la porción cortical del TC se reabsorbe activamente más Na^+. En ausencia de ADH el TC es prácticamente

impermeable al H_2O. Por lo tanto, al reabsorberse más Na^+ sin H_2O, la osmolalidad del fluido tubular en estos segmentos de la nefrona disminuye aun más. En estas condiciones, el fluido que sale de la porción cortical del TC es hiposmótico con respecto al plasma (aproximadamente 100 mOsm/kg H_2O) (**Fig. 11**).

El TC-MI a través de ENaC reabsorbe activamente más Na^+ de tal manera que el fluido tubular se diluye aun más y la orina tendrá una osmolalidad de tan solo unos 50 mOsm/kg H_2O, con concentraciones bajas de Na^+ y urea. El volumen de orina excretado puede llegar a ser aproximadamente del 10% de la tasa de filtración glomerular o en otras palabras de 18L/día debido a la impermeabilidad al H_2O del TC en ausencia de ADH (2).

El intersticio de la medula renal tiene una importancia crítica para concentrar la orina. Su presión osmótica proporciona la energía para reabsorber agua desde la rama fina descendente del asa de Henle mediante AQP1 y luego desde el TC en presencia de ADH debido a la inserción a membrana de AQP2. Los principales solutos del intersticio medular son el Na^+ y la urea, pero su concentración no es uniforme en su interior es decir, existe un gradiente desde la corteza hasta la papila. También se acumulan otros solutos en el intersticio medular como amonio (NH_4^+) y K^+, pero los más abundantes son el Na^+ y la urea (2).

En el límite entre la médula y la corteza, el intersticio tiene una osmolalidad aproximada de 300 mOsm/kg H_2O atribuible prácticamente en su totalidad al Na^+. Las concentraciones de Na^+ y urea aumentan progresivamente hacia la médula. Cuando la concentración de la orina excretada es máxima, la osmolalidad del intersticio es aproximadamente de 1200 mOsm/kg H_2O en la papila. De esta cifra, unos 600 mOsm/kg H_2O corresponden al Na^+ y los otros 600 mOsm/kg H_2O a la urea (**Fig. 11**).

El gradiente de concentración del Na^+ en la medula renal se debe a su acumulación por los segmentos de la nefrona en la médula renal durante el proceso de MPC. La porción más importante es la RAGAH. La acumulación de urea en el intersticio medular es más compleja y se produce con mayor eficacia cuando se excreta una orina hiper-osmótica (**Fig. 11**).

Al producirse orina diluida, la osmolalidad del intersticio medular desciende. Esta reducción se debe casi en su totalidad a la disminución de la concentración de urea en el intersticio medular. En ausencia de ADH se retiran de la membrana los transportadores de urea UTA-1 y UTA-3 y la reabsorción de urea en el TC-MI disminuye (**Fig. 11**).

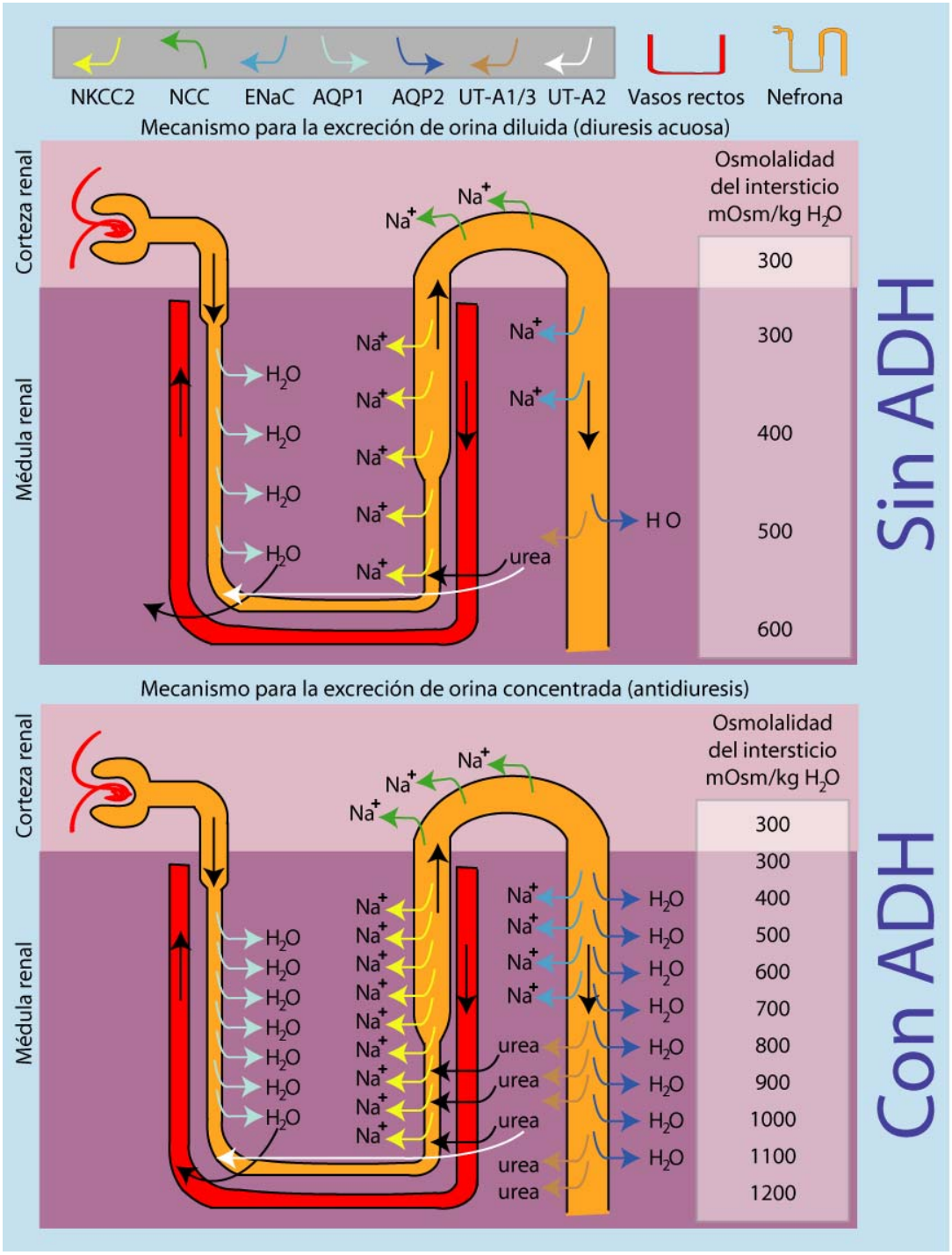

Figura 11. Mecanismo de multiplicación por contracorriente, dilución y concentración urinaria.

La urea se genera en el hígado como un producto del metabolismo de las proteínas y entra en el fluido tubular a través de la filtración glomerular. Como se muestra en la tabla B, la permeabilidad para la urea de la mayoría de los segmentos de la nefrona encargados de la concentración y dilución urinaria es relativamente baja. Una importante excepción es el TC-MI, que tiene una permeabilidad alta y se eleva aún más con la ADH dedido a la activación y llegada a membrana de UTA-1 y UTA-3. Al avanzar el líquido a lo largo de la nefrona y reabsorberse el H_2O en el TC, aumenta la concentración de urea en el fluido tubular. Cuando este líquido con abundante urea llega al TC-MI, donde la permeabilidad para la urea no solo es alta sino que aumenta en presencia de ADH, la urea se reabsorbe por medio de UT-A1 y UT-A3 hacia el líquido intersticial medular, donde se acumula para generar el IMH (2).

Parte de la urea del intersticio entra en RDDAH (a través de UT-A2) y ascendente del asa de Henle. Esta urea queda atrapada entonces en la nefrona hasta que llega de nuevo al TC-MI, donde puede regresar al intersticio medular. Por lo tanto, la urea recircula desde el intersticio a la nefrona. Este proceso de recirculación facilita su acumulación en el intersticio medular (**Fig. 11**).

A continuación se describirá como los riñones pueden excretar una orina concentrada cuando la Osm_p y los valores plasmáticos de ADH son elevados.

Como se ha mencionado, debido a la reabsorción de Na^+ por NKCC2 a lo largo de la RAGAH, el fluido tubular que llega al TC es hipo-osmótico con respecto al líquido intersticial circundante. Una vez presente el IMH y el gradiente de concentración favorable para la reabsorción de H_2O desde el TC, lo único que se requiere es que el TC sea permeable al H_2O, lo anterior se logra en presencia de la ADH quien favorecerá la llegada a membrana de AQP2 en el TC y mediante la reabsorción de H_2O en este segemento de la nefrona comienza el proceso de concentración urinario.

En presencia de ADH se aumenta la permeabilidad a la urea de la última porción del TC medular. Dado que la concentración de urea en el líquido tubular ha aumentado por la reabsorción de agua en la corteza y en la zona externa de la médula, su concentración en el líquido tubular es mayor que en el intersticial y algo de la urea difundirá fuera de la luz tubular hacia el intersticio medular.

La orina producida cuando los valores de ADH son elevados tendrá una osmolalidad de 1200 mOsm/kg H_2O y contendrá concentraciones altas de urea y otros solutos no reabsorbidos. La urea del líquido tubular tiende a equilibrarse con la urea intersticial por lo que su concentración en la orina es semejante a la del intersticio. En estas condiciones, la diuresis puede ser de tan solo 500 mL/día (2).

<u>Mecanismos moleculares de acción de la hormona aldosterona</u>

Por su parte, la homona esteroidea aldosterona favorecerá la secreción de K^+ y la reabsorción de Na^+ en la nefrona distal al modular la actividad de sistemas de transporte iónico localizados en la membrana apical y basolateral de las células epiteliales presentes en este segmento de la nefrona (64).

Para llevar a cabo sus funciones, la aldosterona promoverá la expresión a nivel transcripcional y de proteína de una variedad de genes, entre los que se encuentran aquellos que codifican para: a) la bomba Na^+/K^+ ATPasa, b) subunidad α de ENaC y c) la serina treonina cinasa inducible por suero y por glucocortIcoides tipo 1 (SGK1) (**Fig. 12**). Lo anterior se logra cuando la aldosterona activa a un receptor nuclear que es un factor de transcripción conocido como receptor a mineralocorticoides (RM). La activación del RM por aldosterona involucra la interacción física y formación de un complejo entre la aldosterona y el RM. Una vez formado dicho complejo, este migrará al núcleo celular donde favorecerá la expresión a nivel transcripcional de los genes mencionados (2) (**Fig. 12**).

El incremento en los niveles de expresión de la cinasa SGK1 (65) y su posterior activación mediada por aldosterona, son procesos críticos para promover y sostener la reabsorción de Na^+ y la secreción de K^+ en la parte distal de la nefrona.

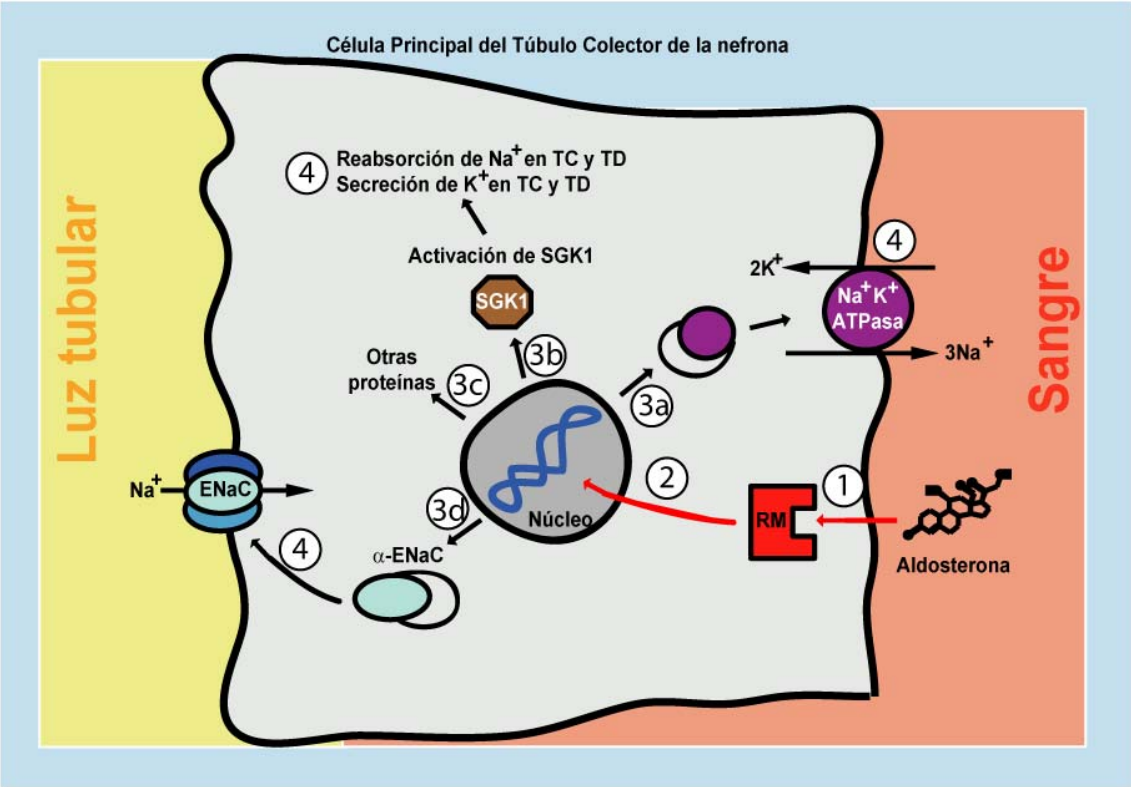

Figura 12. Mecanismo clásico de acción de aldosterona a través del RM. (Los círculos con números señalan el orden de eventos).

Para alcanzar la activación de SGK1, se requieren de eventos de fosforilación a través de una cascada de señalización mediada por la fosfatidil inositol 3-cinasa (P13K) y las cinasas tipo 1 y 2 dependientes de IP_3 (PDK1 y PDK2) (66) (**Fig. 13**).

A través de PI3K y PDK1, se lleva a cabo la fosforilación del residuo de serina 422 presente en SGK1. Una vez fosforilada la serina 422 y con el fin de alcanzar la actividad máxima de SGK1, se promoverá la fosforilación del residuo de treonina 256 por la cinasa PDK2 reclutada por la serina treonina cinasa sin lisina tipo 1 (WNK1) (responsable del desarrollo del Síndrome de Gordon ver más adelante) previamente fosforilada en el residuo de treonina 58 por la proteína cinasa B (PKB) (67) (**Fig. 13**).

La fosforilación de SGK1 en los residuos de treonina 256 y serina 422, le permitirán a SGK1 promover la reabsorción de Na^+ y la secreción de K^+ en la parte distal de la nefrona al llevar a cabo las siguientes acciones:

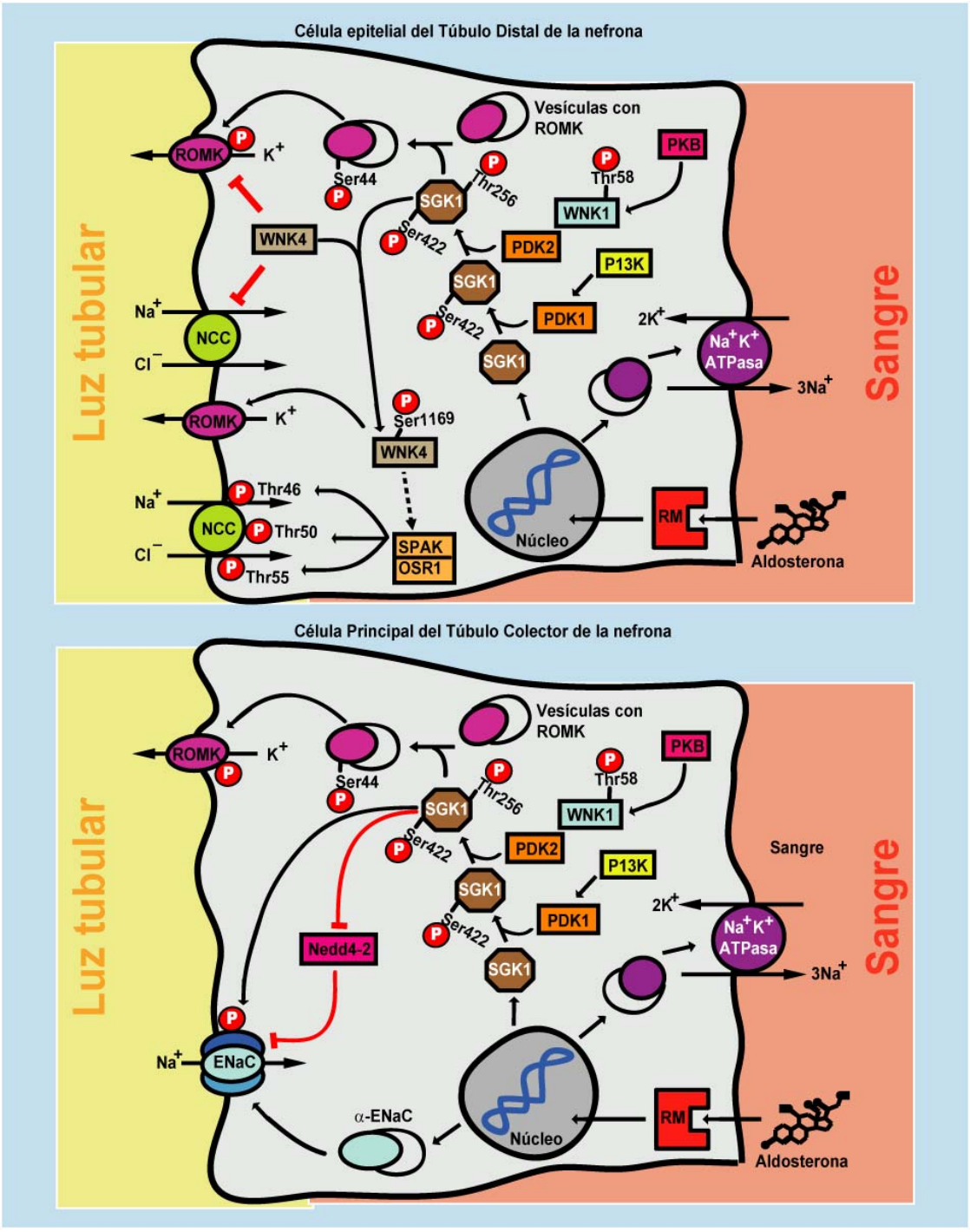

Figura 13. Mecanismo de acción de aldosterona en el TD y TC de la nefrona.

a) Fosforilar a la serina treonina cinasa WNK4 (también responsable del desarrollo del Síndrome de Gordon, ver más adelante) en la serina 1169 y de esa manera eliminar la inhibición ejercida por WNK4 sobre el cotransportador NCC y el canal apical de K^+ conocido como ROMK (68).

b) Fosforilar a ROMK en el residuo de serina 44 y de esa manera promover una mayor llegada a la membrana apical de canales de K^+ y por lo tanto: elevar los niveles de secreción de K^+ (69).

c) Fosforilar a Nedd4-2 en los residuos de serina 221, treonina 246 y serina 327 para prevenir que interactue con ENaC y de esa manera evitar la poli-ubiquitilación de ENaC, su endocitosis, degradación proteosomal y promover una mayor reabsorción de Na^+ a lo largo del TC de la nefrona debido a una mayor cantidad de ENaC en la membrana apical (70-73).

Recienteme se ha encontrado que la aldosterona también favorece la reabsorción de Na^+ en el TD mediante la activación de NCC a través de su fosforilación (al menos en rata) de los residuos amino terminales: treonina 53, treonina 58 y serina 71. Es importante mencionar que dichos residuos son requeridos para sostener la actividad basal de NCC y su activación durante la presencia de la ADH ó maniobras de depleción intracelular de Cl^- (74,75).

La fosforilación de dichos residuos parece ocurrir a través de la cascada de señalización que involucra a las cinasas WNK1 y WNK4 las que a su vez fosforilan y activan a las cinasas SPAK y OSR1 las cuales interactuan fisicamente con NCC y lo fosforilaran en los residuos amino terminales mencionados (ver más adelante) (74) (**Fig. 13**).

Modificaciones en los niveles de presión sanguínea

Hipertensión arterial

La hipertensión arterial (HTA), o P_s elevada es un problema de salud pública, ya que constituye un importante factor de riesgo para el desarrollo de la ateroesclerosis, y de causas comunes de morbilidad y mortalidad como lo son: a) el infarto agudo al miocardio, b) evento vascular cerebral, c) insuficiencia arterial periférica y d) enfermedad renal terminal (76).

Por parte del séptimo reporte del comité nacional conjunto para la prevención, detección, evaluación y tratamiento de la HTA (JNC7 por sus siglas en inglés) (77,78), la clasificación de los niveles de HTA es la mostrada en la tabla C (3):

Clasificación	Presión sistólica (mm Hg)	Presión diastólica (mm Hg)
Normal	<120	<80
Pre-hipertensión	120-139	80-89
Hipertensión etapa 1	140-159	90-99
Hipertensión etapa 2	>160	>100

Tabla 3. Clasificación de los niveles de HTA según JNC7.

A la fecha se ha estimado que la HTA afecta a mil millones de personas alrededor del mundo. En otras palabras, del 20 al 25% de la población adulta en sociedades industrializadas la padecen (76). A partir de estudios clínicos, la HTA ha sido definida como los niveles de P_s en los cuales, una intervención terapéutica produce beneficio sobre la salud del paciente (79).

El tratamiento farmacológico de la HTA ha permitido establecer que mediante la reducción de los niveles de P_s es posible disminuir significativamente el riesgo de evento vascular cerebral, así como de infarto agudo al miocardio y enfermedad renal terminal.

A pesar del importante papel de la HTA como causa de enfermedad, su patogénesis en el 95-97% de los casos es en gran medida desconocida. A dicha situación donde se desconocen las causas precisas que originan el incremento sostenido de los niveles de P_s se le conoce como HTA esencial (80).

Los estudios epidemiológicos han documentado el impacto de una gran variedad de factores entre los que se encuentran: la edad, el género, el índice de masa corporal y la dieta (81). No obstante, el definir las causas de HTA a partir de estudios fisiológicos ha sido difícil debido principalmente a las causas multifactoriales, demográficas y ambientales que la ocasionan (82).

El desconocimiento del número de genes que influyen en el desarrollo de alteraciones en los niveles de P_s, así como la magnitud de sus efectos, ha puesto hoy en día al tratamiento de la HTA como una actividad ampliamente empírica, con alrededor de setenta diferentes fármacos antihipertensivos disponibles (83-91)

Con el fin de avanzar en la comprensión de la patogénesis de la HTA, se han empezado a estudiar raros desordenes Mendelianos en donde los pacientes cursan con variaciones en los niveles de P_s debido a la presencia de una sola mutación en un solo gen (hipertensión o hipotensión monogénica) (92-93).

En años recientes, los mecanismos moleculares de varias formas monogénicas de hipertensión e hipotensión han sido identificados. Como se discutirá más adelante, en todas estas alteraciones de los niveles de P_s, las mutaciones responsables modifican la reabsorción de Na^+ y H_2O mediada por el SRAA en el riñón. Estudios genéticos moleculares han identificado mutaciones en diez genes que ocasionan formas Mendelianas de HTA y mutaciones en doce genes que son responsables del desarrollo de hipotensión arterial (8-16)

<u>Formas monogénicas de hipertensión arterial</u>

A la fecha diez genes y uno aun desconocido pero con localización cromosómica 1q31-q42, han sido descritos como blancos para el desarrollo de enfermedades donde los pacientes cursan con HTA cuando se encuentran mutaciones en ellos (**Tabla 4**). Mutaciones en los genes mostrados en la tabla D son responsables del desarrollo de 7 cuadros clínicos donde se presenta HTA monogénica:

- Exceso aparente de mineralocorticoides (EAM)
- Síndrome de Geller o HTA exacerbada en el embarazo (SG)
- Resistencia a glucocorticoides familiar (RGF)
- Aldosteronismo remediable con glucocorticoides (ARG)
- Hiperplasia adrenal congenita (HAC)
- Síndrome de Liddle (SL)

- Síndrome de Gordon o Pseudohipoaldosteronismo tipo II (PHAII)

Símbolo del gene	Localización cromosómica	Codifica para	Enfermedad con hipertensión monogénica	OMIM
HSD11B2	16q22	11-β- hidroxiesteroide deshidrogenasa tipo 2	Exceso aparente de mineralocorticoides	+218030
NR3C2	4q31.1	Receptor de mineralocorticoides	Síndrome de Geller HTA exacerbada en el embarazo	#605115
NR3C1	5q31.3	Receptor de glucocorticoides	Síndrome de resistencia a glucocorticoides	+138040
CYP11B2	8q21-q22	18-hidroxilasa (Aldosterona sintasa)	Aldosteronismo remediable con glucocorticoides	#103900
CYP11B1	8q21	11-β- hidroxilasa	Hiperplasia adrenal congénita por deficiencia de 11-β-hidroxilasa	#202010
CYP17A1	10q24.3	17-α-hidroxilasa	Hiperplasia adrenal congénita por deficiencia de 17-α-hidroxilasa	#202110
SCNN1B	16p12.2-p12.1	Subunidad β de ENaC	Síndrome de Liddle OMIM #17720	*600760
SCNN1G	16p12	Subunidad γ de ENaC		*600761
WNK1	12p13.3	Serina treonina cinasa WNK1	Síndrome de Gordon c Pseudohipoaldosteronimo tipo 2c	*605232
WNK4	17q21-q22	Serina treonina cinasa WNK4	Síndrome de Gordon b Pseudohipoaldosteronimo tipo 2b	*601844
desconocido	1q31-q42	desconocido	Síndrome de Gordon a Pseudohipoaldosteronimo tipo 2a	inexistente

Tabla 4. Genes responsbles del desarrollo de enfermedades con HTA monogénica.

Exceso aparente de mineralocorticoides (EAM) OMIM +218030

Es una enfermedad autosómica recesiva que cursa con HTA e hipokalemia (bajos niveles séricos de K^+ <3.5 mmol/L) debido a mutaciones del tipo de perdida de función en el gen HSD11B2 que codifica para una enzima, expresada en riñón específicamente en los segmentos de la nefrona donde la aldosterona lleva a cabo sus funciones, conocida como 11-β-hydroxiesteroide deshidrogenasa tipo 2 (11-βHSD2). Como se describirá en los siguientes parrafos, las mutaciones en 11-βHSD2 resultan en la activación del RM por ligandos no fisiológicos como el cortisol (**Fig. 14**).

Uno de los enigmas más grandes en la fisiología renal se presentó después de clonar a nivel molecular el RM y encontrar que el cortisol y la aldosterona poseen la misma afinidad hacia dicho receptor nuclear (94). Dado que las concentraciones plasmáticas de cortisol se encuentran muy por encima de las de aldosterona, resultaba intrigante comprender la especificidad, si es que existía, del efecto mineralocorticoide del cortisol

y la aldosterona. Hoy entendemos mejor como es que puede ocurrir tal especificidad y se basa en la actividad y expresión de la enzima 11-βHSD2. En condiciones normales, la 11-βHSD2 se encarga de transformar el cortisol circulante en cortisona la cual no posee afinidad para el RM. Con lo anterior se puede prevenir que el cortisol pueda unirse y activar al RM en los segmentos de la nefrona donde la aldosterona lleva a cabo sus funciones (TD y TC de la nefrona) (95).

En pacientes con EAM, debido a su imposibilidad para convertir el cortisol a cortisona, se presentan efectos similares a los que ocurren cuando se incrementa la producción de aldosterona y la activación del RM (elevación en los niveles de reabsorción de H_2O y Na^+ y aumento en los niveles de secreción de K^+ en la parte distal de la nefrona) y por lo tanto HTA e hipokalemia (**Fig. 14)**.

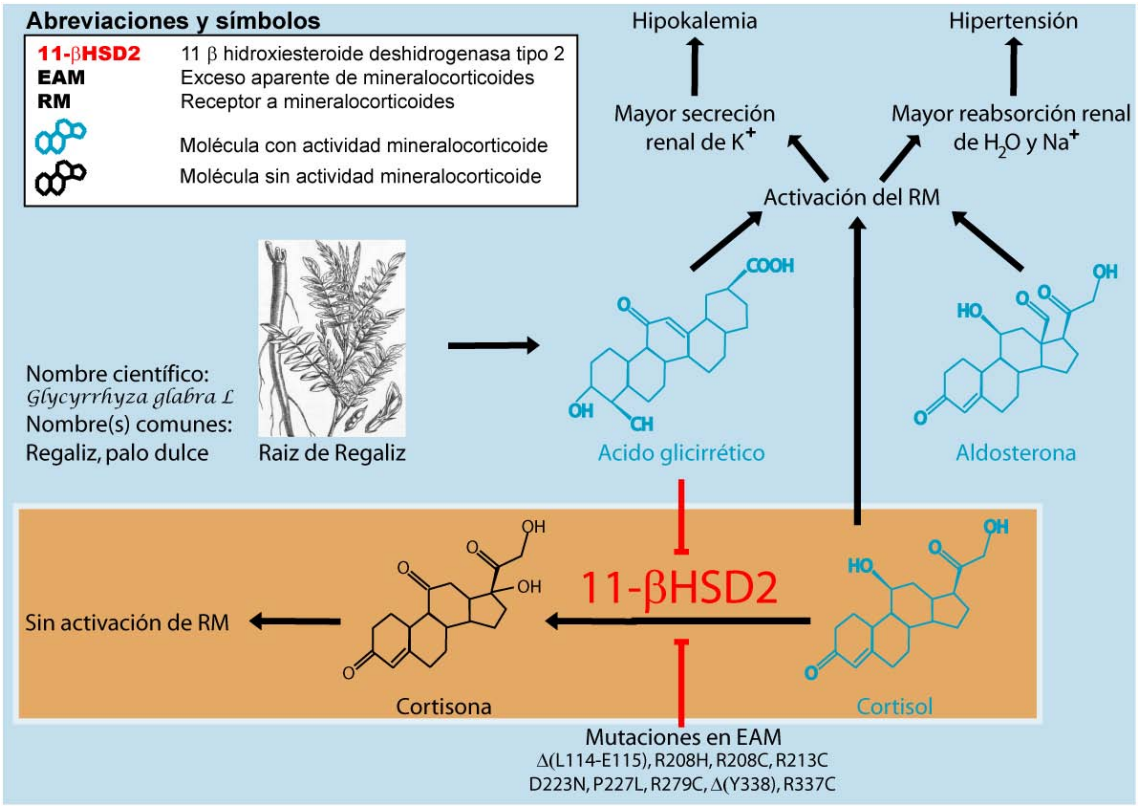

Figura 14. Mecanismo molecular responsable del desarrollo de EAM.

De manera interesante, la ingesta excesiva y crónica de productos fabricados (infusiones, gomas de mascar, caramelos) a partir de extractos de la raiz de la planta *Glycyrrhyza glabra*, también conocida como regaliz, puede resultar en la fenocopia de EAM y por lo tanto el desarrollo de HTA e hipokalemia debido a dos razones

principalmenente: a) uno de los componentes de la raiz del regaliz es una molécula conocida como ácido glicirrético, potente inhibidor de la enzima 11-βHSD2, que impide la transformación de cortisol a cortisona y b) el propio ácido glicirrético posee actividad mineralocorticoide y puede promover la activación del RM y por tanto la secreción de K^+ y reabsorción renal de Na^+ y H_2O, elevando los niveles de P_s (**Fig. 14**).

Síndrome de Geller (SG) OMIM #605115

Un desorden similar al AME, pero con herencia autosómica dominante es el síndrome de Geller (SG). El SG es ocasionado por una mutación localizada en el dominio de unión a ligando localizado en el carboxilo tenrminal del RM (96).

La mutación responsable del desarrollo del SG es del tipo ganancia de la función y consiste en la sustitución del residuo de serina conservado en el RM desde anfibios hasta humanos en la posición 180 por un residuo de leucina (S180L) (96).

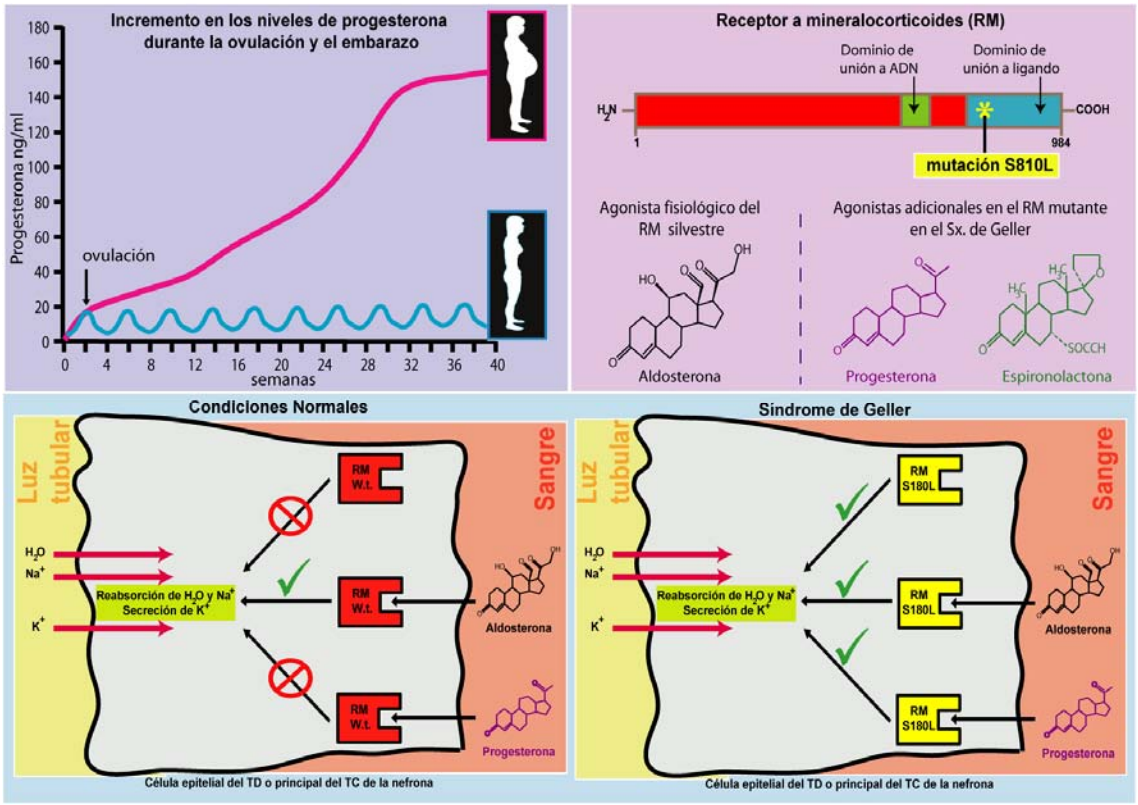

Figura 15. Mecanismo molecular responsable del desarrollo del síndrome de Geller.

Los pacientes con SG cursan con severa HTA e hipokalemia desde muy temprana edad debido a que la mutación S180L en el RM promueve un estado de activación constitutiva del RM que se traduce en un incremento en la secreción de K^+, así como en una elevada reabsorción renal de Na^+ y H_2O en ausencia de aldosterona (**Fig. 15**).

Aunado a lo anterior, la mutación S180L altera la especificidad del RM de tal manera, que potentes antagonistas como la espironolactona o ligandos que en condiciones normales no favorecerían la activación del RM, como la progesterona, se vuelven potentes activadores del RM (**Fig. 15**).

Debido a que durante el embarazo los niveles de progesterona se llegan a incrementar hasta 100 veces con respecto a su valor normal (1), Geller y colaboradores anticiparon de manera correcta que la HTA e hipokalemia en pacientes con la mutación S180L durante el embarazo empeoraría debido a una aberrante activación del RM por progesterona (97) (**Fig. 15**).

Resistencia a los glucocorticoides familiar (RGF) OMIM +138040

Es un desorden genético donde los pacientes presentan insensibilidad parcial o generalizada a los glucocorticoides que se traduce en HTA, alcalosis metabólica (pH sanguíneo mayor a 7.45), fatiga crónica y aumento en los niveles de andrógenos debido a mutaciones en el gen NR3C1 que codifica para el receptor a glucocorticoides (RG) (98). Las mutaciones responsables del desarrollo de RGF son en su mayoría mutaciones puntuales (Val571Ala, Asp641Val, Gly679Ser, Val729Ile, Phe737Leu, Ile747Met, y Leu773Pro) del tipo perdida de la función localizadas en el dominio de unión a ligando del RG, que disminuyen la afinidad de RG por el cortisol y que alteran la retroalimentación negativa a nivel hipotalámico e hipofisario de su síntesis (98).

Como efecto compensador a la insensibilidad o baja respuesta a glucocorticoides, en pacientes con RGF, se promueve mediante la sobreactivación del eje hipotálamo-hipófisis-suprarenal la elevación en los niveles de secreción de la hormona liberadora de corticotropina (CRH) y de la hormona adrenocorticotropa (ACTH) (99).

Con lo anterior, el resultado final es una elevada producción de cortisol, desoxicorticoesterona y corticoesterona, así como en una elevada síntesis de androgenos como A4-androstenediona, dehidropiandrosterona y dehidropiandrosterona-sulfato (99) (**Fig. 16**).

Debido al gran incremento en la síntesis de cortisol y de intermediarios esteroidogénicos con actividad mineralocorticoide como la desoxicorticoesterona y corticoesterona, se supera la capacidad de la enzima 11-βHSD2 y el resultado final es la activación del RM en ausencia de aldosterona y el desarrollo de la enfermedad (**Fig. 16**).

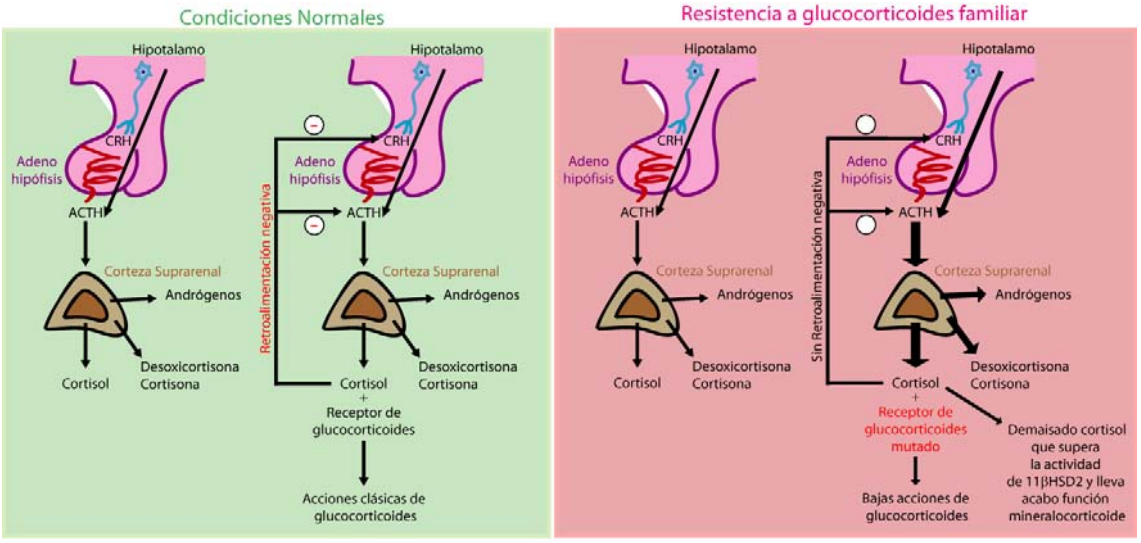

Figura 16. Fisiopatología de la resistencia a a glucocorticoides familiar.

Aldosteronismo remediable con glucocorticoides (ARG) OMIM #103900

Es una desorden genético de herencia autosómica dominante en donde los pacientes a pesar de tener niveles normales o bajos de actividad plasmática de renina, cursan con HTA sensible a Na^+, expansión de volumen y en ocasiones hipokalemia y moderada alcalosis metabólica. Como su nombre lo indica el ARG se puede prevenir completamente mediante la administración exógena de glucocoticoides. Una característica clínica importante en pacientes con ARG es la presencia en orina de grandes cantidades de esteroides con actividad mineralocorticoide (capaces de activar al RM) (100).

El ARG se presenta debido a un entrecuzamiento cromosómico aberrante durante la meiosis celular que resulta en la generación de un gen quimérico entre dos genes áltamente homologos (alrededor de 95% de homología a nivel de secuencia) involucrados en la biosíntesis de mineralocorticoides y localizados *en tandem* en el cromosoma 8 humano. Los genes involucrados en la formación del gen quimérico son: a) el que codifica para la aldosterona sintasa (CYP11B2) y b) el que codifica para la enzima 11β hidroxilasa (CYP11B1) (101-103).

La actividad de la aldosterona sintasa es el paso limitante para la biosíntesis de aldosterona desde la glomerulosa adrenal en respuesta a Angiotensina II, mientras que la actividad de la 11β hidroxilasa es crítica para la biosíntesis del cortisol en la fasciculata adrenal en respuesta a la hormona ACTH.

El gen quimérico resultante consiste en la fusión entre la región promotora del gen para la 11β hidroxilasa y la región codificante para la aldosterona sintasa. En el ARG, gracias a la formación de dicho gen quimérico, la biosíntesis de aldosterona queda bajo el control de los elementos reguladores para la síntesis de glucocorticoides (hormona ACTH) e independiente de los niveles de renina y angiotensina II (101-103) (**Fig. 17**).

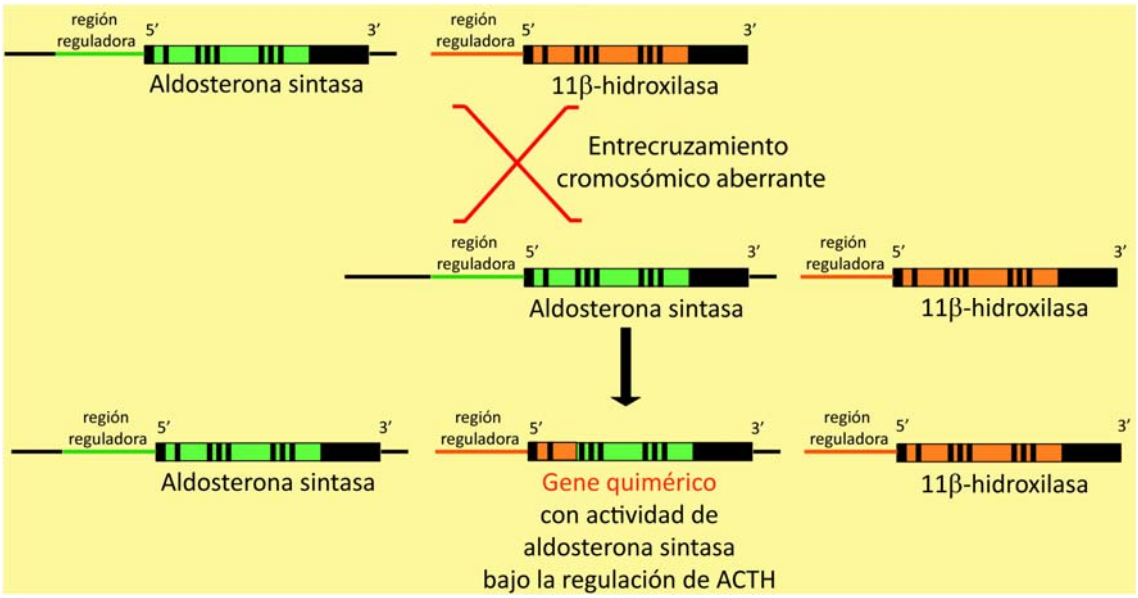

Figura 17. Mecanismo molecular responsable del desarrollo del aldosteronismo remediable con Glucocorticoides.

Hiperplasia adrenal congénita (HAC) por mutaciones en 11β hidroxilasa OMIM #202010 y 17α hidroxilasa OMIM #202110

Son desordenes autosomicos recesivos en los cuales se presentan mutaciones del tipo pérdida de la función en genes involucrados en la síntesis de cortisol y aldosterona. Debido a la presencia de mutaciones en los genes que codifican para la 11β hydroxilasa y la 17α hidroxilasa se altera o interrumpe la síntesis de cortisol resultando en la sobreproducción de ACTH, hiperplasia adrenal y a la acumulación de precursores esteroideos del cortisol con actividad mineralocorticoide los cuales provocarán la activación del RM y el desarrollo de HTA debido a una elevada reabsorción renal de Na^+ y H_2O (104) (**Fig. 18**).

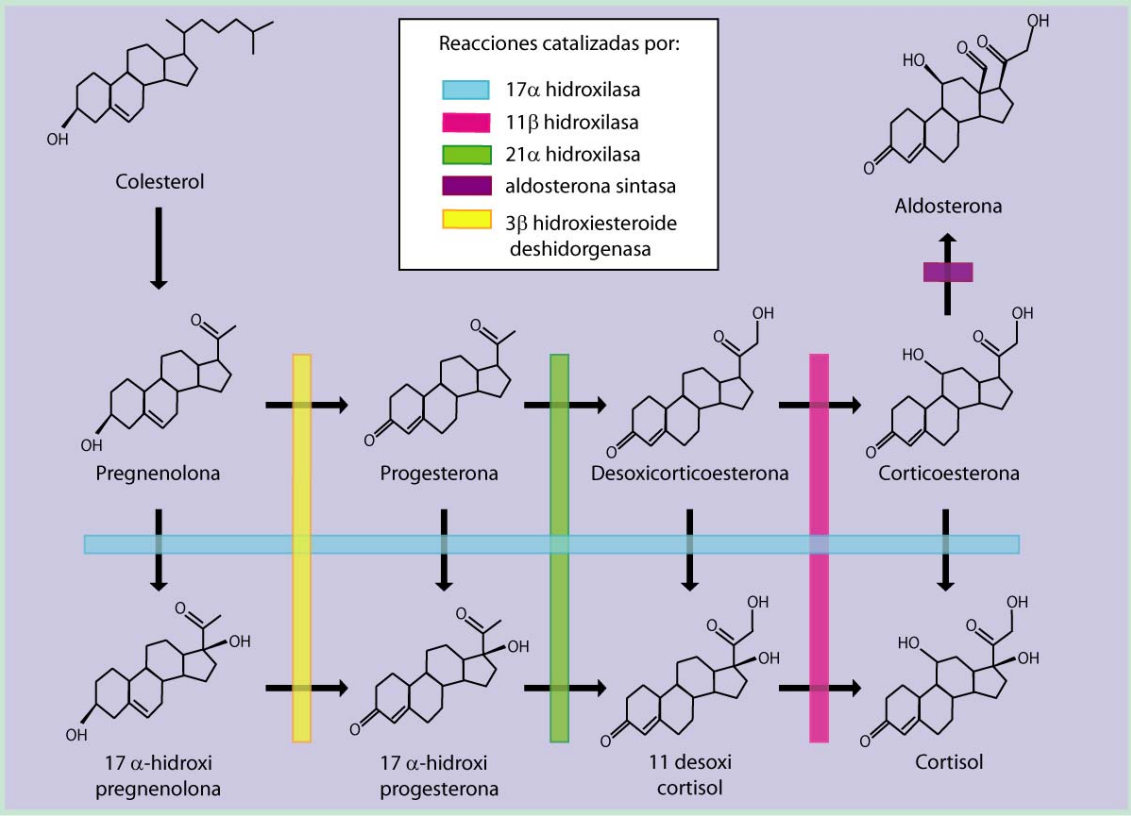

Figura 18. Biosíntesis de cortisol y aldosterona y enzimas involucradas.

Síndrome de Liddle (SL) por mutaciones en α-ENaC, β-ENaC y γ-ENaC

Es una enfermedad autosómica dominante descrita por primera vez en 1960 (105,106), donde los pacientes cursan con HTA, hipokalemia, alcalosis metabólica y bajos niveles

de actividad de renina plasmática y de aldosterona. Se ocasiona por mutaciones en el canal epitelial de sodio ENaC expresado en la membrana apical del TC en la nefrona del riñón (107,108)(1;2) (**Fig. 19**).

ENaC está conformado por 3 subunidades (alfa, beta y gamma) las cuales poseen una estructura similar ya que comparten entre 32-37% de identidad a nivel de secuencia de aminoácidos y están compuestas por dos dominios transmembranales, dos regiones citoplásmicas intracelulares y una gran región extracelular con alto contenido en aminoácidos de cisteina. Se ha propuesto que la forma funcional de ENaC está constituida por dos subunidades alfa, una subunidad beta y una subunidad gamma (109)(3).

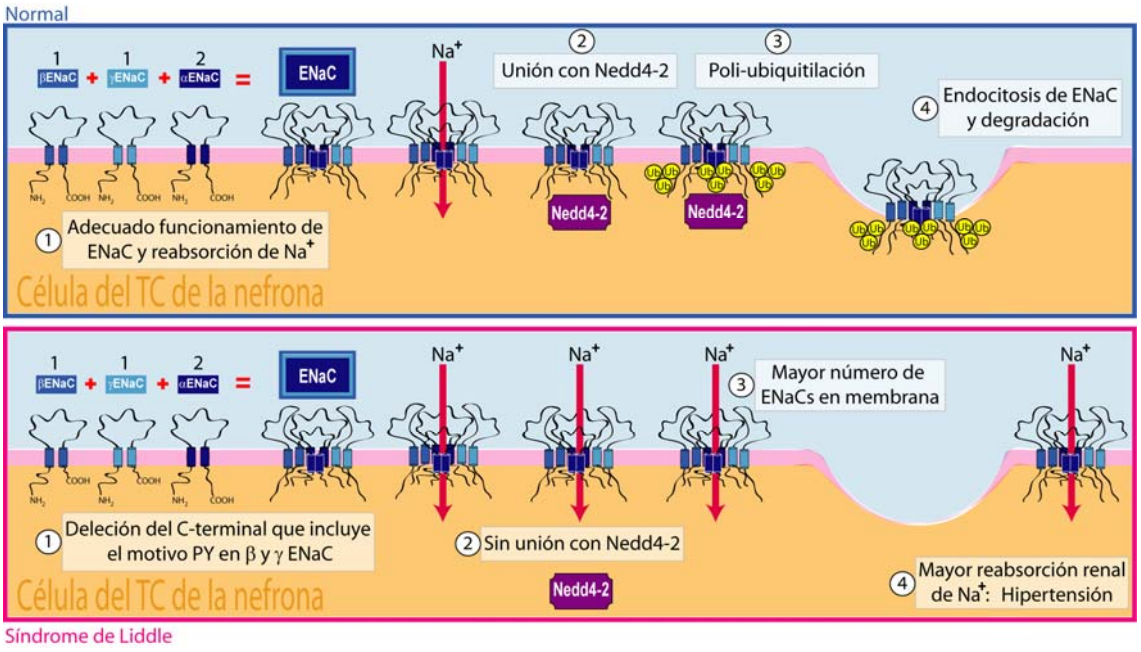

Figura 19. Mecanismo molecular responsable del síndrome de Liddle. (Los círculos con números señalan el orden de eventos).

La subunidad alfa por si sola es capaz de promover el transporte de Na^+ mientras que las subunidades gamma y beta favorecen la actividad de la subunidad alfa. Las primeras mutaciones descritas en ENaC responsables del síndrome de Liddle fueron localizadas en las subunidades gamma y beta y resultaron ser mutaciones que ocasionaban cambios en el marco de lectura o introducían codones de paro en la región carboxilo terminal. Debido a lo anterior, en el Sx. de Liddle las subunidades beta y gamma de ENaC poseen una región carboxilo más corta (45 a 75 aminoácidos menos) (110,111).

A partir del hecho que los pacientes con SL cursan con severa y temprana HTA, se infirió de manera correcta que tales mutaciones favorecerían la reabsorción renal de Na^+. Lo anterior fue corroborado de manera experimental expresando a las subunidades de ENaC con las mutaciones tipo SL en ovocitos de la rana *Xenopus laevis*, donde se observó que la presencia de dichas mutaciones favorecía el transporte de Na^+ debido a una mayor cantidad de canales tipo ENaC presentes en la membrana celular.

Para determinar cuales de los aminoácidos perdidos durante las mutaciones tipo Sx. de Liddle favorecían la actividad de ENaC, se sustituyeron por alanina cada uno de estos residuos y se encontró que la alteración del motivo PY (con secuencia Pro-Pro-Xaa-Tyr) es la causa del desarrollo de dicho síndrome (4)112). Diversos estudios han podido establecer que mediante el motivo PY presente en las subunidades que constituyen a ENaC se puede establecer interacción física con los dominios WW presentes en la E3 ubiquitina ligasa Nedd4-2. Al exisitir mutaciones en elmotivo PY se impide la interacción con Nedd4-2 y de esa manera se previene la poliubiquitilación de ENaC (113). Al no ser blanco de poliubiquitilación, ENaC no puede ser removido de la membrana apical de las células del TC de la nefrona y dirigido a degradación proteosomal o lisosomal por lo que mayor cantidad de canales tipo ENaC permanecen en membrana donde favorecerán la reabsorción renal de Na^+ y el desarrollo de HTA (**Fig. 19**).

Síndrome de Gordon ó pseudohipoaldosteronismo tipo II

Es un desorden autosómico dominante y heterogeneo donde los pacientes cursan con HTA e hiperkalemia, acidosis tubular renal e hipercloremia a pesar de tener niveles de actividad de renina plasmática bajos. Debido a la heterogeneidad genética, el síndrome de Gordon también conocido como pseudohipoaldosteronismo tipo II (PHAII) se puede originar de manera independiente por mutaciones en diferentes genes (114,115)(5;6) (**Tabla 4**).

A la fecha, tres diferentes loci han sido encontrados como responsables del desarrollo de PHAII. El primero se encuentra en 1q31-q42 y es la causa del PHAII clase A (PHAII-A). El segundo locus se encuentra en el gen que codifica para la serina treonina cinasa WNK4 y es el responsable del desarrollo del PHAII clase B (PHAII-B). El tercer locus

es el gen que codifica para la serina treonina cinasa WNK1 y es el responsable de que se presente el PHAII clase C (PHAII-C) (116)(7).

Las mutaciones causantes de PHAII-C se localizan en el cromosoma 12 dentro del primer intron del gen que codifica para WNK1. Dichas mutaciones favorecen un aumento en la expresión de WNK1 (de aproximadamente 5 veces en leucocitos) y consisten en dos grandes deleciones de 21761 ó 41241 pb las cuales eliminan secuencias que reprimen (1 represor y 1 insulator) la expresión transcripcional de WNK1 (116) (**Fig. 20**).

Por otro lado, mutaciones en el cromosoma 17 dentro del gen que codifica para la serina treonina cinasa WNK4 son las causantes PHAII-B. Cuatro mutaciones de manera independiente han sido descritas como causantes del PHAII-B y son: Glu562Lys, Asp564Ala, Gln565Glu y Arg1186Cys (116) (**Fig. 20**).

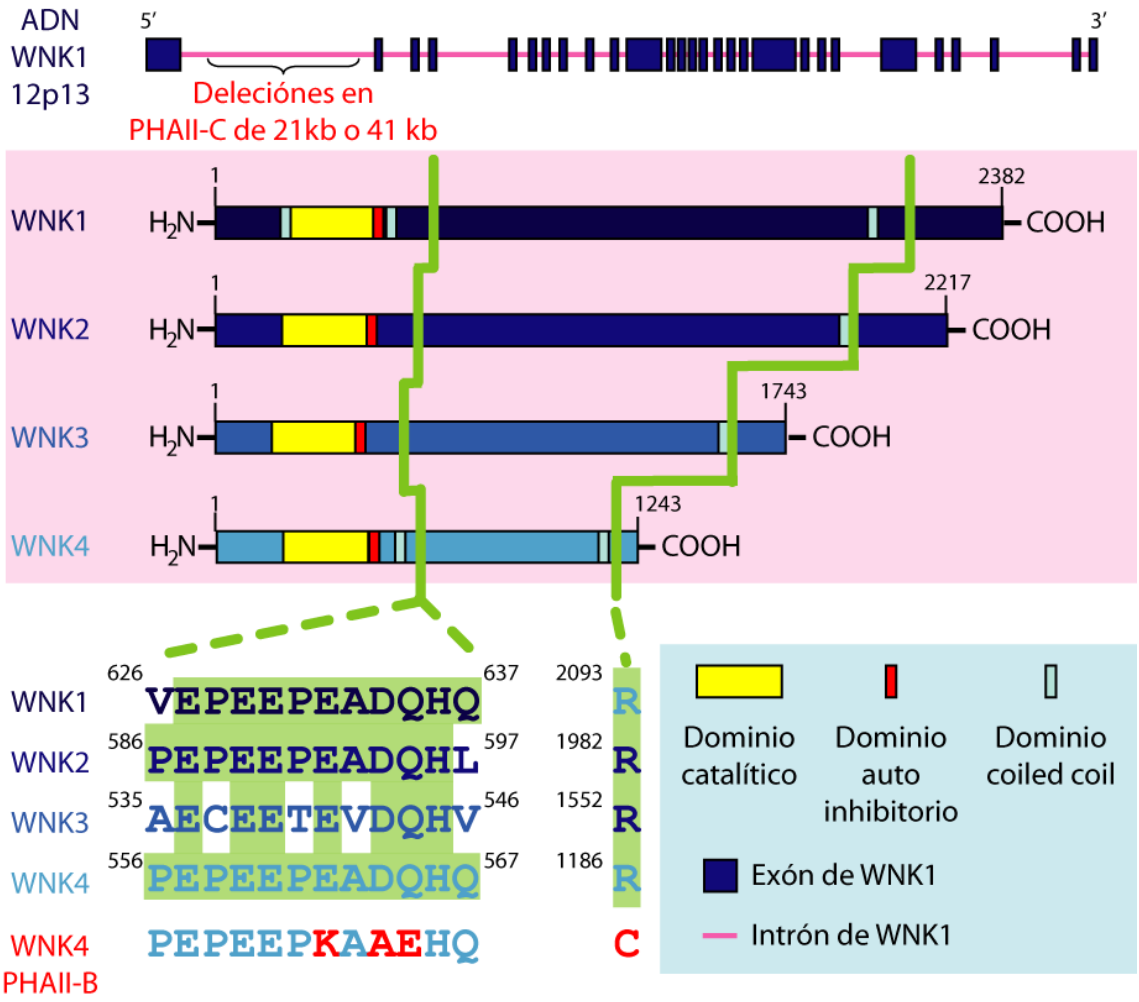

Figura 20. Familia de las cinasas WNK y mutaciones en PHAII-B y PHAII-C.

Todas las mutaciones causantes del PHAII-B se localizan en regiones ampliamente conservadas entre los demás miembros de la familia de cinasas tipo WNK. De manera interesante, las primeras 3 mutaciones (Glu562Lys, Asp564Ala, Gln565Glu) involucran cambios por aminoácidos con carga eléctrica distinta al aminoácido presente en individuos sanos. Dichos cambios se localizan fuera del dominio catalítico de la WNK4 y río abajo del primer dominio de interacción (coiled coil) presente en la región amino terminal de dicha cinasa, mientras que la cuarta mutación (Arg1185C) se localiza río abajo del segundo dominio de interacción coiled coil (116,117) (**Fig. 20**).

Gracias al creciente número de trabajos científicos destinados a comprender el desarrollo y causas del PHAII, hoy sabemos que el cuadro clínico en PHAII se debe principalmente a incrementos en los niveles de reabsorción renal de Na^+ a lo largo la nefrona distal. De manera muy importante en pacientes con PHAII parece destacar la sobreactivación de NCC ya que el fenotipo de pacientes con PHAII se corrije en su totalidad mediante el empleo de diuréticos tipo tiazida (inhibidores específicos de NCC). El aumento en los niveles de reabsorción de Na^+ en el TD ocasiona que menos cantidad de Na^+ llegue a regiones más distales de la nefrona donde se lleva a cabo el intercambio de Na^+ por H^+ y K^+. Debido a lo anterior se excreta menos H^+ y K^+ y los pacientes con PHAII cursan con acidosis tubular hiperkalémica.

Aunque incrementos en la actividad de NCC son clave para el desarrollo de PHAII, en estos pacientes tambien parece estar afectada la actividad de: ENaC en el TC de la nefrona (118), ROMK (119), las claudinas 4 y 7 (proteínas expresadas en las uniones estrechas de las células en la nefrona distal involucradas en el transporte paracelular de Cl^-) (120,121), los canales de Ca^{++} TRPV4 y TRPV5 (122,123) y la actividad de las serina treonina cinasas SPAK y OSR1 las cuales a su vez modularán la actividad de diversas proteínas citoplásmicas y de transpote (124) (ver más adelante).Todas las modificaciones en la actividad de las proteínas mencionadas se presentan porque WNK1 y WNK4 han probado ser importantes reguladores de sus acciones.

Debido a lo anterior, el mecanismo molecular detrás del desarrollo de PHAII es complejo y parece involucrar alteraciones en la homeostasis y manejo de diversos iones en la nefrona del riñón. En los siguientes parrafos nos enfocaremos a describir las modificaciones presentes en PHAII sobre el manejo de K^+ y Na^+ que se encuentran ligadas al desarrollo de HTA e hiperkalemia.

WNK1 y WNK4 se expresan de manera importante a lo largo de la nefrona distal donde NCC lleva a cabo sus funciones. La expresión de WNK1 es citoplasmática, mientras que la de WNK4 además de ser citoplasmática, se presenta en las uniones celulares estrechas (125). WNK1 posee diversas isoformas debido a empalme alternativo dentro de las que se encuentran: una larga (L-WNK1) y una corta (KS-WNK1) ausente de dominio catalítico y expresada en la nefrona distal. L-WNK1 se expresa de manera ubicua y se encuentra involucrada en la respuesta a estrés osmótico mientras que KS-WNK1 se expresa específicamente en riñón y parece estar involucrada en la señalización y respuesta a aldosterona.

En terminos generales, WNK4 regula la actividad de diversas proteinas de transporte mediante diferentes mecanismos celulares, que en ocasiones dependen (NCC, ENaC) y en otras no (Claudina 4-7 y ROMK) de su actividad catalítica. En la mayoría de los casos WNK4 modula la cantidad de proteína presente en la membrana celular y el efecto ejercido por la cinasa WNK4 es prevenido por la L-WNK1, cuyas acciones a su vez son inhibidas por KS-WNK1. Al menos durante la regulación ejercida sobre ROMK, para que KS-WNK1 antagonize las acciones de L-WNK1 quie a su vez inhibe a WNK4 se requieren de: a) sus primeros 30 aminoacidos los cuales son únicos (no se encuentran presentes en L-WNK1) y son codificados por el exon 4a y/ó b) la región que correspondería al dominio autoinhibitorio de L-WNK1 (119).

El mecanismo por el cual un incremento en los niveles de L-WNK1 conduce al desarrollo de hiperkalemia en PHAII-C es el siguiente: L-WNK1 es un potente inhibidor de la actividad de ROMK. En pacientes con PHAII-C al existir elevados niveles de L-WNK1 se promueve la internalización y degradación de ROMK y por lo tanto una severa disminución en los niveles de secreción de K^+ (**Fig. 21**).

El mecanismo por el cual un incremento en los niveles de L-WNK1 conduce al desarrollo de HTA en PHAII-C es el siguiente: L-WNK1 es un regulador negativo sobre la actividad de WNK4 quien a su vez es un inhibor de NCC y ENaC. Al elevarse los niveles de expresión de L-WNK1, se pierde la regulación negativa de WNK4 sobre la reabsorción de Na^+ en la parte distal de la nefrona y con ello el desarrollo de HTA (126) (**Fig. 21**). Consistente con el importante papel de WNK1 para modular la actividad de los niveles de Ps, se ha encontrado que polimorfismos en el gen que cofidica para WNK1 se encuentran asociados a variaciones en los niveles de P_s (127,128) y ratones

knockout heterocigotos para WNK1 ($WNK1^{-}/+$) (con bajos niveles de WNK1) presentan hipotensión arterial (129). De manera similar, mediante análisis de enlace génico en la población de Framingham, un segmento del cromosoma 17 que contiene al gen que codifica para WNK4, fue identificado como positivo para enlace con HTA (130). Un polimorfismo G/A en el intron 10 de WNK4 se encontró presente en el 13% de pacientes caucásicos hipertensos contra un 7% de presencia en pacientes caucásicos normotensos (131). En un estudio de cohorte en una población japonesa de 956 pacientes hipertensos o con falla renal, se pudieron identificar tres mutaciones (Met546Val, Pro556Thr y Pro1173Thr) en 5 pacientes dentro de la región codificante de WNK4 (132).

El mecanismo por el cual mutaciones en WNK1 conducen al desarrollo de PHAII-C es el siguiente: En condiciones normales se ha encontrado que KS-WNK1 previene la actividad de L-WNK1. En el PHAII-C al existir una elevada expresión de L-WNK1, no existe suficiente KS-WNK1 que controle a L-WNK1. Por lo tanto, se interrumpe la inhibición de WNK4 ejercida sobre NCC y ENaC, lo que resulta en un incremento en la cantidad de proteína de NCC y ENaC y por lo tanto, una mayor reabsorción renal de Na^{+}. El mecanismo por el cual mutaciones en WNK4 conducen al desarrollo de PHAII-B es menos comprendido. Lo que se ha podido establecer, principalmente mediante ensayos de expresión funcional heterologa usando ovocitos de la rana *Xenopus laevis*, es que la inhibición de WNK4 sobre NCC requiere de la actividad catalítica de WNK4. No obstante, las mutaciones tipo PHA-II en WNK4 no alteran la actividad catalítica de la cinasa, por lo que probablemente dos o más mecanismos para la regulación de NCC mediada por WNK4 pudiesen existir. Recientemente se ha encontrado que WNK4 favorece la degradación lisosomal de NCC a través de la proteasa leupetina (133) y mediante las acciones de una proteína conocida como sortilina (134,135) (**Fig. 21**).

Con respecto a ROMK, en condiciones normales WNK4 regula de manera negativa la cantidad de ROMK en la membrana y su actividad. Para la inhibición de ROMK mediada por WNK4 no se requiere de la presencia de la actividad catalítica de WNK4 y de manera muy interesante mutaciones tipo PHAII en WNK4 potencían el efecto inhibidor sobre ROMK y por lo tanto una menor secreción de K^{+} y el desarrollo de hiperkalemia (**Fig. 21**).

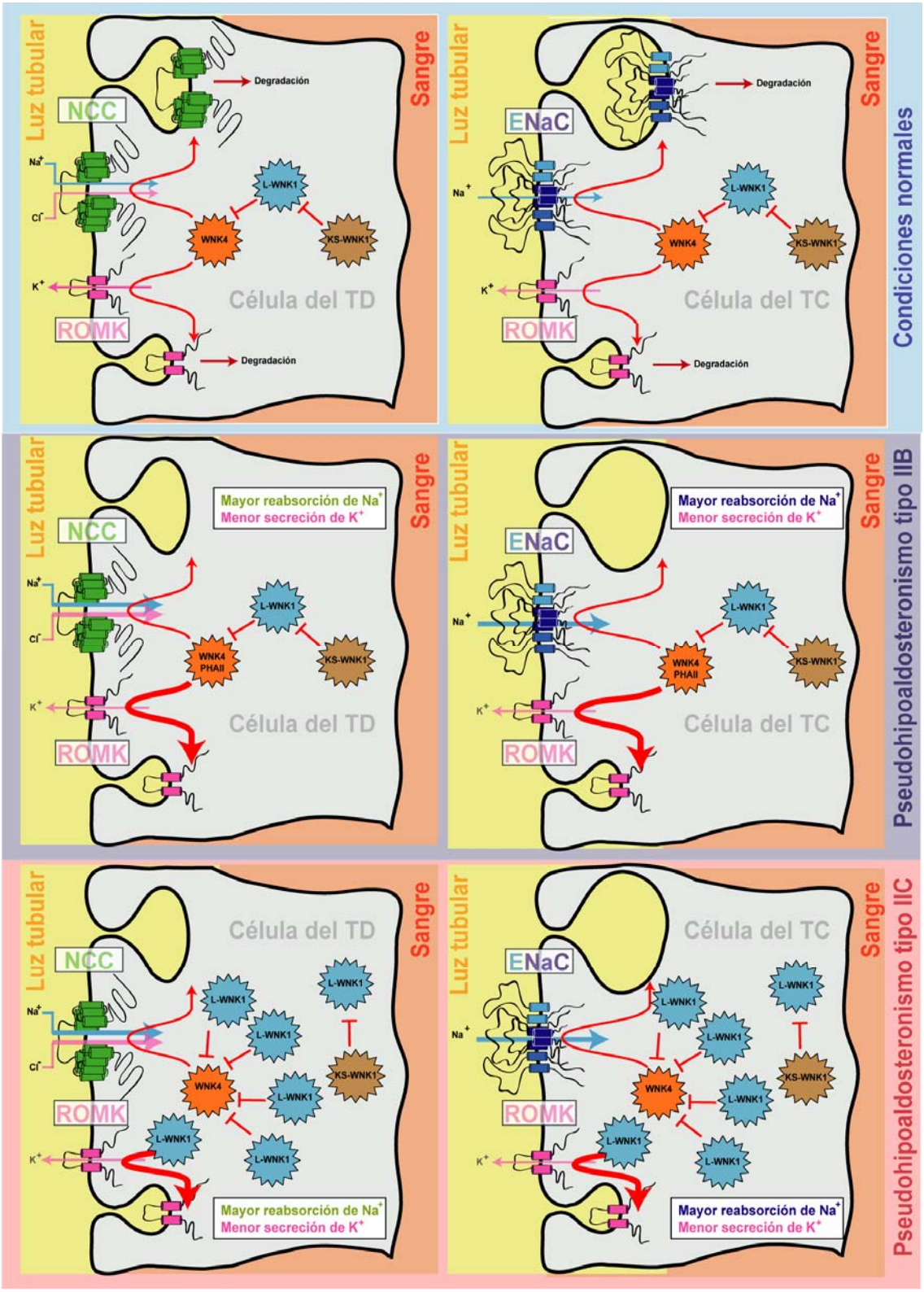

Figura 21. Familia de las cinasas WNK y mutaciones en PHAII-B y PHAII-C.

Evidencias adicionales que confirman que la patogénesis de pacientes con PHAII se debe principalmente a un incremento en la actividad de NCC y reabsorción de Na^+ en el TD se encuentran: a) en modelos experimentales utilizando ratones transgénicos, la

sobrexpresión de WNK4 silvestre resulta en hipotensión e hipokalemia (similar a lo que ocurre en el Síndrome de Gitelman), mientras que la sobrexpresión de WNK4 con mtuaciones PHAII (WNK4-PHAII) resulta en hipertensión e hiperkalemia (similar a lo que se presenta en Síndrome de Gordon), d) la HTA e hiperkalemia desaparecen en la progenie de la cruza entre ratones que sobrexpresan a WNK4-PHAII con aquellos que carecen de la expresión de NCC (ratones KO-NCC) (136).

Formas monogénicas de hipotensión arterial

Así como existen mutaciones en genes que desencadenan el desarrollo de HTA, se han encontrado mutaciones cuyo resultado es el contrario y consiste en una disminución drástica de los niveles de P_s asociada a alteraciones en los niveles de reabsorción renal de Na^+. Consistente con lo discutido anteriormente, aquellas mutaciones que en este caso desfavorezcan la reabsorción renal de Na^+ son responsables de disminuciones en los niveles de la P_s. A la fecha 12 genes han sido encontrados como blancos para el desarrollo de hipotensión arterial monogénica (**Tabla 5**).

Símbolo del gene	Localización cromosómica	Codifica para	Enfermedad con hipotensión monogénica	OMIM
CYP11B2	8q21-q22	18-hidroxilasa (Aldosterona sintasa)	Deficiencia de aldosterona sintasa tipo 1	#203400
CYP21A2	6p21.3	21-hidroxilasa	Hiperplasia adrenal congenita por deficiencia de 21-hidroxilasa	+201910
SCNN1A	12p13	Subunidad α de ENaC	Pseudohipoaldosteronismo tipo 1 (autosómico recesivo) OMIM #264350	*600228
SCNN1B	16p12.2-p12.1	Subunidad β de ENaC		*600760
SCNN1G	16p12	Subunidad γ de ENaC		*600761
NR3C2	4q31.1	Receptor de mineralocorticoides	Pseudohipoaldosteronismo tipo 1 (autosómico dominante)	#177735
SLC12A3	16q13	Cotransportador apical de Na^+Cl^- (NCC)	Síndrome de Gitelman	#263800
SLC12A1	15q15-q21.1	Cotransportador apical de $Na^+K^+2Cl^-$ (NKCC2)	Síndrome de Bartter tipo 1	#601678
KCNJ1	11q24	Canal apical de K^+(ROMK)	Síndrome de Bartter tipo 2	#241200
CLCNKB	1p36	Canal basolateral de Cl^- (CLC-Kb)	Síndrome de Bartter tipo 3	#607364
BSND	1p32.1	Barttina	Síndrome de Bartter tipo 4a	#602522
CASR	3q13-q21	Sensor de Ca^{++}	Síndrome de Bartter tipo 5	+601199

Tabla 5. Desordenes monogénicos con hipotensión arterial.

Deficiencia de aldosterona sintasa (OMIM #203400)

El síndrome de deficiencia de la aldosterona síntasa (DAS), es un desorden autosómico recesivo con características clínicas opuestas a las presentes en el ARG que se ocasiona por mutaciones inactivantes en el gen CYP11B2, el cual codifica para la aldosterona sintasa. La aldosterona sintasa es una enzima que se encarga del último paso en la vía biosíntetica de la aldosterona, donde cataliza la transformación de la corticoesterona en aldosterona en la glomerulosa adrenal. Las mutaciones reportadas como responsables del desarrollo de DAS comprenden desde deleciones de 1 a 5 nucleótidos que resultan en la generación de un codón de paro y la completa ausencia de actividad en la aldosterona sintasa, hasta sustituciones puntuales como Arg181Trp en el exón 3 y Val386Ala en el exón 7 que de igual manera abaten la actividad de dicha enzima (137).

En pacientes con DAS se ve comprometida la biosíntesis de aldosterona y por lo tanto el SRAA no puede llevar a cabo sus funciones y se presentan elevados niveles de actividad de renina plasmática y elevados niveles de la molécula precursora de aldosterona, la corticoesterona (138).

Debido a la ausencia de aldosterona, no se puede promover la adecuada reabsorción de Na^+ y la secreción de K^+ en la parte distal de la nefrona y los pacientes con este síndrome cursan con una severa pérdida renal de Na^+, hipotensión arterial, hiperkalemia y alcalosis metabólica (137,138).

Hiperplasia adrenal congénita por deficiencia de 21-hidroxilasa OMIM +201910

Mutaciones del tipo perdida de la función en el cromosoma 6 dentro del gen CYP21 que codifica para la enzima 21-hidroxilasa son las responsables de aproximadamente el 90% de los casos de HAC. Pacientes con HAC por deficiencia de 21-hidroxilasa cursan con diversas alteraciones entre las que destacan severa hipotensión y virilización.

La actividad de la enzima 21-hidroxilasa es crítica para la biosíntesis del glucocorticoides y mineralocorticoides. Cuando se pierde o disminuye la actividad de la 21-hidroxilasa no existe la adecuada síntesis de aldosterona y cortisol. Al no existir adecuadas concentraciones de mineralocorticoides y corsticoesteroides se promueve la

secreción de ACTH, lo cual desencadena la hiperplasia de las grandulas adrenales (**Fig. 28**).

En pacientes con HAC por deficiencia de 21-hidroxilasa debido a la disminución en los niveles de aldosterona, no existe el adecuado manejo de Na^+ y K^+ en la parte distal de la nefrona. A su vez, la acumulación de precursores de hormonas sexuales ocasiona indiferenciacion sexual o virilización.

El tratamiento para la hiperplasia adrenal congenita por deficiencia de 21-hidroxilasa consiste en la administración de corticoesteroides y mineralocorticoides los cuales revierten los procesos de virilización, pérdida renal de Na^+ e hipotensión.

Pseudohipoaldosteronismo tipo I (PHAI)

El síndrome conocido como pseudohipoaldosteronismo tipo I (PHAI) es un desorden genético donde los pacientes cursan con características clínicas recíprocas a las observadas en el SL. Pacientes con PHAI presentan severa hipotensión arterial al nacer debido a la perdida renal de Na^+, alcalosis metabólica e hiperkalemia a pesar de presentar elevados niveles de actividad plasmática de renina y aldosterona. Fuertes candidatos para el desarrollo de PHAI, una enfermedad con características clínicas contrarias al SL, serían evidentemente los genes que codifican para ENaC o bien aquellos cuyos productos modulen la actividad de ENaC. Lo anterior fue comprobado y hoy sabemos que el PHAI es una enfermedad que se presenta principalmente debido a disminuciones en la actividad de ENaC a lo largo del TC de la nefrona.

El PHAI es un desorden que puede presentar herencia autosómica dominante (PHAI-ad) ó autosómica recesiva (PHAI-ar). En el caso del PHAI-ad lo que ocasiona la enfermedad son mutaciones del tipo pérdida de la función en el cromosoma 4 dentro del gen NR3C2 que codifica para el RM. Al abatirse la actividad del RM, las acciones de la aldosterona en la parte distal de la nefrona para activar a NCC, ROMK y ENaC se interrumpen y los pacientes cursan con severa hipotensión arterial e hiperkalemia a pesar de presentar elevados niveles de aldosterona.

El desarrollo del PHAI-ar se debe a mutaciones del tipo pérdida de la función en los genes que codifican para las subunidades alfa beta y gamma que constituyen a ENaC (139). Al disminuir la actividad de ENaC, no existe una adecuada reabsorción de Na^+ en el TC de la nefrona y los pacientes desarrollan hipotensión arterial, alcalosis metabólica e hiperkalemia.

Síndrome de Gitelman OMIM #263800

Es un desorden autosómico recesivo con características clínicas recíprocas a las presentes en el PHAII. El síndrome de Gitelman se encuentra asociado a hipotensión arterial, alcalosis metabólica, hipokalemia, hipocalciuria e hipermagnesuria. Esta enfermedad se ocasiona por la presencia de mutaciones del tipo pérdida de la función en el cromosoma humano 16 dentro del gen SLC12A3 el cual codifica para el cotransportador de Na^+/Cl^- conocido como NCC. Este cotransportador se expresa en la membrana apical del TD de la nefrona donde actúa como el principal responsable de la reabsorción transcelular de Na^+ y como blanco farmacológico de los diuréticos tipo tiazida.

En pacientes con síndrome de Gitelman, las disminuciones en la actividad de NCC resultan en severa deshidratación, pérdida renal de Na^+ e hipotensión arterial. Al no reabsorberse Na^+ de manera adecuada a lo largo del TD, mayor cantidad de Na^+ llega al TC donde se promueve su intercambio por H^+ y K^+ resultando en alcalosis metabólica hipokalémica.

Recientemente mediante elegantes estudios utilizando ratones knockout para NCC se ha aclarado la visión por la que se explica el desarrollo de hipocalciuria en el Síndrome de Gitelman (140). Al parecer la disminución en los niveles de excreción de Ca^{++} se debe a un incremento en la reabsorción de este ión a lo largo del TP de la nefrona. El desarrollo de la hipermagnesuria en pacientes con síndrome de Gitelman es poco comprendido. Lo que se ha podido establecer es que en ratones knockout para NCC o en aquellos tratados con tiazidas se promueve la inhibición de la expresión del canal epitelial de Mg^{++} conocido como TRPM6 el cual se encarga de la reabsorción de este catión a lo largo del TD de la nefrona. El mecanismo por el cual se promueve la inhibición de TRPM6 no ha sido establecido (140).

Reabsorción de $Na^{\pm}$ en la rama ascendete gruesa del asa de Henle

NKCC2 juega un papel muy importante en la reabsorción de Na^+ en la RAGAH (141), dicha reabsorción de Na^+ en este segmento de la nefrona impermeable al H_2O es crítica y necesaria para: a) la generación de un IMH requerido durante el proceso de concentración urinaria (8)142), b) el adecuado manejo ácido base (9;10)143,144) y c) la reabsorción paracelular de Na^+ y cationes divalentes como el Mg^{++} y el Ca^{++} (27;145,146).

El movimiento de Na^+ a través de la membrana apical de las células de la RAGAH mediado por NKCC2 es electroneutro debido a la simultanea reabsorción de un ion K^+ y de dos iones de Cl^-. Debido al cotransporte de Na^+ con K^+ y Cl^-, el manejo de K^+ y Cl^- a lo largo de la RAGAH se encuentra íntimamente ligado a una correcta reabsorción de Na^+ por NKCC2 (147).

En condiciones normales el K^+ reabsorbido por NKCC2 requiere ser recirculado hacia la luz tubular por medio del canal apical de K^+, conocido como ROMK, para continuar con la reabsorción de Na^+ por una razón muy importante: las concentraciones de K^+ (4 mM) en la luz tubular son menores que las de Na^+ (56 mM) y si no existese una recirculación de K^+ hacia la luz tubular para mantener constante las concentraciones de K^+, llegaría el momento en donde las concentraciones de K^+ disminuirían tanto que se comprometería el cotransporte de Na^+ (147).

El Cl^- reabsorbido por NKCC2 atravesará la membrana basolateral principalmente mediante dos canales de Cl^- conocidos como CLC-Ka y CLC-Kb, constituidos por una subunidad α y una subunidad β en común conocida como Barttina. El Na^+ por su aparte atravesará la membrana basolateral mediante la bomba Na^+/K^+/ATPasa constituida por las subunidades $\alpha\beta$ y γ (**Fig. 12**)

El transporte transcelular de Na^+ genera un gradiente electroquímico y un voltaje positivo (10 mV) en la luz tubular que favorecerá la reabsorción paracelular de Na^+, Mg^{++} y Ca^{++}, por lo que una adecuada función de NKCC2 es necesaria para la correcta reabsorción y manejo de estos iones (26,145) (**Fig. 18**).

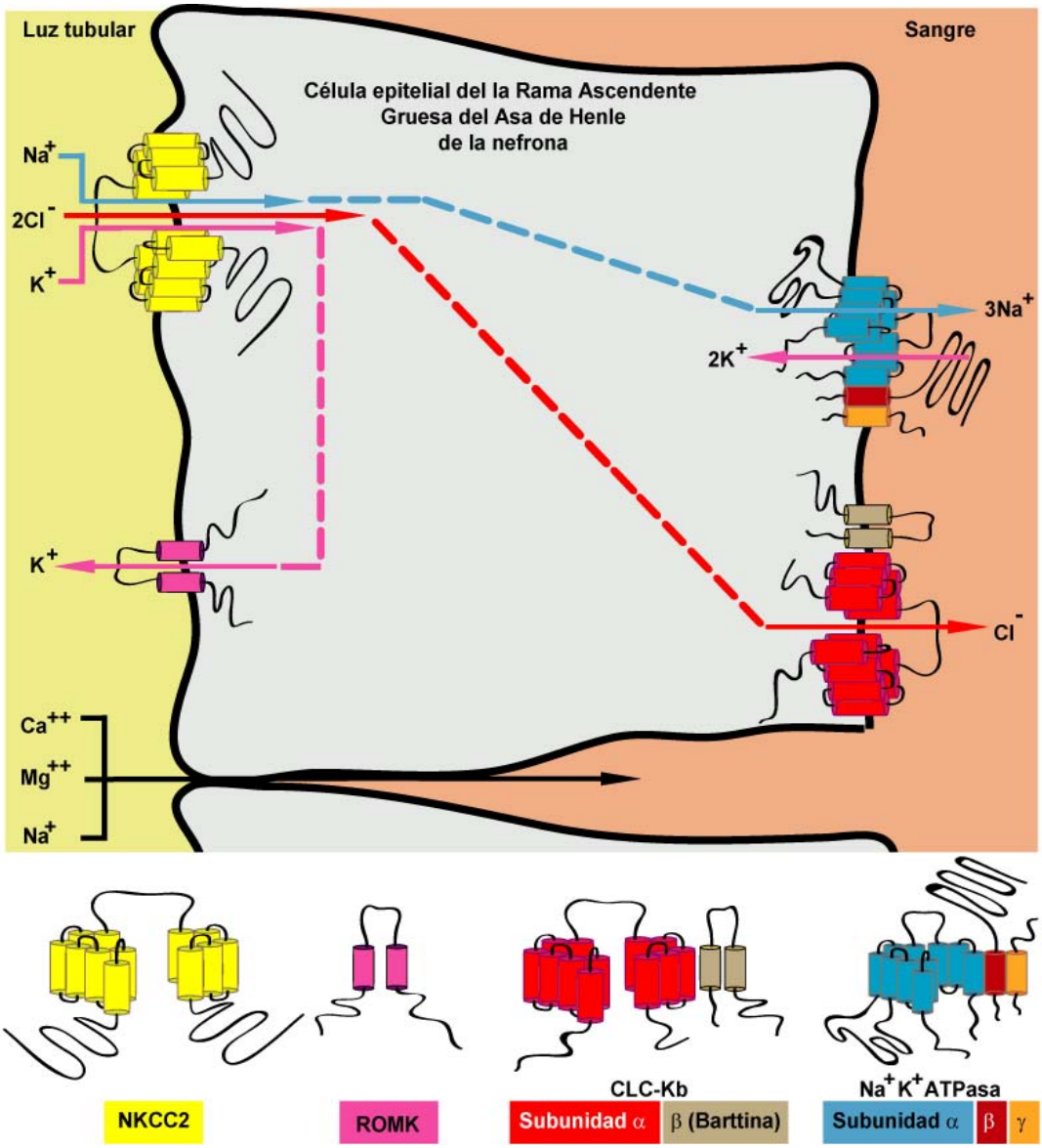

Figura 22. Secreción de K^+ y reabsorción de Na^+, Cl^-, Ca^{++} y Mg^{++} a lo largo de la RAGAH.

NKCC2 y el síndrome de Bartter

El importante papel de NKCC2 en la fisiología renal y en la regulación de los niveles de P_s ha quedado plenamente demostrado por varias razones (147). Una muy importante es la basada en que se han identificado mutaciones inactivantes, la mayoría mutaciones sin sentido, pero también cambios en el marco abierto de lectura por microdeleciones o inserciones en el gen SLC12A1, que codifica para NKCC2, como responsables del síndrome de Bartter tipo I (OMIM #601678) (148-151) (**Fig. 10**).

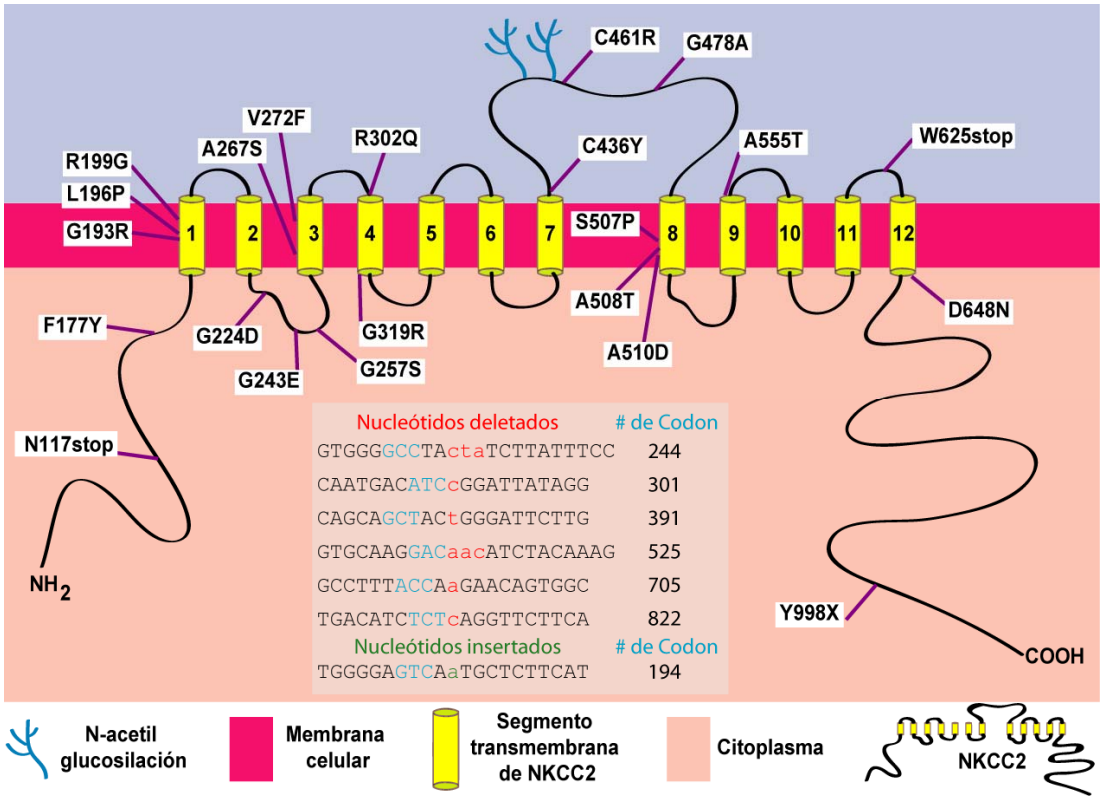

Figura 23. Mutaciones en NKCC2 reportadas como causantes del Sx. de Bartter tipo I.

En los pacientes con síndrome de Bartter tipo I debido a una disminución o perdida de la reabsorción de Na^+ a lo largo de la RAGAH cursan con: a) incapacidad para generar el intersticio medular hiperosmótico que se traduce en poliuria (inhabilidad para concentrar la orina), b) perdida del gradiente electroquímico y del voltaje positivo en la luz tubular, mediado por el transporte transcelular, que impide la reabsorción paracelular de Ca^{++} y resulta en hipercalciuria (Ca^{++} >0.1 mmol/kg/24h en orina), c) normotensión arterial a expensas de la hipertrofia del aparato yuxtaglomerular y la activación del SRAA (hiperrreninemia e hiperaldosteronismo), d) elevación en los niveles de secreción de K^+ que resulta en hipokalemia (niveles séricos de K^+ <3.5mM) e incremento en la secreción de H^+ que se traduce en alcalosis metabólica (pH sanguíneo >7.45) debido a los elevados niveles de aldosterona y sus acciones en la parte distal e la nefrona (152).

Hoy en día sabemos gracias a estudios de enlace génico (genetic linkage) que el síndrome de Bartter, descrito por primera vez en 1962 (153), es una enfermedad monogénica, pero a la vez heterogénea ya que puede resultar de mutaciones en varios

genes cuyos productos participan en la reabsorción de Na^+ a lo largo de la RAGAH. Mutaciones en: a) NKCC2 son responsables del síndrome de Bartter tipo I (148-151), b) ROMK del síndrome de Bartter tipo II (OMIM #241200) (154-161), c) la subunidad α de CLC-Kb del síndrome de Bartter tipo III (OMIM #607364) (162), d) la Barttina o subunidad β de CLC-Kb del síndrome de Bartter tipo IVa (OMIM #602522) (163) y e) en el sensor de Ca^{++} (CaSR) del síndrome de Bartter tipo V (OMIM +601199) (164,165) (**Tabla 6**).

Símbolo del gene	Localización cromosómica	Codifica para	Enfermedad	OMIM
SLC12A1	15q15-q21.1	Cotransportador apical de $Na^+K^+2Cl^-$ (NKCC2)	Síndrome de Bartter tipo 1	#601678
KCNJ1	11q24	Canal apical de K^+(ROMK)	Síndrome de Bartter tipo 2	#241200
CLCNKB	1p36	Canal basolateral de Cl^- (CLC-Kb) subunidad α	Síndrome de Bartter tipo 3	#607364
BSND	1p32.1	(CLC-Kb) subunidad β o Barttina	Síndrome de Bartter tipo 4a	#602522
CASR	3q13-q21	Sensor de Ca^{++}	Síndrome de Bartter tipo 5	+601199

Tabla 6. Genes responsables del desarrollo del síndrome de Bartter.

Todas las mutaciones responsables del síndrome de Bartter disminuirán o detendrán la reabsorción de Na^+ a lo largo de la RAGAH y por lo tanto el desarrollo de poliuria, hiperreninemia, hiperaldosteronismo, hipokalemia, alcalosis metabólica e hipercalciuria (152)(11).

En el síndrome de Bartter tipo I se impide la reabsorción de Na^+ de manera directa al disminuir o abatir la actividad de NKCC2, mientras que en el tipo II se altera la reabsorción de Na^+ de manera indirecta al impedir la recirculación de K^+ a través de mutaciones en ROMK (152,157;166).

Con respecto al Bartter tipo III y IVa, se cree que al afectarse la salida de Cl^- a través de la membrana basolateral de una u otra forma la actividad de NKCC2 y por lo tanto la reabsorción de Na^+ en la RAGAH se disminuye. En el Bartter tipo V a diferencia de los demás tipos de síndromes de Bartter, la herencia es autosómica dominante y se provoca por mutaciones activantes en el CaSR que promueven la inhibición de la actividad de

NKCC2 y ROMK y de esa manera se impide la adecuada reabsorción de Na^+ a lo largo de la RAGAH (152) (**Fig. 24**).

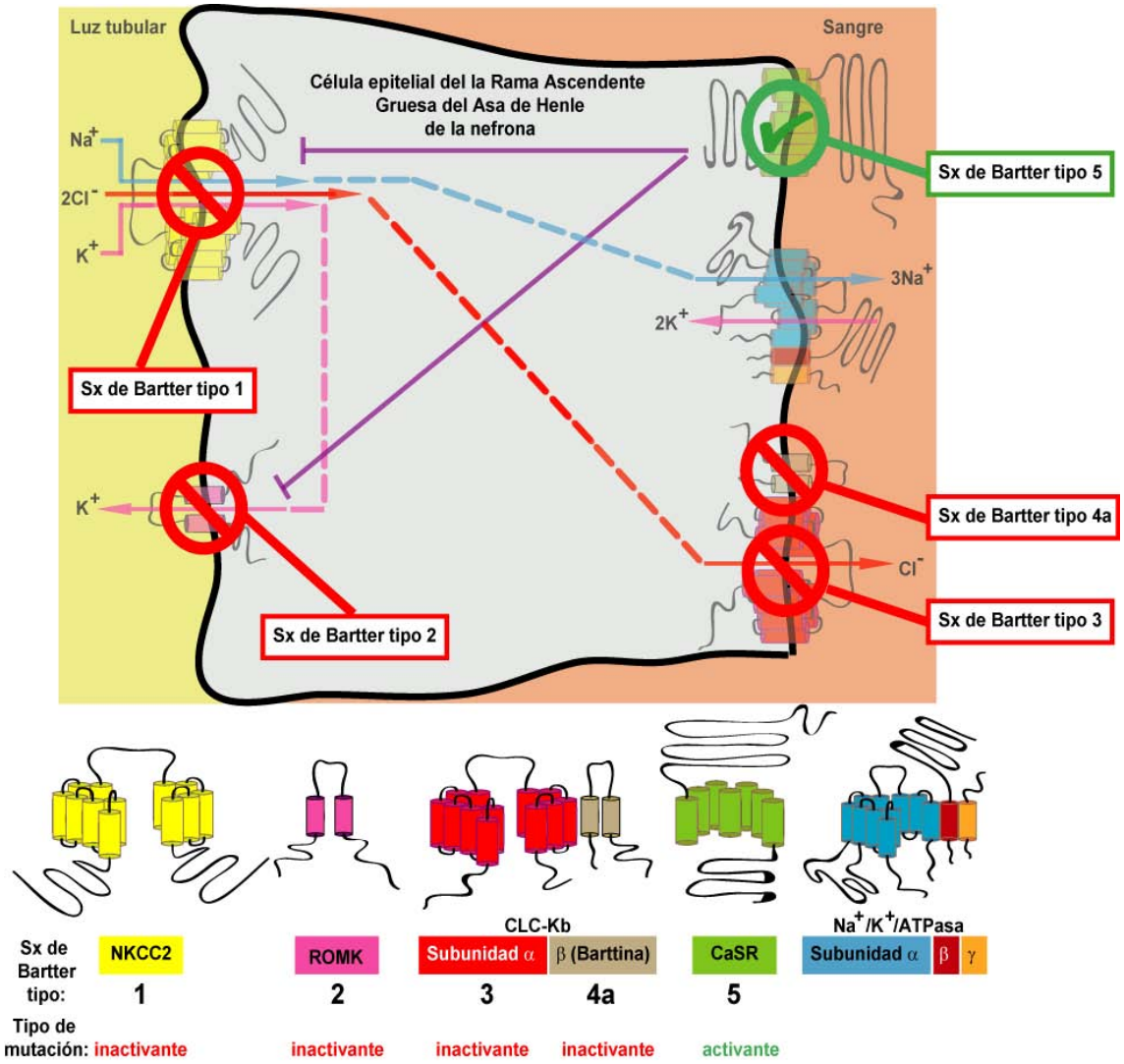

Figura 24. Proteínas involucradas en el desarrollo del síndrome de Bartter.

<u>Diferencias clínicas entre los tipos de síndromes de Bartter</u>

Pacientes que cursan con síndromes de Bartter tipo I y II llegan a presentar las manifestaciones clínicas más severas y notorias ya que dichos pacientes llegan a ser clínicamente aparentes desde el embarazo en forma de polihidramnios (presencia excesiva o aumento de líquido amniótico, por lo general mayor a los 2 litros alrededor del feto antes de que este nazca) (167,168). Pacientes con Bartter tipo III, IV y V llegan a ser clínicamente aparentes en etapas posteriores como durante la infancia o niñez debido a una severa poliuria y deshidratación. Como común denominador, en los

pacientes con síndrome de Bartter, los niveles de P_s van desde bajos (por la severa perdida renal de Na^+) a normales (debido al efecto compensador que consiste en la activación del SRAA) (169). De manera similar, una característica que se comparte entre los síndromes de Bartter y que se origina de igual forma por la hiperreninemia e hiperaldosteronismo como efectos compensadores a la pérdida de Na^+ y depleción de volumen es la presencia de hipokalemia y alkalosis metabolica debido a una mayor secreción de K^+ y H^+ en el TC de la nefrona (169).

En general, en todos los síndromes de Bartter es común la presencia de alteraciones en los mecanismos de concentración-dilución urinaria (169). Como se describió en secciones anteriores, dado que la reabsorción transcelular de Na^+ y el mecanismo de reciclaje de K^+ a través de la membrana apical favorecen la generación del voltaje transepitelial el cual es neceario para la adecuada reabsorción paracelular de Ca^{++} y Mg^{++}. En los síndromes de Bartter tipo I y II es muy frecuente observar alteraciones graves en el manejo de iones divalentes por lo que es notoria la presencia de hipermagnesuria e hipercalciuria que resultan en una severa nefrocalcinosis (formación de depósitos de iones divalentes principalmente de Ca^{++} en el riñón que ocasionan falla renal) (167,168).

Una característica clínica importante presente en pacientes con el síndrome de Bartter tipo II es que al nacimiento se presenta hiperkalemia a diferencia de los otros síndromes de Bartter donde existe hipokalemia debido a una elevada secreción de K^+ (170). De manera importante la hiperkalemia presente en pacientes con Bartter tipo II a lo largo del desarrollo se convierte en hipokalemia. El cambio en los niveles séricos de K^+ en pacientes con Bartter tipo II (de hiperkalemia a hipokalemia) se ha explicado de la siguiente manera: la hiperkalemia neonatal se ocasiona porque ROMK no puede llevar a cabo sus funciones de secreción de K^+ y por lo tanto se disminuye la secreción de este ión (170,171). Con forme va pasando el tiempo y el desarrollo del paciente se lleva cabo, debido al impedimento en la recirculación de K^+ se altera la reabsorción de Na^+ en la RAGAH. Al alterarse los niveles de reabsorción renal de Na^+, los niveles de P_s disminuyen y se promueve como efecto compensador la activación del SRAA. Como se ha venido discutiendo a lo largo de este manuscrito, la aldosterona promoverá la secreción de K^+ principalmente a través de ROMK. Al no exisitir ROMK funcional en pacientes con Bartter tipo II se ha postulado que otros mecanismos compensadores

(probablemente canales de K^+ conocidos como BK) son activados y se favorece el desarrollo de hipokalemia (172,173).

Usualmente el síndrome de Bartter tipo III es el menos severo y de manera importante no se desarrolla nefrocalcinosis y los niveles de poliuria y deshidratación son menores. Lo anterior ocurre probablemente porque existen otros medios para el movimiento de Cl^- a través de la membrana basolateral que pudiesen tomar papeles compensadores como el canal de cloruro CLC-Ka (174).

En comparación con los pacientes que presentan síndrome de Bartter tipo III, los pacientes con Bartter tipo IV presentan una más severa hipokalemia alcalósis metabólica y perdida de Na^+ (175). Lo anterior ocurre debido a que la subunidad β o Barttina es necesaria para la función de los dos canales basolaterales de Cl^- CLC-Ka y CLC-Kb. Por tal motivo se ha postulado que al mutarse la subunidad β, ambos canales pierden función y se interrumpe de manera completa la reabsorción de Cl^- a través de la membrana basolateral (175). Como se describió anteriormente, para la correcta reabsorción de Na^+ se requiere de la salida de Cl^- desde las celulas tubulares de la RAGAH a través de la membrana basolateral.

Como característica clínica distintiva entre los demás síndromes de Bartter, el tipo IV presenta sordera sensorineural (176,177). Lo anterior ha sido explicado de la siguiente manera: CLC-Kb/Barttina además de expresarse en la RAGAH, se expresan en la stria del oido interno donde se encargan de recircular el Cl^- secretado por el cotransportador $Na^+/K^+/ 2Cl^-$ conocido como NKCC1. La correcta recirculación de Cl^- (análoga a la recirculación de K^+ por ROMK en la RAGAH) es necesaria para el adecuado funcionamiento de NKCC1 y como resultado final la correcta secreción de K^+ hacia el lumen por canales de potasio conocidos como KCNQ1/KCNQE. Todo lo anterior es necesario para el proceso auditivo. Al existir mutaciones en la Barttina que es una subunidad del canal de Cl^- CLC-Kb se interrumpe todo este proceso y existen alteraciones en el proceso auditivo (176).

Biología molecular de NKCC2

NKCC2 es una proteína en humano de 1099 aminoacidos con peso molecular de 121.47 kDa que se ha sugerido actúa en forma de dímeros (178), posee 12 segmentos transmembrana (TM), dos sitios de N-acetil glucosilación críticos para sostener su actividad localizados en el asa extracelular presente entre los TM 7-8 (posiciones en rata N442 y N452) (179) y grandes regiones amino (174 aminoácidos) y carboxilo citoplásmicas (454 aminoácidos) las cuales se han postulado como blancos de eventos de fosforilación para modular la actividad de NKCC2 debido a la presencia de sitios concenso de fosforilación o de unión a diversas proteínas cinasas (180-186) (**Fig. 25**).

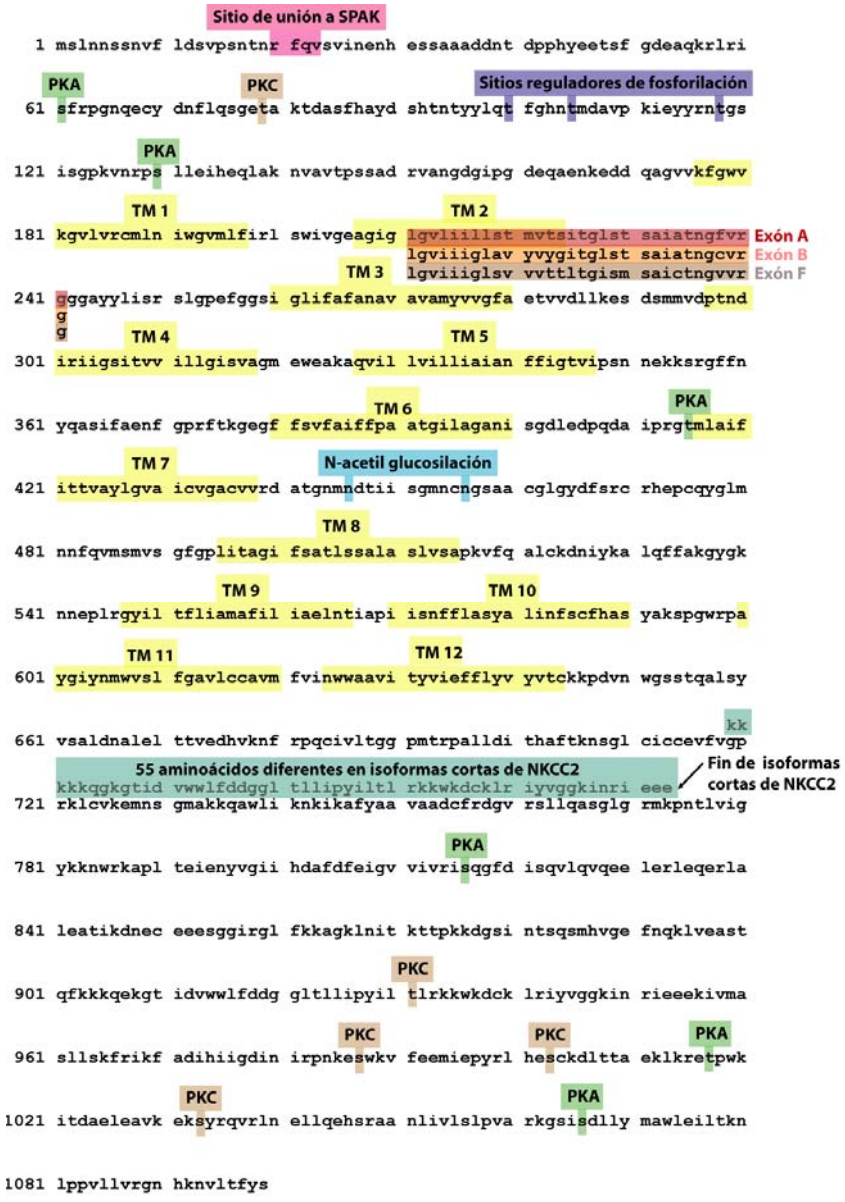

Figura 25. Secuencia de NKCC2 humana.

En roedor al menos 6 isoformas para NKCC2, productos de dos eventos independientes de empalme alternativo, han sido descritas (187). El primer empalme alternativo comprende la incorporación de tres exones mutuamente excluyentes denominados A, B y F, de 96 nucleótidos, precedidos del exón número 3. A nivel de proteína dichos exones conforman parte de la TM 2 y el asa citoplásmica número 1. Como resultado de dicho empalme alternativo se producen las isoformas "largas" de NKCC2 denominadas NKCC2A, NKCC2B, y NKCC2F las cuales difieren en su expresión a lo largo de la RAGAH, así como en sus cinéticas de transporte para Na^+ K^+ y Cl^-. En roedores, la isoforma NKCC2B expresada principalmente en la región cortical de la RAGAH poseé la mayor afinidad para sus sutratos de transporte, seguida por la isoforma NKCC2A que se expresa a todo lo largo de la RAGAH y de la isoforma NKCC2F con expresión restringida a la región medular de la RAGAH (**Fig. 26**).

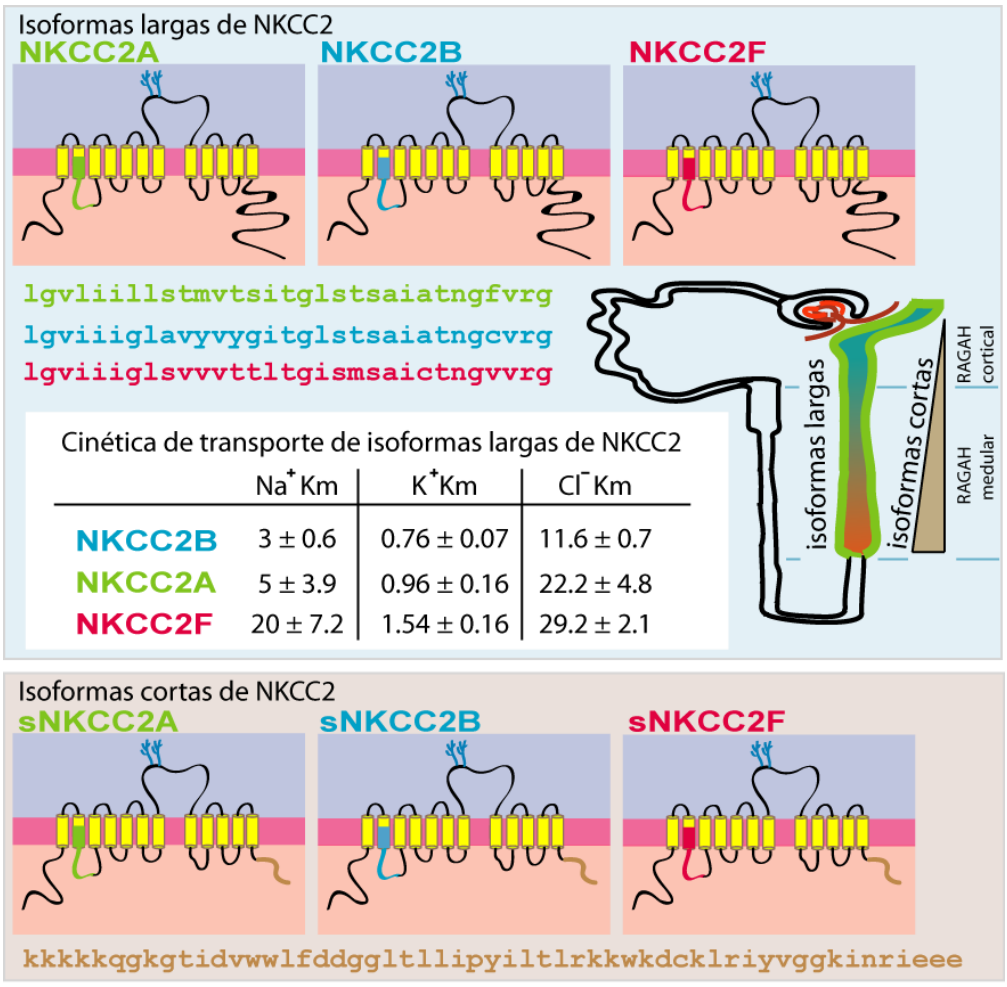

Figura 26. Isoformas cortas y largas de NKCC2.

Como resultado del segundo empalme alternativo y al uso de un segundo sitio de poliadenilación en el exón 16 se producen isoformas de NKCC2 denominadas "cortas" de tan solo 773 aminoácidos. Las isoformas cortas de NKCC2 poseen una región carboxilo de 129 aminoácidos, en donde los últimos 55 residuos son completamente distintos a las isoformas largas (187) (**Figs. 21 y 22**).

NKCC2 y la familia de cotransportadores electroneutros SLC12A

De acuerdo a la clasificación de la base de datos del comité de nomenclatura de la organización del genoma humano (HUGO Human Genome Organization www.genenames.org), NKCC2 pertenece a la familia de cotransportadores electroneutros de cationes acoplados a Cl^- conocida como SLC12A (solute carrier family 12A).

Según análisis filogenéticos, SLC12A está conformada por nueve miembros divididos en 3 ramas:

a) *La rama que utiliza la concentración extracelular del Na^+ (140 mM) como gradiente de transporte*. Está conformada por 3 genes que codifican para proteínas conocidas de manera grupal como NKCCs. Los NKCCs comparten un 50% de identidad a nivel de secuencia de aminoácidos y están constituidos por 12 TM, regiones amino y carboxilo citoplásmicas y una asa extracelular glucosilada entre los TM 7 y 8. Los genes que forman parte de esta rama son: SLC12A1 y SLC12A2 que codifican para NKCC2 y NKCC1 (cotransportadores de $Na^+/K^+/2Cl^-$) y el gen SLC12A3 que codifica para el cotransportador de Na^+/Cl^-, conocido como NCC, responsable del desarrollo de hipotensión arterial y del síndrome de Gitelman (OMIM #263800) cuando se encuentran mutaciones inactivantes en su secuencia debido a una disminución en la reabsorción de Na^+ a lo largo del TD de la nefrona (189).

b) *La rama que utiliza la concentración intracelular de K^+ (120 mM) como gradiente de transporte*. Está conformada por 4 genes que codifican para cotransportadores de K^+/Cl conocidos de manera grupal como KCCs. Los KCCs comparten un 67% de identidad a nivel de secuencia de aminoácidos y están constituidos por 12 TM, regiones

amino y carboxilo citoplásmicas y una asa extracelular glucosilada entre los TM 5 y 6. El gen SLC12A4 codifica para KCC1 que se expresa de manera ubicua y juega un papel importante en la regulación del volumen celular (190,191), SLC12A5 codifica para KCC2 que se expresa en el sistema nervioso central (SNC) y modula la respuesta al ácido gamma aminobutírico (GABA) (192,193), SLC12A6 codifica para KCC3 que es expresado en SNC y responsable del desarrollo de defectos neurodegenerativos y agénesis del cuerpo calloso (síndrome de Anderman, OMIM #601678) cuando se encuentran mutaciones inactivantes en su secuencia (194,195) y por último, el gen SLC12A7 que codifica para KCC4 que se expresa de manera abundante en las células intercaladas del TD de la nefrona así como en las células ciliares del oído interno (196,197).

c*) La rama que incluye a los genes SLC12A8 y SLC12A9.* SLC12A8 es un gen que ha sido asociado al desarrollo de psoriasis vulgaris (198) y codifica para un cotransportador de poliaminas-aminoácidos conocido como CCC9 (199). SLC12A9 codifica para una proteína denominada CIP probablemente con funciones de transporte, pero sin sustratos establecidos, capaz de interactuar con NKCC1 y prevenir su actividad (200) (**Fig. 27**).

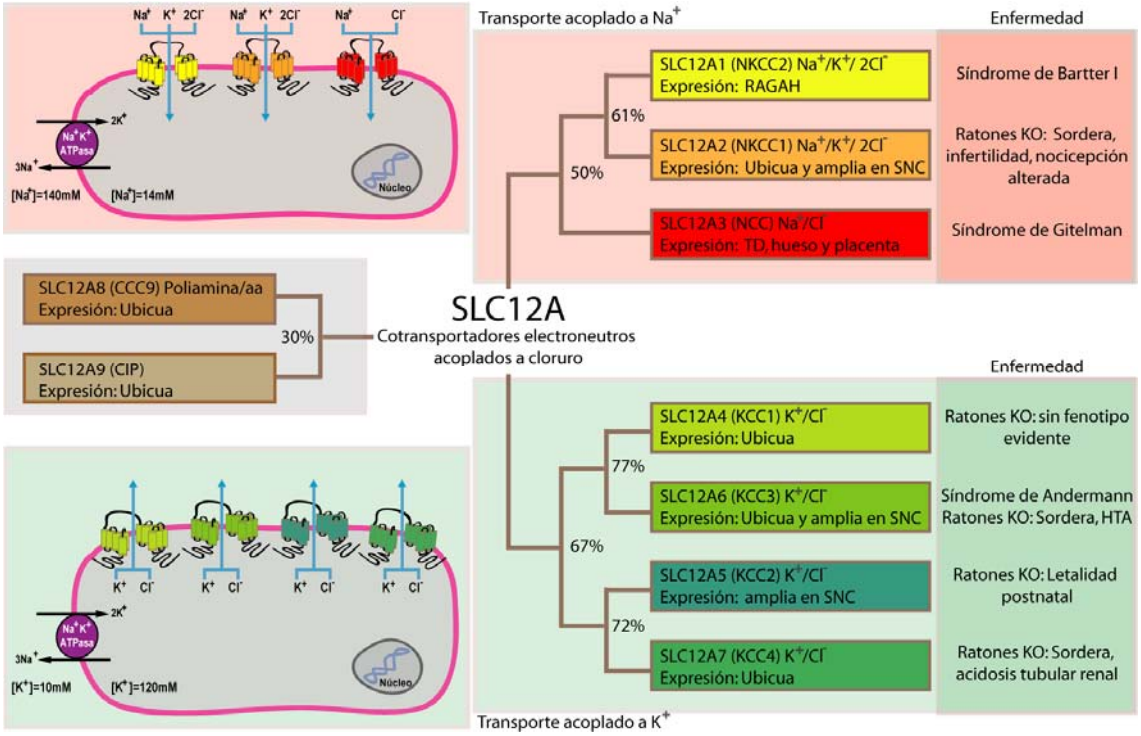

Figura 27. Clasificación y función de los miembros de SLC12A.

Los miembros de SLC12A son considerados cotransportadores secundarios ya que para su función no requieren de la hidrólisis de moléculas de adenosin trifosfato (ATP), pero sí del gradiente de concentración del Na^+ y K^+ generado por la bomba Na^+/K^+/ATPasa. Los NKCCs mueven iones desde fuera hacia adentro de la célula acoplando el transporte de Cl^- en el caso de NCC y de $K^+/2Cl^-$ en el caso de NKCC1 y NKCC2 al gradiente de concentración favorable para el Na^+. Los KCCs acoplan el movimiento de Cl^- desde adentro hacia afuera de la célula al gradiente de concentración favorable para el K^+ (**Fig. 27**).

Debido a la actividad recíproca entre los NKCCs (entrada de Cl^-) y KCCs (salida de Cl^-) se ha propuesto que existe una vía de señalización común que regula su actividad (22)201).

Dentro de las funciones celulares en las que la $[Cl^-]_i$ juega un papel importante se encuentran: la regulación del volumen celular (V_{cel}) y la excitabilidad neuronal.

Las células mantienen su V_{cel} constante mediante el movimiento de Cl^- y de osmolitos orgánicos para igualar la osmolaridad intracelular y extracelular (202,203). Cambios en la osmolaridad se acompañan de movimiento de H_2O a favor de su gradiente que resulta en cambios en el V_{cel}.

Cuando una célula se expone a un líquido extracelular (LEC) no isotónico se activan respuestas reguladoras en segundos o minutos para restablecer el V_{cel}. Por ejemplo, un aumento en la osmolaridad del LEC provocará una disminución en el V_{cel} debido a la salida de H_2O desde la célula.

Para contrarrestar disminuciónes en el V_{cel} se llevará a cabo el proceso conocido como incremento regulador del volumen (IRV). Durante el IRV se promoverá la entrada de Cl^- mediante la activación de NKCC1 e inhibición de los KCCs, así como el ingreso de osmolitos orgánicos a través de diversos cotransportadores. El incremento de osmolitos intracelulares y de la presión osmótica celular será acompañado de la reincorporación de H_2O a la célula y el restablecimiento del V_{cel}.

De manera contraria, durante una disminución en la osmolaridad del LEC se provocará un aumento en el V_{cel} debido a la entrada de H_2O. Para contrarrestar aumentos en el V_{cel} se llevará a cabo el proceso conocido como reducción reguladora del volumen (RRV). A través del RRV se promoverá la salida de Cl^- mediante la activación de los KCCs e inhibición de NKCC1, así como la salida de osmolitos orgánicos. La disminución de osmolitos intracelulares y de la presión osmótica celular será acompañada de la salida de H_2O desde la célula y el restablecimiento del V_{cel} (**Fig. 28**).

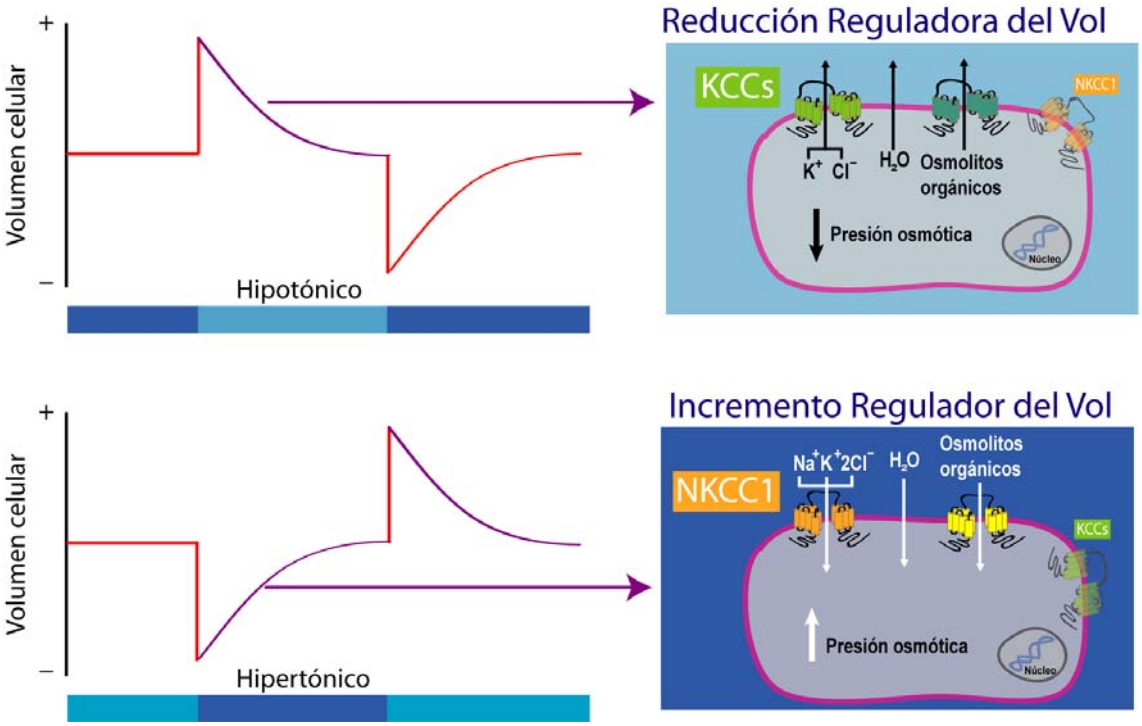

Figura 28. Regulación del volumen celular, NKCC1 y KCCs.

Durante el proceso de excitabilidad neuronal o inhibición presináptica, en donde se presentan cambios en el potencial de membrana debido al transporte de iones a través de la membrana celular, la $[Cl^-]_i$ juega un papel muy importante en la respuesta al neurotransmisor GABA, cuyo receptor ($GABA_A$) es un complejo multimérico que constituye un canal iónico acoplado a Cl^-.

Si la $[Cl^-]_i$ se encuentra por debajo de su potencial de equilibrio, la liberación de GABA favorecerá la hiperpolarización de la neurona y el efecto inhibidor presináptico debido a la entrada de Cl^-. De manera contraria, si la $[Cl^-]_i$ se encuentra por arriba de su potencial

de equilibrio se favorecerá la despolarización celular y excitación neuronal debido a la salida de Cl^- (**Fig. 29**).

Durante etapas neonatales, los efectos de GABA son excitatorios debido a que existe una mayor expresión de NKCC1 con respecto a KCC2 que resulta en una elevada $[Cl^-]_i$. En etapas posteriores del desarrollo, debido a una mayor expresión de KCC2 sobre NKCC1, los efectos de GABA son inhibitorios por la disminución en la $[Cl^-]_i$ (**Fig. 29**).

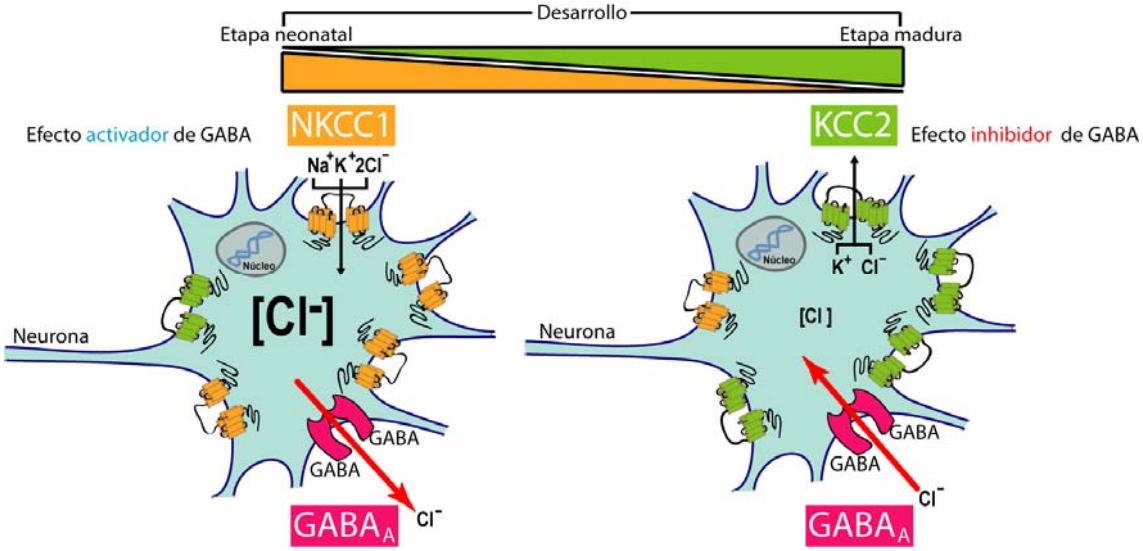

Figura 29. Relación entre $[Cl^-]_i$, excitabilidad neuronal**,** GABA**,** NKCC1 y KCC2.

<u>Maniobras de depleción de cloruro intracelular como activadores de NKCC1 y NCC</u>

De manera muy importante, durante maniobras de depleción de $[Cl^-]_i$ la actividad y estado de fosforilación de NKCC1 y NCC se incrementan de manera significativa.

NKCC1 fue el primer cotransportador miembro de SLC12A cuya actividad se reportó se favorecía durante maniobras de depleción de $[Cl^-]_i$. Durante tales maniobras, la fosforilación de al menos 3 residuos localizados en la región amino terminal se demostró estaba correlacionada con la activación de NKCC1. Y de manera importante la activación de NKCC1 durante eventos de depleción de $[Cl^-]_i$ se previno por la coexpresión de la serina treonina cinasa SPAK catalíticamente inactiva (ver más adelante).

Los tres aminoácidos fosfoaceptores fueron identificados en la región amino terminal de NKCC1 de tiburón en las posiciones Thr184 Thr189 y Thr202 utilizando cromatografía líquida de alta presión (HPLC). Mediante la generación de un fosfoanticuerpo (conocido como R5 y dirigido contra los dos primeros residuos Thr184 y Thr189) se ha podido establecer que el estado de fosforilación de NKCC1 se encuentra íntimamente ligado al nivel de activación del cotransportador ya que la Thr184 y la Thr189 son necesarias para la activación máxima de NKCC1 en presencia de diversos estímulos.

Cabe resaltar que nnguno de los residuos fosforilados durante la activación de NKCC1 se presenta dentro del contexto de sitios consenso para serina treonina cinasas conocidas. Sin embargo, los tres residuos se localizan en una region que muestra 80% de homología entre NKCC1, NKCC2 y NCC y además se localizan cerca de un sitio conservado de unión a la proteína fosfatasa 1 con la secuencia (Arg-Val-Xaa-Phe).

Consistente con el papel que juegan eventos de fosforilación para modular la actividad de los NKCCs se ha enonctrado al menos para el caso de NKCC1 que inhibidores para proteina fosfatasa 1 favorecen su estado de fosforilación y de actividad.

Debido a la conservación a lo largo de las especies de los tres residuos amino terminales entre NKCC1, NKCC2 y NCC, se ha sugerido que se comparte un mecanismo fosforegulador entre los miembros de la rama de SLC12A que utiliza la concentración extracelular del Na^+ como gradiente de transporte. Al parecer la fosforilación de estos residuos es una vía final de activación de los NKCCs ya que diversos estímulos pueden favorecer su fosforilación. Por ejemplo durante la activación de NCC y NKCC2 por la ADH se favorece la fosforilación de estos residuos amino terminales.

Para el caso de NCC, nuestro grupo de investigación ha establecido que durante dos maniobras de depleción de $[Cl^-]_i$ (coexpresión con KCC2 e incubación en una disolución hipotónica baja en cloruro) la atividad de NCC se incrementa alrededor de tres veces. Las dos maniobras utilizadas para depleción de $[Cl^-]_i$ tuvieron efectos sinérgicos y fueron dosis dependiente sobre la actividad de NCC.

El incremento en la actividad de NCC durante maniobras de depleción de $[Cl^-]_i$ se encontró asociado elevaciones en los niveles de fosforilación de los residuos de Thr53 y

Thr58. De manera consistente la sustitución de estos residuos por alanina en conjunto con un residio adicional Ser71 eliminó por completo la respuesta a NCC a maniobras de depleción de $[Cl^-]_i$.

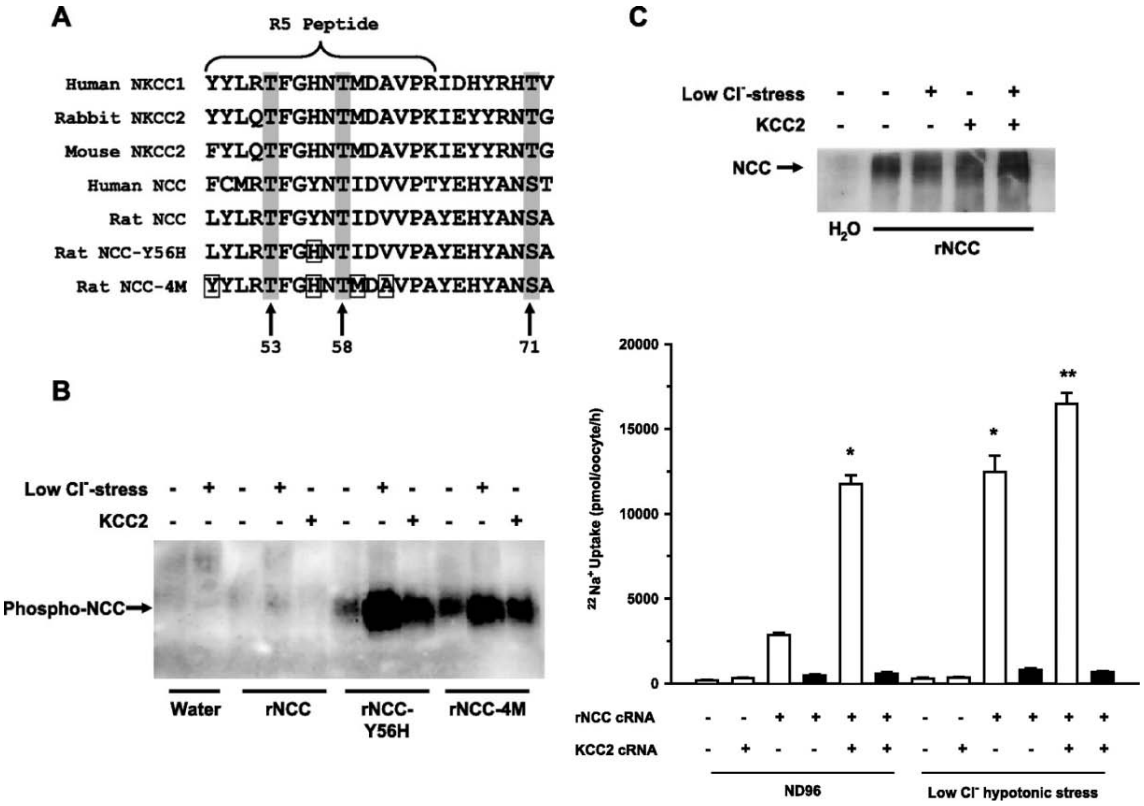

Figura 30. Activación y fosforilación de NCC durante maniobras de depleción de cloruro intracelular (tomado y modificado de Pacheco-Alvarez et al 2006)

Las cinasas WNK como reguladores de SLC12A

Recientemente se han empezado a descubrir los mecanismos moleculares por los que se pudiera regular de manera coordinada la actividad de los NKCCS-KCCs y por lo tanto la $[Cl^-]_i$. Numerosos estudios han sugerido que eventos de defosforilación activarán a los KCCs e inhibirán a los NKCCs, mientras que la fosforilación inactivará a los KCCs y activará a los NKCCs (204,205). Empleando ovocitos de la rana *Xenopus laevis* como sistema de expresión heteróloga se ha encontrado que la serina treonina cinsasa conocida como WNK3, miembro de la subfamilia de proteínas cinasas WNK (ver más adelante), podría ser la cinasa sensora de la $[Cl^-]_i$ debido a que regula de manera coordinada la actividad de los NKCCs y de los KCCs (183;206,207).

La coexpresión de WNK3 resulta en un efecto positivo sobre la actividad de los NKCCs en condiciones isotónicas e inclusive en condiciones hipotónicas donde la actividad de los NKCCs se encuentra normalmente abatida. El incremento en la actividad de los NKCCs se encuentra asociado a la fosforilación de residuos de treonina ampliamente conservados y presentes en su región amino terminal citoplásmica (posiciones en NKCC2 de humano: T100 y T105) (183).

Con respecto a los KCCs, la coexpresión de WNK3 resulta en la inhibición del transporte de K^+ y Cl^- aún en condiciones hipotónicas donde se favorece normalmente la actividad de los KCCs (206).

La eliminación de actividad catalítica en WNK3, favorece la inhibición de los NKCCs mediante la defosforilación de residuos de treonina amino terminales y la activación de los KCCs aún en condiciones hipertónicas donde se promueve su inhibición (206). Recientemente se ha demostrado que la defosforilación de dos residuos de treonina ampliamente conservados localizados en la región carboxilo terminal (posiciones en KCC3 de humano: T991 y T1048) es necesaria para la activación de los KCCs (208) (**Fig. 31**).

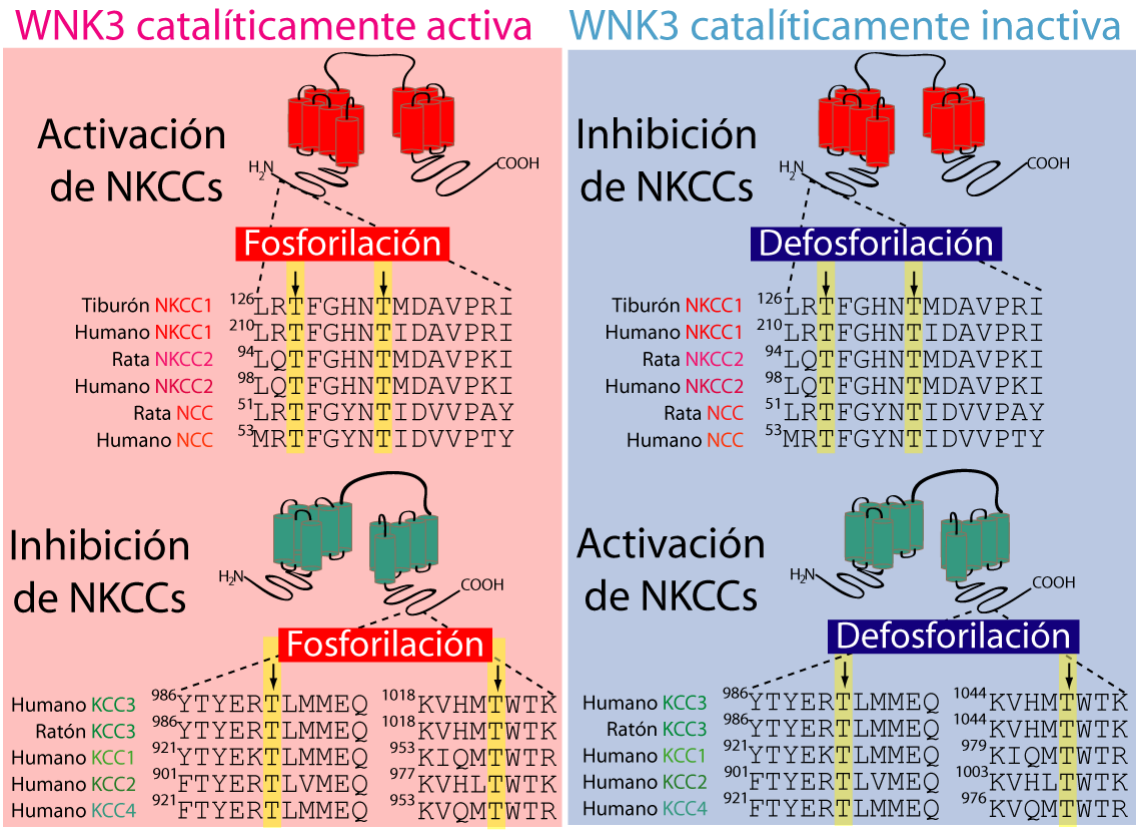

Figura 31. Relación entre $[Cl^-]_i$, excitabilidad neuronal**,** GABA**,** NKCC1 y KCC2.

Dado que la activación de los KCCs por la coexpresión de WNK3 catalíticamente inactiva se puede prevenir con inhibidores específicos para la proteína fosfatasa 1 y para la proteína fosfatasa 2B, se ha postulado que WNK3 modula el equilibrio entre actividades cinasas y fosfatasas para regular la $[Cl^-]_i$ (206).

Hoy sabemos que los miembros de la subfamilia de serina treonina cinasas conocidas como WNK por sus siglas en inglés (With No K=lysine) son importantes reguladores de la actividad de diversas proteínas entre las que se encuentran miembros de SLC12A (209-212).

Las WNKs fueron llamadas así porque son únicas dentro de la superfamilia de proteínas cinasas en el sentido de que carecen de un residuo de lisina conservado y localizado en el subdominio II entre las cinasas para la unión de ATP (213). En las WNK este residuo de lisina en el subdominio II es remplazado por un residuo de cisteina, asparagina o serina dependiendo de la especie (214) (**Fig. 32**).

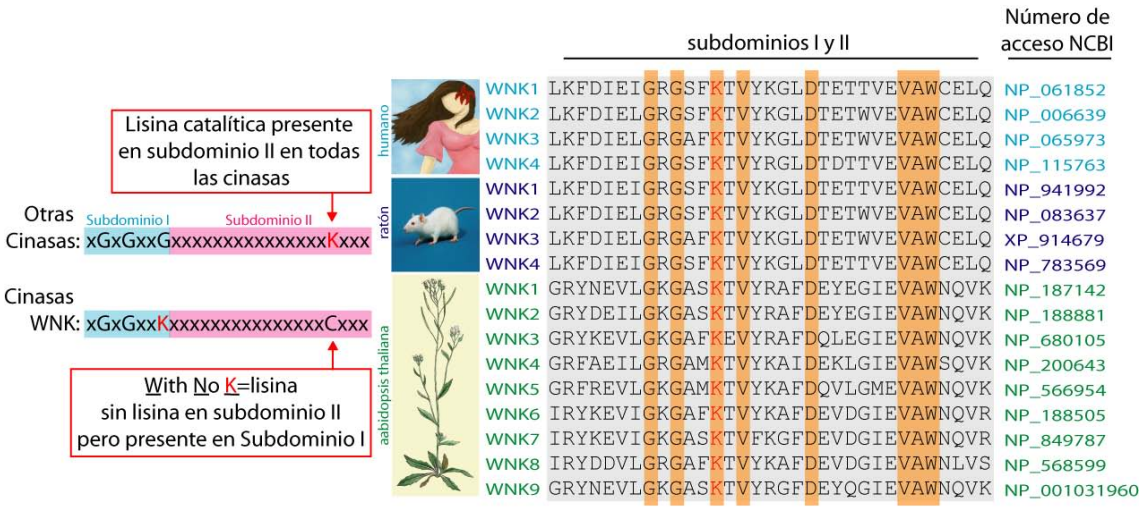

Figura 32. Cinasas tipo WNK en humano, ratón y arabidopsis thaliana.

Mediante análisis de modelaje proteíco, así como de mutagénesis se ha encontrado que un residuo de lisina distinto y localizado en el subdominio I es el empleado y necesario para la actividad catalítica de estas cinasas (215,216). A pesar de estar localizado en diferentes partes del dominio cinasa, a nivel estructural el residuo de lisina empleado por las WNK, localizado en el subdominio I, apunta hacia la hendidura formada en el sitio activo como lo hace el residuo de lisina clásico de las serina treonina cinasas en el subdominio II.

A nivel de estructura, las WNK poseen en su región amino terminal el dominio catalítico típico de las serina treonina cinasas, con un nivel de identidad de 85-90%. Además de la región cinasa, las WNK contienen un dominio autoinhibitorio que puede prevenir o suprimir la actividad catalítica y en la región carboxilo un segmento regulador, con baja identidad entre las WNK, en la cual se encuentran numerosos motivos de interacción proteícos como aquellos con la secuencia PXXP ricos en reisudos de prolina y de uno a dos dominios coiled-coil.

A nivel de expresión, las cinasas tipo WNK se han encontrado únicamente presentes en organismos pluricelulares. En ratón y humano existen cuatro WNK (WNK1 a WNK4), expresadas en diversidad de tejidos. A nivel de ARNm: WNK1 se expresa predominantemente en riñón, cerebro y músculo (217). WNK2 se expresa principalmente en SNC, corazón y colon (218-221). WNK3 se distribuye en diversidad de tejidos como cerebro, riñón, hígado e intestino delgado (222,223), mientras que

WNK4 lo hace preferencialmente en riñón, piel, colón, hígado y pulmón (224-227) (**Fig. 33**).

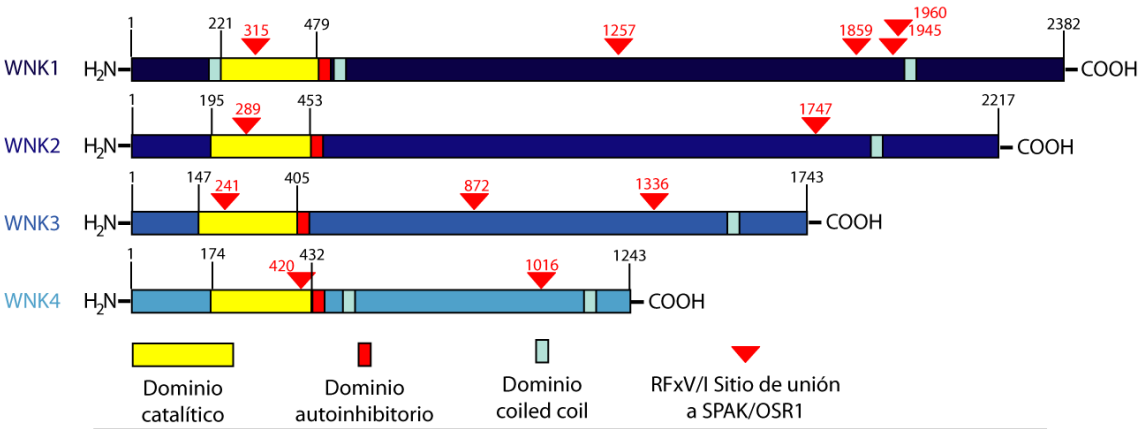

Gene	Localización cromosómica	Número de exones	Expresión	Peso molecular de la proteína	Sitios de unión a SPAK/OSR1
WNK1	12p13.3	28	Riñón, cerebro, músculo	251 kDa	5
WNK2	9q22.31	31	SNC, corazón, colon	243 kDa	2
WNK3	Xp11.23-21	24	Cerebro, hígado, intestino delgado, riñón	192 kDa	3
WNK4	17q21-q22	19	Riñón, piel, colon, hígado, pulmón	135 kDa	2

Figura 33. Características de las serina treonina cinasas WNK en humano.

Desde el descubrimiento y clonación molecular en el año 2000 de la primera cinasa tipo WNK (WNK1), la acumulación de diversos estudios ha permitido establecer que los miembros de las cinasas tipo WNK participan en diversidad de procesos celulares como regulación del balance iónico, desarrollo, señalización, superviviencia y proliferación celular.

Como se discutió anteriormente, la adecuada función de miembros de las WNK es crítica para sostener la salud humana. Mutaciones en el exón HSN2 de la isoforma neural de WNK1 son responsables del desarrollo de la neuropatía sensorial humana tipo II (228), mientras que mutaciones en WNK4 o la sobreexpresión de la isoforma renal larga de WNK1 (L-WNK1) son responsables del desarrollo del Síndrome de Gordon, también conocido como pseudohipoaldosteronismo tipo II (PHAII) (OMIM 145260) (229).

Las cinasas SPAK y OSR1

Además de las cinasas WNK, dos serina treonina cinasas: SPAK (Ste20p-SPS1-related Proline Alanine rich Kinase) y OSR1 (Oxidative Stress Responsive Kinase 1) han sido propuestas como reguladores de la actividad de diversas proteínas dentro de las que se encuentran miembros de la familia de cotransportadores electroneutros de cationes acoplados a Cl^- (230-234).

SPAK y OSR1 comparten un 68% de identidad a nivel de secuencia de aminoácidos y se encuentran dentro de las 28 cinasas identificadas en humano relacionadas a la cinasa conocida como Ste20p (sterile 20 protein) de la levadura *Saccharomyces cerevisiae*.

Las cinasas relacionadas a Ste20p participan en una gran diversidad de procesos celulares dentro de los que destacan la regulación de transporte iónico y homestasis del volumen celular.

A la fecha las cinasas relacionadas a Ste20p han sido divididas en dos familias: las cinasas PAK (p21 Activated Kinases) caracterizadas por tener su dominio cinasa en la región carboxilo terminal y las cinasas GCKs (germinal center kinases) las cuales poseen su dominio catalítico en la región amino terminal (235) (**Fig. 34**).

La familia de las cinasas tipo PAK está a su vez dividida en dos subfamilias (PAK1 y PAK2), mientras que la familia de las GCKs es dividida en 8 subfamilias (GCK1-GCKVIII).

Las cinasas SPAK y OSR1 forman parte de la subfamilia VI de las GCKs y se postularon inicialmente como reguladoras de la actividad de miembros de SLC12A porque se encontró mediante ensayos de doble híbrido en levadura que eran capaces de interactuar a través de su región carboxilo terminal con el motivo Lys/Arg-Phe-Xaa-Val/Iso presente en NKCC1, NKCC2 y KCC3a (**Fig. 34**).

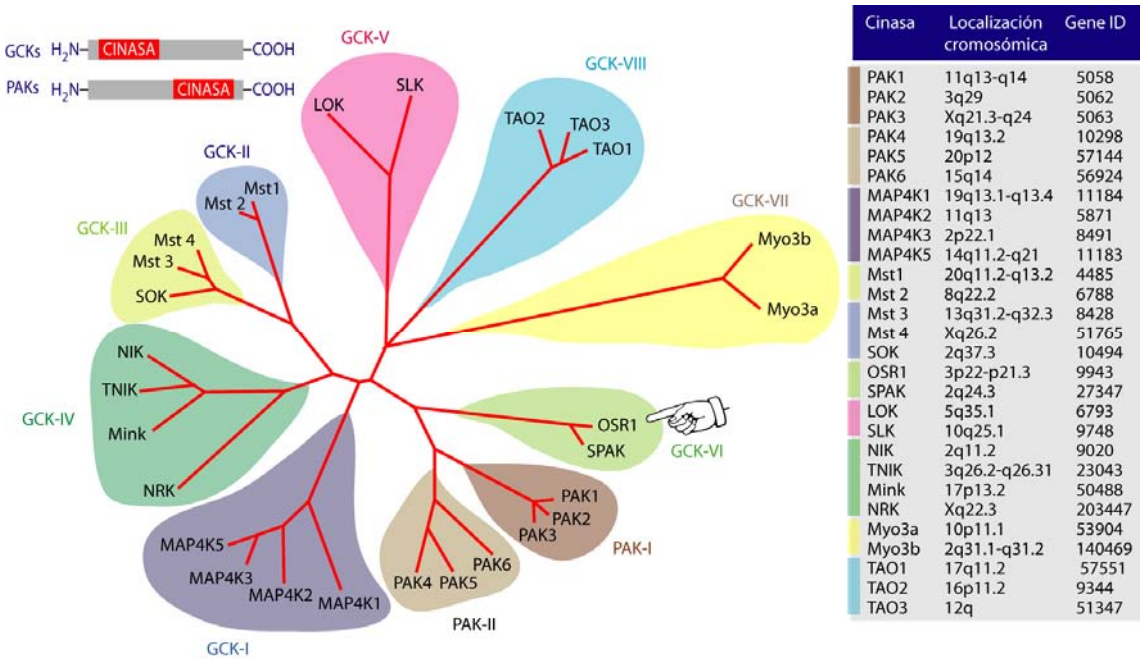

Cinasa	Localización cromosómica	Gene ID
PAK1	11q13-q14	5058
PAK2	3q29	5062
PAK3	Xq21.3-q24	5063
PAK4	19q13.2	10298
PAK5	20p12	57144
PAK6	15q14	56924
MAP4K1	19q13.1-q13.4	11184
MAP4K2	11q13	5871
MAP4K3	2p22.1	8491
MAP4K5	14q11.2-q21	11183
Mst1	20q11.2-q13.2	4485
Mst 2	8q22.2	6788
Mst 3	13q31.2-q32.3	8428
Mst 4	Xq26.2	51765
SOK	2q37.3	10494
OSR1	3p22-p21.3	9943
SPAK	2q24.3	27347
LOK	5q35.1	6793
SLK	10q25.1	9748
NIK	2q11.2	9020
TNIK	3q26.2-q26.31	23043
Mink	17p13.2	50488
NRK	Xq22.3	203447
Myo3a	10p11.1	53904
Myo3b	2q31.1-q31.2	140469
TAO1	17q11.2	57551
TAO2	16p11.2	9344
TAO3	12q	51347

Figura 34. Dendograma de las cinasas en humano relacionadas a la cinasa Ste20p de levadura.

Mediante ensayos de expresión funcional se ha podido establecer que la actividad catalítica de SPAK así como su interacción física con NKCC1 y NCC es necesaria para mantener la actividad normal de estos cotransportadores (236). Consistente con lo anterior, la sobreexpresión de SPAK catalíticamente inactiva previno la fosforilación de los residuos amino terminales en NKCC1 y NCC requeridos para sostener la actividad basal, su activación mediada por WNK3 y al menos para el caso de NKCC1 su activación durante maniobras de depleción de la concentración de cloruro intracelular. De manera importante la sobrexpresión de SPAK catalíticamente inactiva resultó en la activacion de KCC2. En resumen, la actividad de diversos miembros de SLC12A parece depender de los efectos que las cinasas SPAK y OSR1 ejerzan sobre ellos.

El interés en comprender el papel de las cinasas SPAK y OSR1 se incrementó de manera notoria al descubrir que estas dos cinasas son blancos de fosforilación de WNK1 y WNK4 las cuales están mutadas en pacientes con PHAII.

De manera interesante las cinasas SPAK y OSR1 son capaces de interactuar y estimular la actividad del cotransportador $Na^+/K^+/2Cl^-$ (NKCC1) en presencia de las cinasas

WNK1 y WNK4, así como modular la actividad del cotransportador NKCC1 en relación con cambios a la $[Cl^-]_i$ (237-238).

La interacción entre las cinasas SPAK/OSR1 y proteínas con motivo Lys/Arg-Phe-Xaa-Val/Iso involucra 92 aminoácidos 79% idénticos a nivel de secuencia, localizados en la región carboxilo, que en conjunto han sido llamados como CCT (conserved carboxy terminal domain) por sus siglas en ingles (239).

Mediante el empleo de ensayos tipo doble híbrido, Piechotta y colaboradores han establecido que SPAK y OSR1 también pueden establecer interacción física con otras proteínas entre las que se encuentran: AATYK1, AATYK3, gelsolina, otoferlina, HSP105. Esta observación indica que SPAK y OSR1 se encuentran probablemente involucradas en múltiples pocesos celulares algunos de los cuales parecen se completamente independientes de la modulación del transporte iónico.

A pesar de que el ensayo de doble híbrido es una técnica muy valiosa y utlizada para descubrir interacciones proteína-proteína, en muchas ocasiones no todas las posibles interacciones proteícas pueden ser descifradas mediante su empleo. Recientemente, mediante búsquedas *in silico* utilizando el proteoma de ratón se ha podido establecer que 130 proteínas presentan a nivel de secuencia al menos un motivo de interacción con las cinasas SPAK y OSR1.

Cabe mencionar que todos los miembros de las WNK poseen al menos un motivo de uníón a SPAK y OSR1. Si bien es cierto que la presencia a nivel de secuencia de tal motivo de unión a SPAK y OSR1 no garantiza la interacción, lo anterior abre la posibilidad de que las cinasas SPAK y OSR1 desempeñen papeles muy importantes a nivel celular (**Fig. 28**).

PLANTEAMIENTO DEL PROBLEMA

Un determinante importante de los niveles de P_s es la reabsorción de Na^+ en la nefrona, donde en RAGAH, el principal responsable es el cotransportador NKCC2. Las mutaciones en NKCC2, CLC-Kb, y Barttina son responsables del desarrollo del síndrome de Bartter tipo I, III y IV respectivamente.

A la fecha, no se conoce el mecanismo por cual el bloqueo de la actividad de CLC-Kb (Bartter tipo III ó IV) disminuye la reabsorción de Na^+ mediada por NKCC2, pero es probable que el bloqueo de CLC-Kb y Barttina conduzca a un aumento en la $[Cl^-]_i$, el cual resulte en la inhibición de la expresión y/o función de NKCC2, ocasionando el desarrollo de la enfermedad.

De manera importante, la disminución en las $[Cl^-]_i$, modulan mediante eventos de fosforilación en residuos conservados dentro de la región amino terminal, la actividad de NKCC1 y NCC, cotransportadores que pertencen a la misma familia (SLC12A) de cotransportadores electroneutros de cationes acoplados a Cl^- que NKCC2 y con los cuales comparte un 61 y 50% de identidad a nivel de secuencia de aminoácidos respectivamente.

A lo largo de mis estudios de doctorado mi objetivo principal fue demostrar si cambios en las $[Cl^-]_i$ mediante eventos de fosforilación en la región amino terminal modificaban la actividad de NKCC2 de manera similar a lo que ocurre en NKCC1 y NCC.

Si cambios en las $[Cl^-]_i$ son capaces de modular la actividad de NKCC2, entonces probabalemente un aumento en la $[Cl^-]_i$, sea el responsable del bloqueo de la expresión y/o función de NKCC2 en el síndrome de Bartter tipo III y IV. Asimismo, durante mi doctorado me di a la tarea de establecer el mecanismo molecular por el cual cambios en $[Cl^-]_i$ modulan la actividad de NKCC2, en donde dos proteinas cinasas WNK3 y SPAK/OSR1 han sido sugeridas como sensoras de cambios en $[Cl^-]_i$ debido que modulan la actividad de miembros de SLC12A.

OBJETIVO GENERAL

Avanzar en la comprensión del mecanismo de regulación de la actividad del cotransportador NKCC2 por cambios en la $[Cl^-]_i$, probablemente responsables del síndrome de Bartter tipo III y IV así como el mecanismo molecular por el cual cambios en $[Cl^-]_i$ modulan la actividad de NKCC2

OBJETIVOS PARTICULARES

Determinar el efecto de dos maniobras de depleción de $[Cl^-]_i$ (coexpresión del cotransportador K^+/Cl^- KCC2 e incubación en una solución hipotónica con bajas concentraciones de Cl^-) sobre la fosforilación de dos residuos de treonina 96 y 101 y su relación con la actividad de NKCC2.

Establecer el papel de las cinasas WNK3 y SPAK catalíticamente activas e inactivas (WNK3 D294A y SPAK K104R) sobre la actividad basal del NKCC2, así como durante maniobras de depleción de $[Cl^-]_i$

Determinar el papel del motivo de unión a SPAK en la región carboxilo terminal de la cinasa WNK3 mediante su eliminación con la mutación puntual F1337A.

METODOLOGIA

El presente estudio fue llevado a cabo mediante la combinación de tres disciplinas: a) la biología molecular, b) la bioquímica y c) la expresión funcional heteróloga utilizando ovocitos de la rana *Xenopus laevis* (**Fig. 35**).

Los ovocitos de la rana *Xenopus laevis* se pueden microinyectar con ARNm o ARNc exógeno con ayuda de un micromanipulador y con la ayuda de un microscopio estereoscópico. Dicho sistema de expresión funcional heteróloga ha provado ser útil para la expresión y estudio de diversas proteínas de varias especies ya que el ARNm o ARNc que codifica para dichas proteinas puede ser procesado y traducido con gran eficiencia. De esta manera, después de microinyectar ovocitos de la rana *Xenopus laevis* con el ARNc que codifica para NKCC2 se puede evaluar la actividad de NKCC2 anclado a membrana mediante la captación o incorporación a la célula de sustratos de transporte como el $^{86}Rb^+$ ó el $^{22}Na^+$. La captación de dicho material radiaoctivo sensible o inhibida por bumetanida (inhibidor específico de NKCC2) puede entonces ser correlacionada al nivel de actividad de NKCC2 expresado en los ovocitos.

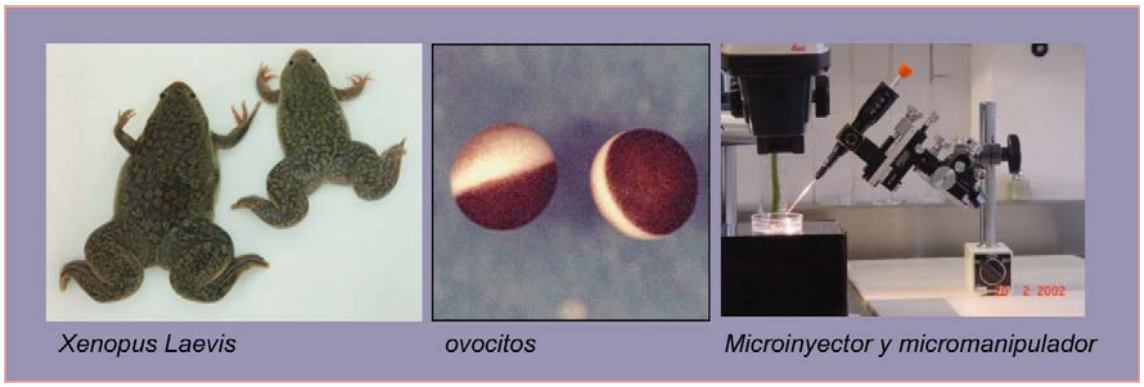

Figura 35. Rana *Xenopus laevis*, ovocitos, microinyector y micromanipulador utilizados durante los ensayos de expresión funcional heteróloga

Extracción e inyección de ovocitos de Xenopus laevis

La obtención y preparación de ovocitos se llevó a cabo siguiendo la metodología que hemos utilizado en repetidas ocasiones (240-245). En resumen, los ovocitos se obtienen de ranas hembras adultas *Xenopus laevis*, se defoliculan manualmente e incuban durante toda la noche en la solución conocida como ND96 (en [mM]: 96 NaCl, 2 KCl, 1.8 $CaCl_2$, 1 $MgCl_2$, y 5 HEPES/Tris, pH 7.4) y al día siguiente se microinyectan con 50 nl de agua con o sin ARNc de nuestros genes a estudiar.

Se utilizaron de 10 a 15 ovocitos por cada grupo, de manera tal que cada experimento requiere de la microinyección de aproximadamente 350 a 400 ovocitos. Después de la microinyección de ARNc, los ovocitos se incuban durante 3 a 4 días en ND96 suplementado con 2.5 mM de piruvato de Na^+ como fuente de energía y 0.5 mg/L de gentamicina para prevenir contaminación bacteriana.

Clonas, síntesis e inyección del ARN complementario

El ADNc que utilizamos en el estudio es el que codifica para NKCC2 de rata, para KCC2 de humano, para WNK3 de humano y para SPAK de ratón. El ARNc fue sintetizado a partir del ADNc de cada una de las clonas silvestres ó clonas con mutaciones puntuales utilizando el estuche mMESSAGE mMACHINE® T7 de la marca Ambion. La calidad del ARNc fue comprobada mediante electroforesis en gel de

agarosa/formaldehído y su concentración fue determinada por espectrofotometría de ácidos nucleicos y por análisis densitométrico de las bandas observadas en el gel. Para la microinyección, el ARNc se disolvió en H_2O libre de RNAsas y DNAsas y se inyectó en ovocitos a razón de 50 nL por ovocito de una disolución usualmente a 0.2 µg/µL (10 ng de ARNc/ovocito).

Determinación de la expresión funcional o actividad de NKCC2

Las propiedades funcionales y farmacológicas de las clonas silvestres o mutadas las llevamos a cabo siguiendo los protocolos que hemos utilizado previamente. En resumen, la actividad del cotransportador NKCC2 se determinó como la captación o incorporación de $^{22}Na^+$ o de $^{86}Rb^+$, dependiente de Cl^- y sensible a bumetanida.

Las disoluciones de precaptación y de captación utilizadas fueron diseñadas según las necesidades de cada experimento. En general se incuban lo ovocitos en precaptación con amiloride y ouabaina en ausencia de K^+. La ouabaina inhibe a a la Na^+/K^+ ATPasa, la amiloride previene la captación de Na^+ por canales de sodio (ENaC) ó por el intercambiador Na^+/H^+ (NHE) y la ausencia de K^+ previene la captación por NKCC1 ó NKCC2. Posteriormente, se cambian los ovocitos a una disolución de captación con las mismas drogas, pero en presencia de Na^+, K^+ y Cl^- y con 2 µCi/mL de $22Na^+$ ó $86Rb^+$. La captación de estos isótopos radioactivos fue determinada mediante centelleo líquido de cada ovocito en presencia de 500 µL de SDS al 10% w/v.

Maniobras para disminuir la concentración intracelular de cloruro

Se utilizaron dos maniobras diferentes para disminuir la $[Cl^-]_i$ en el ovocito. Una fue la expresión del cotransportador KCC2. Este cotransportador de K^+/Cl^- es la única isoforma de las cuatro que es activa en condiciones isotónicas y por lo tanto, durante los tres o cuatro días de incubación post microinyección produce salida de K^+ y Cl^- del ovocito. El potasio es regresado a la célula por la actividad de la Na^+/K^+/ATPasa, con lo que se disminuyen las $[Cl^-]_i$. La segunda maniobra fue la incubación de los ovocitos 12 horas antes de la captación de radionúclidos en una solución ligeramente hipotónica y

sin Cl^-. Dicha incubación resulta en apertura de canales de Cl^- del ovocitos y por tanto la disminución en la $[Cl^-]_i$. A esta maniobra la conocemos como estrés hipotónico bajo en Cl^-. Ambas maniobras han sido utilizadas por nosotros y por otros grupos para disminuir la $[Cl^-]_i$ y en ambos casos se ha determinado la efectividad de las maniobras para disminuir las $[Cl^-]_i$ a partir de la medición de este ion dentro de la célula con electrodos sensibles a Cl^-.

Mutagénesis

Las mutaciones puntuales utilizadas en el presente estudio se llevaron a cabo con el estuche comercial QuickChange de Stratagene siguiendo las instrucciones del fabricante. Los iniciadores (primers) específicos para realizar cada mutación fueron sintetizados por Sigma-Aldrich. Las mutaciones introducidas en los ADNc fueron las siguientes: NKCC2-TM: Esta es la triple mutante de NKCC2 en que las treoninas 96, 101 y 113 fueron sustituidas por alanina. Con esto eliminamos las treoninas en la región amino terminal, que para el caso de NKCC1 y NCC se ha demostrado que son importantes en la regulación de su actividad. WNK3-D294A: WNK3 en la que el ácido aspártico de la posición 294 fue sustituido por alanina. Con esto la cinasa WNK3 pierde su actividad catalítica. WNK3 F1337A: WNK3 en el que la fenilalanina 1337 fue sustituida por alanina. Con esto se elimina el único sitio potencial en WNK3 para su interacción con la cinasa SPAK. SPAK-K104R: SPAK en la que la lisina 104 es sustituida por arginina y con esto pierde su actividad catalítica. Todas las mutaciones se corroboraron mediante secuenciación automátizada del ADNc.

Analisis de transferencia tipo Western

Se utilizó análisis de transferencia tipo Western (Western blot) para conocer la cantidad de proteína de NKCC2 en los ovocitos inyectados con ARNc de NKCC2 y expuestos a las maniobras de depleción de $[Cl^-]_i$ así como para determinar el estado de fosforilación de las treoninas 96 y 101 de la región amino terminal. Para el primer caso utilizamos anticuerpos policlonales generados contra la región amino terminal de NKCC2 generosamente obsequiados por Mark Knepper. Para el segundo caso utilizamos el

fosfoanticuerpo conocido como R5 que reconoce a las treoninas 184 y 189 de NKCC1 cuando están fosforiladas. Este anticuerpo fue donado por Biff Forbush y debido a que el péptido de 16 amino ácidos que se utilizó para hacer el anticuerpo, incluyendo las dos treoninas, está altamente conservado en NKCC2, los anticuerpos R5 pueden reconocer las treoninas 96 y 101 de NKCC2 cuando están fosforiladas. Para llevar a cabo los Western blots se extrajeron proteínas de 15 ovocitos por grupo, se homogenizaron en buffer de lisis a razón de 10 µL/ovocito, se centrifugaron en dos ocasiones a 14000 rpm (16464 unidades g) durante 10 minutos a 4^{o}C y se recolectó el sobrenadante. Para cada carril se utilizó el equivalente a un ovocito.

Análisis estadístico

La diferencia de medias entre dos grupos se analizó mediante la prueba de *t* de Student. La significancia estadística entre los grupos se llevó a cabo con ANOVA de una vía y corrección de Bonferroni para comparaciones múltiples. Los resultados se presentan como media ± error estandar.

La metodología a detalle utilizada en mis proyectos de investigación realizados durante mi doctorado se encuentra anexada en las publicaciones siguientes.

RESULTADOS

Los resultados obtenidos a lo largo de mi doctorado permitieron alcanzar los objetivos trazados en mi proyecto y dichos resultados lograron ser publicados en el artículo que lleva por nombre: "***Regulation of NKCC2 by a chloride-sensing mechanism involving the WNK3 and SPAK kinases***". Dicha publicación se encuentra en la revista "Proceedings of the nacional Academy of Sciences" dentro del volumen y tomo en las páginas. La publicación se encuentra anexa en páginas posteriores, así como un breve resumen y discusión en la que se resaltan las principales conclusiones obtenidas en dicho trabajo.

Regulation of NKCC2 by a chloride-sensing mechanism involving the WNK3 and SPAK kinases

José Ponce-Coria*, Pedro San-Cristobal*, Kristopher T. Kahle†, Norma Vazquez*, Diana Pacheco-Alvarez*‡, Paola de los Heros*, Patricia Juárez*, Eva Muñoz§, Gabriela Michel*, Norma A. Bobadilla*, Ignacio Gimenez§, Richard P. Lifton¶, Steven C. Hebert‖**, and Gerardo Gamba*††

*Molecular Physiology Unit, Instituto Nacional de Ciencias Médicas y Nutrición Salvador Zubirán and Instituto de Investigaciones Biomédicas, Universidad Nacional Autónoma de México, Tlalpan, 14000 Mexico City, Mexico; †Department of Neurosurgery, Massachusetts General Hospital, Harvard Medical School, Boston, MA 02114; ‡Escuela de Medicina, Universidad Panamericana, 03920 Mexico City, Mexico; §Department of Pharmacology and Physiology, School of Medicine, University of Zaragoza, 50009 Zaragoza, Spain; and Departments of ¶Genetics and ‖Molecular and Cellular Physiology, Howard Hughes Medical Institute, Yale University School of Medicine, New Haven, CT 06510

Contributed by Steven C. Hebert, April 2, 2008 (sent for review December 7, 2007)

The Na^+:K^+:2Cl^- cotransporter (NKCC2) is the target of loop diuretics and is mutated in Bartter's syndrome, a heterogeneous autosomal recessive disease that impairs salt reabsorption in the kidney's thick ascending limb (TAL). Despite the importance of this cation/chloride cotransporter (CCC), the mechanisms that underlie its regulation are largely unknown. Here, we show that intracellular chloride depletion in *Xenopus laevis* oocytes, achieved by either coexpression of the K-Cl cotransporter KCC2 or low-chloride hypotonic stress, activates NKCC2 by promoting the phosphorylation of three highly conserved threonines (96, 101, and 111) in the amino terminus. Elimination of these residues renders NKCC2 unresponsive to reductions of $[Cl^-]_i$. The chloride-sensitive activation of NKCC2 requires the interaction of two serine-threonine kinases, WNK3 (related to WNK1 and WNK4, genes mutated in a Mendelian form of hypertension) and SPAK (a Ste20-type kinase known to interact with and phosphorylate other CCCs). WNK3 is positioned upstream of SPAK and appears to be the chloride-sensitive kinase. Elimination of WNK3's unique SPAK-binding motif prevents its activation of NKCC2, as does the mutation of threonines 96, 101, and 111. A catalytically inactive WNK3 mutant also completely prevents NKCC2 activation by intracellular chloride depletion. Together these data reveal a chloride-sensing mechanism that regulates NKCC2 and provide insight into how increases in the level of intracellular chloride in TAL cells, as seen in certain pathological states, could drastically impair renal salt reabsorption.

ion transport | loop of Henle | protein serine-threonine kinases | hypertension | diuretics

The renal-specific Na^+:K^+:2Cl^- cotransporter (NKCC2) is the major salt transport pathway of the apical membrane of the mammalian thick ascending limb (TAL) of Henle's loop. The activity of NKCC2 is critical for salt reabsorption, countercurrent multiplication, acid-base regulation, and divalent mineral cation metabolism (1). NKCC2 is the main pharmacological target of loop diuretic drugs used worldwide for the treatment of edematous states. The fundamental role of NKCC2 in human physiology and blood pressure regulation has been established by the finding that inactivating mutations in *SLC12A1*, the gene encoding NKCC2, causes Bartter syndrome type I (2), an autosomal recessive syndrome featuring severe volume depletion, hypokalemia, metabolic alkalosis, and hypercalciuria.

NKCC2 is an electroneutral cation-coupled chloride cotransporter (CCC) in the *SLC12* gene family that contains seven members encompassing two different branches. The sodium-driven branch (Na-[K]-Cl) comprises the thiazide-sensitive Na^+:Cl^- cotransporter NCC and two different isoforms of the Na^+:K^+:2Cl^- cotransporter—the ubiquitous NKCC1 and the kidney-specific NKCC2. The potassium-driven branch (KCCs) comprises four different K^+-Cl^- cotransporters, KCC1–KCC4. Studies have shown that CCCs are regulated by intracellular chloride concentration $[Cl^-]_i$ by means of phosphorylation and dephosphorylation events. Phosphorylation activates Na-[K]-CCs and inhibits KCCs, whereas dephosphorylation has the opposite effect (3–5). Extensive work performed with NKCC1 (6–11) has established that cotransporter activation by low intracellular chloride is associated with phosphorylation of specific threonines in its amino terminus. This phosphorylation appears to be due to the activation of a kinase, rather than the inhibition of a protein phosphatase; the existence of a kinase whose activity is modulated by $[Cl^-]_i$ has been proposed to account for these phenomena (12).

In recent years, serine/threonine kinases from two different gene families have been shown to fit the profile of "Cl^--sensing kinases." One is the WNK family, from which two members (WNK1 and WNK4) are mutated in pseudohypoaldosteronism type II, a Mendelian form of human hypertension. WNK3 increases the activity of the sodium-driven cotransporters Na-[K]-CCs, promoting Cl^- influx, but decreases the activity of the potassium-driven cotransporters KCC1–KCC4 to prevent Cl^- efflux. Through these reciprocal actions on cellular Cl^- influx and efflux pathways, WNK3 regulates the level of $[Cl^-]_i$ (13–15). The Ste20-type kinases SPAK/OSR1 become phosphorylated in response to decreases in $[Cl^-]_i$ and also regulate the activity of NKCC1 (12, 16–19). A link between these two different kinase families has been established by the finding that WNK1 and WNK4 interact with and phosphorylate SPAK/OSR1, which enables SPAK/OSR1 to physically associate with, phosphorylate, and activate NKCC1 (20–22).

Here, we show NKCC2 is regulated by $[Cl^-]_i$ and that phosphorylation of two conserved threonines in its amino terminal domain is involved. Activation of NKCC2 by intracellular chloride depletion requires an interaction between WNK3 and SPAK; WNK3 is positioned upstream of SPAK and appears to be the chloride-sensitive kinase. These observations define a regulatory pathway for NKCC2 and provide insight into how increases in $[Cl^-]_i$ in Bartter syndrome type III, which results from inactivating mutations in the TAL's basolateral Cl^- efflux channel CLC-KB, could lead to the inhibition of NKCC2 activity.

Results

NKCC2 Activity and Phosphorylation Are Increased by Intracellular Chloride-Depletion Maneuvers. We evaluated whether NKCC2 is regulated by $[Cl^-]_i$ by employing two experimental approaches

Author contributions: J.P.-C., P.S.-C., K.T.K., D.P.-A., N.A.B., I.G., R.P.L., S.C.H., and G.G. designed research; J.P.-C., P.S.-C., N.V., D.P.-A., P.d.l.H., P.J., E.M., G.M., I.G., and G.G. performed research; J.P.-C., P.S.-C., N.A.B., I.G., S.C.H., and G.G. analyzed data; and J.P.-C., P.S.-C., K.T.K., N.A.B., I.G., R.P.L., S.C.H., and G.G. wrote the paper.

The authors declare no conflict of interest.

**Deceased April 15, 2008.

††To whom correspondence should be addressed. E-mail: gamba@biomedicas.unam.mx.

This article contains supporting information online at www.pnas.org/cgi/content/full/0802966105/DCSupplemental.

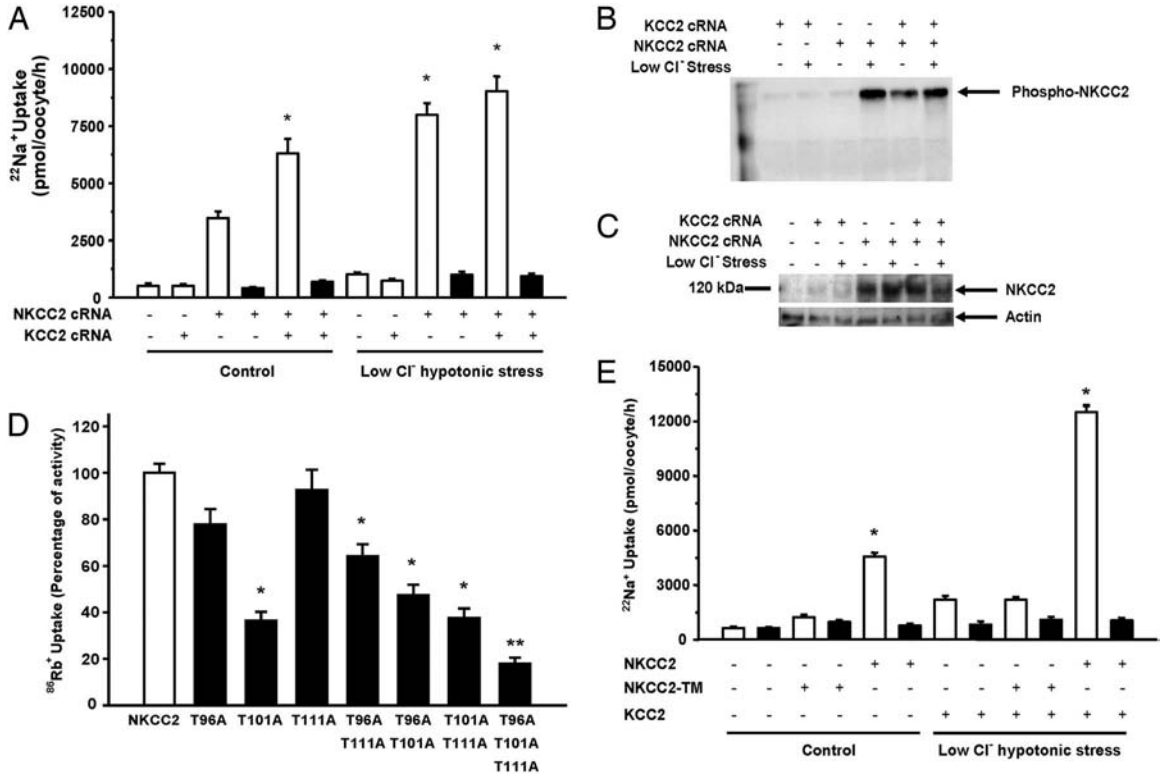

Fig. 1. Regulation of NKCC2 by intracellular chloride-depletion maneuvers. *Xenopus* oocytes were injected with water or 10 ng per oocyte of wild-type or mutant NKCC2 cRNA alone or together with 10 ng per oocyte of KCC2 cRNA, as stated. Four days later, influx experiments or Western blot analyses were performed in control conditions or under low-chloride stress. (*A*) $^{22}Na^+$ uptake was assessed in absence (open bars) or presence (filled bars) of 100 μM bumetanide. (*B*) A representative Western blot analysis performed by using the R5 phosphoantibody (26). (*C*) A representative Western blot analysis performed with polyclonal anti-NKCC2 and anti-actin antibody (41). (*D*) Uptake of $^{86}Rb^+$ was assessed in oocytes injected with water, wild-type, or mutant NKCC2. Mean value of wild-type NKCC2-injected oocytes was taken as 100%, and the value observed in mutants was normalized. *, significantly different from the uptake observed in wild-type NKCC2; **, significantly different to uptake observed in T101A. (*E*) Uptake of $^{22}Na^+$ in oocytes injected with water, wild-type NKCC2 cRNA, or triple-mutant NKCC2 exposed to control conditions and both chloride-depletion maneuvers as stated. Uptake of $^{22}Na^+$ was performed in the absence (open bars) or presence (filled bars) of 100 μM bumetanide. This is a representative experiment, and each bar represents the mean ± SEM of 10 oocytes. *, significantly different from the uptake observed in the corresponding control.

that have been used successfully to induce a sustained depletion of $[Cl^-]_i$ (7, 8, 21, 23, 24). The first strategy used coexpressing KCC2, a transporter that promotes chloride efflux in isotonic conditions (3). The second strategy used exposing oocytes to "low-Cl^- hypotonic stress," which induces the opening of Cl^- channels promoting Cl^- efflux (25). Oocytes expressing NKCC2 alone exhibited an increase in bumetanide-sensitive $^{22}Na^+$ uptake versus water-injected oocytes (Fig. 1*A*). Coexpression with KCC2 or incubation of oocytes in low-chloride hypotonic stress augmented bumetanide-sensitive $^{22}Na^+$ uptake (Fig. 1*A*). Exposing oocytes to both intracellular chloride-depletion maneuvers did not result in further activation of NKCC2.

Intracellular chloride depletion could augment NKCC2 function by increasing the phosphorylation of residues necessary for its activation, as has been shown previously to occur with shark NKCC1 (7) and NCC (24). In this regard, the amino terminal domain threonines that become phosphorylated in NKCC1 (T184 and T189) and NCC (T53 and T58) in response to chloride depletion are conserved in NKCC2 (T96 and T101); a third phospho-acceptor residue implicated in regulation of NKCC1 (T202) and NCC (S71) also is conserved in NKCC2 (T111) (24). R5 antibody, which recognizes phospho-threonines 184 and 189 in NKCC1, also is able to recognize phospho-threonines 96 and 101 in NKCC2 (26), and the phosphorylation of these threonines in NKCC2 has been shown to have a regulatory role *in vivo* (27). By using R5 antibody, phospho-NKCC2 was detected in homogenates extracted from oocytes expressing NKCC2 and exposed to low chloride stress and in homogenates from oocytes expressing both NKCC2 and KCC2, but not in those injected with water or expressing KCC2 and exposed to low chloride stress or oocytes expressing NKCC2 alone and exposed to control conditions during uptake (Fig. 1*B*). The amount of NKCC2 in oocytes was not affected by the intracellular chloride-depletion strategies (Fig. 1*C*). Densitometric analysis revealed that the ratio between phospho-NKCC2 (Fig. 1*B*) over total NKCC2 signals (Fig. 1*C*) of 0.14 in control condition increased to 1.06 after low-Cl^- stress, 1.03 after coinjection of KCC2, and 1.41 when both maneuvers were applied together. Thus, intracellular chloride depletion is associated with increased activity and phosphorylation of NKCC2 at the amino terminal threonines T96 and T101.

Elimination of the Amino Terminal Threonines T96, 101, and 111 Prevents NKCC2 Activation by Intracellular Chloride Depletion. Site-directed mutagenesis was used to substitute threonines 96, 101, and/or 111 of NKCC2 with alanine to produce single, double, or triple NKCC2 mutants. As shown in Fig. 1*D*, no significant effect was observed by the elimination of T96 or T111 on NKCC2 activity. However, NKCC2 activity was reduced 60% by mutation of T101. NKCC2 activity in the double mutant T96,111A was reduced by 40%, and double mutants in which T101 was involved had activity similar to the single mutant T101A. A triple mutant NKCC2 exhibited a further reduction of activity to nearly 85%. Thus, activity in the triple mutant was significantly lower

than in T101A. Thus, the behavior of the NKCC2 mutants differs from that of NKCC1 (7) or NCC (24), in which basal transporter activity depends on the presence of the second threonine. We exposed oocytes expressing wild-type NKCC2 or triple-mutant NKCC2 to both chloride-depletion maneuvers together (coexpression of KCC2 plus low-chloride hypotonic stress). As shown in Fig. 1*E*, a significant increase in NKCC2 activity was observed when both maneuvers were applied to oocytes expressing wild-type NKCC2. In contrast, the activity of triple mutant NKCC2 was not increased by chloride-depletion maneuvers. Thus, threonines 96, 101, and 111 not only become phosphorylated when NKCC2 is activated by intracellular chloride depletion, but also are required for its activation.

Regulation of NKCC2 Activity by WNK3 and SPAK Kinases. We next investigated whether the proposed "Cl^--sensing kinases" WNK3 and/or SPAK were involved in the mechanism by which intracellular chloride depletion increases NKCC2 activity because these kinases have been shown to regulate other CCCs. Similar to our previous findings (15), the coexpression of NKCC2 with WNK3 resulted in a significant increase in NKCC2 activity by >2-fold [supporting information (SI) Fig. S1]. No effect was observed when SPAK was coexpressed with NKCC2, but the coexpression of SPAK with WNK3 and NKCC2 resulted in a greater increase in bumetanide-sensitive $^{86}Rb^+$ uptake than was seen in oocytes expressing WNK3 and NKCC2 (Fig. S1). Because oocytes express WNK and SPAK orthologs that might be important for the functional regulation of heterologous-expressed NKCC2, we analyzed the effect of reducing the endogenous activity of these kinases by coexpressing NKCC2 together with catalytically inactive forms of WNK3 (D294A, termed WNK3-DA) (15) or SPAK (K104R, termed SPAK-KR) that serve as dominant-negative-type mutants or as inhibitors (16). Basal activity of NKCC2 was reduced 65 ± 6.5% ($P < 0.05$) by coinjecting WNK3-DA cRNA and 47 ± 2.6% ($P < 0.05$) with SPAK-KR coexpression. A similar type of inhibition has been observed for NKCC1 when coexpressed with inactive SPAK-KR (12, 19). Thus, although wild-type SPAK had no effect on NKCC2 (Fig. S1), inactive SPAK-KR significantly reduces basal NKCC2 activity. These data show that NKCC2 is inhibited by the catalytically inactive forms of WNK3 and SPAK and suggest that both kinases are required to maintain NKCC2 basal activity.

WNK3 Lies Upstream of SPAK for NKCC2 Activation. WNK1 and WNK4 lie upstream of SPAK in the regulation of NKCC1 (20, 21). Because both WNK3-DA and SPAK-KR inhibit NKCC2, we tested whether WNK3 and SPAK function in the same pathway in the regulation of NKCC2 by injecting WNK3-DA cRNA or SPAK-KR cRNA alone or both inactive kinases together. To increase our ability for detecting additive effects, lesser amounts of each kinase cRNA were injected. Data were normalized to the $^{86}Rb^+$ uptakes in oocytes injected with only NKCC2 (Fig. 2, filled bars). As shown in Fig. 2*A*, coexpression of WNK3-DA or SPAK-KR resulted in a significant 25% inhibition of NKCC2. When both inactive kinases were coexpressed, no further inhibition was observed. These data suggest that WNK3 and SPAK operate in series, and not parallel pathways, to regulate NKCC2.

We next coexpressed inactive WNK3-DA or SPAK-KR in combination with the wild-type SPAK or WNK3, respectively, to determine which kinase is able to rescue NKCC2 from the inhibitory effect of the other's inactive form. Wild-type WNK3 activated NKCC2 in the presence of SPAK-KR (Fig. 2*B*). In contrast, in the presence of WNK3-DA, the coexpression of wild-type SPAK did not activate NKCC2 (Fig. 2*C*). These observations suggest that WNK3 is positioned upstream of SPAK.

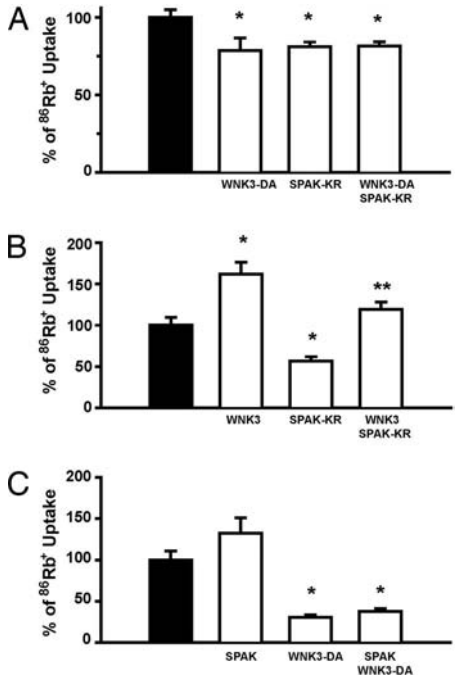

Fig. 2. Effect of the catalytically inactive kinases WNK3-DA and SPAK-KR on the functional expression of NKCC2. For all figures, oocytes were injected with water or 10 ng per oocyte of NKCC2 cRNA alone or together with the active or inactive kinases as stated. Three days later, $^{86}Rb^+$ uptake was assessed. Values observed in oocytes injected with NKCC2 alone were taken as 100% for normalization purpose. (*A*) Oocytes were injected with NKCC2 cRNA alone (filled bar) or together with 2.5 ng per oocyte of WNK3-DA cRNA or SPAK-KR cRNA alone or both inactive kinases together (open bars) as stated. (*B*) Oocytes were injected with NKCC2 cRNA alone (filled bar) or together with 5 ng/oocyte of wild-type WNK3 cRNA with or without 5 ng/oocyte of SPAK-KR cRNA (open bars). (*C*) Oocytes were injected with NKCC2 cRNA alone (filled bar) or together with 5 ng per oocyte of WNK3-DA cRNA with or without 5 ng per oocyte of wild-type SPAK cRNA (open bars). *, significantly different from the uptake observed in the NKCC2 cRNA group; **, significantly different from the uptake observed in the NKCC2 cRNA plus SPAK-KR cRNA group.

A SPAK-Binding Motif in WNK3 Is Necessary for WNK3's Activation of NKCC2. According to a recent genome-wide analysis (28), the sequence GRFQVITI in the carboxyl-terminal regulatory domain of WNK3 represents a unique SPAK-binding site that is conserved in mouse, rat, and human WNK3. Thus, the effect of wild-type or WNK3-F1337A on NKCC2 activity and WNK3-SPAK interaction was analyzed. Wild-type WNK3 was able to increase activity, but this effect was completely absent with WNK3-F1337A (Fig. 3*A*). Consistent with this observation, HA-SPAK was coprecipitated with wild-type c-Myc-WNK3, but not with c-Myc-WNK3-F1337A (Fig. 3*B*), suggesting that to activate NKCC2, WNK3 and SPAK form a protein complex. The lack of WNK3-F1337A effect on NKCC2 could be alternatively explained if the mutation F1337A reduces WNK3 kinase expression and/or activity, but this scenario is unlikely for three reasons. First, expression of c-Myc-WNK3 or c-Myc-WNK3-F1337A was similar (Fig. 3*C*). Second, WNK3 without catalytic activity (Fig. 2*A*) inhibits NKCC2, whereas WNK3-F1337A mutant does not (Fig. 3*A*). Third, the effect of WNK3-F1337A on KCC4 demonstrates that this construct contains catalytic activity. Both wild-type WNK3 and WNK3-F1337A reduced the activity of KCC4 when oocytes were incubated in hypotonic conditions. Because catalytic activity of WNK3 is required for KCC4 inhibition (13), this observation demonstrates that WNK3-F1337A is an active kinase. Interestingly, this observation also shows that the mechanisms by which WNK3 activates

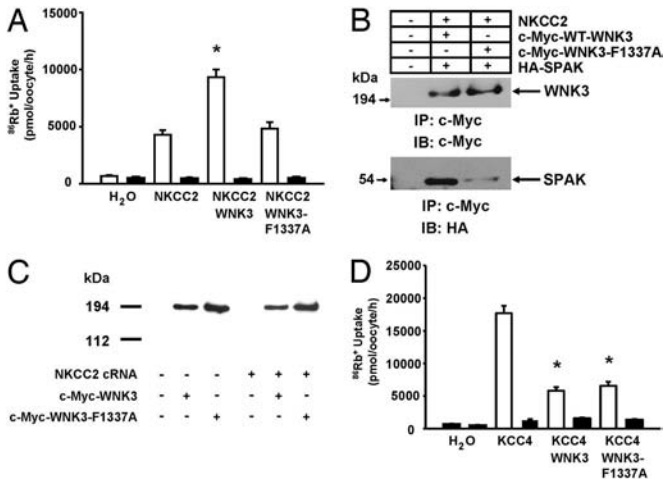

Fig. 3. Effect of elimination of the unique SPAK binding site of WNK3 on the kinase expression and its effects on NKCC2 and KCC4. (*A*) Uptake of $^{86}Rb^+$ in oocytes injected with water, NKCC2 cRNA alone or together with wild-type c-Myc-WNK3 cRNA, or c-Myc-WNK3-F1337A cRNA. Uptake was performed in isotonic conditions in the absence (open bars) or presence (filled bars) of 100 μM bumetanide. *, significantly different from the uptake observed in NKCC2 cRNA group. (*B*) Oocytes were injected with water, NKCC2 cRNA, c-Myc-WNK3 cRNA, c-Myc-WNK3-F1337A cRNA, and/or HA-SPAK cRNA as stated. Three days later, c-Myc-WNK3 or c-Myc-WNK3-F1337A were immunoprecipitated from corresponding protein homogenates, resolved in SDS/PAGE, and transferred to PDFV membranes. Western blot analyses were performed by using anti-c-Myc or anti-HA monoclonal antibodies as stated. (*C*) Representative Western blot analysis of proteins extracted from oocytes 3 days after injection with water or NKCC2 cRNA alone or together with wild-type c-Myc-WNK3 cRNA or c-Myc-WNK3-F1337A cRNA as stated. Similar results were observed in the absence of NKCC2 cRNA injections. (*D*) Uptake of $^{86}Rb^+$ in oocytes injected with water, KCC4 cRNA alone or together with wild-type c-Myc-WNK3 cRNA, or c-Myc-WNK3-F1337A cRNA in hypotonic conditions in the presence (open bars) or absence (filled bars) of extracellular chloride. *, significantly different from the uptake observed in the KCC4 cRNA group.

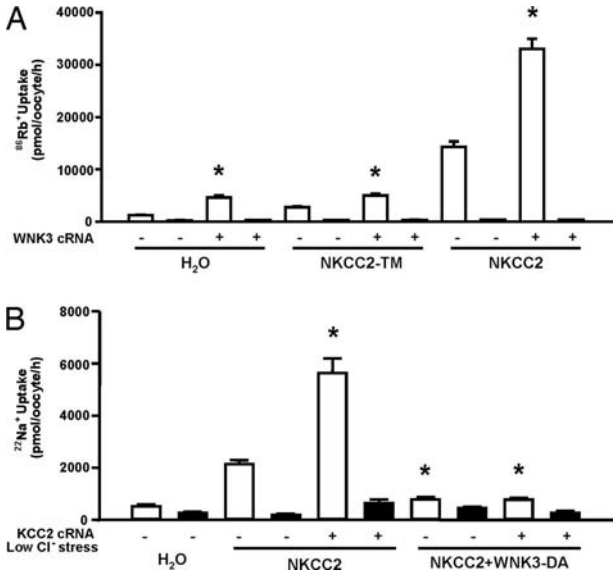

Fig. 4. Effect of elimination of the threonines 96, 101, and 111 in NKCC2 (NKCC2-TM) or coinjection of wild-type NKCC2 and WNK3-DA on the response to wild-type WNK3 or chloride depletion maneuvers. (*A*) Oocytes injected with water, wild-type NKCC2, and triple-mutant NKCC2 were coinjected with WNK3 cRNA as stated. Four days later, $^{86}Rb^+$ uptake was assessed in control isotonic conditions. Values observed in water-injected oocytes were subtracted to all groups. *, significantly different from the uptake observed in the corresponding group in the absence of WNK3. (*B*) *Xenopus laevis* oocytes were injected with water, with NKCC2 cRNA alone, or together with KCC2 cRNA and/or WNK3-DA as stated. Uptakes of $^{22}Na^+$ were performed in control isotonic conditions or under low-chloride hypotonic stress in the absence (open bars) or presence (filled bars) of 100 μM bumetanide. *, significantly different from the uptake observed in the NKCC2 control group.

NKCC2 or inhibits KCCs activity are different: Interaction between WNK3 and SPAK is required for NKCC2 activation, but is not necessary for KCC4 inhibition. In this regard, another difference is that WNK3-DA inhibitory effect on NKCC2 is a dominant-negative type of effect, whereas activation of KCCs is not (Fig. S2). Moreover, we have previously shown that activation of KCCs by WNK3-DA is prevented by protein phosphatase inhibitors (13), although this is not the case for NKCC2 inhibitory effect on WNK3-DA or SPAK-KR (Fig. S3).

Amino Terminal Threonines 96, 101, and 111 Are Required for WNK3-Induced Activation of NKCC2. We have previously shown that increased activity of NKCC2 by WNK3 is associated with phosphorylation of threonines 96 and 101, as detected by the R5 phosphoantibody (15). Thus, we analyzed the effect of WNK3 on NKCC2 harboring the triple mutation (T96,101,111A) that eliminates the response to intracellular chloride depletion (Fig. 1*D*). As shown in Fig. 4*A*, WNK3 increased the activity of wild-type NKCC2, but had no effect on the NKCC2 triple mutant in which all three threonines were eliminated. These data suggest that the activation of NKCC2 by WNK3 is due to phosphorylation and requires the presence of threonines 96, 101, and 111. Because intracellular chloride depletion also activates NKCC2 by phosphorylating these residues, we reasoned that WNK3 could be the kinase translating the decrease of $[Cl^-]_i$, into NKCC2 activation, and, in this case, catalytically inactive WNK3-DA should prevent the activation of NKCC2 by intracellular chloride-depletion maneuvers. We therefore tested the effect of both chloride-depletion maneuvers together (coexpression of KCC2 plus low-chloride stress) on NKCC2 activity coexpressed with WNK3-DA. In the presence of WNK3-DA, the activity of NKCC2 was significantly reduced, as shown previously. Intracellular chloride depletion, however, failed to increase the $^{86}Rb^+$ uptake mediated by NKCC2 under these conditions (Fig. 4*B*). These data show that NKCC2's activation by intracellular chloride depletion is prevented by WNK3-DA.

Discussion

In the present study, we demonstrate that rat NKCC2 expressed in oocytes is activated by intracellular chloride depletion and is associated with phosphorylation of the cotransporter at threonines 96 and 101. Elimination of these two residues, together with T111, renders NKCC2 less active and unresponsive to reduction of $[Cl^-]_i$. The regulation of NKCC2 by intracellular chloride depletion requires interaction between WNK3 and SPAK, in a pathway in which WNK3 lies upstream of SPAK. This is demonstrated by the fact that eliminating the unique SPAK-binding site in WNK3 (F1337A) prevents the activation of NKCC2 by this kinase. Mutation of threonines 96, 101, and 111 also prevented the response of NKCC2 to WNK3, and overexpression of the catalytically inactive WNK3-DA completely prevented the activation of NKCC2 by intracellular chloride depletion. These data together suggest that changes in $[Cl^-]_i$ are sensed by WNK3, which in turn interacts with and activates SPAK, promoting the phosphorylation of NKCC2 at threonines 96, 101, and 111, which results in increased activity of the cotransporter.

The regulation of WNK kinases by $[Cl^-]_i$ has been previously demonstrated. When Xu *et al.* (29) first cloned the cDNA encoding WNK1, they observed that, from a variety of potential stimuli to regulate WNK1, the only positive one was NaCl

PHYSIOLOGY

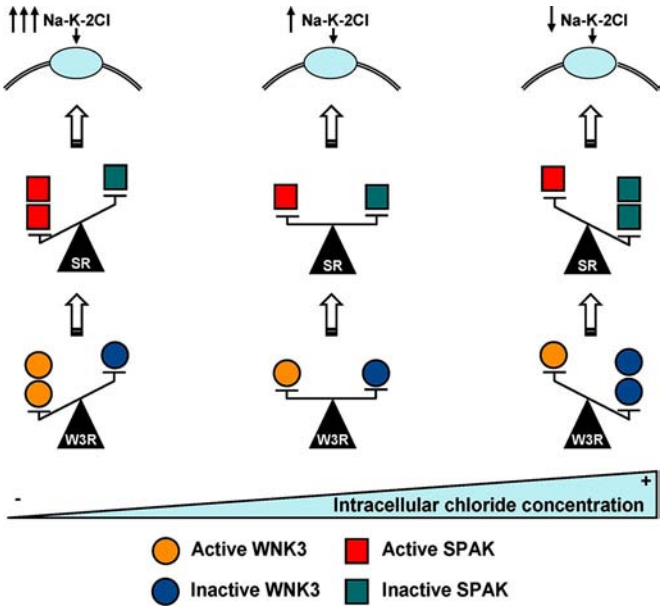

Fig. 5. Proposed model for intracellular chloride, WNK3, and SPAK interaction in the control of NKCC2 activity.

concentration. Later, Lenertz *et al.* (30) showed that WNK1 is activated by osmotic challenges in a variety of cell lines. Moriguchi *et al.* (21) observed in HEK293 cells that the activity of WNK1 and of SPAK/OSR1 kinases is increased by lowering $[Cl^-]_i$ and proposed that WNK1 behaves as an activator of SPAK/OSR1 in response to a decrease in the $[Cl^-]_i$. It remains to be determined how changes in $[Cl^-]_i$ affect the kinase activity of WNK3, if WNK3 directly phosphorylates SPAK, and how a WNK3–SPAK interaction phosphorylates NKCC2.

Fig. 5 depicts our proposed model for the WNK3–SPAK pathway in the regulation of NKCC2. We propose that variations in $[Cl^-]_i$ are associated with changes in the ratio of active versus inactive WNK3 kinase (W3R). Injecting oocytes with wild-type WNK3 cRNA, by increasing W3R, mimics a situation in which $[Cl^-]_i$ is reduced. Increased W3R in turn increases the active versus inactive SPAK kinase ratio (SR) that promotes NKCC2 phosphorylation, thereby increasing the activity of the cotransporter. In contrast, injecting oocytes with WNK3-DA cRNA, by decreasing the W3R, mimics increases in $[Cl^-]_i$, which in turn decreases SR and thus prevents phosphorylation and activation of NKCC2. Injecting oocytes with wild-type SPAK cRNA alone cannot mimic the activation of NKCC2 seen with the reduction of $[Cl^-]_i$ because, although the number of SPAK copies increases, they are not activated by the low amount of WNK3. In contrast, injecting oocytes with inactive SPAK-KR cRNA simulates an increase in $[Cl^-]_i$ because the overexpression of this inactive kinase reduces SR. This model also helps to explain why wild-type SPAK is unable to reverse NKCC2 inhibition by WNK3-DA, but wild-type WNK3 can overcome the inhibition of NKCC2 by SPAK-KR. The latter occurs because, even in the presence of SPAK-KR, overexpression of wild-type WNK3 will increase the SR via activation of endogenous SPAK. By disrupting the SPAK-binding motif of WNK3 (WNK3–F1337A), WNK3 is no longer able to interact with SPAK and thus cannot increase the SR. Thus, NKCC2 activation does not occur. Finally, because the catalytically inactive WNK3-DA exerts a dominant negative-type effect on endogenous WNK3, intracellular chloride depletion no longer activates NKCC2 in the presence of WNK3-DA.

Bartter's syndrome is a heterogeneous disease in which inactivating mutations in NKCC2, the potassium channel ROMK, and the basolateral chloride channel ClC-KB have been shown to cause Bartter's syndrome type I, II, and III, respectively (31). The mechanisms of disease in Bartter's syndrome type I and II are easily understood; inactivation of NKCC2 directly impairs salt flux through transporter, whereas mutations in ROMK disrupt the potassium-recycling mechanism necessary for continued NKCC2 function. Both types are clinically evident since birth or even before as polyhydramnios. In contrast, the mechanisms by which mutations in ClC-KB cause disease are unclear. Patients with the type III variant show a less severe phenotype that is not clinically evident until late in the first year of life, often exhibiting combined features of Bartter's and Gitelman's syndrome (another form of Mendelian hypotension due to mutations in NCC). In the case of Bartter's type III, CLC-KB-inactivating mutations, by preventing chloride efflux from cells, might indirectly impair the activity of NKCC2 in the TAL and in some cases also of NCC in the DCT, but the clinical consequences takes time to develop until the nephron reaches its maximum development in the early postnatal life (32). Consistent with this hypothesis are the data from this and a previous study (24) that NKCC2 and NCC are regulated by intracellular chloride. Thus, we believe that our observations help to define a regulatory pathway of NKCC2 that provides insight into how increases in $[Cl^-]_i$ in Bartter's syndrome type III could lead to the inhibition of NKCC2 (and NCC) activity.

In conclusion, our data demonstrate that NKCC2 is activated by intracellular chloride depletion by a mechanism that involves WNK3 and SPAK kinases. WNK3 appears to be the Cl^--sensing kinase that in turn physically interacts with SPAK by means of a unique SPAK-binding site. The interaction results in the activation of SPAK and then in the phosphorylation of NKCC2 at the amino terminal domain threonines 96, 101, and probably 111, which, in turn, results in an increase in NKCC2 activity.

Methods

Clones and Mutagenesis. The cDNAs used in this study were previously described (15, 33–38). Site-directed mutations (QuikChange; Stratagene) were performed to substitute threonines 96, 101, and/or 111 of NKCC2 and WNK3 phenylalanine 1337 for alanine. c-Myc-epitope-tag was introduced into WNK3 after the ATG starting codon by using double-step PCR. A construct containing a fragment of WNK3 from residues 410–482 was done by PCR, and a flag epitope tag was engineered in frame with the rest of coding region. DNA sequencing was used to confirm all mutations. All primers were custom made (Sigma).

Assessment of the Na^+:K^+:2Cl^- and K^+-Cl^- Cotransporters' Function. rNKCC2 activity was assessed by functional expression in *Xenopus laevis* oocytes as described (15, 33, 39). Oocytes were injected with water or rNKCC2 cRNA (10 ng/oocyte) and exposed to two different conditions that promote a decrease in the $[Cl^-]_i$: coinjection with the K^+:Cl^- cotransporter KCC2 cRNA (10 ng/oocyte), and low-Cl^- hypotonic stress (24). For influx details and all solutions contents, see *SI Methods*.

Western Blot Analysis and NKCC2 Phosphoantibody Studies. Immunoblots were performed by using a rabbit polyclonal anti-NKCC2 antibody following our previously published protocol (41). Expression of proteins harboring the FLAG (for WNK3–410-482 fragment), HA (for SPAK or SPAK-KR), and c-Myc epitopes (for WNK3, WNK3-DA or WNK3-F1337A) were detected by using the appropriate peroxidase-conjugated monoclonal antibodies (Sigma). R5 antibody was used to detect the phosphorylation status of T96 and T101 in NKCC2 as described previously (26).

Data Analysis. All results presented are based on a minimum of three different experiments with at least 10 oocytes per group in each experiment. Statistical significance is defined as two-tailed, with $P < 0.05$, and the results are presented as mean ± SEM. The significance of the differences between groups was tested by one-way ANOVA with multiple comparisons using Bonferroni's correction.

ACKNOWLEDGMENTS. This work was supported, in part, by National Institutes of Health Grant DK-64635 (to G.G.), El Consejo Nacional de Ciencia y Tecnología (Mexico) Grant 59992 (to G.G.), and a Foundation Leducq for the Transatlantic Network on Hypertension-Renal Salt Handling in the Control of Blood Pressure grant (to G.G, S.C.H., and R.P.L.).

1. Gamba G (1999) Molecular biology of distal nephron sodium transport mechanisms. *Kidney Int* 56:1606–1622.
2. Simon DB, *et al*. (1996) Bartter's syndrome, hypokalaemic alkalosis with hypercalciuria, is caused by mutations in the Na-K-2Cl cotransporter NKCC2. *Nat Genet* 13:183–188.
3. Gamba G (2005) Molecular physiology and pathophysiology of the electroneutral cation-chloride cotransporters. *Physiol Rev* 85:423–493.
4. Adragna NC, Fulvio MD, Lauf PK (2004) Regulation of K-Cl cotransport: From function to genes. *J Membr Biol* 201:109–137.
5. Flatman PW (2007) Cotransporters, WNKs and hypertension: Important leads from the study of monogenetic disorders of blood pressure regulation. *Clin Sci (London)* 112:203–216.
6. Darman RB, Flemmer A, Forbush B (2001) Modulation of ion transport by direct targeting of protein phosphatase type 1 to the Na-K-Cl cotransporter. *J Biol Chem* 276:34359–34362.
7. Darman RB, Forbush B (2002) A regulatory locus of phosphorylation in the N terminus of the Na-K-Cl cotransporter, NKCC1. *J Biol Chem* 277:37542–37550.
8. Flemmer AW, Gimenez I, Dowd BF, Darman RB, Forbush B (2002) Activation of the Na-K-Cl transporter NKCC1 detected with a phospho-specific antibody. *J Biol Chem* 277:37551–37558.
9. Lytle C, Forbush B, III (1992) The Na-K-Cl cotransport protein of shark rectal gland. II Regulation by direct phosphorylation. *J Biol Chem* 267:25438–25443.
10. Lytle C, McManus T (2002) Coordinate modulation of Na-K-2Cl cotransport and K-Cl cotransport by cell volume and chloride. *Am J Physiol* 283:C1422–C1431.
11. Lytle C, Forbush B, III (1996) Regulatory phosphorylation of the secretory Na-K-Cl cotransporter: Modulation by cytoplasmic Cl. *Am J Physiol* 270:C437–C448.
12. Dowd BF, Forbush B (2003) PASK (proline-alanine-rich STE20-related kinase), a regulatory kinase of the Na-K-Cl cotransporter (NKCC1). *J Biol Chem* 278:27347–27353.
13. De Los Heros P, *et al*. (2006) WNK3 bypasses the tonicity requirement for K-Cl cotransporter activation via a phosphatase-dependent pathway. *Proc Natl Acad Sci USA* 103:1976–1981.
14. Kahle, *et al*. (2005) WNK3 modulates transport of Cl- in and out of cells: Implications for control of cell volume and neuronal excitability. *Proc Natl Acad Sci USA* 102:16783–16788.
15. Rinehart, *et al*. (2005) WNK3 kinase is a positive regulator of NKCC2 and NCC, renal cation-Cl− cotransporters required for normal blood pressure homeostasis. *Proc Natl Acad Sci USA* 102:16777–16782.
16. Gagnon KB, England R, Delpire E (2006) Characterization of SPAK and OSR1, regulatory kinases of the Na-K-2Cl Cotransporter. *Mol Cell Biol* 26:689–698.
17. Piechotta K, Lu J, Delpire E (2002) Cation chloride cotransporters interact with the stress-related kinases Ste20-related proline-alanine-rich kinase (SPAK) and oxidative stress response 1 (OSR1). *J Biol Chem* 277:50812–50819.
18. Piechotta K, Garbarini N, England R, Delpire E (2003) Characterization of the interaction of the stress kinase SPAK with the Na+-K+-2Cl− cotransporter in the nervous system: Evidence for a scaffolding role of the kinase. *J Biol Chem* 278:52848–52856.
19. Delpire E, Gagnon KB (2006) SPAK and OSR1, key kinases involved in the regulation of chloride transport. *Acta Physiol (Oxford)* 187:103–113.
20. Vitari AC, Deak M, Morrice NA, Alessi DR (2005) The WNK1 and WNK4 protein kinases that are mutated in Gordon's hypertension syndrome, phosphorylate and active SPAK and OSR1 protein kinases. *Biochem J* 391:17–24.
21. Moriguchi, *et al*. (2005) WNK1 regulates phosphorylation of cation-chloride-coupled cotransporters via the STE20-related kinases, SPAK and OSR1. *J Biol Chem* 280:42685–42693.
22. Vitari, *et al*. (2006) Functional interactions of the SPAK/OSR1 kinases with their upstream activator WNK1 and downstream substrate NKCC1. *Biochemistry* 397:223–231.
23. Keicher E, Meech R (1994) Endogenous Na^+-K^+(or NH_4^+)-2Cl− cotransport in *Rana* oocytes; anomalous effect of external NH_4^+ on PH_i. *J Physiol* 475:45–57.
24. Pacheco-Alvarez D, *et al*. (2006) The Na-Cl cotransporter is activated and phosphorylated at the amino terminal domain upon intracellular chloride depletion. *J Biol Chem* 281:28755–28763.
25. Ackerman MJ, Wickman KD, Clapham DE (1994) Hypotonicity activates a native chloride current in *Xenopus* oocytes. *J Gen Physiol* 103:153–179.
26. Gimenez I, Forbush B (2005) Regulatory phosphorylation sites in the N-terminus of the renal Na-K-Cl cotransporter (NKCC2). *Am J Physiol* 289:F1341–F1345.
27. Gimenez I, Forbush B, (2003) Short-term stimulation of the renal Na-K-Cl cotransporter (NKCC2) by vasopressin involves phosphorylation and membrane translocation of the protein. *J Biol Chem* 278:26946–26951.
28. Delpire E, Gagnon KB (2007) Genome-wide analysis of SPAK/OSR1 binding motifs. *Physiol Genomics* 28:223–231.
29. Xu B, *et al*. (2000) WNK1, a novel mammalian serine/threonine protein kinase lacking the catalytic lysine in subdomain II. *J Biol Chem* 275:16795–16801.
30. Lenertz LY, *et al*. (2005) Properties of WNK1 and implications for other family members. *J Biol Chem* 280:26653–26658.
31. Hebert SC (2003) Bartter syndrome. *Curr Opin Nephrol Hypertens* 12:527–532.
32. Horster M (2000) Embryonic epithelial membrane transporters. *Am J Physiol* 279:F982–F996.
33. Gamba G, *et al*. (1994) Molecular cloning, primary structure and characterization of two members of the mammalian electroneutral sodium-(potassium)-chloride cotransporter family expressed in kidney. *J Biol Chem* 269:17713–17722.
34. Plata C, Meade P, Vazquez N, Hebert SC, Gamba G (2002) Functional properties of the apical Na+:K+:2Cl− cotransporter isoforms. *J Biol Chem* 277:11004-11012.
35. Song L, *et al*. (2002) Molecular, functional, and genomic characterization of human KCC2, the neuronal K-Cl cotransporter. *Brain Res Mol Brain Res* 103:91–105.
36. Mount DB, *et al*. (1999) Cloning and characterization of KCC3 and KCC4, new members of the cation-chloride cotransporter gene family. *J Biol Chem* 274:16355–16362.
37. Gagnon KB, England R, Delpire E (2006) Volume sensitivity of cation-Cl− cotransporters is modulated by the interaction of two kinases: Ste20-related proline-alanine-rich kinase and WNK4. *Am J Physiol* 290:C134–C142.
38. Garzon-Muvdi T, *et al*. (2007) WNK4 kinase is a negative regulator of K+-Cl− cotransporters. *Am J Physiol* 292:F1197–F1207.
39. Meade P, *et al*. (2003) cAMP-dependent activation of the renal-specific Na+-K+-2Cl− cotransporter is mediated by regulation of cotransporter trafficking. *Am J Physiol* 284:F1145–F1154.
40. Mercado A, Song L, Vazquez N, Mount DB, Gamba G (2000) Functional comparison of the K+-Cl− cotransporters KCC1 and KCC4. *J Biol Chem* 275:30326–30334.
41. Paredes A, *et al*. (2006) Activity of the renal Na+:K+:2Cl− cotransporter is reduced by mutagenesis of *N*-glycosylation sites: Role for protein surface charge in Cl− transport. *Am J Physiol* 290:F1094–F1102.

CONCLUSIONES GENERALES

En el trabajo publicado "***Regulation of NKCC2 by a chloride-sensing mechanism involving the WNK3 and SPAK kinases***" hemos demostrado que la actividad de NKCC2 se incrementa por maniobras que reducen la $[Cl^-]_i$, y que este evento se asocia con fosforilación de las treoninas 96, 101 y 113 de la región amino terminal. La eliminación de estos residuos disminuye la actividad basal de NKCC2 y previene por completo su activación por las maniobras utilizadas que reducen la $[Cl^-]_i$

Por otro lado, mostramos que la actividad basal y la respuesta de NKCC2 a la disminución de la $[Cl^-]_i$ es regulada por las cinasas WNK3 y SPAK. La cinasa WNK3 está "río arriba" de la cinasa SPAK; dentro de una cascada de señalización que conduce a la fosforilación de los residuos amino terminales (treoninas 96, 101 y 113) y la consecuente activación de NKCC2.

Al eliminar las treoninas amino terminales en NKCC2, se previene la activación del cotransportador por la cinasa WNK3 y durante maniobras de depleción de $[Cl^-]_i$. De manera consistente, la coexpresión de la cinasa WNK3-D294A catalíticamente inactiva, impide la activación del cotransportador durante disminuciones en $[Cl^-]_i$.

Con los resultados obtenidos a partir de dicha publicación nos permiten proponer que la [Cl-]i regula la actividad de WNK3 y que esta a su vez regula la actividad de SPAK, la cual probablemente se encarga de fosforilar al NKCC2 en la región amino terminal, y con lo anterior, modular su actividad.

Muy probablemente en los síndromes de Bartter tipo III y IV, mediante el incremento de la $[Cl^-]_i$, la via de señalización WNK3 y SPAK para la activación de NKCC2 se encuentre interrumpida y por lo tanto, la actividad de NKCC2 se reduzca, conduciendo al desarrollo de la enfermedad.

RESULTADOS AUN NO PUBLICADOS

Durante mis estudios de doctorado también me dediqué a estudiar el papel del sitio de interacción con las cinasas SPAK-OSR1 presente en la secuencia de NKCC2 de rata. Este sitio de interacción con las cinasas SPAK-OSR1 se encuentra conservado a lo largo de las especies y de manera importante, el humano no es la excepción.

Utilizando ensayos de doble híbrido en levadura se ha podido establecer que mediante la sustitución de la fenilalanina, presente en el motivo de interacción con SPAK-OSR1 por un residuo de alanina, se puede eliminar la interacción física entre dichas cinasas y las proteínas al momento evaluadas.

En NKCC2 de rata, la fenilalanina presente dentro del motivo de unión a SPAK-OSR1 se localiza en la posición 17 dentro de la región amino terminal citoplásmica. Con el fin de evaluar el papel del sitio de interacción a SPAK-OSR1 en NKCC2, nos dimos a la tarea de generar la clona NKCC2-F17A. En dicha clona, se logró de manera exitosa sustituir la fenilalanina en la posición 17, por un residuo de alanina y por lo tanto eliminar el sitio de unión a SPAK-OSR1.

Al evaluar el papel de la eliminación del sitio de unión a SPAK-OSR1 sobre la actividad basal de NKCC2 encontramos que su eliminación redujo significativamente en un 50% la actividad basal de NKCC2 (**Fig. 36A**). La inhibición o reducción de la actividad de NKCC2 F17A, no se debió a diferentes cantidades de ARN complementario (ARNc) utilizado para la microinyección de los ovocitos de la rana *Xenopus laevis* (**Fig. 36B**), ni a una disminución de los niveles totales de proteína de NKCC2-F17A evaluados mediante análisis de transferencia tipo western blot y normalizados con la cantidad de actina endógena (**Fig. 36C**).

Posteriormente, nos dimos a la tarea de evaluar el efecto de la coexpresión de la cinasa WNK3 sobre la actividad del cotransportador NKCC2-F17A. De manera similar a lo que ocurre con un NKCC2 silvestre, la coexpresión de WNK3 resultó en un incremento estadísticamente significativo sobre la actividad de NKCC2-F17A (**Fig. 37**). En otras palabras, si bien es cierto que la eliminación del sitio de unión SPAK-OSR1 en NKCC2 reduce significativamente en un 50% su actividad basal, NKCC2 F17A ausente del sitio

de unión a SPAK continua siendo estimulado por la coexpresión de la cinasa WNK3 (**Fig. 2A**)

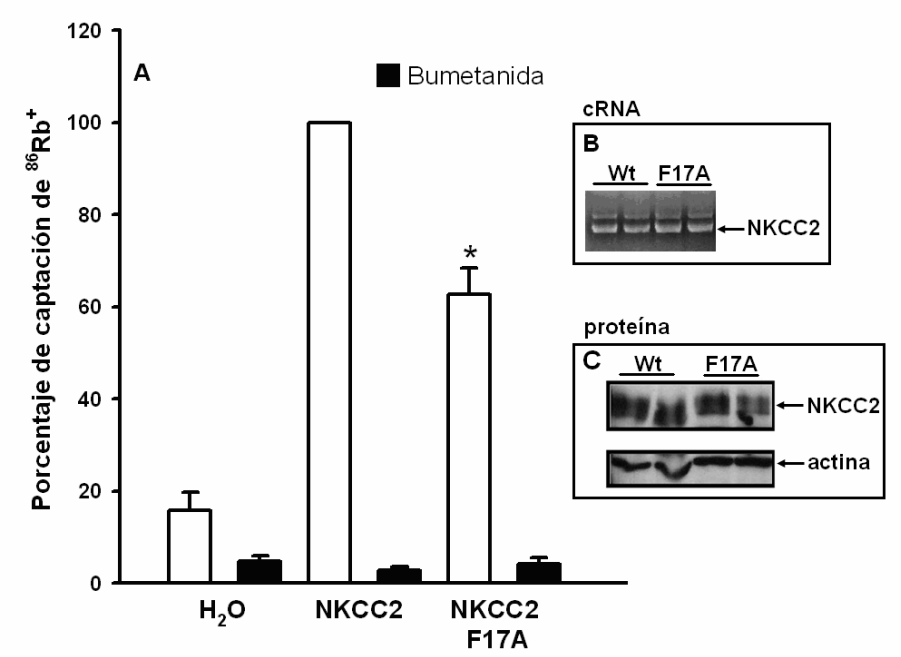

Figura 36. Efecto de la eliminación del sitio de unión a la cinasa SPAK presente en NKCC2.

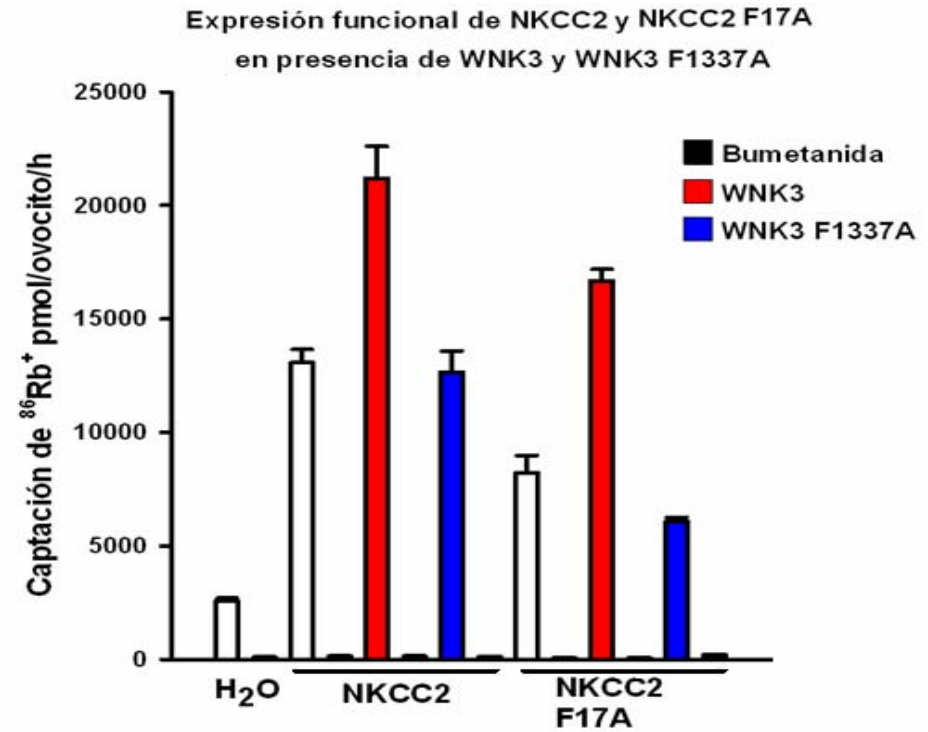

Figura 37. Efecto de WNK3 y WNK3 F1337A sobre la actividad de NKCC2 silvestre y NKCC2-F17A.

Creemos que a pesar de que la interacción entre NKCC2 y SPAK se encuentra abatida en NKCC2-F17A, sigue exisitiendo la interacción entre WNK3 y SPAK la cual puede continuar resultando en la activación de NKCC2.

Para demostrar lo anterior, nos dimos a la tarea de evaluar el efecto de la cinasa WNK3-F1337A sobre la actividad de NKCC2-F17A ausente del sitio de unión a la cinasa SPAK-OSR1. Como se demostró en el trabajo central de esta tesis (Ponce-Coria et al 2008), para la activación de NKCC2 por WNK3 es necesaria la interaccion física entre WNK3 y SPAK. En la figura 37 podemos observar que la coexpresión de la cinasa WNK3-F1337A tuvo el mismo efecto sobre NKCC2 silvestre y NKCC2-F17A (**Fig. 37**). Con lo anterior se puede concluir que de igual forma a la que ocurre con NKCC2 silvestre, WNK3-F1337A no puede activar a NKCC2-F17A y la interacción clave para activar a NKCC2 parece ser la existente entre WNK3 y SPAK, mientras que para sostener la actividad basal de NKCC2, la unión entre SPAK y NKCC2 parece ser crítica.

A la fecha, SPAK y OSR1 han sido observadas como cinasas con actividades redundantes principalmente porque: a) comparten un alto grado de homología a nivel de secuencia de aminoacidos (~60%) que las ubica en la misma subfamilia (GCK-VI) de las cinasa Ste20p, b) comparten sitios de expresión a nivel proteíco y son capaces de interactuar con aquellas proteínas que presentan el motivo de aminoácidos (Arg-Phe-Xaa-Val), c) parecen ser blancos comunes de fosforilación al menos para las cinasas WNK1 y WNK4 para promover la actividad y el estado de fosforilación de NKCC1.

Si bien es cierto que lo anterior ha sido demostrado de manera clara, debe existir algo entre SPAK y OSR1 que las diferencíe y por lo tanto, les confiera cierta especificidad para que a lo largo de la evolución se hayan coservado ambos genes. Evidencia a nivel funcional que sostiene lo anterior es el hecho de que ratones knock-out para SPAK son viables sin fenotipo aparente, mientras que ratones knock-out para OSR1 son inviables (Eric Delpire comunicación personal) (**Fig. 38**). A nivel estructural, una diferencia adicional importante entre SPAK y OSR1 es que SPAK posee una región en el extremo amino terminal (conocida como caja PAPA) con una cantidad muy elevada de residuos de prolina y alanina. De 62 aminoácidos en la región amino terminal 26 son alaninas y 14 son prolinas. En otras palabras, el 64% de residuos en la caja PAPA son prolinas o alaninas.

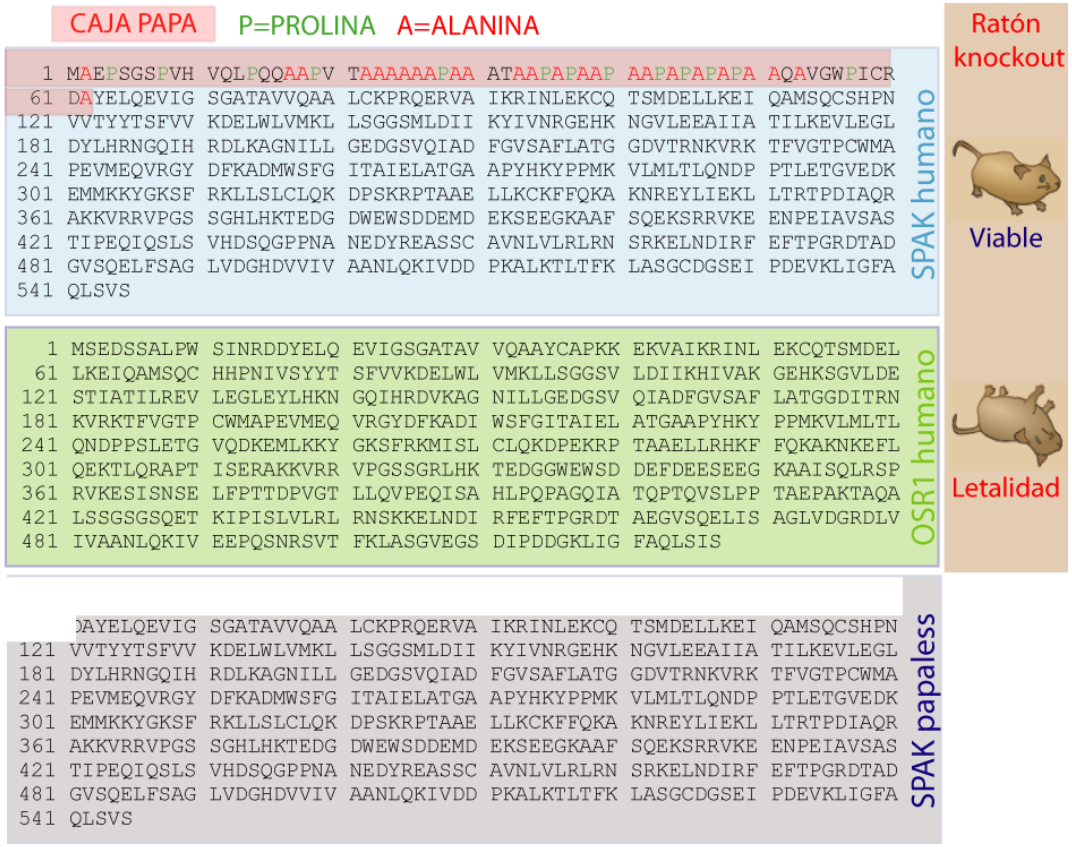

Figura 38. Secuencias de SPAK y OSR1 humanas y fenotipo de ratones KO.

Con el fin de empezar a establecer posibles diferencias de funciones entre SPAK y OSR1. Decidimos evaluar: a) el papel de cada cinasa silvestre por separado y simultaneo sobre la actividad de NKCC1 y NKCC2, b) el efecto sobre NKCC1 y NKCC2 de las versiones de SPAK y OSR1 catalíticamente inactivas (SPAK K104R y OSR1 T185A) y c) el efecto de la deleción de la caja PAPA presente en SPAK (SPAK PAPALESS) sobre la actividad de NKCC1 y NKCC2 (**Fig. 39A**).

Como se puede observar en la figura 39A la coexpresión de SPAK slvestre no tuvo mayor efecto sobre la actividad de NKCC1 y NKCC2. Consistente con lo previamente publicado, la ausencia de actividad catalítica de SPAK (SPAK K104R) redujo la activiadad de tanto NKCC1 como NKCC2. De manera más específica la reducción de la actividad de NKCC1 fue de aproximadamente un 80%, mientras que la reducción en la actividad de NKCC2 fue solo de alrededor de un 50% (**Fig. 39A**).

Al evaluar el efecto de la coexpresión de la cinasa OSR1 sobre la activida de NKCC1 y NKCC2 observamos que OSR1 redujo de manera importante (~50%) e independiente de su actividad catalítica la funciónm de NKCC2. Con respecto a NKCC1 la coexpresión de OSR1 no presentó mayor efecto aun en ausencia de su actividad catalítica.

Al evaluar el efecto de la coexpresión de OSR1 y SPAK se pudo observar que la inhibición ejercida por OSR1 se previno de manera completa. En el caso de NKCC1, su coexpresión con OSR1 y SPAK no cambió el efecto observado con las cinasas de manera individual.

Por último al evaluar el papel de la eliminación de la caja PAPA en SPAK (SPAK PAPALESS) se encontró que ahora SPAK era un inhibidor de la actividad de NKCC2. Lo anterior es consistente con los datos obtenidos al expresar a OSR1 con NKCC2. OSR1 de alguna manera inhibe a NKCC2 y al parecer la caja PAPA juega un papel muy importante para determinar el efecto de SPAK sobre NKCC2 (**Fig. 39A**).

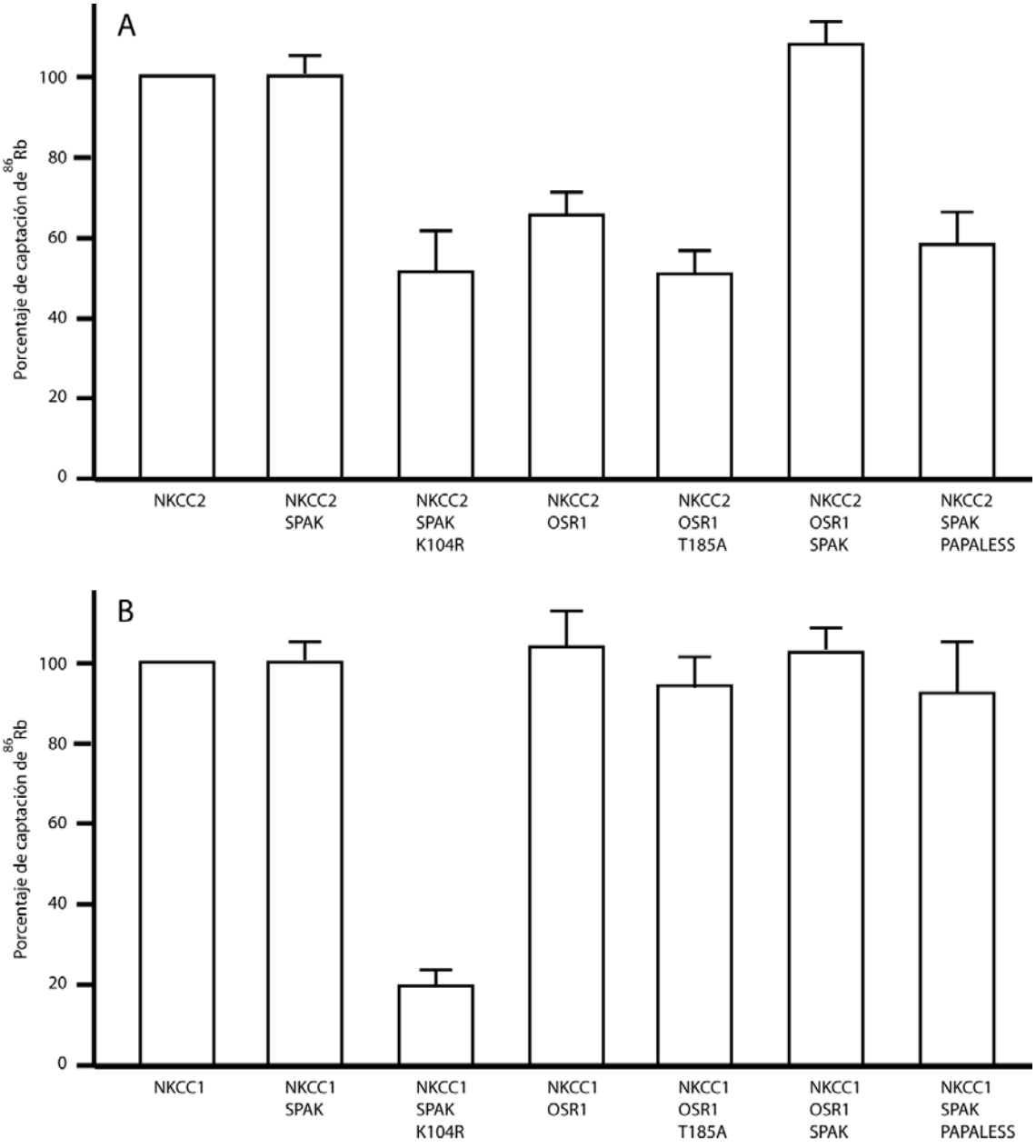

Figura 39. Efecto de SPAK y OSR1 sobre la activiadad de NKCC1 y NKCC2.

Conclusiones de los resultados aún no publicados

La eliminación del sitio de unión a SPAK en el cotransportador NKCC2 resulta en una disminución del 50% sobre su actividad.

Eliminar el sitio de unión a la cinasa SPAK-OSR1 en el cotransportador NKCC2 no impide que la coexpresión de la cinasa WNK3 silvestre resulte en la activación del cotransportador.

A diferencia de lo que ocurre con la coexpresión de la cinasa SPAK, la coexpresión de la cinasa OSR1 resulta en una disminución del 50% de la actividad de NKCC2. Dicha inhibición es independiente de la actividad catalítica de la cinasa OSR1 y es rescatada por la coexpresión de la cinasa SPAK silvestre. Por lo anterior la inhibición de NKCC2 por la cinasa OSR1 probablemente sea debido a un efecto dominante negativo sobre la cinasa SPAK endogena.

La remoción de la región conocida como caja PAPA en la cinasa SPAK ocasiona que la cinasa SPAK "PAPALESS" se convierta en un inhibidor de la actividad del cotransportador NKCC2, simulando el efecto de la cinasa OSR1.

OTROS ARTÍCULOS PUBLICADOS

Adicionalmente al artículo de primer autor "**Regulation of NKCC2 by a chloride sensing mechanism involving the WNK3 and SPAK kinases**" cuyo trabajo fue el central para el desarrollo de la presente tesis, durante mi doctorado tuve la oportunidad de participar en la publicación de tres artículos científicos originales y 1 revisión:

"WNK4 kinase is a negative regulator of K^+-Cl^- cotransporters"
Am J Physiol Renal Physiol. 2007 Apr; 292 (4): F1197-207.

"Renal Na^+-K^+-Cl^- cotransporter activity and vasopressin-induced trafficking are lipid raft-dependent"
Am J Physiol Renal Physiol. 2008 Sep; 295 (3): F789-802.

"WNK3 and WNK4 amino-terminal domain defines their effect on the renal Na^+-Cl^- cotransporter"
Am J Physiol Renal Physiol. 2008 Oct; 295 (4): F1199-206.

"WNK kinases, renal ion transport and hypertension"
Am. J. Nephrol. 2008; 28 (5):860-70. Review.

A lo largo de las siguientes páginas se añaden los artículos mencionados, así como un breve resumen del trabajo plasmado en dichas publicaciones.

En el trabajo titulado "***WNK4 kinase is a negative regulator of K^+-Cl^- cotransporters"*** se evaluó por primera vez el efecto de la coexpresión de la cinasa WNK4 silvestre ó catalíticamente inactiva sobre la actividad de los cotransportadores KCC. De manera interesante, WNK4 es un potente inhibidor de la actividad de los KCC en condiciones de hipotonicidad (situación de activación de los KCC). Para tal inhibición, se requiere de la actividad catalítica de dicha cinasa y las mutaciones tipo PHAII no alteran la inhibición. Un hallazgo muy interesante en este trabajo fue la observación de que en condiciones de isotonicidad, la coexpresión de WNK4 D294A (ausente de actividad

catalítica), favoreció la activación de KCC2 y KCC3. Tal activación se incrementó significativamente en presencia de la cinasa SPAK K104R (ausente de actividad catalítica). En conclusión, se pudo demostrar que las cinasas WNK4 y SPAK son reguladoras de la actividad de los KCC.

En el trabajo titulado "***Renal Na^+-K^+-Cl^- cotransporter activity and vasopressin-induced trafficking are lipid raft-dependent"*** se determinó que el 40-70% de NKCC2, se encuentra localizado en estructuras conocidas como balsas lipídicas que pueden estar en membrana ó en vesículas citoplásmicas. La eliminación de las balsas lípidicas, mediante la incubación con metil beta ciclodextrina, disminuyó la cantidad de $^{86}Rb^+$ incorporado por NKCC2. Consistente con el papel de las balsas lipídicas en la modulación de la llegada a membrana de este cotransportador; la incubación con la ADH (un clásico activador de NKCC2) promueve que exista una mayor fracción o cantidad de este cotransportador en balsas lipídicas. En conclusión, la cantidad de NKCC2 presente en balsas lípidicas parece ser un determinante importante de la reabsorción transepitelial de Na^+.

En el trabajo titulado "***WNK3 and WNK4 amino-terminal domain defines their effect on the renal Na^+-Cl^- cotransporter***" se pudo determinar mediante el intercambio de regiones entre la cinasa WNK3 y la cinasa WNK4 (construcción de proteínas quiméricas) que la región amino terminal de WNK3 (primeros 146 aminoácidos) es aquella que contiene las "señales" necesarias para la activación de NCC. Para la inhibición de NCC, la región amino terminal de WNK4 (primeros 173 aminoácidos) es aquella que "dirige" tal efecto sobre el cotransportador. En conclusión, las diferencias en los efectos de las cinasas WNK3 y WNK4 sobre NCC radican y estan determinadas por la región amino terminal de dichas cinasas.

En la revisión titulada "***WNK kinases, renal ion transport and hypertension***" se discute el papel de la familia de cinasas WNK sobre las modificaciones en los niveles de presión sanguínea, presentes en pacientes con PHAII. Se hace énfasis también en la regulación del transporte ionico a nivel renal, por las diferentes isoformas de las cinasas WNK. Se analizan los efectos de WNK1 y WNK4 sobre la nefrona distal y los modelos animales de PHAII.

Al momento de escribir esta tesis, se sometió a publicación la revisión titulada ***"Los cotransportadores de $Na^+/K^+/2Cl^-$: expresión regulación y su papel en la salud".*** Tal revisión se pretende sea publicada en la sección del rincón del residente de la revista de investigación clínica, dicha revista constituye el órgano oficial de los institutos nacionales de salud. La carta del editor asociado donde se notifica la recepción del manuscrito y el contenido del mismo, se añaden al final de los artículos publicados durante mi doctorado.

Am J Physiol Renal Physiol 292: F1197–F1207, 2007.
First published December 19, 2006; doi:10.1152/ajprenal.00335.2006.

WNK4 kinase is a negative regulator of K^+-Cl^- cotransporters

Tomas Garzón-Muvdi,[1] Diana Pacheco-Alvarez,[1] Kenneth B. E. Gagnon,[2] Norma Vázquez,[1] José Ponce-Coria,[1] Erika Moreno,[1] Eric Delpire,[2] and Gerardo Gamba[1]

[1]*Molecular Physiology Unit, Instituto Nacional de Ciencias Médicas y Nutrición Salvador Zubirán and Instituto de Investigaciones Biomédicas, Universidad Nacional Autónoma de México, Mexico City, Mexico; and* [2]*Department of Anesthesiology, Vanderbilt University Medical Center, Nashville, Tennessee*

Submitted 24 August 2006; accepted in final form 16 December 2006

Garzón-Muvdi T, Pacheco-Alvarez D, Gagnon KB, Vázquez N, Ponce-Coria J, Moreno E, Delpire E, Gamba G. WNK4 kinase is a negative regulator of K^+-Cl^- cotransporters. *Am J Physiol Renal Physiol* 292: F1197–F1207, 2007. First published December 19, 2006; doi:10.1152/ajprenal.00335.2006.—WNK kinases [with no lysine (K) kinase] are emerging as regulators of several membrane transport proteins in which WNKs act as molecular switches that coordinate the activity of several players. Members of the cation-coupled chloride cotransporters family (solute carrier family number 12) are one of the main targets. WNK3 activates the Na^+-driven cotransporters NCC, NKCC1, and NKCC2 and inhibits the K^+-driven cotransporters KCC1 to KCC4. WNK4 inhibits the activity of NCC and NKCC1, while in the presence of the STE20-related proline-alanine-rich kinase SPAK activates NKCC1. Nothing is known, however, regarding the effect of WNK4 on the K^+-Cl^- cotransporters. Using the heterologous expression system of *Xenopus laevis* oocytes, here we show that WNK4 inhibits the activity of the K^+-Cl^- cotransporters KCC1, KCC3, and KCC4 under cell swelling, a condition in which these cotransporters are maximally active. The effect of WNK4 requires its catalytic activity because it was lost by the substitution of aspartate 318 for alanine (WNK4-D318A) that renders WNK4 catalytically inactive. In contrast, three different WNK4 missense mutations that cause pseudohypoaldosteronism type II do not affect the WNK4-induced inhibition of KCC4. Finally, we observed that catalytically inactive WNK4-D318A is able to bypass the tonicity requirements for KCC2 and KCC3 activation in isotonic conditions. This effect is enhanced by the presence of catalytically inactive SPAK, was prevented by the presence of protein phosphatase inhibitors, and was not present in KCC1 and KCC4. Our results reveal that WNK4 regulates the activity of the K^+-Cl^- cotransporters expressed in the kidney.

intraneuronal chloride concentration; transepithelial salt absorption

THE K^+-CL^- COTRANSPORTERS belong to the cation-coupled chloride cotransporter's gene family of membrane proteins (*SLC12*). This family is divided into two branches. One branch is represented by the K^+-driven K^+-Cl^- cotransporters KCC1 to KCC4 and the other one by the Na^+-driven Na^+:Cl^-, NCC, and Na^+:K^+:2Cl^- cotransporters NKCC1 and NKCC2 (18). Four genes encode isoforms of the K^+:Cl^- cotransporter. These genes are known as *SLC12A4*, *SLC12A5*, *SLC12A6*, and *SLC12A7* and encode the K^+-Cl^- cotransporter isoforms KCC1, KCC2, KCC3, and KCC4, respectively. KCC1 exhibits ubiquitous expression and its primary role seems to be cell volume regulation. KCC2 is only present in neurons in which its activity is critical to define intraneuronal chloride concentration. KCC3 and KCC4 are expressed in several tissues, including the central nervous system and the kidney, and may play a role in several physiological processes such as transepithelial salt absorption, renal K^+ secretion and reabsorption, myocardial K^+ loss during ischemia, and vascular smooth muscle cell relaxation (18, 33, 37).

Several lines of evidence suggest the presence of basolateral K^+-Cl^- cotransporter systems in proximal tubule (PT) (6, 29), thick ascending limb of Henle's loop (TALH) (3, 22), and collecting duct (CD) (43, 55), as well as in the apical membrane of the distal convoluted tubule (DCT), in which the K^+-Cl^- cotransporter plays a role in K^+ secretion (4, 15, 45). Immunolocalization studies in the kidney have shown that KCC3 and KCC4 are present in the basolateral membrane of the proximal tubule and KCC4 is also expressed in the basolateral membrane of the TALH, DCT, and the α-intercalated cells of the CD (7, 35, 46). The distribution of KCC1 protein along the nephron has not been determined. Inactivating mutations of KCC3 are the cause of a rare neurological syndrome known as Anderman's disease featuring agenesis of the corpus callosum with motor and sensory neuropathy, mental retardation, and psychosis (23). Targeted disruption of KCC3 in mice results in a complex neurological phenotype, without major disturbances in renal function, but with the development of arterial hypertension, probably related to a role of KCC3 in vascular smooth muscle cell relaxation (2, 8, 42). No disease has been linked to KCC4, but targeted disruption of this cotransporter gene in mice produces a syndrome of deafness and renal tubular acidosis (7).

A recently discovered family of serine/threonine kinase proteins named WNK [with no lysine (K)] has been shown to regulate the activity of several membrane proteins (19), in particular members of the *SLC12* family and other Cl^- transport pathways (25, 26). Deletions of intron 1 of WNK1 or missense mutations in a conserved acidic region of WNK4 are the cause of a salt-dependent form of arterial hypertension known as pseudohypoaldosteronism type II (PHAII) (48), featuring also hyperkalemia and metabolic acidosis. PHAII-type mutations in WNK4 affect the WNK4-related regulation of the thiazide-sensitive Na^+:Cl^- cotransporter NCC (9, 49, 53), the apical potassium channel ROMK (28), and paracellular claudins (26, 52). In addition to NCC, WNK4 also modulates the function of other Cl^- transport pathways such as the basolateral Na^+:K^+:2Cl^- cotransporter NKCC1 and the anion exchanger CFEX that mediates several different Cl^-:base exchange activities (25). WNK1 modulates the activity of WNK4 (54) and also regulates ROMK (10) and the apical

Address for reprint requests and other correspondence: G. Gamba, Molecular Physiology Unit, Vasco de Quiroga No. 15, Tlalpan 14000, México City, México (e-mail: gamba@biomedicas.unam.mx or gamba@quetzal.innsz.mx).

The costs of publication of this article were defrayed in part by the payment of page charges. The article must therefore be hereby marked "*advertisement*" in accordance with 18 U.S.C. Section 1734 solely to indicate this fact.

amiloride-sensitive Na^+ channel in CD (51). Therefore, WNK kinases are emerging as important regulators of Cl^- transport pathways in both epithelial and nonepithelial cells. In the present study, we thus analyzed the effect of WNK4 on the activity of the renal K^+-Cl^- cotransporters KCC1, KCC3, and KCC4.

METHODS

Xenopus laevis oocyte preparation. Adult female *X. laevis* frogs were purchased from NASCO (Fort Atkinson, MI) and kept at the animal facility under constant control of room temperature (16°C). All animal procedures followed were in accordance with our institutional guidelines. Oocytes were surgically collected from anesthetized animals under 0.17% tricaine and incubated for 1 h under vigorous shaking in Ca^{2+}-free frog Ringer ND96 (in mM: 96 NaCl, 2 KCl, 1 MgCl, and 5 HEPES/Tris, pH 7.4) in the presence of 2 mg/ml of collagenase B. Oocytes were then washed four times in regular ND96, manually defolliculated, and incubated overnight in ND96 at 18°C. The next day, mature oocytes were injected with 50 nl of water alone or containing 0.2 μg/μl of cRNA in vitro transcribed from cotransporters cDNAs or 0.1 μg/μl of cRNA in vitro transcribed from kinases described below. Oocytes were incubated at 18°C for 4 days in ND96 supplemented with 2.5 mM sodium pyruvate and 5 mg/100 ml of gentamicin; this incubation medium was changed every 24 h. On the day of the influx measurement, 2 h before the uptake assay, oocytes were switched to Cl^--free ND96 (in mM: 96 Na^+ isethionate, 2 K^+-gluconate, 6.0 Ca^{2+} gluconate, 1.0 Mg^{2+}-gluconate, 5 mM HEPES, 2.5 sodium pyruvate, 5 mg/ml gentamicin, pH 7.4).

Assessment of the K^+-Cl^- cotransporter function. K^+-Cl^- cotransport was assessed by measuring tracer $^{86}Rb^+$ uptake (New England Nuclear) in experimental groups of at least 10 oocytes. Since KCC1, KCC3, and KCC4 express minimal activity under isotonic conditions (34, 35), $^{86}Rb^+$ uptake was generally assessed in oocytes preswollen by a 30-min incubation period in a hypotonic K^+- and Cl^--free medium [in mM: 50 *N*-methyl-D-glucamine (NMDG)-gluconate, 4.6 Ca^{2+}-gluconate, 1.0 Mg^{2+}-gluconate, 5 HEPES/Tris, pH 7.4] with 1 mM ouabain, followed by a 60-min uptake period in a hypotonic Na^+-free medium (10 mM K^+-gluconate, 40 mM NMDG-Cl^-, 1.8 mM $CaCl_2$, 1 mM $MgCl_2$, 5 mM HEPES, pH 7.4), supplemented with 1 mM ouabain and 2.0 μCi of $^{86}Rb^+$. To define the amount of tracer $^{86}Rb^+$ uptake due to the K^+-Cl^- cotransporter activity, uptake in all experimental groups was assessed in parallel in the presence or absence of extracellular chloride. When uptake in isotonic conditions was measured, the isotonic condition was generated by supplementing the incubation and uptake solutions with 3.5 g/100 ml sucrose to reach isosmolar conditions for oocytes (~210 mosmol/kgH_2O). Ouabain was added to prevent $^{86}Rb^+$ uptake via the Na^+-K^+-ATPase. The absence of extracellular Na^+ and the hypotonicity of the uptake medium prevented $^{86}Rb^+$ uptake via the endogenous Na^+:K^+:$2Cl^-$ cotransporter that is present in oocytes (17).

All uptakes were performed at 32°C temperature. At the end of the uptake period, oocytes were washed five times in ice-cold uptake solution without isotope to remove extracellular fluid tracer. Oocytes were dissolved in 10% sodium dodecyl sulfate and tracer activity was determined for each oocyte by β-scintillation counting.

cDNA constructs and mutations. The full-length rabbit KCC1, human KCC2, human KCC3, and mouse KCC4 cDNAs are subcloned into the high expression vector pGEMHE (34, 35, 44). The full-length mouse SPAK and WNK4 kinases are inserted into the amphibian oocyte expression vector pBF and were previously described (16). Site-directed mutagenesis was performed on WNK4 cDNA to generate kinase dead WNK4 (WNK4-D318A), kinase dead SPAK (SPAK-K104R), or to introduce PHAII-type mutations (E559K, D561A, and Q562E) into the WNK4 sequence. Complementary sense and antisense oligonucleotides containing the appropriate mutations were custom made (Sigma). Mutations were performed using the QuickChange kit following the manufacturer's recommendations (Stratagene, La Jolla, CA). In addition, by means of double-step PCR, the sequence of the epitope tag HA was introduced in frame into the wild-type WNK4 and SPAK cDNAs. Then, using the appropriate restriction enzymes the tagged sequence was pasted into the catalytically inactive WNK4-D318A and SPAK-K104R cDNAs. To prepare cRNA, KCC1 and KCC4 cDNAs were linearized at their 3′-end with *Nhe*I, and KCC3 cDNA with *Not*I and transcribed in vitro using a T7 RNA polymerase mMESSAGE kit (Ambion). To prepare cRNA from the wild-type or mutant kinases WNK4 and SPAK cDNAs were linearized with *Mlu*I and transcribed in vitro using a SP6 RNA polymerase mMESSAGE kit (Ambion). Transcription product integrity was confirmed on agarose gels and concentration was determined by absorbance reading at 260 nm (DU 640, Beckman, Fullerton, CA). cRNA was stored in aliquots at −80°C until used.

Nested RT-PCR amplification of SPAK/OSR1 from X. laevis oocytes. External and internal primers for nested RT-PCR amplification of SPAK/OSR1 from *X. laevis* oocyte mRNA were custom made (Sigma) based on the *X. laevis* SPAK/OSR1 homolog serine threonine kinase 39 sequence deposited in the GenBank database (accession number BC077748). External primer sequences were sense 5′-TCCATCAACAGGGACGACTA-3′ and antisense 5′-ATGACCTCTGGTGCCATCCA-3′ and amplify a fragment of 563 bp. Internal primer sequences were sense 5′-CATCAAGAGAATAAACCTGG-3′ and antisense 5′-GTACAGATCCATCGTCACCC-3′ and amplify a fragment of 349 bp. Total RNA from *X. laevis* oocytes was isolated using the Tripure system (Roche) following the manufacturer's recommendations. Reverse transcription (RT) was carried out using 2.5 μg of total RNA at 37°C for 60 min in a total volume of 20 μl using 200 units of the Moloney murine leukemia virus reverse transcriptase (Invitrogen). The 563-bp fragment obtained with external primers was gel purified and used as template for the internal PCR. Products were resolved in 5% acrylamide gels.

Western blot analysis of wild-type and mutants HA-WNK4 and HA-SPAK. Total proteins were extracted from 10 to 15 oocytes per group by passing oocytes several times through a 0.4-mm needle syringe in lysis buffer using 4 μl per oocyte (200 mM sucrose; 0.5 mM EDTA, 5 mM Tris·HCl, pH 7.0; inhibitor protease cocktail complete). The homogenates were centrifuged at 14,000 rpm for 10 min at 4°C, and the supernatant was collected. Protein concentrations were assessed in duplicate using a Bio-Rad DC Protein assay (Bio-Rad, Hercules, CA). For Western blot analysis, 20 μg of proteins were diluted in 10 μl loading buffer and subsequently denatured by boiling for 5 min. Proteins were resolved by SDS-PAGE and then transferred to polyvinylidine difluoride membranes (Amersham Pharmacia Biotech; 2 h at 400 mA). Prestained Rainbow markers (Amersham) were used as molecular mass standards. Nonspecific binding sites were blocked overnight at 4°C in 500 mM NaCl, 20 mM Tris-buffered saline containing 0.4% nonfat dry milk. Thereafter, membranes were incubated with 1:2,000 dilutions of a specific monoclonal anti-HA peroxidase-conjugated antibody (Sigma) diluted in blocking buffer (TTBS, 0.05% Tween 20) for 1.5 h at room temperature. Membranes were subsequently washed three times in TTBS for 10 min and immunoreactive species were detected using the ECL Plus Western blotting detection system (Amersham).

Statistical analysis. Statistical significance is defined as two-tailed $P < 0.05$ and the results are presented as means ± SE. The significance of the differences between groups was tested by nonpaired *t*-test when two groups were compared or by one-way ANOVA with multiple comparisons using the Bonferroni correction. Although all experiments were performed at least twice, most of the observations are based on more than two experiments.

RESULTS

WNK4 reduces the activity of K^+-Cl^- cotransporters in swollen oocytes. We previously showed that microinjection of *X. laevis* oocytes with KCC1, KCC3, or KCC4 cRNAs (34, 35) resulted in significant K^+-Cl^- cotransport activity, compared with control oocytes that were injected with water. Activity of these K^+-Cl^- cotransporters is evident, however, only when uptakes were performed under hypotonic conditions, supporting what has been demonstrated in several cell types, that the K^+-Cl^- cotransporters expressed in oocytes are also activated by cell swelling (1). Figure 1 shows the combined results of several experiments in which *X. laevis* oocytes were injected with water, K^+-Cl^- cotransporter cRNA alone, or together with WNK4 cRNA. Tracer $^{86}Rb^+$ uptake assays were performed 4 days later under hypotonic conditions in the absence or presence of extracellular chloride. Microinjection with KCC cRNA resulted in a significant increase in $^{86}Rb^+$ uptake over the water-injected oocytes. The values observed were KCC1 8,840 ± 434 pmol·oocyte^{-1}·h^{-1}, KCC3 24,893 ± 626 pmol·oocyte^{-1}·h^{-1}, and KCC4 18,146 ± 601 pmol·oocyte^{-1}·h^{-1}. In all cases, the level of uptake was dramatically reduced in the absence of extracellular chloride, indicating that observed uptake was due to the activity of the exogenous K^+-Cl^- cotransporter. As shown in Fig. 1, coinjection of *X. laevis* oocytes with the wild-type WNK4 kinase cRNA resulted in a significant reduction of the $^{86}Rb^+$ uptake induced by K^+-Cl^- cotransporters. KCC1 activity was reduced by 60% (KCC1+WNK4 4,274 ± 519 pmol·oocyte^{-1}·h^{-1}, $P <$ 0.01 vs. KCC1 alone), KCC3 activity by 40% (KCC3+WNK4 15,592 ± 2,129 pmol·oocyte^{-1}·h^{-1}, $P < 0.01$ vs. KCC3 alone), and KCC4 activity by 55% (KCC4+WNK4 7,464 ± 552 pmol·oocyte^{-1}·h^{-1}, $P < 0.01$ vs. KCC4 alone). Thus coexpression of the K^+-Cl^- cotransporters KCC1, KCC3, and KCC4 with WNK4 resulted in a significant reduction in their activity.

SPAK does not affect the activity of nonneuronal K^+-Cl^- cotransporters in swollen oocytes. We showed previously that the STE20 kinase SPAK modulates the activity of other members of the cation-coupled chloride cotransporter, such as the Na^+-K^+-$2Cl^-$ cotransporter NKCC1 (16) and interact at the protein-protein level with KCC3 (40). Moreover, KCC3 possesses what appears to be a real SPAK binding motif (RVXF) at the NH_2-terminal domain. Thus we assessed the effect of SPAK on the activity of the K^+-Cl^- cotransporter in microinjected oocytes exposed to hypotonicity. As shown in Fig. 2, however, no effect of SPAK was observed. Tracer $^{86}Rb^+$ uptake in KCC1, KCC3, and KCC4 when injected alone was 9,248 ± 502, 24,435 ± 615, and 18,840 ± 580 pmol·oocyte^{-1}·h^{-1}, respectively, while in the presence of SPAK, the $^{86}Rb^+$ uptake in KCC1+SPAK, KCC3+SPAK, or KCC4+SPAK cRNA-injected oocytes was 8,319 ± 684, 25,029 ± 543, or 16,493 ± 742, respectively. The values in the presence of SPAK were not statistically different to those observed in its absence.

Presence of SPAK does not change the WNK4 inhibitory effect on K^+-Cl^- cotransporters activity in swollen oocytes. We previously showed that WNK4 effect on NKCC1 is changed by the presence of SPAK (16). We thus analyzed whether SPAK could also change the type of effect that WNK4 has on the K^+-Cl^- cotransporters. Experiments were designed to analyze the effect of the WNK4+SPAK combination on K^+-Cl^- cotransporter activity. *X. laevis* oocytes were injected with KCC1, KCC3, or KCC4 cRNA alone, or in combination with WNK4 cRNA or WNK4 + SPAK cRNA. The combined

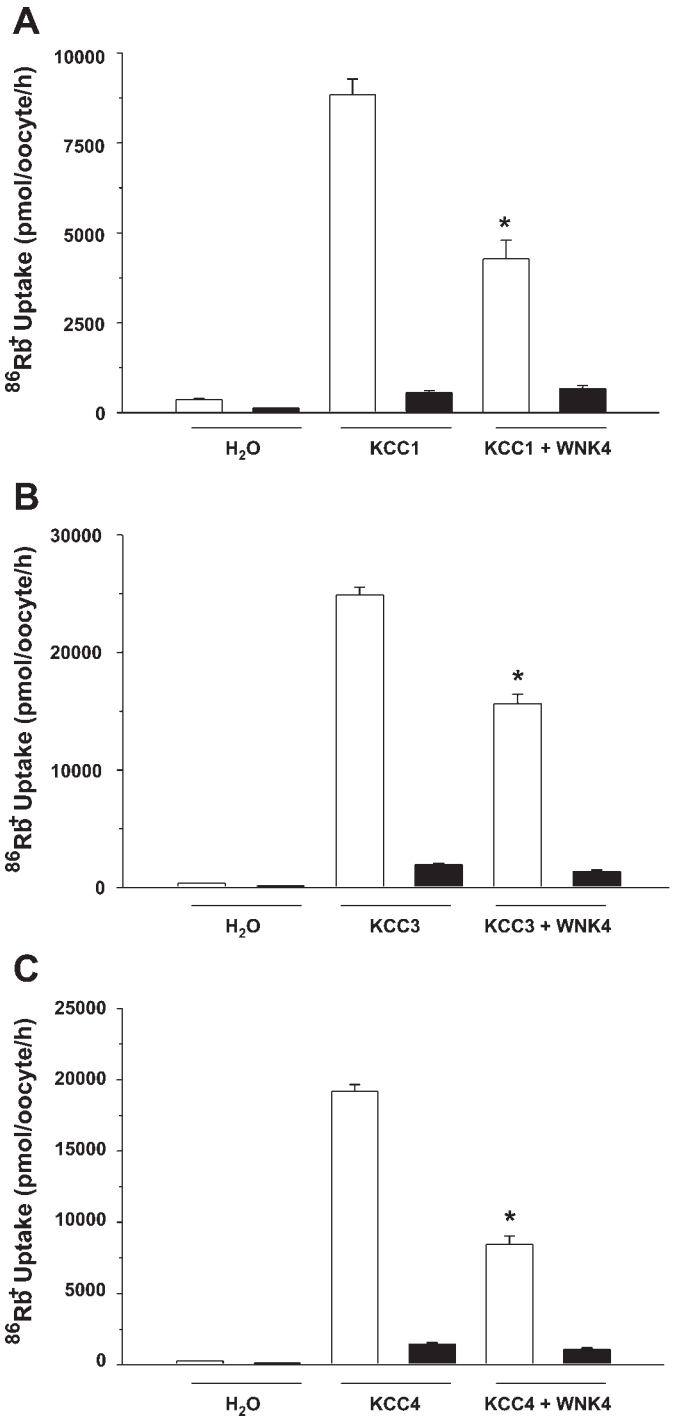

Fig. 1. Effect of wild-type WNK4 on KCC cotransport activity induced by cell swelling under hypotonic conditions. *Xenopus laevis* oocytes were injected with water or 0.2 μg/μl each of KCC1 (*A*), KCC3 (*B*), or KCC4 (*C*) cRNA alone or together with WNK4 cRNA. $^{86}Rb^+$ uptake was assessed 4 days later in hypotonic conditions (110 mosmol/kgH_2O) in the presence (open bars) or absence (filled bars) of Cl^- in the uptake medium. The pooled data from at least 5 different experiments are shown, with means ± SE of at least 50 oocytes for each group. *Significantly different from the uptake observed in the corresponding control (absence of WNK4, $P < 0.01$).

results of five experiments for KCC1, four experiments for KCC3, and six experiments for KCC4 are shown in Fig. 3. As shown above, coinjection of KCC cRNA with WNK4 cRNA alone resulted in significant reduction of the K^+-Cl^- cotrans-

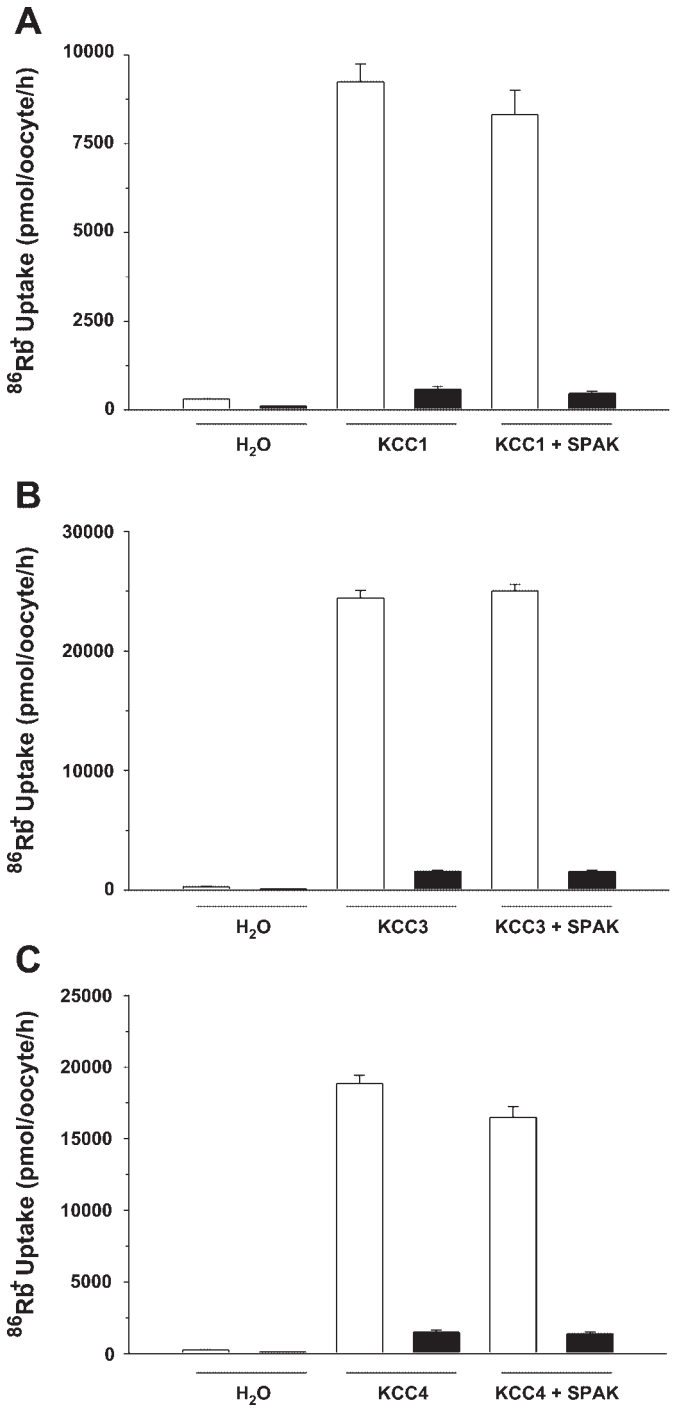

Fig. 2. Effect of wild-type SPAK on KCC cotransport activity induced by cell swelling under hypotonic conditions. *X. laevis* oocytes were injected with water or 0.2 μg/μl each of KCC1 (*A*), KCC3 (*B*), or KCC4 (*C*) cRNA alone or together with SPAK cRNA. $^{86}Rb^+$ uptake was assessed 4 days later in hypotonic conditions (110 mosmol/kgH_2O) in the presence (open bars) or absence (filled bars) of Cl^- in the uptake medium. The pooled data from at least 5 different experiments are shown, with means ± SE of at least 50 oocytes for each group. No difference was observed between groups of oocytes injected with KCCs alone or together with SPAK.

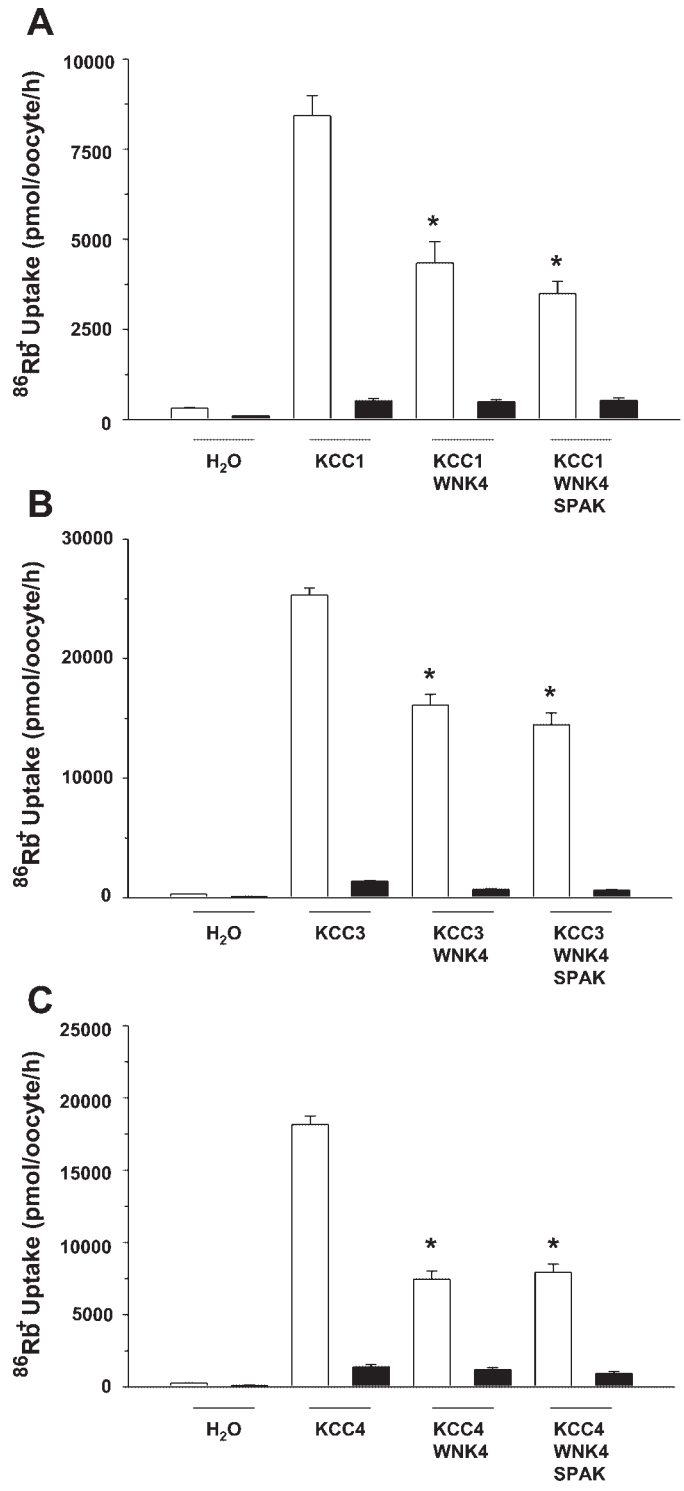

Fig. 3. Effect of wild-type SPAK on WNK4-induced inhibition of KCC activity induced by cell swelling under hypotonic conditions. *X. laevis* oocytes were injected with water or 0.2 μg/μl each of KCC1 (*A*), KCC3 (*B*), or KCC4 (*C*) cRNA alone or together with WNK4 cRNA or WNK4 cRNA and SPAK cRNA, as stated. $^{86}Rb^+$ uptake was assessed 4 days later in hypotonic conditions (110 mosmol/kgH_2O) in the presence (open bars) or absence (filled bars) of Cl^- in the uptake medium. The pooled data from 4 experiments for KCC1 or KCC3 and 6 for KCC4 are shown, with means ± SE of at least ~40, ~40, and ~60 oocytes for each group, respectively. *Significantly different from the uptake observed in the corresponding control (absence of WNK4, $P < 0.01$).

porter activity. Tracer $^{86}Rb^+$ uptake in KCC1, KCC3, and KCC4 in the presence of WNK4 was 4,341 ± 596, 16,129 ± 867, and 7,464 ± 552 pmol·oocyte^{-1}·h^{-1}, respectively. These values were significantly different from those observed in the absence of WNK4. When SPAK cRNA was added to the microinjected cocktail, the uptake observed in KCC1 was further reduced to 3,490 ± 347 pmol·oocyte^{-1}·h^{-1}. However, the difference did not reach significance. For KCC3 and KCC4 cRNA-injected oocytes, addition of SPAK cRNA did not increase the WNK4-induced inhibition of the K^+-Cl^- cotransporter activity. Uptake observed in the presence of WNK4+SPAK for KCC3 was 14,471 ± 981 pmol·oocyte^{-1}·h^{-1} and for KCC4 was 7,942 ± 552 pmol·oocyte^{-1}·h^{-1}. These values were not different from the uptake observed in the presence of WNK4 alone. Thus, in contrast to observations of Gagnon et al. (16) that SPAK changes the type of WNK4 effect on NKCC1, the presence of SPAK does not change the WNK4-induced inhibition of K^+-Cl^- cotransporter activity. As shown in Fig. 4*A*, nested RT-PCR analysis demonstrated the presence of SPAK/OSR1 transcript in *X. laevis* oocytes, indicating that this kinase is expressed endogenously. In addition, endogenous expression of SPAK/OSR1 was suggested by our previous observation that the SPAK-stimulated NKCC1 activity in oocytes is reduced in the presence of the catalytically inactive SPAK (16). We thus coinjected oocytes with KCC4 cRNA alone, KCC4 + wild-type WNK4, or KCC4 + wild-type WNK4 + the catalytically inactive SPAK harboring the K104R substitution that confers dominant negative activity (SPAK-KR) (16, 36). As shown in Fig. 4*B*, the WNK4-induced inhibition of KCC4 activity was not affected by the presence of the catalytically inactive SPAK-K104R, suggesting that the WNK4 inhibitory effect of KCC4 is probably not requiring the endogenous SPAK.

Inhibition of KCCs by WNK4 is dependent on WNK4 catalytic activity. Previous studies with WNK1, WNK3, and WNK4 showed that catalytic activity of these kinases is required for regulation of some, but not for all of the WNKs target proteins. Catalytically inactive WNKs can be obtained by a single point mutation in which an aspartic acid of the kinase domain is substituted by alanine (50). The mutations D368A, D294A, and D318A have been used for WNK1 (36, 47, 50), WNK3 (41), and WNK4 (9, 47, 49), respectively. For instance, the ability of WNK4 to reduce the NCC activity is lost by the D318A substitution (9, 21, 49), while its ability to inhibit the potassium channel ROMK is not affected by this mutation (28). We thus analyzed whether the effect of WNK4 on K^+-Cl^- cotransporters requires the kinase catalytic activity. To this end, experiments were performed in which *X. laevis* oocytes were injected with KCC1, KCC3, or KCC4 cRNA alone or coinjected with similar amounts of either wild-type WNK4 cRNA or the catalytically inactive WNK4 D318A cRNA. Four days later, $^{86}Rb^+$ uptake was assessed in all groups. The results of these series of experiments are shown in Fig. 5. As shown in Fig. 5*A*, the KCC1-induced uptake of 7,655 ± 546 pmol·oocyte^{-1}·h^{-1} was reduced to 3,616 ± 501 pmol·oocyte^{-1}·h^{-1} by wild-type WNK4, and to 5,377 ± 385 pmol·oocyte^{-1}·h^{-1} by WNK4-D318A. The difference between the KCC1 vs. KCC1+WNK4-D318A groups was significant. However, the difference between KCC1+WNK4 and KCC1+WNK4-D318A groups was also significant. As shown in Fig. 5, *B* and *C*, the KCC3 and KCC4-induced uptake of

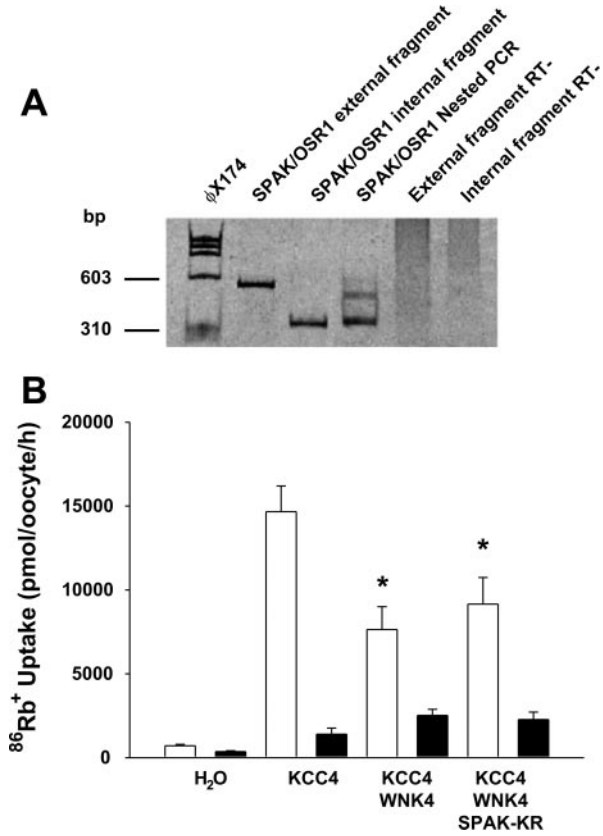

Fig. 4. Effect of dominant negative SPAK-K104R on WNK4-induced inhibition of KCCs activity under hypotonic conditions. *A*: nested PCR from *X. laevis* oocytes mRNA with specific external and internal primers to amplify SPAK/OSR1. Primers were designed using the reported sequence of *X. laevis* SPAK/OSR1 (accession number BC077748). The gel shows amplification of the expected size bands of both external and internal fragments from reverse transcriptase template and the nested PCR fragment obtained when the external band was used as template. The last 2 lines depict PCR analysis of external and internal fragments from mRNA not exposed to reverse transcriptase. *B*: oocytes were injected with water or 0.2 μg/μl each of KCC4 cRNA alone or together with WNK4 cRNA or WNK4 cRNA and SPAK-K104R cRNA, as stated. $^{86}Rb^+$ uptake was assessed 4 days later in hypotonic conditions (110 mosmol/kgH_2O) in the presence (open bars) or absence (filled bars) of Cl^- in the uptake medium. The pooled data from 3 experiments are shown. *Significantly different from the uptake observed in the corresponding control (absence of WNK4, $P < 0.01$). No difference was observed between the KCC+WNK4 group when compared with the KCC+WNK4+SPAK group.

23,839 ± 108 and 19,078 ± 1,067 pmol·oocyte^{-1}·h^{-1}, respectively, was significatively reduced by WNK4. In contrast, no significant effect was observed by WNK4-D318A since uptake in KCC3 or KCC4 oocytes coinjected with WNK4-D318A was 24,489 ± 1,264 and 16,136 ± 839 pmol·oocyte^{-1}·h^{-1}, respectively. Thus the inhibitory effect of WNK4 on KCC1 was significatively reduced and on KCC3 and KCC4 was completely prevented by eliminating the catalytic activity of WNK4.

Protein expression of wild-type and mutant WNK4 and SPAK in oocytes. Western blot analysis was performed to find out whether the protein expression of the wild-type and mutant forms of WNK4 and SPAK were not affected by introduction of the mutations used to generate the catalytically inactive forms or by coexpression of two kinases together. To perform these experiments, the DNA sequence encoding the HA-tag epitope was introduced in frame into the wild-type and mutant kinases. Then, oocytes were injected with KCC1, KCC3, or

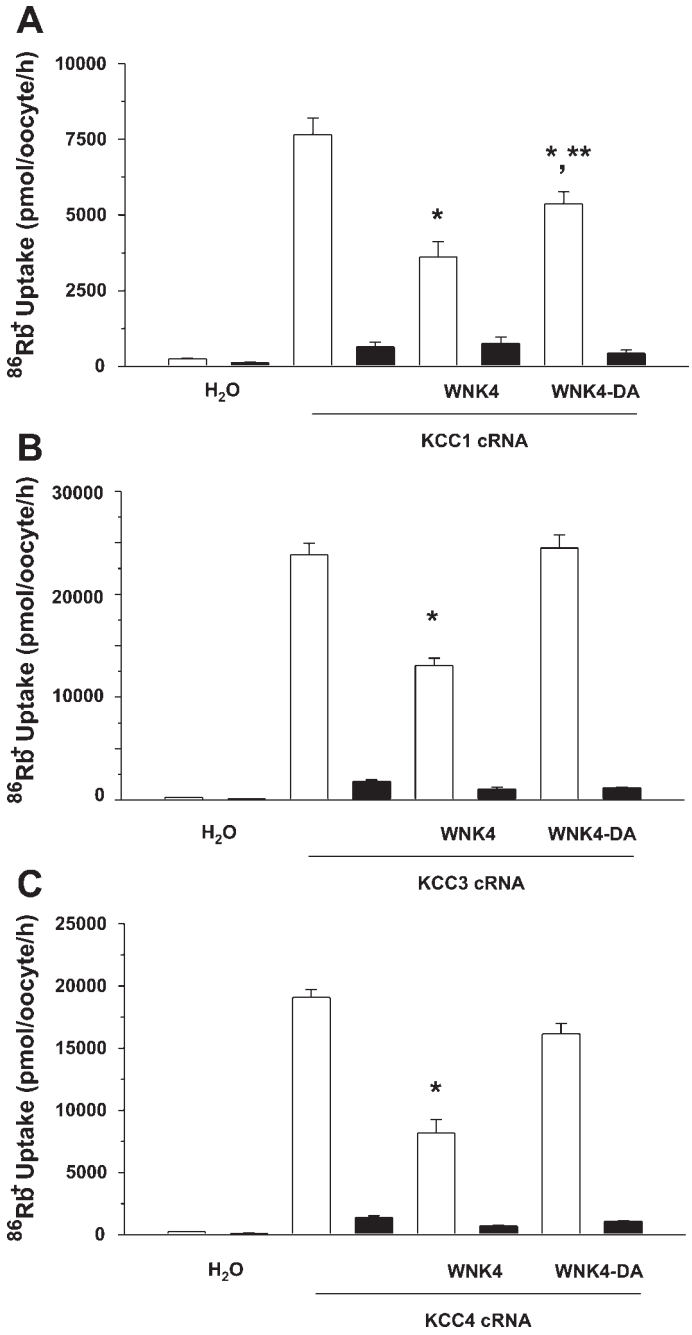

Fig. 5. Catalytic activity of WNK4 is required for WNK4-induced inhibition of KCC cotransporters. *X. laevis* oocytes were injected with water or 0.2 μg/μl each of KCC1 (*A*), KCC3 (*B*), or KCC4 (*C*) cRNA alone or together with WNK4 cRNA or catalytically inactive WNK4 harboring the D318A mutation, as stated. $^{86}Rb^+$ uptake was assessed 4 days later in hypotonic conditions (110 mosmol/kgH_2O) in the presence (open bars) or absence (filled bars) of Cl^- in the uptake medium. The pooled experiments from 2 experiments are shown, with means ± SE of at least 20 oocytes for each group. *Significantly different from the uptake observed in the corresponding control (absence of WNK4, $P < 0.01$). **Significantly different from uptake in KCC1+WNK4 group ($P < 0.05$).

KCC4 cRNA alone or together with wild-type or mutant WNK4 and/or SPAK cRNA. Three to four days later, one-half of the oocytes were used to assess functional expression by measuring $^{86}Rb^+$ uptake in the absence or presence of extracellular chloride. The other half were used to extract proteins for Western blot analysis using an anti-HA monoclonal antibody. Functional experiments exhibited similar results as those presented in Figs. 1 to 4. That is, when oocytes were incubated in hypotonic conditions, the KCC activity was inhibited by wild-type HA-WNK4, but not by wild-type HA-SPAK or the catalytically inactive HA-WNK4-D318A. The level of inhibition observed by the coinjection of wild-type HA-WNK4 together with the catalytically inactive HA-SPAK-K104R was similar to that observed by HA-WNK4 alone. Thus the presence of the HA epitope did not affect the behavior of the wild-type and mutant kinases. Figure 6 shows a representative Western blot obtained from one of these experiments from KCC4 cRNA-injected oocytes. Results were similar when proteins were extracted from experiments in which KCC1 or KCC3 was the K^+-Cl^- cotransporter cRNA injected (data not shown). As shown in Fig. 6, no protein bands were detected by anti-HA antibodies in proteins extracted from *X. laevis* oocytes injected with water or with KCC4 cRNA alone. A band corresponding to WNK4 molecular mass (~135 kDa) was detected in oocytes injected with HA-WNK4 cRNA. The presence and intensity of WNK4 bands were similar in oocytes injected with KCC4 plus wild-type HA-WNK4 cRNA compared with those injected with KCC4 plus HA-WNK4-D318A, HA-WNK4 and HA-SPAK, or HA-WNK4 and HA-SPAK-K104R. Thus expression of the mutant WNK4-D318A was similar to wild-type WNK4, and the presence of wild-type or mutant SPAK had no effect on WNK4 expression. In addition, a band corresponding to SPAK molecular mass (~58 kDa) was observed in oocytes injected with wild-type or mutant SPAK. The intensity of the band was similar in the absence or presence of WNK4.

PHAII-type mutations do not affect the inhibition of KCCs by WNK4. Missense mutations of an acidic domain of WNK4 are the cause of PHAII syndrome that features arterial hyper-

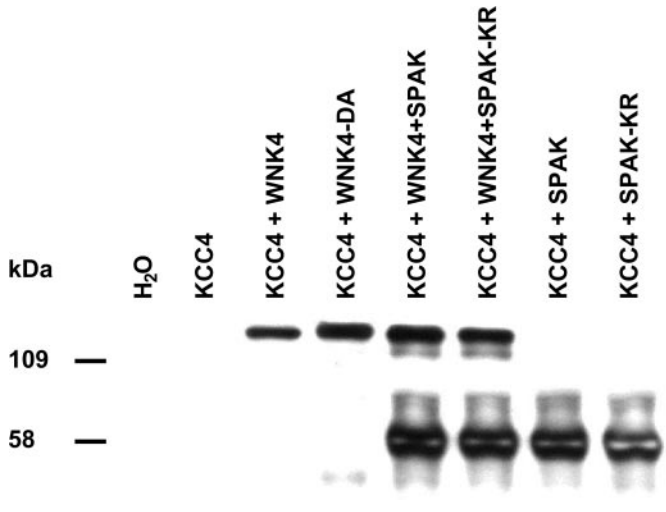

Fig. 6. Protein expression of HA-tagged active and inactive WNK4 and SPAK kinases. Representative image of a Western blot analysis of proteins extracted from *X. laevis* oocytes injected with water, KCC4 cRNA alone, or together with active and inactive HA-tagged kinases cRNAs, as stated is shown. Immunoblot was performed using monoclonal anti-HA antibody. No bands were observed in water- or KCC4 cRNA-injected oocytes. The bands of ~130 kDa correspond to wild-type HA-WNK4 or mutant HA-WNK4-D318A, while the bands of ~60 kDa correspond to wild-type HA-SPAK or mutant HA-SPAK-K104R. No differences in protein expression were observed between the active and inactive kinases or when any pair of cRNAs was coinjected.

tension and metabolic acidosis among other clinical manifestations. It has been proposed that these mutations alter the way in which WNK4 regulates the activity of several membrane transport proteins. In some cases, as occurs with the inhibitory effect of WNK4 on NCC (9, 49), the mutations prevent this effect. In other cases, like the WNK4-induced inhibition of ROMK (28) or the WNK4-induced phosphorylation of claudins (26, 52), the PHAII mutations increased the effect on its targets. In other words, PHAII-type mutations can behave as "loss-of-function" or "gain-of-function" mutations (19). Because KCC4 is expressed in α-intercalated cells of the cortical collecting duct and its targeted deletion resulted in metabolic acidosis (7), we wanted to know whether the PHAII-type mutations affected the WNK4-induced inhibition of KCC4. The results, however, as shown in Fig. 7 revealed that wild-type WNK4 reduced the activity of KCC4 to a similar degree to WNK4 harboring any of the PHAII type mutations E559K, D561A, or Q562E.

Catalytically inactive WNK4 activates KCC2 and KCC3 in isotonic conditions. We showed before that WNK3 in its catalytically active and inactive form is able to bypass the tonicity requirement for regulation of the cation-chloride cotransporters. For example, wild-type WNK3 activates NKCC1 cotransporter, even when oocytes are incubated in hypotonic conditions in which NKCC1 is inhibited. In contrast, catalytically inactive WNK3-D294A inhibits NKCC1, even when oocytes are incubated in hypertonic solutions in which NKCC1 is activated. Similarly, wild-type WNK3 prevents the cell swelling-induced activation of all four K^+-Cl^- cotransporters, while WNK3-D294A is able to activate the four K^+-Cl^- cotransporters in isotonic conditions in which they are normally inactive (11, 27, 41). Therefore, we analyzed the effect of wild-type WNK4 and the catalytically inactive WNK4-D318A on K^+-Cl^- cotransporters in isotonic conditions. We first observed that in isotonic conditions, WNK4 has no effect on the K^+-Cl^- cotransporter's activity. Then, we performed experiments in which oocytes were injected with the K^+-Cl^- cotransporter cRNA alone or together with WNK4-D318A cRNA, the catalytically inactive form of SPAK (SPAK-K104R) cRNA or both inactive kinases simultaneously (WNK4-D318A + SPAK-K104R). Then, $^{86}Rb^+$ uptake was assessed by incubating the oocytes in isotonic conditions. As shown in Fig. 8, *A* and *B*, coinjection of KCC1 or KCC4 with the catalytically inactive forms of WNK4 and/or SPAK had no effect on these cotransporters activity. In contrast, coinjection of KCC2 or KCC3 with WNK4-D318A resulted in a significant increase in the Cl^--dependent $^{86}Rb^+$ uptake. $^{86}Rb^+$ uptake in oocytes injected with KCC2 or KCC3 alone was 1,003 ± 74 and 715 ± 133 pmol·oocyte^{-1}·h^{-1}, respectively, while in oocytes injected with KCC2 or KCC3 and WNK4-D318A cRNA $^{86}Rb^+$ uptake was 5,161 ± 723 and 2,446 ± 434 pmol·oocyte^{-1}·h^{-1}, respectively. The increase was significant ($P < 0.01$) compared with its respective control. In addition, although $^{86}Rb^+$ uptake was not affected by SPAK-K104R, neither in KCC2 nor in KCC3, coinjection of these cotransporters cRNA with WNK4-D318A cRNA and SPAK-K104R cRNA resulted in further increase in activity since $^{86}Rb^+$ uptake in KCC2 oocytes increased to 13,184 ± 1,751 pmol·oocyte^{-1}·h^{-1} ($P < 0.01$ vs. KCC2+WNK4-DA group) and in KCC3 oocytes to 4,483 ± 603 pmol·oocyte^{-1}·h^{-1} ($P < 0.01$ vs. KCC3+WNK4-DA group). Thus our data suggest that catalytically inactive WNK4-D318A is able to induce activation of KCC2 and KCC3 in isotonic conditions, but not of KCC1 and KCC4.

The activation of KCC2 and KCC3 observed by WNK4-D318A is similar to what we previously observed with the catalytically inactive form of WNK3 (WNK3-D294A) (11) and it is also similar to what would be expected with activation of the protein phosphatases, suggesting that WNK4-D318A is also able to activate some of the endogenous protein phosphatases in the oocytes. To test this possibility, we assessed the effect of the PP1 inhibitor calyculin A and/or the PP2B inhibitor cyclosporine A on the WNK4-D318A-induced activation of KCC2 or KCC3 in isotonic conditions. As shown in Fig. 9*A*, the activity of KCC2 was increased by WNK4-D318A and the increment was partially inhibited by calyculin A or cyclospirne A, and completely prevented by the combination of both inhibitors. Interestingly, the activation of KCC2 achieved by the combination of both inactive kinases WNK4-D318A and SPAK-K104R was not inhibited by calyculin A or cyclosporine A alone but was significantly decreased by the combination of both inhibitors. As Fig. 9*B* shows, the activation of KCC3 either by WNK4-D318A alone or both inactive kinases together was completely prevented by calyculin A.

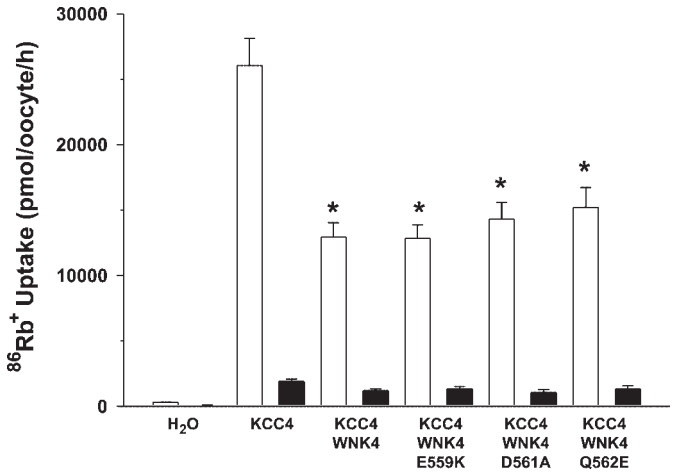

Fig. 7. PHAII-type mutations do not change the WNK4-induced inhibition of KCC4 activity. *X. laevis* oocytes were injected with water or 0.2 μg/μl each of wild-type KCC4 or KCC4 cRNA together with similar amounts of KCC4 + wild-type WNK4 or KCC4 + WNK4 harboring the PHAII-type mutations E559K, D561A, or Q562A, as stated. $^{86}Rb^+$ uptake was assessed 4 days later in hypotonic conditions (110 mosmol/kgH_2O) in the presence (open bars) or absence (filled bars) of Cl^- in the uptake medium. The pooled data from 5 experiments are shown, with means ± SE of at least 50 oocytes for each group. *Significantly different from the uptake observed in the corresponding control (absence of WNK4, $P < 0.01$).

DISCUSSION

In the present study, we analyzed the effect of the serine/threonine kinase WNK4 on the functional expression of the K^+-Cl^- cotransporter isoforms KCC1, KCC3, and KCC4. We observed that cell swelling-induced activation of K^+-Cl^- cotransporters is partially (~50%) inhibited by WNK4. The catalytic activity of WNK4 is required since the catalytically inactive WNK4-D318A, in which the aspartate 318 was substituted by alanine, lost the inhibitory effect of WNK4. The presence and/or activity of the STE20 kinase SPAK did not

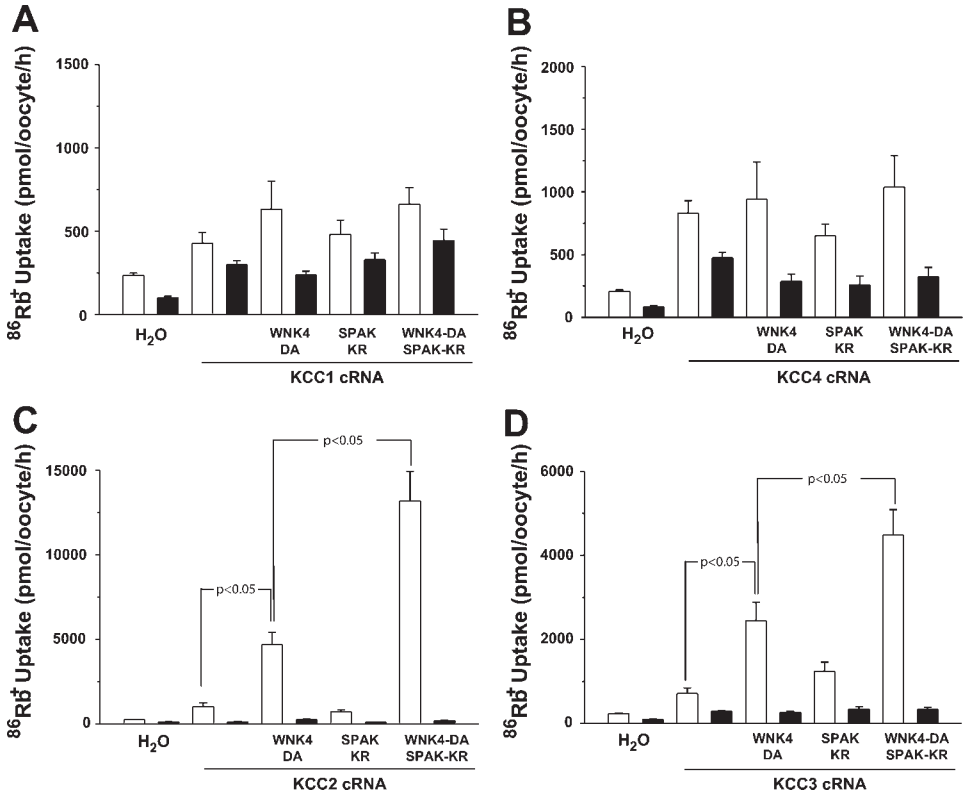

Fig. 8. Effect of catalytically inactive WNK4-D318A and SPAK-K104R on KCCs activity under isotonic conditions. *X. laevis* oocytes were injected with water or 0.2 μg/μl each of KCC1 (*A*), KCC4 (*B*), KCC2 (*C*), or KCC3 (*D*) cRNA alone or together with WNK4-D318A cRNA, SPAK-K104R cRNA, or both, as stated. $^{86}Rb^+$ uptake was assessed 4 days later in isotonic conditions (220 mosmol/kgH_2O) in the presence (open bars) or absence (filled bars) of Cl^- in the uptake medium. The pooled data from 3 experiments are shown.

affect the inhibitory effect of WNK4 on KCCs. In addition, PHA-II type mutations in WNK4 did not affect the WNK4 ability to reduce K^+-Cl^- cotransporter activity. Finally, when activity of the cotransporters was assessed in isotonic conditions, we observed that catalytically inactive WNK4 is able to bypass the tonicity requirements for activation of KCC3 (and KCC2), but not for KCC1 and KCC4.

WNK kinases are emerging as powerful regulators of several transport pathways in many tissues. Among these transport mechanisms are the cation-coupled chloride cotransporters. The hypothesis that WNK kinases are regulators of salt transport mechanisms is supported by evidence indicating that WNK kinase activity is regulated by hypertonicity and hypotonicity (31). In the kidney, WNK4 is most highly expressed in the distal nephron. In this region, the modulation of NCC and ROMK activity by WNK4 has been proposed to be critical for balancing the renal reabsorption of salt and secretion of potassium. WNK4 inhibits NCC and ROMK by different mechanisms. NCC inhibition requires the catalytic activity of WNK4 and is lost by PHAII-type mutations (9, 21, 49), whereas ROMK inhibition is independent of WNK4 catalytic activity and is enhanced by PHAII-type mutations (28). Thus it has been proposed that distinct states of WNK4 activity and regulation, presumably by aldosterone, may allow variations in WNK4 activity toward salt reabsorption and K^+ secretion mechanisms, endowing the kidney with the ability for K^+ secretion when K^+ in plasma is increased, without having to activate salt reabsorption mechanisms, or increasing salt reabsorption, when required, without having to increase K^+ secretion (28). Outside the kidney, WNK4 is expressed in several polarized epithelial cells and modulates the activity of NKCC1 (16, 25).

Another member of WNK kinases with remarkable effects on SLC12 cotransporters is WNK3. This kinase possesses the ability to bypass the tonicity requirements for activation or inhibition of the cotransporters. Wild-type WNK3 activates NCC, NKCC1, and NKCC2, and inhibits all four KCCs, even during cell swelling. In contrast, the catalytically inactive WNK3-D294A inhibits NCC, NKCC1, and NKCC2, and remarkably activates KCCs, even when oocytes are incubated in isotonic conditions (11, 27, 41). Interestingly, WNK4 without catalytic activity (WNK4-D318A) loses its inhibitory effect on NCC, while WNK3 without catalytic activity not only loses its ability to activate NCC but actually turns into a powerful inhibitor of this cotransporter.

WNK1 does not seem to directly regulate the activity of *SLC12* members. However, WNK1 has been proposed to be a major regulator of other WNK kinases. The WNK4-induced inhibition of NCC activity is prevented by WNK1 (53) and biochemical analysis has shown that WNK2 and WNK4 kinases can be phosphorylated and regulated by WNK1 (31). In addition, WNK kinases not only interact with each other. Recent observations indicate that WNK kinases also interact with STE20-like kinases such as SPAK (or PASK) and OSR1, which have been shown to regulate NKCC1 activity (13, 39). Gagnon et al. (16) observed that in the presence of SPAK, the effect of WNK4 on NKCC1 turned stimulatory when oocytes were incubated in isotonic conditions, but has no further effect when oocytes were exposed to hypertonicity, suggesting that WNK4+SPAK together are able to bypass the tonicity requirement for NKCC1 activation. Simultaneously, Vitari et al. (47) and Moriguchi et al. (36) using combinations of WNK1 or WNK4 with SPAK observed that NCC, NKCC1, or NKCC2 become phosphorylated at their NH_2-terminal domain only

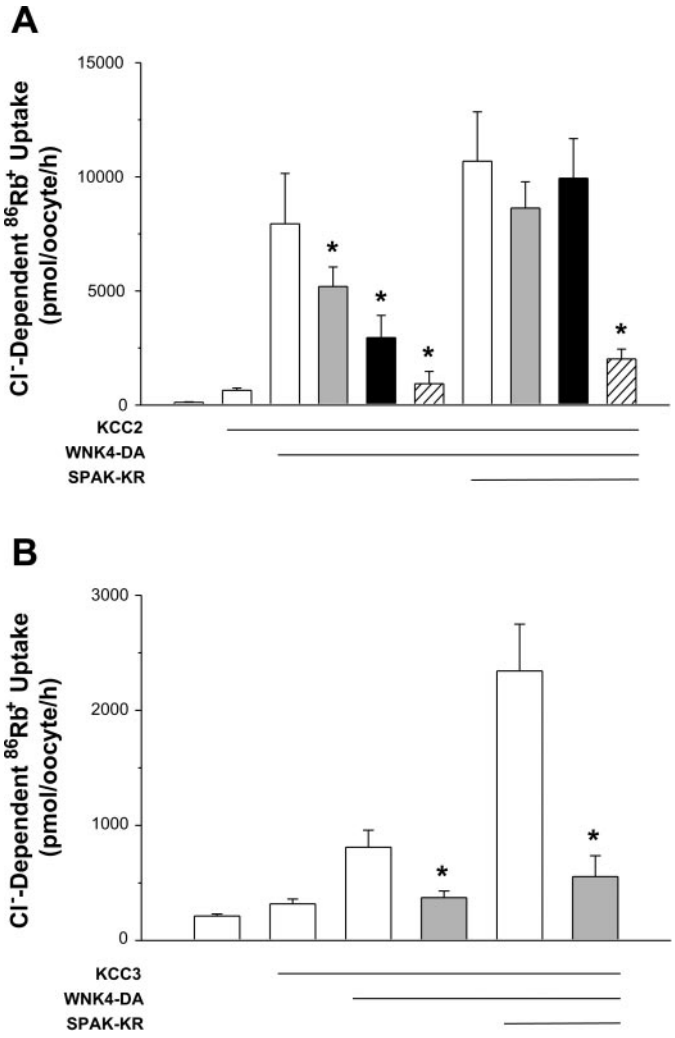

Fig. 9. Effect of the protein phosphatases inhibitors calyculin A and/or cyclosporine A on the WNK4-DA or WNK4-DA + SPAK-KR-induced activation of KCC2 or KCC3 activity under isotonic conditions. *X. laevis* oocytes were injected with water or 0.2 μg/μl each of KCC2 (*A*) or KCC3 (*B*) cRNA alone or together with WNK4-D318A cRNA or WNK4-D318A and SPAK-K104R cRNA, as stated. $^{86}Rb^+$ uptake was performed 3 days later in control conditions (open bars) or in the presence of 100 nM calyculin A (gray bars), 25 μg cyclosporine A (black bars), or both inhibitors together (stripped bars). $^{86}Rb^+$ uptake is expressed as the Cl^--dependent fraction. *Significantly different from the same group in the absence of inhibitor ($P < 0.05$).

when both WNK and SPAK kinases were expressed together, suggesting that WNK kinases lie upstream of SPAK (20). Recently, it was shown that WNK1, but not WNK4, is able to regulate OSR1 kinase in HeLa cells (5).

In the present study, we show that WNK4 also modulates the activity of the K^+-Cl^- cotransporter isoforms that are expressed outside the central nervous system. We previously observed that KCC2 is partially inhibited by WNK4 (16). The activity of KCC1, KCC3, and KCC4 is reduced by 50% when these cotransporters where coexpressed with WNK4. Thus the K^+-Cl^- cotransporters are another Cl^- transport pathway to be regulated by WNK4. Kahle et al. (25) showed that WNK4 inhibits the activity of NKCC1, whereas Gagnon et al. (16) showed that in the presence of SPAK, WNK4 increases the NKCC1 activity. Supporting these observations, Vitari et al. (47) and Moriguchi et al. (36) presented evidence that WNK1 and WNK4 are able to phosphorylate SPAK, which in turn interacts and phosphorylates the NH_2-terminal domain of NKCC1. In the present study, we observed that WNK4 is a negative regulator of the K^+-Cl^- cotransporters and that this type of effect is not changed by the presence of SPAK. This conclusion is based on the following observations. Although *X. laevis* oocytes exhibit endogenous expression of SPAK/OSR1 (Fig. 4), the activity of KCCs was not affected by coinjection of KCCs cRNA with SPAK cRNA (Fig. 2), the WNK4 effect on KCCs was not changed by coinjection of the KCCs with WNK4 and SPAK cRNA (Fig. 3), and dominant negative SPAK-K104R did not affect the inhibitory effect of WNK4 (Fig. 4). Thus WNK4 alone inhibits NKCC1 (25) and in the presence of SPAK activates NKCC1 (16, 36, 47). In contrast, WNK4 alone or coexpressed with SPAK inhibits all K^+-Cl^- cotransporters. Therefore, WNK4 (in the presence of SPAK) activates Cl^- influx and inhibits Cl^- efflux through members of the *SLC12* family. This is a similar situation to that observed previously for WNK3 that activates Cl^- influx pathways (NCC, NKCC1, and NKCC2) and inhibits Cl^- efflux pathways (KCC1 to KCC4).

Three isoforms of the K^+-Cl^- cotransporters are expressed in the kidney. Immunolocalization of KCC1 along the nephron has not been addressed. At the mRNA level, KCC1 transcripts have been shown to be expressed along the nephron (12, 32). KCC3 and KCC4 are present in the PT basolateral membrane (7, 35, 46) in which their role has been proposed to be the regulation of cell volume, since large amounts of solute and water are transported by PT cells (24, 37). For instance, stimulation of the Na^+-glucose cotransporter in the apical membrane of PT increases the load of salt and water into cells, presumably increasing cell volume, and activates a K^+ efflux mechanism that is barium insensitive and inhibitable by 1 mM furosemide, strongly suggesting that the activated pathway is a K^+-Cl^- cotransporter (6). Null mice in which KCC3 or KCC4 was disrupted, however, did not show major disturbances in renal function attributable to PT cells. It is possible that the presence of one cotransporter is enough to compensate for the absence of the other, suggesting that double knockout mice will be required to clarify the role of K^+-Cl^- cotransporters in PT cells. In TALH, the presence of a K^+-Cl^- cotransporter pathway has been clearly demonstrated to be present in the basolateral membrane (3, 22) and immunolocalization studies indicate that it is the KCC4 isoform. In DCT KCC4 is expressed in the basolateral membrane. However, physiological studies have also suggested the presence of an apical K^+-Cl^- cotransporter (4, 14, 45). Because neither KCC3 nor KCC4 has been observed in DCT apical membrane, it is highly likely that KCC1 is the isoform responsible for such observations. Finally, KCC4 has a clear role in CD acid secretion. This isoform is expressed in the basolateral membrane of α-intercalated cells and targeted disruption of KCC4 resulted in renal tubular acidosis (7). The proposed mechanism is that KCC4 is required for basolateral Cl^- efflux that maintains the gradient for the basolateral Cl^-:HCO_3^- exchanger to be functional. If the activity of this exchanger is reduced, the accumulation of HCO_3^- within the intercalated cell will prevent H^+ production and secretion in the apical membrane, reducing the urinary acidification.

Because WNK4 is most highly expressed in DCT and CD, it is expected that regulation of KCCs by WNK4 will affect the function of these cotransporters in the distal nephron, adding another pathway for the WNK4-induced inhibition of K^+ secretion. Interestingly, WNK4 inhibition of the potassium channel ROMK does not require the kinase catalytic activity (28). In contrast, WNK4-induced inhibition of K^+-Cl^- cotransporters requires the WNK4 catalytic activity. This increases the diversity of regulatory possibilities by WNK4, because it is possible that WNK4 is inhibiting two different K^+ secretory mechanism in DCT by different mechanisms. The requirement of catalytic activity of WNK4 to inhibit K^+-Cl^- cotransporters suggests that WNK4 induces phosphorylation of KCCs because it is known that KCC remains inactive when these proteins are phosphorylated (1). In addition, WNK4 could also be involved in regulating urine acidification. The expression of WNK4 along the CD has been demonstrated by three studies (30, 38, 48). None of them, however, specifically shows that WNK4 is expressed at the α-intercalated cells. If this were the case, then the inhibition of KCC4 by WNK4 could decrease the H^+ secretion by α-intercalated cells of the CD following the proposed mechanism by Boettger et al. (7). We explored the effect of PHAII-type mutations on KCC4 inhibition by WNK4 as a potential mechanism to explain part of the metabolic acidosis seen in these patients. However, our data do not support this possibility. In contrast to what has been observed for NCC (9, 49), ROMK (28), and claudins (26, 52), PHAII-type mutations in WNK4 do not affect its inhibitory properties on KCC4. Because outside the kidney WNK4 is expressed in several Cl^--transporting polarized epithelia (25), the regulation of KCCs in these places could play a role in transepithelial K^+ transport.

We previously observed that eliminating the catalytic activity of WNK3 by the D294A substitution (41) switch this kinase affects members of the *SLC12* family. Wild-type WNK3 activates NCC, NKCC1, and NKCC2, while the catalytically inactive WNK3-D294A completely inhibits the activity of these Na^+-driven cotransporters (27, 41). A similar situation occurs with KCCs. Wild-type WNK3 completely inhibits the activity of all four KCC cotransporters, even when oocytes were exposed to hypotonicity in which KCCs are maximally active, whereas WNK3-D294A activates the KCC cotransporters, even when oocytes are incubated in isotonic medium during the uptake where it is known that KCCs are inactive (11). KCC activation by WNK3-D294A apparently is due to WNK3-D294A-induced activation of protein phosphatases 1 and 2B (11). Thus WNK3 has the ability to bypass the tonicity requirements for regulation of the *SLC12* family members. In the present study, we explored whether a similar situation occurs by eliminating the catalytic activity of WNK4. Interestingly, we observed that KCC2 and KCC3 but not KCC1 or KCC4 were activated by WNK4-D318A. When catalytically inactive SPAK-K104R cRNA was added to the coinjection cocktail, further activation of KCC2 and KCC3 was observed. These effects of the catalytically inactive kinases were partially or completely prevented by the protein phosphatase inhibitors calyculin A or cyclosporine A (Fig. 9), suggesting that, as we previously observed with the catalytically inactive form of WNK3 (11), WNK4-D318A-induced increase in $^{86}Rb^+$ uptake by KCC2 and KCC3 is associated with activation of the protein phosphatases. Because KCC1 and KCC4 were not activated in the same way, it is possible that unique sequences or motifs within KCC2 and KCC3 endow these isoforms with the ability to be activated by WNK4-D318A. Further studies will be required to clarify these possibilities.

In summary, in the present study we show that K^+-Cl^- cotransporters are inhibited by WNK4, adding another Cl^- transport mechanism that is regulated by this kinase. WNK4 inhibits KCCs by mechanisms in which WNK4 catalytic activity is required. PHAII-type mutations do not change the effect of WNK4 on KCC cotransporters. Finally, the catalytically inactive WNK4 is able to activate KCC2 and KCC3 in isotonic conditions.

ACKNOWLEDGMENTS

We thank all members of the Molecular Physiology Unit for suggestions and assistance.

GRANTS

This work was supported in part by National Institutes of Health Grants DK-36803 and DK-64635 to G. Gamba and NS-36758 to E. Delpire.

REFERENCES

1. **Adragna NC, Fulvio MD, Lauf PK.** Regulation of K-Cl cotransport: from function to genes. *J Membr Biol* 201: 109–137, 2004.
2. **Adragna NC, White RE, Orlov SN, Lauf PK.** K-Cl cotransport in vascular smooth muscle and erythrocytes: possible implication in vasodilation. *Am J Physiol Cell Physiol* 278: C381–C390, 2000.
3. **Amlal H, Paillard M, Bichara M.** Cl^--dependent $NH4^+$ transport mechanisms in medullary thick ascending limb cells. *Am J Physiol Cell Physiol* 267: C1607–C1615, 1994.
4. **Amorim JB, Bailey MA, Musa-Aziz R, Giebisch G, Malnic G.** Role of luminal anion and pH in distal tubule potassium secretion. *Am J Physiol Renal Physiol* 284: F381–F388, 2003.
5. **Anselmo AN, Earnest S, Chen W, Juang YC, Kim SC, Zhao Y, Cobb MH.** WNK1 and OSR1 regulate the Na^+, K^+, $2Cl^-$ cotransporter in HeLa cells. *Proc Natl Acad Sci USA* 103: 10883–10888, 2006.
6. **Avison MJ, Gullans SR, Ogino T, Giebisch G.** Na^+ and K^+ fluxes stimulated by Na^+-coupled glucose transport: evidence for a Ba^{2+}-insensitive K^+ efflux pathway in rabbit proximal tubules. *J Membr Biol* 105: 197–205, 1988.
7. **Boettger T, Hubner CA, Maier H, Rust MB, Beck FX, Jentsch TJ.** Deafness and renal tubular acidosis in mice lacking the K-Cl cotransporter Kcc4. *Nature* 416: 874–878, 2002.
8. **Boettger T, Rust MB, Maier H, Seidenbecher T, Schweizer M, Keating DJ, Faulhaber J, Ehmke H, Pfeffer C, Scheel O, Lemcke B, Horst J, Leuwer R, Pape HC, Volkl H, Hubner CA, Jentsch TJ.** Loss of K-Cl cotransporter KCC3 causes deafness, neurodegeneration and reduced seizure threshold. *EMBO J* 22: 5422–5434, 2003.
9. **Cai H, Cebotaru V, Wang YH, Zhang XM, Cebotaru L, Guggino SE, Guggino WB.** WNK4 kinase regulates surface expression of the human sodium chloride cotransporter in mammalian cells. *Kidney Int* 69: 2162–2170, 2006.
10. **Cope G, Murthy M, Golbang AP, Hamad A, Liu CH, Cuthbert AW, O'Shaughnessy KM.** WNK1 affects surface expression of the ROMK potassium channel independent of WNK4. *J Am Soc Nephrol* 17: 1867–1874, 2006.
11. **De Los Heros P, Kahle KT, Rinehart J, Bobadilla NA, Vazquez N, San Cristobal P, Mount DB, Lifton RP, Hebert SC, Gamba G.** WNK3 bypasses the tonicity requirement for K-Cl cotransporter activation via a phosphatase-dependent pathway. *Proc Natl Acad Sci USA* 103: 1976–1981, 2006.
12. **Di Stefano A, Jounier S, Wittner M.** Evidence supporting a role for KCl cotransporter in the thick ascending limb of Henle's loop. *Kidney Int* 60: 1809–1823, 2001.
13. **Dowd BF, Forbush B.** PASK (proline-alanine-rich STE20-related kinase), a regulatory kinase of the Na-K-Cl cotransporter (NKCC1). *J Biol Chem* 278: 27347–27353, 2003.
14. **Ellison DH, Velazquez H, Wright FS.** Stimulation of distal potassium secretion by low lumen chloride in the presence of barium. *Am J Physiol Renal Fluid Electrolyte Physiol* 248: F638–F649, 1985.

15. **Ellison DH, Velazquez H, Wright FS.** Unidirectional potassium fluxes in renal distal tubule: effects of chloride and barium. *Am J Physiol Renal Fluid Electrolyte Physiol* 250: F885–F894, 1986.
16. **Gagnon KB, England R, Delpire E.** Volume sensitivity of cation-Cl^- cotransporters is modulated by the interaction of two kinases: Ste20-related proline-alanine-rich kinase and WNK4. *Am J Physiol Cell Physiol* 290: C134–C142, 2006.
17. **Gamba G, Miyanoshita A, Lombardi M, Lytton J, Lee WS, Hediger MA, Hebert SC.** Molecular cloning, primary structure and characterization of two members of the mammalian electroneutral sodium-(potassium)-chloride cotransporter family expressed in kidney. *J Biol Chem* 269: 17713–17722, 1994.
18. **Gamba G.** Molecular physiology and pathophysiology of the electroneutral cation-chloride cotransporters. *Physiol Rev* 85: 423–493, 2005.
19. **Gamba G.** Role of WNK kinases in regulating tubular salt and potassium transport and in the development of hypertension. *Am J Physiol Renal Physiol* 288: F245–F252, 2005.
20. **Gamba G.** WNK lies upstream of kinases involved in regulation of ion transporters. *Biochem J* 391: e1–e3, 2005.
21. **Golbang AP, Cope G, Hamad A, Murthy M, Liu CH, Cuthbert AW, O'Shaughnessy KM.** Regulation of the expression of the Na/Cl cotransporter (NCCT) by WNK4 and WNK1: evidence that accelerated dynamin-dependent endocytosis is not involved. *Am J Physiol Renal Physiol* 291: F1369–F1376, 2006.
22. **Greger R, Schlatter E.** Porpierties of the basolateral membrane on the cortical thick ascending limb of Henle's loop of rabbit kidney. A model for secondary active chloride transport. *Pflügers Arch* 396: 325–334, 1983.
23. **Howard HC, Mount DB, Rochefort D, Byun N, Dupre N, Lu J, Fan X, Song L, Riviere JB, Prevost C, Horst J, Simonati A, Lemcke B, Welch R, England R, Zhan FQ, Mercado A, Siesser WB, George AL Jr, McDonald MP, Bouchard JP, Mathieu J, Delpire E, Rouleau GA.** The K-Cl cotransporter KCC3 is mutant in a severe peripheral neuropathy associated with agenesis of the corpus callosum. *Nat Genet* 32: 384–392, 2002.
24. **Jentsch TJ.** Chloride transport in the kidney: lessons from human disease and knockout mice. *J Am Soc Nephrol* 16: 1549–1561, 2005.
25. **Kahle KT, Gimenez I, Hassan H, Wilson FH, Wong RD, Forbush B, Aronson PS, Lifton RP.** WNK4 regulates apical and basolateral Cl^- flux in extrarenal epithelia. *Proc Natl Acad Sci USA* 101: 2064–2069, 2004.
26. **Kahle KT, MacGregor GG, Wilson FH, Van Hoek AN, Brown D, Ardito T, Kashgarian M, Giebisch G, Hebert SC, Boulpaep EL, Lifton RP.** Paracellular Cl^- permeability is regulated by WNK4 kinase: insight into normal physiology and hypertension. *Proc Natl Acad Sci USA* 101: 14877–14882, 2004.
27. **Kahle KT, Rinehart J, De Los HP, Louvi A, Meade P, Vazquez N, Hebert SC, Gamba G, Gimenez I, Lifton RP.** WNK3 modulates transport of Cl^- in and out of cells: implications for control of cell volume and neuronal excitability. *Proc Natl Acad Sci USA* 102: 16783–16788, 2005.
28. **Kahle KT, Wilson FH, Leng Q, Lalioti MD, O'Connell AD, Dong K, Rapson AK, MacGregor GG, Giebisch G, Hebert SC, Lifton RP.** WNK4 regulates the balance between renal NaCl reabsorption and K^+ secretion. *Nat Genet* 35: 372–376, 2003.
29. **Kone BC, Brady HR, Gullans SR.** Coordinated regulation of intracellular K^+ in the proximal tubule: Ba^{2+} blockade downregulates the Na^+,K^+-ATPase and upregulates two K^+ permeability pathways. *Proc Natl Acad Sci USA* 86: 6431–6435, 1989.
30. **Lalioti MD, Zhang J, Volkman HM, Kahle KT, Hoffmann KE, Toka HR, Nelson-Williams C, Ellison DH, Flavell R, Booth CJ, Lu Y, Geller DS, Lifton RP.** Wnk4 controls blood pressure and potassium homeostasis via regulation of mass and activity of the distal convoluted tubule. *Nat Genet* 38: 1124–1132, 2006.
31. **Lenertz LY, Lee BH, Min X, Xu BE, Wedin K, Earnest S, Goldsmith EJ, Cobb MH.** Properties of WNK1 and implications for other family members. *J Biol Chem* 280: 26653–26658, 2005.
32. **Liapis H, Nag M, Kaji DM.** K-Cl cotransporter expression in the human kidney. *Am J Physiol Cell Physiol* 275: C1432–C1437, 1998.
33. **Mercado A, Mount DB, Gamba G.** Electroneutral cation-chloride cotransporters in the central nervous system. *Neurochem Res* 29: 17–25, 2004.
34. **Mercado A, Song L, Vazquez N, Mount DB, Gamba G.** Functional comparison of the K^+-Cl^- cotransporters KCC1 and KCC4. *J Biol Chem* 275: 30326–30334, 2000.
35. **Mercado A, Vazquez N, Song L, Cortes R, Enck AH, Welch R, Delpire E, Gamba G, Mount DB.** Amino-terminal heterogeneity in the KCC3 K^+-Cl^- cotransporter. *Am J Physiol Renal Physiol* 289: F1246–F1261, 2005.
36. **Moriguchi T, Urushiyama S, Hisamoto N, Iemura S, Uchida S, Natsume T, Matsumoto K, Shibuya H.** WNK1 regulates phosphorylation of cation-chloride-coupled cotransporters via the STE20-related kinases, SPAK and OSR1. *J Biol Chem* 280: 42685–42693, 2005.
37. **Mount DB, Gamba G.** Renal potassium-chloride cotransporters. *Curr Opin Nephrol Hypertens* 10: 685–691, 2001.
38. **O'Reilly M, Marshall E, Macgillivray T, Mittal M, Xue W, Kenyon CJ, Brown RW.** Dietary electrolyte-driven responses in the renal WNK kinase pathway in vivo. *J Am Soc Nephrol* 17: 2402–2413, 2006.
39. **Piechotta K, Garbarini N, England R, Delpire E.** Characterization of the interaction of the stress kinase SPAK with the Na^+-K^+-$2Cl^-$ cotransporter in the nervous system: evidence for a scaffolding role of the kinase. *J Biol Chem* 278: 52848–52856, 2003.
40. **Piechotta K, Lu J, Delpire E.** Cation chloride cotransporters interact with the stress-related kinases Ste20-related proline-alanine-rich kinase (SPAK) and oxidative stress response 1 (OSR1). *J Biol Chem* 277: 50812–50819, 2002.
41. **Rinehart J, Kahle KT, De Los HP, Vazquez N, Meade P, Wilson FH, Hebert SC, Gimenez I, Gamba G, Lifton RP.** WNK3 kinase is a positive regulator of NKCC2 and NCC, renal cation- Cl^- cotransporters required for normal blood pressure homeostasis. *Proc Natl Acad Sci USA* 102: 16777–16782, 2005.
42. **Rust MB, Faulhaber J, Budack MK, Pfeffer C, Maritzen T, Didie M, Beck FX, Boettger T, Schubert R, Ehmke H, Jentsch TJ, Hubner CA.** Neurogenic mechanisms contribute to hypertension in mice with disruption of the K-Cl cotransporter KCC3. *Circ Res* 98: 549–556, 2006.
43. **Schafer JA, Troutman SL.** Potassium transport in cortical collecting tubules from mineralocorticoid-treated rat. *Am J Physiol Renal Fluid Electrolyte Physiol* 253: F76–F88, 1987.
44. **Song L, Mercado A, Vazquez N, Xie Q, Desai R, George AL, Gamba G, Mount DB.** Molecular, functional, and genomic characterization of human KCC2, the neuronal K-Cl cotransporter. *Brain Res Mol Brain Res* 103: 91–105, 2002.
45. **Velazquez H, Ellison DH, Wright FS.** Luminal influences on potassium secretion: chloride, sodium and thiazide diuretics. *Am J Physiol Renal Fluid Electrolyte Physiol* 262: F1076–F1082, 1992.
46. **Velazquez H, Silva T.** Cloning and localization of KCC4 in rabbit kidney: expression in distal convoluted tubule. *Am J Physiol Renal Physiol* 285: F49–F58, 2003.
47. **Vitari AC, Deak M, Morrice NA, Alessi DR.** The WNK1 and WNK4 protein kinases that are mutated in Gordon's hypertension syndrome, phosphorylate and active SPAK and OSR1 protein kinases. *Biochem J* 391: 17–24, 2005.
48. **Wilson FH, Disse-Nicodeme S, Choate KA, Ishikawa K, Nelson-Williams C, Desitter I, Gunel M, Milford DV, Lipkin GW, Achard JM, Feely MP, Dussol B, Berland Y, Unwin RJ, Mayan H, Simon DB, Farfel Z, Jeunemaitre X, Lifton RP.** Human hypertension caused by mutations in WNK kinases. *Science* 293: 1107–1112, 2001.
49. **Wilson FH, Kahle KT, Sabath E, Lalioti MD, Rapson AK, Hoover RS, Hebert SC, Gamba G, Lifton RP.** Molecular pathogenesis of inherited hypertension with hyperkalemia: the Na-Cl cotransporter is inhibited by wild-type but not mutant WNK4. *Proc Natl Acad Sci USA* 100: 680–684, 2003.
50. **Xu B, English JM, Wilsbacher JL, Stippec S, Goldsmith EJ, Cobb MH.** WNK1, a novel mammalian serine/threonine protein kinase lacking the catalytic lysine in subdomain II. *J Biol Chem* 275: 16795–16801, 2000.
51. **Xu BE, Stippec S, Chu PY, Lazrak A, Li XJ, Lee BH, English JM, Ortega B, Huang CL, Cobb MH.** WNK1 activates SGK1 to regulate the epithelial sodium channel. *Proc Natl Acad Sci USA* 102: 10315–10320, 2005.
52. **Yamauchi K, Rai T, Kobayashi K, Sohara E, Suzuki T, Itoh T, Suda S, Hayama A, Sasaki S, Uchida S.** Disease-causing mutant WNK4 increases paracellular chloride permeability and phosphorylates claudins. *Proc Natl Acad Sci USA* 101: 4690–4694, 2004.
53. **Yang CL, Angell J, Mitchell R, Ellison DH.** WNK kinases regulate thiazide-sensitive Na-Cl cotransport. *J Clin Invest* 111: 1039–1045, 2003.
54. **Yang CL, Zhu X, Wang Z, Subramanya AR, Ellison DH.** Mechanisms of WNK1 and WNK4 interaction in the regulation of thiazide-sensitive NaCl cotransport. *J Clin Invest* 115: 1379–1387, 2005.
55. **Zhou X, Xia SL, Wingo CS.** Chloride transport by the rabbit cortical collecting duct: dependence on H,K-ATPase. *J Am Soc Nephrol* 9: 2194–2202, 1998.

Am J Physiol Renal Physiol 295: F789–F802, 2008.
First published June 25, 2008; doi:10.1152/ajprenal.90227.2008.

Renal Na^+-K^+-Cl^- cotransporter activity and vasopressin-induced trafficking are lipid raft-dependent

Pia Welker,[1]* Alexandra Böhlick,[1]* Kerim Mutig,[1] Michele Salanova,[1] Thomas Kahl,[1] Hartmut Schlüter,[2] Dieter Blottner,[1] Jose Ponce-Coria,[3] Gerardo Gamba,[3] and Sebastian Bachmann[1]

[1]*Department of Anatomy, Charité-Universitätsmedizin Berlin, Berlin;* [2]*Department of Nephrology, Charité-Universitätsmedizin Berlin, Berlin, Germany; and* [3]*Instituto Nacional de Ciencias Médicas y Nutrición Salvador Zubirán and Instituto de Investigaciones Biomédicas, Universidad Nacional Autónoma de México, Mexico City, Mexico*

Submitted 1 April 2008; accepted in final form 17 June 2008

Welker P, Böhlick A, Mutig K, Salanova M, Kahl T, Schlüter H, Blottner D, Ponce-Coria J, Gamba G, Bachmann S. Renal Na^+-K^+-Cl^- cotransporter activity and vasopressin-induced trafficking are lipid raft-dependent. *Am J Physiol Renal Physiol* 295: F789–F802, 2008. First published June 25, 2008; doi:10.1152/ajprenal.90227.2008.—Apical bumetanide-sensitive Na^+-K^+-$2Cl^-$ cotransporter (NKCC2), the kidney-specific member of a cation-chloride cotransporter superfamily, is an integral membrane protein responsible for the transepithelial reabsorption of NaCl. The role of NKCC2 is essential for renal volume regulation. Vasopressin (AVP) controls NKCC2 surface expression in cells of the thick ascending limb of the loop of Henle (TAL). We found that 40–70% of Triton X-100-insoluble NKCC2 was present in cholesterol-enriched lipid rafts (LR) in rat kidney and cultured TAL cells. The related Na^+-Cl^- cotransporter (NCC) from rat kidney was distributed in LR as well. NKCC2-containing LR were detected both intracellularly and in the plasma membrane. Bumetanide-sensitive transport of NKCC2 as analyzed by $^{86}Rb^+$ influx in *Xenopus laevis* oocytes was markedly reduced by methyl-β-cyclodextrin (MβCD)-induced cholesterol depletion. In TAL, short-term AVP application induced apical vesicular trafficking along with a shift of NKCC2 from non-raft to LR fractions. In parallel, increased colocalization of NKCC2 with the LR ganglioside GM1 and their polar translocation were assessed by confocal analysis. Apical biotinylation showed twofold increases in NKCC2 surface expression. These effects were blunted by mevalonate-lovastatin/MβCD-induced cholesterol deprivation. Collectively, these findings demonstrate that a pool of NKCC2 distributes in rafts. Results are consistent with a model in which LR mediate polar insertion, activity, and AVP-induced trafficking of NKCC2 in the control of transepithelial NaCl transport.

thick ascending limb; lipid raft; *Xenopus* oocyte; cholesterol depletion

THE KIDNEY-SPECIFIC, apical Na^+-K^+-$2Cl^-$ cotransporter (NKCC2 or BSC1; *SLC12A1*) is strongly expressed on the luminal membrane of renal tubular cells of the thick ascending limb of Henle's loop (TAL) (14, 32), where it is crucial for normal Na^+, K^+, Cl^-, Mg^{2+}, and Ca^{2+} reabsorption (16). It also serves to maintain the corticomedullary osmotic gradient that drives urinary concentration in response to the antidiuretic hormone vasopressin (AVP) (14, 18). In the specialized cells of TAL constituting the macula densa, NKCC2 mediates signaling at the juxtaglomerular apparatus (32, 33, 47). The fundamental role of NKCC2 in renal salt reabsorption has further been firmly established in the context of salt wasting disorders and NKCC2-deficient mice (37, 52).

Data on the intracellular regulation of NKCC2 are scarce (13). Amino-terminal phosphorylation at three threonine residues (15), mediated by kinases such as WNK3 (39), may play a major role herein. AVP, glucagon, several other hormones, paracrine factors, and osmolality have been shown to influence NaCl transport as well as trafficking and biosynthesis of NKCC2 (14, 24, 27, 34, 46). AVP is particularly effective in enhancing NKCC2 and salt transport via $G\alpha_s$-coupled V2 receptor (V2R), cAMP release, and PKA activation preferentially in medullary TAL (1, 14, 18, 27, 29). Localization of NKCC2 in subapical vesicles suggested membrane translocation of the transporter in the acute response to AVP/cAMP (31). In accordance with this, acute AVP-dependent phosphorylation of NKCC2 was associated with vesicular trafficking of the transporter to the luminal membrane (14).

Membrane proteins can be organized in microdomains (lipid rafts, LR). LR are liquid-ordered phase, discrete domains enriched in glycosphingolipids and cholesterol. The raft hypothesis proposes that phase separation causes these lipids and proteins to aggregate in LR, determining their insolubility in nonionic detergents (for review, see Refs. 4, 36, 50). In the biosynthetic pathway, proteins may enter LR at the Golgi level and form complexes with other membrane proteins. Their shuttling between the Golgi and the cell membrane is probably a way for the cell to exert regulatory control over the surface expression of the proteins (30, 51). Lipid-binding proteins such as caveolins or flotillins may help to organize LR (9, 44). Although there has been controversy about proper definitions in the raft concept, there is now little doubt about their functional involvement in polar sorting, turnover, and signaling properties of membrane proteins (4, 22, 48). Meanwhile, it has been shown that apart from hydrophobicity, other factors such as transmembrane domain amino acid sequence, membrane-proximal cytoplasmic or extracellular motifs, or components of adhering macromolecular complexes may affect raftophilicity (2, 4, 6, 11, 38, 53). Accordingly, there is now growing literature to demonstrate that membrane-multispanning ion channels and transporters such as the Na^+/H^+ exchanger 3 (NHE3), Na^+-P_i cotransporter-2 (NaPi-IIa), epithelial Na^+ channel (ENaC), and basolateral Na^+-K^+-ATPase (NKA) may distribute in LR (20, 21, 28, 55).

In this study we hypothesized whether surface expression, activity, and vesicular trafficking of NKCC2 depend on its distribution in LR. We have studied a functional role for the lipid environment in NKCC2-dependent ion transport using an

* P. Welker and A. Böhlick contributed equally to this work.

Address for reprint requests and other correspondence: S. Bachmann, Institute of Anatomy, Charité-Universitätsmedizin Berlin, Philippstr. 12, 10115 Berlin, Germany (e-mail: sbachm@charite.de).

The costs of publication of this article were defrayed in part by the payment of page charges. The article must therefore be hereby marked "*advertisement*" in accordance with 18 U.S.C. Section 1734 solely to indicate this fact.

oocyte system with heterologous expression of NKCC2 (27, 39). The Brattleboro rat model of central diabetes insipidus was used to study the effect of AVP on the pool of LR-associated NKCC2 in apical trafficking. The cell biological detail of LR-related trafficking and delivery of NKCC2 to the apical cell pole was investigated in cultured TAL cells.

EXPERIMENTAL PROCEDURES

Animals. Adult male Sprague-Dawley (SD), Long Evans (LE), and Brattleboro rats with hereditary hypothalamic diabetes insipidus (DI) weighing between 200 and 250 g were used. LE and DI rats had been obtained from Harlan (Indianapolis IN) for breeding. All rats were bred in the local animal facility under conditions agreed to by the German law for animal protection (Berlin registration no. G357/05). Homozygous DI and control LE rats received treatments to induce trafficking of NKCC2; the selective V2 vasopressin receptor agonist 1-deamino-8-D-arginine vasopressin (dDAVP; 1 μg/kg body wt) or vehicle (0.9% NaCl) were given to both strains by intraperitoneal injections (4 groups, total $n = 20$ rats). To obtain kidneys for cell isolation or biochemical analysis, rats were isoflurane anesthetized and kidneys were removed via opening of the abdominal cavity 1 h after drug application. For histochemical evaluation of kidneys, rats were given an intraperitoneal injection of Nembutal (40 mg/kg body wt) and were aldehyde-fixed by retrograde perfusion through the abdominal aorta (46). Kidneys were then removed and prepared for cryostat sectioning or paraffin embedding. For immunoelectron microscopy, samples were postfixed in 3% paraformaldehyde (PFA) and 0.05% glutaraldehyde and then embedded in LR-White resin.

Cells. Cultured SV40-transformed rabbit TAL cells (rbTAL) were obtained from rabbit kidney medulla. Cells were seeded on culture dishes or glass coverslips and cultured in DMEM/Ham's F-12 medium containing L-glutamine, 15 mM HEPES, 1% penicillin/streptomycin, 5% fetal calf serum, 1% L-glutamine, and 1% nonessential amino acids (GIBCO; 7.5% CO_2, 37°C). Cells were utilized up to the 10th passage (55). For immunohistochemistry, cells were seeded in multiwell tissue culture plates into which either coverslips coated with aminosilane (Sigma) or, alternatively, membrane inserts with a pore size of 0.4 μm (Falcon) had been placed. Cells were grown to confluent monolayers and incubated with 7.5% CO_2 at 37°C. Culture medium was changed every 2 days. Cell viability was tested using trypan blue (Sigma).

AVP treatment. For AVP treatment, cells were incubated in culture flasks or on coverslips with 0.l μM AVP (Sigma) in culture medium for 15, 30, or 60 min and 4, 6, or 24 h, harvested, and prepared for Western blot or immunostaining as detailed below. To study responsiveness to the cAMP signaling pathway under AVP stimulation (34), rbTAL cells were incubated for 1 h with the cAMP agonist 8-bromoadenosine 3′,5′-cyclic monophosphate (8-Br-cAMP; 10 nM; Biolog) or the PKA inhibitors H-89 (10 nM; Biaffin) or the *Rp* diastereomer of adenosine 3′,5′-cyclic monophosphorothioate (*Rp*-cAMPS; 20 nM; Biolog) in the presence or absence of AVP. Cells had been preincubated for 45 min with 0.5 mM 3-isobutyl-1-methyl xanthine (Sigma) to inhibit the activity of cAMP phosphodiesterase. Cells were then washed with cold PBS, harvested, counted in a Neubauer chamber, frozen and thawed twice, and centrifuged at 800 *g*. cAMP was detected in the supernatants using an ELISA kit (R&D Systems). Influence of AVP on NKCC2 translation was studied by preincubation of rbTAL cells with 0.1 mM cycloheximide (Sigma) for 4 h, followed by an incubation for 1 or 4 h with AVP (0.1 μM) in the continued presence of cycloheximide. Whole cell lysates were analyzed by Western blotting. To study the role of the cytoskeleton, the actin-depolarizing agent cytochalasin-B (20 μM; Sigma) was applied in the presence or absence of AVP.

Functional expression of NKCC2 in Xenopus laevis oocytes. Functional expression of NKCC2 was assessed as previously described (27, 35). In brief, defolliculated stage V–VI *Xenopus laevis* oocytes were injected with water or NKCC2 cRNA at 0.2 μg/μl and incubated for 3 days in frog Ringer ND96 containing sodium pyruvate and gentamicin. The next day, oocytes were exposed to 30 min of incubation in K^+- and Cl^--free ND96 medium supplemented with 1 mM ouabain, followed by a 60-min uptake period in ND96 with 1 mM ouabain and 2.0 μCi of $^{86}Rb^+$. Because *X. laevis* oocytes express an endogenous Na^+-K^+-$2Cl^-$ cotransporter (12), the mean value observed in water-injected oocytes was subtracted from the uptake observed in NKCC2-injected oocytes from each experiment. $^{86}Rb^+$ uptake was assessed in the absence or presence of bumetanide. Values observed in parallel groups of oocytes injected with water were subtracted from values in corresponding groups of oocytes injected with NKCC2 cRNA to define the $^{86}Rb^+$ uptake induced by NKCC2. At the end of the uptake period, oocytes were washed five times in ice-cold uptake solution without isotope, dissolved in 10% sodium dodecyl sulfate, and counted by beta scintillation counting. Each experiment was performed in duplicate.

Depletion of membrane cholesterol. For cholesterol depletion (CD), rbTAL cells were cultured in the presence or absence of 4 μM lovastatin and 0.25 mM mevalonate for 24 h and subsequently for 1 h with 10 mM methyl-β-cyclodextrin (MβCD; all from Sigma). To confirm CD cytochemically, coverslips or membrane inserts were incubated for 15 min with green fluorescent filipin (125 μg/ml in PBS at room temperature; Sigma), followed by nuclear staining with 4,6-diamidino-2-phenylindole (DAPI; dilution 1:10,000; Abcam). Coverslips or inserts were placed on microscopic slides in the presence of antifading fluorescence mounting medium (DAKO). Oocytes were exposed to 10 mM MβCD alone for a total of 90 or 180 min, including the uptake period of 60 min. The use of MβCD to induce CD in *X. laevis* oocytes has been previously validated (45).

In situ hybridization. In situ hybridization was performed on perfusion-fixed, paraffin-embedded tissue as described previously (29). Digoxygenin (DIG)-11-UTP-labeled antisense V2R riboprobes were hybridized and recognized with sheep anti-DIG-alkaline phosphatase-conjugated antibody (DAKO) diluted 1:50 in blocking medium. Signal was generated using 4-nitroblue tetrazolium chloride. Sections were analyzed in bright-field microscopy.

Antisera. Antibodies used for NKCC2 in this study were guinea pig anti-rat NKCC2 antibody (2.1; 1:250 dilution) (29, 46), rabbit anti-rat NKCC2 antibody (1:250 dilution; Biotrend), and mouse monoclonal anti-rabbit NKCC1/2 antibody (T4; 1:250 dilution; Developmental Studies Hybridoma Bank). Other antibodies used in this study were rabbit anti-human THP (1:200 dilution) (46), mouse monoclonal anti-flotillin-1 antibody (1:500 dilution; BD Biosciences), mouse monoclonal anti-caveolin-1 antibody (1:200 dilution; Santa Cruz Biotechnology), rabbit anti-human zonula occludens (ZO)-1 antibody (1:500 dilution; Invitrogen), mouse monoclonal anti-clathrin antibody (1:200 dilution; Progene), rabbit polyclonal anti-vasopressin receptor (V2R) antibody (1:300 dilution) (29), and rabbit polyclonal anti-ganglioside asialoGM1 (1:500 dilution, Abcam). For double staining, specific sera were combined with FITC-conjugated phalloidin, staining actin filaments (Molecular Probes). Secondary antibodies were coupled to horseradish peroxidase (HRP; DAKO), Cy3, or Cy2 (both from Dianova).

Immunohistochemical analysis. Cryostat sections (7 μm) or paraffin sections (4 μm) were prepared for immunohistochemical study of kidneys. For immunoelectron microscopy, ultrathin LR-White sections were prepared on grids. To analyze cultured cells, these were grown on coverslips and fixed with cold methanol or, alternatively, 3% PFA in PBS. In brief, sections and cells were blocked with 5% milk powder dissolved in PBS and incubated with specific antibodies dissolved in the blocking solution overnight at 4°C; after thorough rinsing in PBS, appropriate secondary antibodies were applied at room temperature (55). Monolayers from primary cell culture were selected for evaluation when a proportion of 20–30% of the cells was NKCC2 immunoreactive. Immunoelectron microscopy staining was performed on grids, and signal was detected with 10-nm IgG-coupled

immunogold (Auroprobe). All antibodies used for immunohistochemistry had been previously characterized elsewhere; specificity was therefore controlled only by omitting the first antibody.

Conventional fluorescence microscopy and quantitative confocal laser scanning microscopy. Conventional fluorescence microscopy was performed in a DMRB microscope (Leica) equipped with a digital camera (Spot 32; Diagnostic Instruments); images were digitized using Metaview software (Visitron). For confocal microscopy and quantitative evaluation of the cell culture experiments, a confocal laser scanning microscope equipped with a multilaser system (argon laser, 458–514 nm; helium-neon laser, 543 nm; and helium-neon laser, 633 nm; Leica) and a Leica confocal software package was used. The observer was blinded to the treatment of the individual samples. From each experiment, five slides per individual condition, cytochemically labeled by single or double staining, were analyzed by randomly selecting five optical fields per slide. Multichannel detection was checked by sequential scanning analysis to avoid overlapping of fluorescence emission signals in double-stained conditions. Per field, the sum of pixel intensities in the selected stacks of interest of the apical vs. basolateral cell compartments were evaluated. The dynamic range was set such that sites with the most intensive fluorescence had only a few saturated pixels. Fluorescence signal intensities were quantified under standard digital scanning conditions with the basic microscope settings (laser intensity, photomultiplier tube offset, and gain) adjusted uniformly for the evaluation of the individual samples.

Cholera toxin-NKCC2 double staining. To study potential colocalization of NKCC2 with the LR component ganglioside GM1, primary TAL cells and rbTAL cells grown on coverslips were incubated with a cholera toxin-B chain (CT-B)-Alexa 594 conjugate (10 μg/ml) that binds to GM1, followed by incubation with antibody to CT-B; the conjugates were then cross-linked with PFA according to the manufacturer's instructions (Vybrant lipid raft labeling kit; Sigma). Next, the cells were incubated with anti-NKCC2 (2:1) for double staining, followed by staining with Cy3-coupled secondary antibody.

Tissue and cell homogenization and fractionation. Tissue blocks of kidney inner stripe or cortex were frozen in liquid nitrogen, ground in a mortar, and thawed in *buffer I* [250 mM sucrose, 10 mM triethanolamine, protease inhibitors (Complete; Roche Diagnostics), pH 7.5] (55); alternatively, 500 mM sodium carbonate, 5 mM dithiothreitol, and the protease inhibitors were used at pH 11. rbTAL cells grown to confluence were harvested in ice-cold PBS with a plastic scraper (20 petri dishes per experiment, diameter 9 cm; Falcon) and pelleted. The pellet was frozen in liquid nitrogen and then thawed in *buffer I*. Tissues and cells were subsequently lysed by ultrasonication (5 × 5 s with 4°C cooling intervals) to produce extracts. These were centrifuged at 300 *g* (10 min, 4°C) to remove nuclei and whole cells or, alternatively, at 4,000 *g* (15 min, 4°C) to also remove mitochondria (P1). For preparation of membrane fractions, the resulting postnuclear supernatant (S1) was centrifuged at 18.000 *g* (60 min, 4°C) to obtain a pellet containing plasma membrane and adherent vesicular structures (P2) and a supernatant (S2) containing the intracellular fraction with cytoplasmic and vesicular components.

Detergent extraction using Triton X-100. The postnuclear supernatant (S1) was centrifuged at 120,000 *g.* (60 min, 4°C) to concentrate the plasma membrane and cytoplasmic vesicular structures. The pellet was homogenized in *buffer I* with a 26G syringe and incubated with ice-cold. Triton X-100 (final concentration 1%, 60 min, 4°C). Alternatives to Triton X-100 (Triton X-114, Brij-98, and CHAPS) have been tested as well.

Sucrose gradient fractionation (floating assay). Triton X-100-treated cell or kidney homogenates were resuspended in *buffer I* and processed using two alternative floatation techniques that differed with respect to gradient composition (55). In brief, the detergent-insoluble fraction was resuspended in 1 ml of *buffer I* containing 40% sucrose, overlayed with 2 ml of 30% sucrose plus 2 ml of 5% sucrose in *buffer I* (discontinuous floating assay). Both gradients were then centrifuged at 200,000 *g* (16 h, 4°C). From the discontinuous gradients, 3 fractions (1 ml of 40%, 2 ml of 30%, and 2 ml of 5% sucrose) for overview study and parallel lipid analysis or 10 fractions (200 μl each) for high-resolution analysis were sequentially collected from the top of the gradients and analyzed using gel electrophoresis and Western blotting. For control purpose, cell or kidney homogenates were incubated with Triton X-100 (1%) at 37°C for 1 h to study disintegration of LR.

Gel electrophoresis and immunoblotting. Protein concentrations were measured with the BCA protein assay reagent kit (Pierce), and 20 μg of protein per lane were separated on 8 or 10% SDS polyacrylamide minigels. After electrophoretic transfer to nitrocellulose membranes, equity in protein loading and blotting was verified by membrane staining using 0.1% Ponceau red. Membranes were blocked with 5% skim milk in PBS and exposed to the specific antibodies for 90 min at room temperature, followed by HRP-conjugated secondary antibody (DAKO) for 45 min at room temperature. Immunoreactive bands were detected by chemiluminescence, using an enhanced chemiluminescence (ECL-) kit and exposed to Amersham Hyperfilm ECL X-ray films (both from GE Healthcare). BIO-PROFIL Bio-1D image software (Vilber Lourmat) was used for densitometric evaluation of the resulting bands.

Lipid analysis. Fractions of floating assays derived from rat kidney outer medullary membrane preparations were resuspended in 50 mM Tris·HCl, 150 mM NaCl, 0.5% Na-deoxycholate, and 20% methanol (pH 7.4), blotted onto nitrocellulose, verified by Ponceau red, and analyzed by dot-blot staining for GM1 using specific antibody and peroxidase detection. For further lipid detection, extracts were resuspended in 100 μl of 50 mM HEPES adjusted to pH 8.0 in HEPES and mixed with 200 μl of methanol-chloroform (1:1). After Bligh-Dyer two-phase extraction, lipids were separated by thin-layer chromatography (TLC) using a mixture of chloroform-methanol-H_2O (65:25:4). Lipids were visualized using 20% H_2SO_4 at 120°C. Cholesterol, phosphatidylcholine, and sphingomyelin were used as standards (all from Sigma). Dot blot and TLC signals were evaluated densitometrically.

Liquid chromatography-tandem mass spectrometry for identification of NKCC2 in membrane raft fractions. LR preparations of kidney outer medullary tissue from control rats were used to verify NKCC2 in raft fractions by liquid chromatography-tandem mass spectrometry (LC-MS/MS) (see Supplemental Material 1). (Supplemental data for this article is available online at the *American Journal of Physiology-Renal Physiology* website.)

Ultrastructural analysis of LR. LR fractions from floating assays with membrane preparations from rat kidney outer medulla were resuspended in HEPES (pH 7.3) and prepared for fixation or Western blot control using anti-flotillin-1 antibody. Pooled pellets were fixed in 3% PFA and 0.05% glutaraldehyde and embedded in LR-White resin. Immunogold labeling on the grids was performed with anti-NKCC2 antibody (T4) and 10-nm size immunogold for detection as described above. Ultrathin sections were examined in a Zeiss EM 12.

Surface biotinylation. Control rbTAL cells as well as cholesterol-depleted and AVP-treated rbTAL cells were prepared as detailed above. Cells were grown in culture flasks and washed with ice-cold PBS (pH 7.5) for surface biotinylation using sulfo-NHS-biotin (Pierce) according to the manufacturer's instructions. In brief, cells were incubated for 30 min with the biotin reagent, followed by removal of the solution and quenching of remaining reagent with PBS containing 100 mM glycine. Cells were then scraped, washed with cold PBS, and centrifuged to produce a postnuclear supernatant (S1) that was further centrifuged at 18,000 *g* for 30 min to obtain the membrane fraction (P2) and a supernatant (S2; cytoplasmic and vesicular fraction). P2 and S2 fractions were incubated with protein G-coupled microbeads for magnetic cell separation (MACS, Miltenyi) according to the manufacturer's instructions. The protein G-coupled beads were incubated with rabbit anti-NKCC2 antibody (1:200 dilution) and mixed with the P2 and S2 fractions for 1 h on a rotating platform at 4°C. Beads were then bound to columns placed in a magnetic field, and

columns were washed by sucrose buffer three times to remove unbound proteins. Immunoprecipitated protein was then eluted from the columns. Eluates were analyzed by Western blot. To this end, beads were run on 8% SDS-PAGE, blotted onto nitrocellulose, and detected with streptavidin-coupled HRP (1:5,000 dilution; DAKO) or guinea pig anti-NKCC2 (1:250 dilution); signal was generated by anti-guinea pig antibody coupled to HRP (1:4,000 dilution; DAKO).

RT-PCR. Total RNA was isolated from whole kidney homogenates or cell lysates using the RNeasy total RNA kit (Qiagen). To perform RT-PCR, genomic DNA was digested by DNase. cDNA was synthesized by reverse transcription of 5 μg of total RNA using a cDNA synthesis kit (Invitrogen). For amplification of V2 vasopressin receptor, 5′-TgT ggC TCT gTT TCA AgT gC-3′ forward primer and 5′-gTg CCA CAA ACA CCA TCA Ag-3′ reverse primers were used. For amplification of NKCC2, 5′-gCC ACT ggg AgC ATg AAT gAC-3′ forward primer and 5′-AAA CCC TgA CAC CAT gCT CAT-3′ reverse primer were used. For specific detection of three alternatively spliced NKCC2 cassette exons (33), 5′-gTC TTg gAg TTg TCA TAA TT-3′ forward primer and 5′-CTC CAC gAA CAA ACC CgT TA-3′ reverse primer for the A-isoform, 5′-gTC TTg gTg TgA TTA TCA TC-3′ forward primer and 5′-CTC CTC TgA CAT ATC CAT TT-3′ reverse primer for the B-isoform, and 5′-ATC gTC ATT ggC CTg AgT gT-3′ forward primer and 5′-CTC CTC TTA CTA CTC CAT TT-3′ reverse primer for the F-isoform were used. RT-PCR reactions were carried out in an automated thermal cycler (Perkin Elmer, Boston, MA) using *Taq* polymerase (GIBCO). Reactions were controlled by PCR amplification of the housekeeping gene β-actin. Quantitative gene expression studies were performed using TaqMan gene expression assays for NKCC1 and NKCC2 (Applied Biosystems) in a 7500 Fast Real-Time PCR System (Applied Biosystems). GAPDH expression was used as an endogenous control.

Presentation of data and statistical analyses. Results are means ± SD. Statistical significance was determined using Student's unpaired *t*-test. $P < 0.05$ was considered significant.

RESULTS

Rat kidney and cultured TAL cells specifically express vasopressin receptor along with NKCC2. To study the effect of AVP on NKCC2 in association with LR, we have confirmed histochemically the key gene products expressed in the studied tissue and cells. NKCC2 immunostaining and concomitant V2R mRNA expression have been demonstrated in rat outer medullary TAL (29). Cultured rbTAL cells showed NKCC2 diffusely distributed in the cytoplasm and apical cell region (Fig. 1, *A–C*). Preincubation of the antibody with peptide used for immunization resulted in a near-complete lack of NKCC2 immunoreactivity (Fig. 1, *D–F*). Cell borders showed continuous ZO-1-immunoreactive junctional belts. Lysates from rbTAL cells expressed mRNA encoding for NKCC2 with its A-, B-, and F-isoforms and V2R receptor (Fig. 1, *G* and *H*). Comparing expression levels of the kidney-specific NKCC2 with the ubiquitous transporter NKCC1 by sensitive real-time PCR, extracts from rabbit and rat kidneys as well as rbTAL cells showed differences in the 1,000-fold range, indicating very low expression of NKCC1 (Fig. 1, *I* and *J*). NKCC2 mRNA expression level in rbTAL cells was ~15% that of rabbit kidney. These data thus demonstrate viability for the models used in this study.

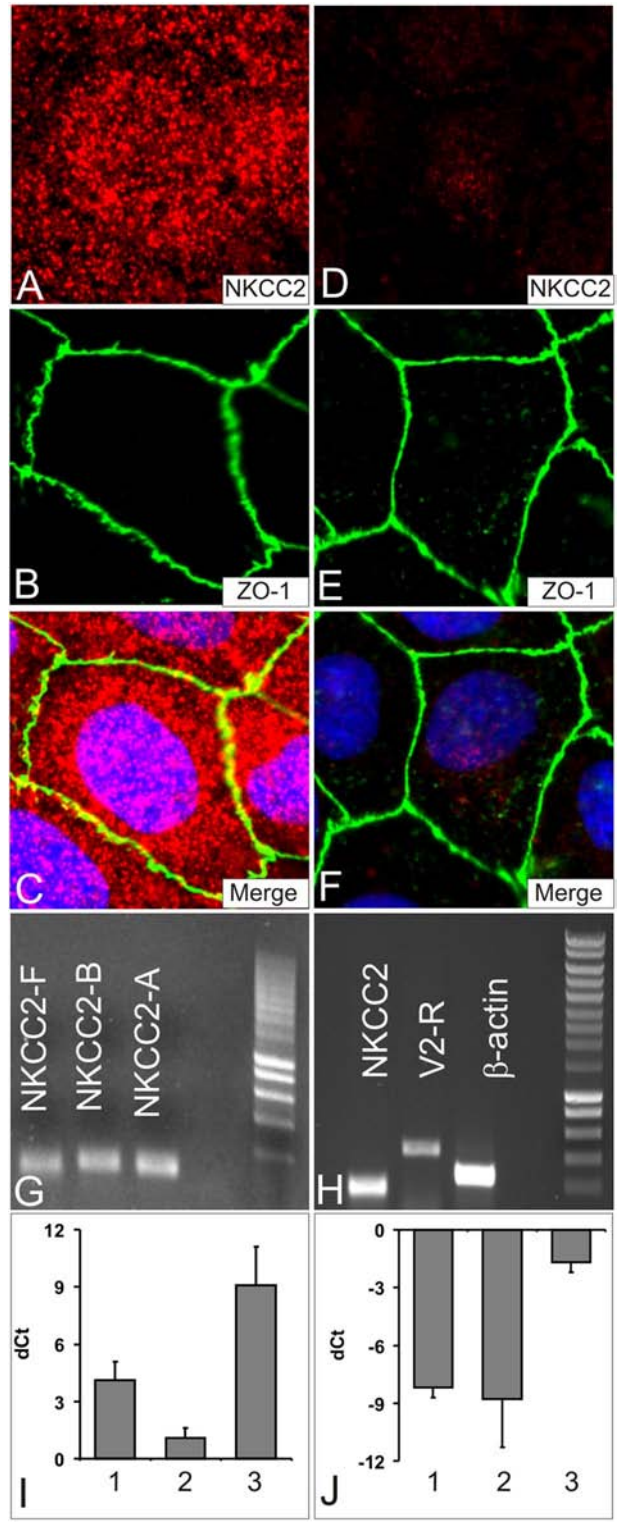

Fig. 1. Cytochemistry and RT-PCR characterize rabbit cells of the thick ascending limb of the loop of Henle (rbTAL) cell monolayers as used in lipid raft (LR) studies. *A–C*: conventional immunofluorescence shows Na^+-K^+-Cl^- cotransporter 2 (NKCC2; red) in a widespread distribution across the cell; cell borders are zonula occludens (ZO)-1-positive (green), nuclei are 4,6-diamidino-2-phenylindole (DAPI)-stained (blue). *D–F*: preincubation peptide blockade (10-fold excess) of the antibody against NKCC2 reveals near-total absence of specific signal. *G* and *H*: RT-PCR showing the presence of mRNA coding for NKCC2 and its 3 isoforms (F, B, and A) with specific, distinct primers and of vasopressin receptor (V2R) mRNA. *I* and *J*: real-time PCR assay showing representative expression of NKCC2 (*I*) vs. NKCC1 mRNA (*J*) in rabbit kidney (*1*), rbTAL cells (*2*), and rat kidney extracts (*3*) from 4 independent experiments. Data are normalized for GAPDH mRNA, which was run in the same well, and are expressed as the change in cycle threshold (dC_t).

There is a pool of NKCC2 in detergent-resistant, cholesterol- and sphingolipid-enriched membranes in rat kidney and cultured TAL cells. Major criteria to establish the association of proteins with LR are used to demonstrate that the protein is insoluble in cold detergent and that it shifts from lighter to heavier membrane fractions after CD based on density gradient fractionation (50). Detergent solubilization of membrane extracts from rat kidney and rbTAL cell homogenates and subsequent centrifugation resulted in the separation of detergent-soluble and -insoluble membranes. Lipid composition analysis by dot blot for GM1 and by TLC for cholesterol, phosphatidylcholine, and sphingomyelin re-

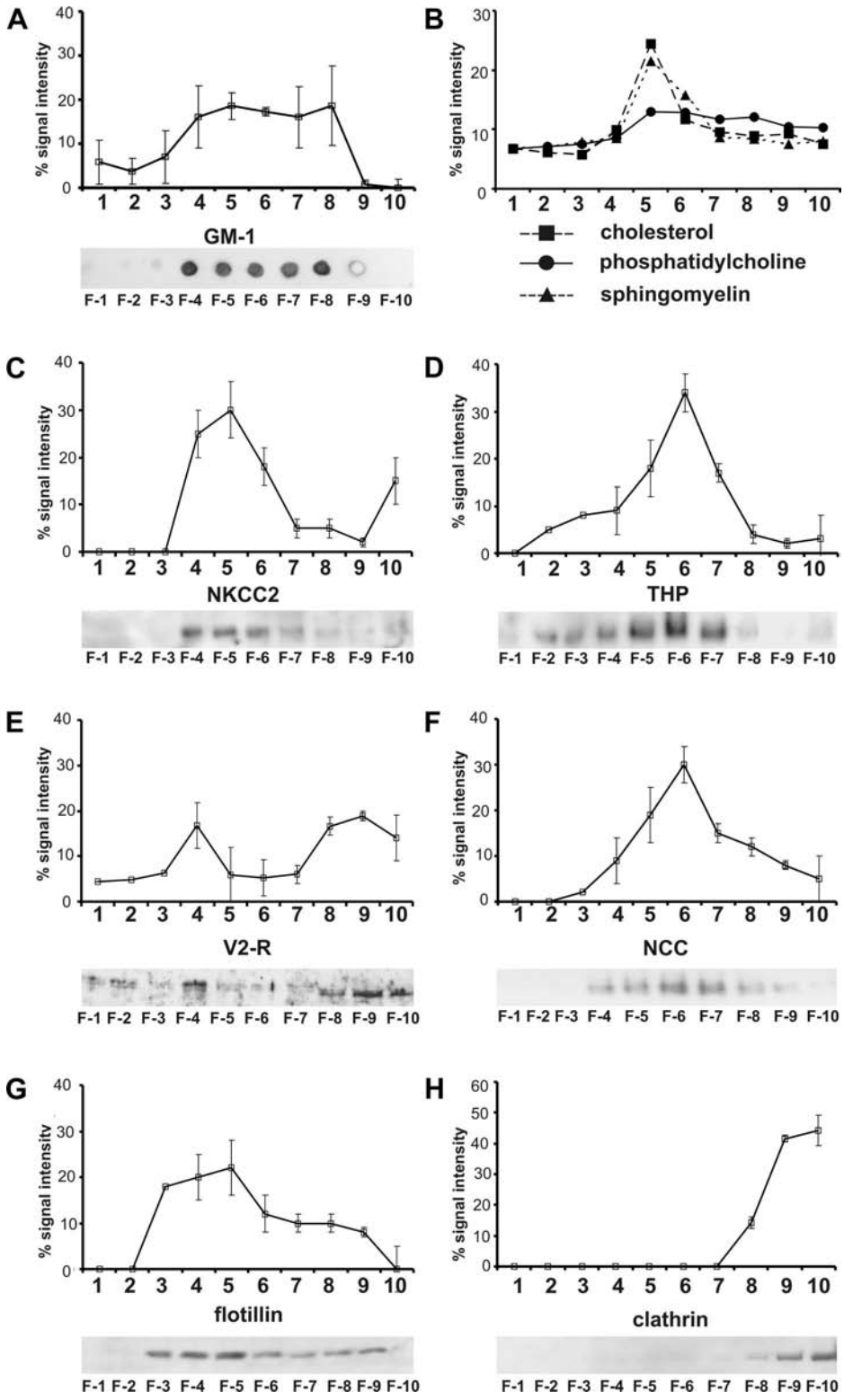

Fig. 2. A pool of membrane NKCC2 and related proteins from rat kidney is associated with LR-specific lipids. Purified membrane preparations from rat kidney extracts were solubilized with cold 1% Triton X-100 and assayed in sucrose gradient floating assays. Fractions show distribution of GM1 by dot blot (*A*), cholesterol, phosphatidylcholine, and sphingomyelin by TLC (*B*), and NKCC2 (*C*), co-localized THP (*D*), V2R (*E*), and Na^+-Cl^- cotransporter (NCC) (*F*) by Western blots in the low-density LR raft fractions. The reference protein flotillin distributes in rafts (*G*), whereas clathrin is typically absent from LR (*H*). Densitometric scanning analysis of blots and TLC bands from at least 4 independent experiments is shown above the respective representative samples for the gradients. Products are enriched in the LR fractions ranging near 20% sucrose. The bands for NKCC2 were located at 160 kDa, THP at 98 kDa, V2R at 50 kDa, NCC at 165 kDa, flotillin at 48 kDa, and clathrin at 180 kDa.

vealed enrichment of these lipids in the low-density fractions from rat kidney extracts separated by floating assay (Fig. 2, *A* and *B*). Plots indicate a heterogeneous distribution of these components along the different fractions. Western blots showed that 40–70% of NKCC2 was associated with the Triton X-100-insoluble fractions and the other 60–30% with the Triton X-100-soluble fractions at 160 kDa (Fig. 2*C*). Among different nonionic detergents tested for NKCC2's resistance to solubilization, Triton X-100 produced the most marked NKCC2 insolubility. Reacting homogenates with warm (37°C) instead of cold Triton X-100 resulted in LR disruption and absence of NKCC2 and flotillin from the low-density fractions. The GPI-anchored glycoprotein THP, which is coexpressed with NKCC2 in the TAL, fractionated in parallel (Fig. 2*D*). The V2 receptor and the thiazide-sensitive Na^+-Cl^- cotransporter NCC, a second major member of the Na^+-K^+-Cl^- cotransporters that is located in the downstream nephron segment ensuing TAL, fractionated in the buoyant membranes as well (Fig. 2, *E* and *F*). Flotillin and clathrin served as positive and negative controls, respectively (Fig. 2, *G* and *H*).

Identification of NKCC2 by LC-MS/MS in LR fractions. To corroborate Western blot identification of NKCC2 in LR, a high-specificity proteomic approach was performed using LC-MS/MS from rat kidney medullary LR fractions. The results demonstrated highly significant occurrence of a 19-amino acid NKCC2-specific peptide (ISQGFDISPVLQVQDELEK) from a COOH-terminal cytoplasmic tail of NKCC2 located next to the TM12 domain (see Supplemental Material 1).

Ultrastructural analysis of LR membranes. LR membranes prepared from purified rat outer medulla revealed vesicles 100–200 nm in diameter and membrane fragments. Immunogold staining with T4 antibody against NKCC2 showed labeling over some but not all of the membranes, reflecting that some but not all LR were from TAL (Fig. 3). For control, negative staining for clathrin (Fig. 3*A*) and positive staining for THP and GM1 (Fig. 3, *C* and *D*) of the same preparation further characterized this result.

Depletion of cholesterol reduces the pool of NKCC2 in LR. To evaluate the effect of CD in rbTAL monolayers, cells had been treated with mevalonate-lovastatin and MβCD; absence of cytochemical staining for filipin confirmed CD in the treated cells as described (55). Trypan blue staining of the cholesterol-depleted cells confirmed their viability, since no intracellular penetration of the dye was registered. CD caused a significant shift in the distribution of NKCC2 and flotillin from the low- to the high-density fractions, indicating partial solubilization of NKCC2 and the control protein (Fig. 4, *A–C*). The detection of clathrin in the high-density fraction was not influenced by this treatment.

Depletion of cholesterol reduces NKCC2 activity in Xenopus laevis oocytes. Oocytes were exposed to MβCD for a total of 90 or 180 min, including the uptake period of 60 min. The activity of NKCC2 was significantly reduced by CD in a time-dependent fashion (Fig. 4, *D* and *E*). At 90 min, the observed reduction was from 4,676 ± 313 pmol·oocyte^{-1}·h^{-1} in the absence of MβCD to 3,121 ± 258 pmol·oocyte^{-1}·h^{-1} in its presence ($P < 0.05$; Fig. 4*D*). At 180 min of exposure, the reduction was more pronounced. NKCC2-induced $^{86}Rb^+$ uptake was reduced from 5,859 ± 570 pmol·oocyte^{-1}·h^{-1} in the absence of MβCD to 802 ± 109 pmol·oocyte^{-1}·h^{-1} in its presence ($P < 0.01$; Fig. 4*D*). The observed reduction with these times of incubation represented 33 and 87% NKCC2 inhibition, respectively (Fig. 4*E*). These observations strongly suggest a functional background for an association between NKCC2 expressed in oocytes and their membrane cholesterol content.

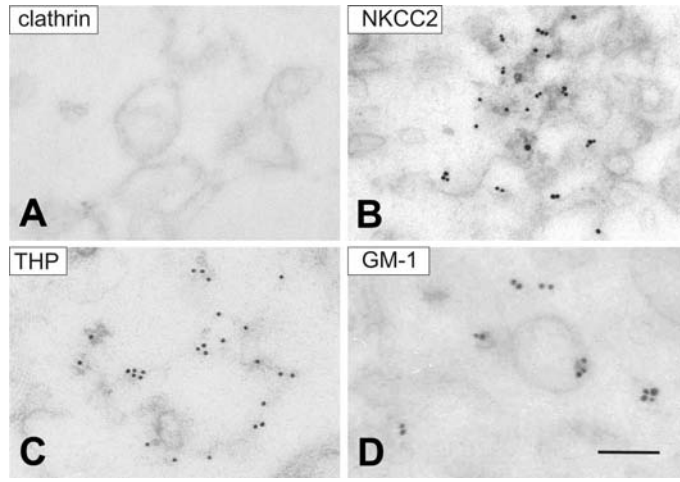

Fig. 3. Ultrastructural immunogold labeling of LR isolated from rat kidney outer medulla shows NKCC2-positive membranes. LR were prepared from purified membrane preparations after solubilization with cold 1% Triton X-100 and sucrose density gradient centrifugation technique. The detergent generates vesicle-like and fragmentary LR ~200 nm in diameter. Rafts were incubated with antibodies against clathrin (*A*), NKCC2 (T4 antibody; *B*), THP (*C*), and GM1 (*D*). A subset of LR shows positive NKCC2 immunostaining. Bar, 200 nm.

Effect of short-term AVP administration on apical trafficking and the association of NKCC2 with LR. To study whether V2R-mediated polar delivery of NKCC2 is related to cholesterol-dependent, LR-associated trafficking upon AVP stimulation, we performed experiments in vivo, in cultured rbTAL monolayers, and in primary TAL cell culture. V2R mRNA was strongly expressed in medullary TAL profiles of LE and DI rats (Fig. 5, *A* and *B*). In LE rats, and more drastically in Brattleboro DI rats, treatment with AVP (intraperitoneal injection of a bolus of 1 μg/kg, 1 h) showed significant changes in apical NKCC2 abundance compared with the respective controls receiving vehicle injection (Fig. 5, *C* and *D*). In rbTAL cells, an AVP-induced shift of immunoreactive NKCC2 toward the luminal membrane was observed along with a general increase in apical signal intensity for NKCC2 (Fig. 5, *E* and *F*; vehicle vs. 10^{-7} M AVP, 1 h). In vivo, NKCC2 also fractionated to a significantly increased proportion (almost 2-fold) into the low-density range of the plasma membrane fractions as used throughout for the floating assays; this was independent of the general increase in NKCC2 signals upon AVP (Fig. 6*A*). Flotillin was unaffected under this condition (Fig. 6*B*). Analogous observations were made in cultured rbTAL cells (see Supplemental Material 2). In these cells, the AVP-dependent shift from a juxtanuclear position of immunoreactive NKCC2 toward an apical concentration was further specified using confocal series of stacks (Fig. 7*A*). A sharp increase in mean apical fluorescence intensity was detectable as early as after 15 min, followed by further augmentation after 4 h. Parallel evaluation by Western blot showed a moderate increase in NKCC2 abundance as early as after 1 h and a more marked increase after 4 h of AVP treatment, whereas after 24 h, signal was decreased to near control level (Fig. 7*B*). Cycloheximide, an inhibitor of protein translation, did not prevent the rise in NKCC2 signal after

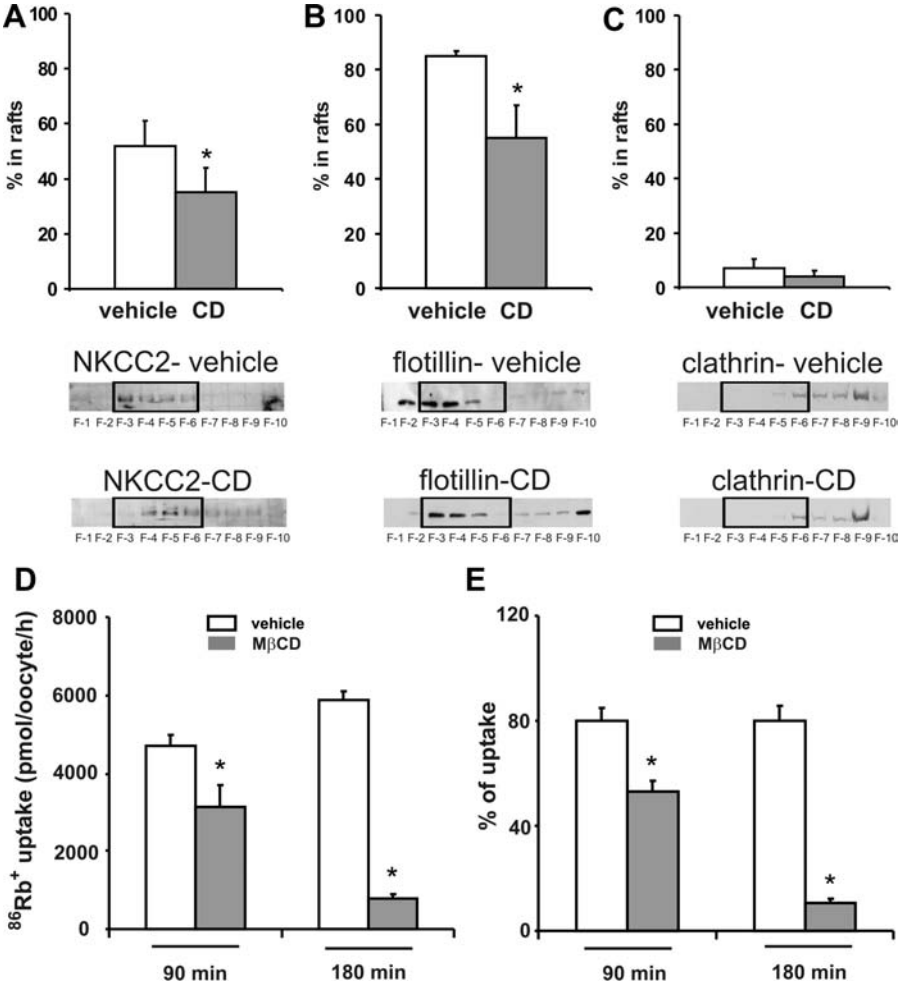

Fig. 4. Cholesterol depletion (CD) influences polar delivery of NKCC2 in TAL and blunts ion transport function of NKCC2 in *Xenopus laevis* oocytes. *A–C*: CD reduces the pool of NKCC2 in LR of rbTAL cells. Cells underwent CD by combined mevalonate-lovastatin and methyl-β-cyclodextrin (MβCD) treatment to inhibit cholesterol synthesis and disrupt LR. Rafts were prepared from purified membrane preparations after solubilization with cold 1% Triton X-100. Floating assays demonstrated cholesterol dependence in the partitioning of NKCC2 (*A*) and flotillin (*B*), but not clathrin (*C*), in LR. Densitometric scanning analysis of Western blots from 5 independent experiments is shown above the respective, representative Western blots. CD caused significant rightward shifts of NKCC2 in the LR fractions ranging near 20% sucrose. $*P < 0.05$ compared with vehicle. *D* and *E*: NKCC2 activity in *X. laevis* oocytes is reduced by CD. Oocytes were injected with water or NKCC2 cRNA, and $^{86}Rb^+$ uptake was assessed. *D*: NKCC2-dependent $^{86}Rb^+$ uptake in the absence (vehicle) or presence of 10 mM MβCD during 90 or 180 min, as indicated. *E*: normalized NKCC2-dependent $^{86}Rb^+$ uptake (after subtraction of uptake in water-injected oocytes) in the absence of MβCD set as 100%. $*P < 0.05$ compared with vehicle. Data in both *D* and *E* are pooled results from 2 independent experiments with 10 oocytes per group each.

1 h of AVP treatment but blunted the increase after 4 h (Fig. 7*C*). Specificity of the AVP-induced changes was verified by incubating the cells with 8-Br-cAMP, leading to adluminal increase of NKCC2 fluorescence close to the level that was reached after AVP application (Fig. 7*D*). Further controls included the PKA inhibitors H-89 and *Rp*-cAMPS, both of which reduced AVP-dependent stimulation of NKCC2 significantly. Cytochalasin B markedly blunted the effect of AVP as well, suggesting that apical trafficking of NKCC2 depends on actin polymerization.

LR markers such as CT-B, staining ganglioside GM1, produce fluorescent patches in the cell, indicating LR sites. These may copatch with LR proteins, resulting in an overlapping fluorescence signal. Copatching was therefore used as a microscopy assay for raft association. After 1 h of AVP treatment, NKCC2 revealed a clear increase in copatching of the two signals in confocal imaging as visualized by the merge images; the individual signals not only for NKCC2 but also for CT-B were enhanced. The overlap is demonstrated semiquantitatively (Fig. 8). These findings were corroborated using rat primary cultured TAL cells from the inner stripe (see Supplemental Material 3). CD by combined mevalonate-lovastatin/MβCD application led to mildly reduced steady-state NKCC2 signal and blunted the effect of AVP (Fig. 9*A*). Western blotting from rbTAL cell lysates also revealed a decrease in NKCC2 abundance after CD and demonstrated that the AVP-induced increase in NKCC2 signal was blunted by CD (Fig. 9*B*). To study the potential impact of CD on AVP signaling, cAMP levels were determined in the supernatants from rbTAL cells incubated for 1 h in the presence or absence of AVP, combined with CD. Augmentation of cAMP levels by AVP was pronounced; under CD, these changes were still significant, albeit to a reduced amount (Fig. 9*C*).

Biotinylation assays show the amount of surface-expressed NKCC2 is increased upon short-term AVP stimulation of rbTAL cells in a cholesterol-dependent manner. We ultimately aimed to consolidate our hypothesis that AVP not only causes apical trafficking of NKCC2 but also promotes luminal insertion of a pool of NKCC2 in a cholesterol-dependent manner to modulate transepithelial NaCl transport via LR. To this end, the surface of live rbTAL cell monolayers was biotinylated. The monolayers were then homogenized and cell membrane and intracellular fractions prepared. Fractions were immunoprecipitated with anti-NKCC2 antibody. The abundance of biotinylated NKCC2, which was determined by streptavidin-peroxidase labeling, was compared with the total abundance of NKCC2, as determined using a different anti-NKCC2 antibody, in the respective fractions (Fig. 10). Samples receiving vehicle showed dramatic reductions in NKCC2 in the membrane fractions upon CD with either detection system (Fig. 10, *A* and *B*), whereas in the intracellular fractions, total NKCC2 was not significantly changed (Fig. 10, *C* and *D*). As expected, the amount of intracellular biotinylated NKCC2 was very low

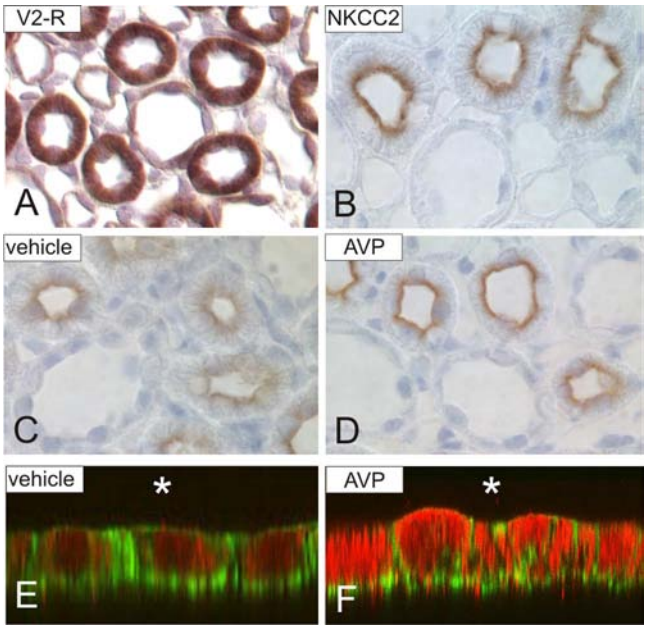

Fig. 5. NKCC2 surface expression of rat medullary TAL and cultured rbTAL cells increases upon treatment with vasopressin (AVP). V2R mRNA (*A*) and immunoreactive NKCC2 (*B*) distributed in untreated control Long Evans (LE) rat medullary TAL. Intraperitoneal bolus injections of vehicle (0.9% NaCl; *C*) or 1-deamino-8-D-arginine vasopressin (dDAVP; 1 μg/kg; *D*) in Brattleboro rats with diabetes insipidus (DI rats) after 1 h; adluminal immunoreactive NKCC2 signal is enhanced upon treatment with dDAVP. *A*, in situ hybridization; *B–D*, immunoperoxidase staining with anti-NKCC2. Comparable effects are shown in vehicle (*E*) and AVP (1×10^{-7} M; 1 h)-treated rbTAL cells (*F*). Confocal merge signals of NKCC2 (red) and phalloidin identifying intracellular F-actin (green) are shown in the *Z*-axis with the apical side oriented toward the asterisk. Significant augmentation of red fluorescent NKCC2 label along with a shift toward the apical cell pole (asterisk) are shown.

in the respective fractions (Fig. 10, *C* and *D*). Mirroring the histochemical results shown in Fig. 5, *E* and *F*, and Fig. 7*A*, Fig. 10, *A* and *B*, further shows pronounced increases for biotinylated NKCC2 (nearly 3-fold) and total NKCC2 in the cell membrane fraction after 1 h of AVP stimulation. Both effects were blunted by CD. These observations permit the conclusion that both steady-state as well as AVP-stimulated surface expressions of NKCC2 are markedly cholesterol dependent. This finding agrees with the concept that LR-dependent trafficking may be relevant for NKCC2 in its active, luminally inserted form. Corresponding to the increases in total cell NKCC2 shown in Fig. 7*B*, intracellular NKCC2 abundance showed a pronounced stimulation upon AVP; this increase was effectively blunted by CD (Fig. 10, *C* and *D*). In agreement with our results from the floating assays and the confocal analysis, the latter observation reflects intensified packing of NKCC2 in LR-containing intracellular membranes upon the stimulatory effect of AVP. Packing into LR thus appears to be linked to the cellular adjustment of NKCC2 abundance.

DISCUSSION

Evidence for partitioning of NKCC2 into cholesterol- and sphingolipid-enriched LR. Results of this study have extended the current concepts of cellular distribution, function, and regulated polar delivery of the major renal epithelial cotransporter NKCC2. Our first major point was to confirm the hypothesis that NKCC2 may distribute in LR with a functional background. As a biochemical hallmark for LR localization, we have applied the procedure of cold extraction with nonionic detergent to isolate LR, relying on their relative, differential insolubility in the detergent in sucrose gradient fractionation, which is based on the close packing of acyl chains and stabilization via cholesterol interdigitation (50).

We have shown that a pool of both intracellular and plasma membrane NKCC2 is LR associated based on the following observations. *1*) Forty to seventy percent of NKCC2 obtained from the extracted plasma membrane preparations including adherent vesicular membranes was detected in the low-density range of the floating assays. The presence of the transporter in LR fractions was identified by Western blot and highly specific LC-MS/MS. *2*) LR properties were confirmed by the typical enrichment in ganglioside GM1, sphingolipid, and cholesterol selectively in the low-density fractions (55). *3*) NKCC2 was detected immunoelectron microscopically in a subset of membrane fragments obtained from sucrose fractionation, reflecting data on intestinal LR proteins (7). *4*) Binding of CT-B to GM1-containing LR, a natural process adapted for experimental LR recognition (17), showed copatching of a subset of CT-B and NKCC2 within the cell and on the surface. *5*) LR association of NKCC2 depended on cholesterol availability as a widely used criterion (19, 28, 55). Localization of NKCC2 in LR of the plasma membrane further agrees with its histochemical localization of NKCC2 in subapical and apical TAL epithelium (14, 31). The occurrence of LR carrying NKCC2 in intracellular fractions suggested their involvement in apical delivery of NKCC2, as described for other membrane-spanning proteins (19, 28). Parallel detection of the structurally related cotransporter NCC (13) in LR frac-

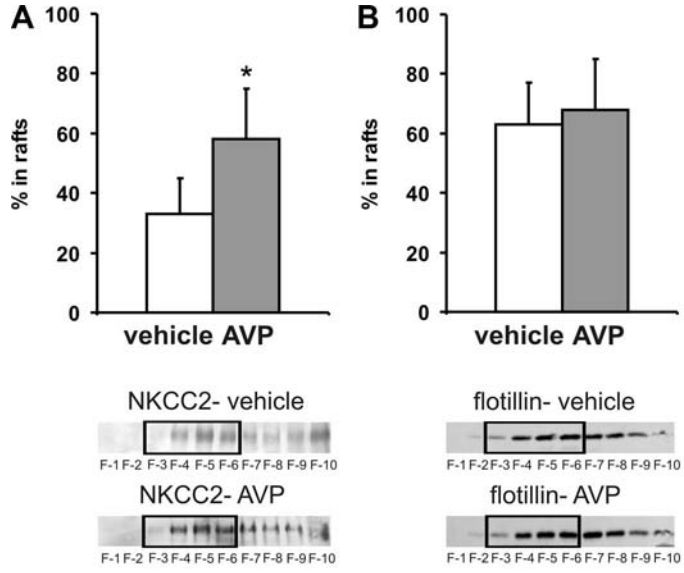

Fig. 6. AVP administration increases the pool of NKCC2 in LR from rat kidney outer medulla. An intraperitoneal bolus injection of vehicle (0.9% NaCl) compared with dDAVP (1 μg/kg) in DI rats after 1 h increased the proportion of NKCC2 (*A*) but not flotillin (*B*) partitioned in LR. Rafts were prepared from purified outer medullary membrane preparations after solubilization with cold 1% Triton X-100 and sucrose gradient floatation technique. Densitometric analysis of Western blots from 4 independent experiments with fractions F3–F6 were evaluated cumulatively. Representative Western blots are shown at *bottom* with the evaluated fractions boxed (discontinuous gradients). *$P < 0.05$ compared with vehicle.

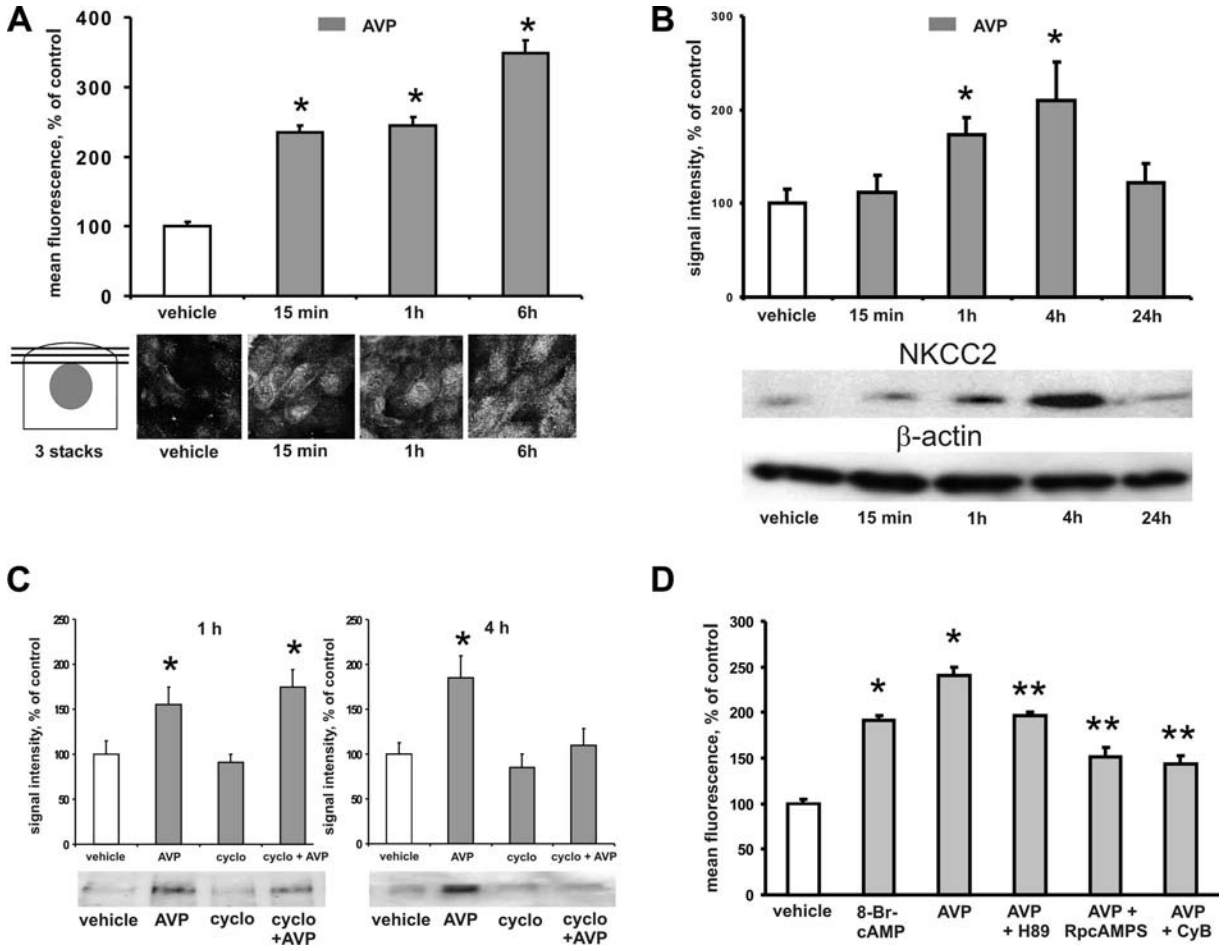

Fig. 7. Time-dependent effects of AVP stimulation on NKCC2 trafficking and protein abundance in rbTAL cells. *A*: time-dependent effects of AVP on NKCC2 surface expression are shown by semiquantitative evaluation of apical NKCC2 fluorescent signal. Values represent mean fluorescence intensity from 3 pooled apical confocal stacks. Baseline apical fluorescence was set at 100%. Representative confocal images are shown at *bottom*. *B*: time-dependent effects of AVP on NKCC2 protein abundance are shown by semiquantitative evaluation of Western blots from whole cell lysates and densitometric scanning. Results are normalized for the housekeeping protein β-actin. Representative blots are shown at *bottom*. *C*: as in *B*, time-dependent effects of AVP (1 and 4 h) on NKCC2 abundance are shown in the absence vs. presence of cycloheximide (cyclo). *D*: specificity of the AVP-induced changes in NKCC2 surface expression was demonstrated by application of the cAMP analog 8-bromo-cAMP (8-Br-cAMP), AVP alone, the PKA inhibitors H-89 and *Rp*-cAMPS, and cytochalasin B (CyB), each combined with AVP. Values were obtained from confocal microscopy of apical NKCC2 immunofluorescent signal. Values represent mean fluorescence intensity from pooled apical confocal stacks. Results are from 3 (*A*), 4 (*B*), 5 (*C*), and 3 independent experiments (*D*), respectively. $*P < 0.05$ compared with vehicle. $**P < 0.05$ compared with AVP.

tions from rat kidney further strengthened our view; apparently the two products are using similar posttranscriptional pathways during biosynthesis.

Protein markers for raft and non-raft domains confirm LR association of NKCC2. Among the positive reference proteins, flotillin-1 as a well-established LR marker (44) and THP as a GPI-anchored raft- and TAL-specific product (5) were detected in the buoyant membrane fractions along with NKCC2. Apart from demonstrating specificity of the assays, the presence of flotillin suggests a role to organize LR as specialized membrane domains interacting with the cytoskeleton (4). Another well-defined, intrinsic component of LR is caveolin, which may target other proteins to LR in certain cell types (9). However, caveolins are not solely responsible for LR association of proteins, and the known caveolin isoforms were not detected in TAL (3, 42). The coated pit-related protein clathrin was used as an established non-raft marker (20, 55).

Cholesterol depletion allows mechanistic insight into polar delivery of NKCC2 in TAL and ion transport function of NKCC2 in the oocyte system. We have administered cholesterol-depleting agents to study whether the liquid-ordered biophysical properties stabilizing LR may influence NKCC2 characteristics. MβCD, a cyclic oligosaccharide acting like an external sponge to remove membrane cholesterol by adhesional contact to the cell surface, was applied acutely to withdraw lipid from the plasma membrane and reduce LR under established conditions (28, 43, 45). To prevent LR association of proteins during their transit through the Golgi apparatus and polar trafficking (28, 51), CD was reached in a two-step approach using mevalonate-lovastatin during 24 h to inhibit de novo synthesis of cholesterol, added with a final short period of MβCD treatment. Cholesterol in the entire cell may thus be reduced to near 80% (10). Neither this measure nor MβCD alone should cause general deficits in membrane structure and function (28, 45, 55).

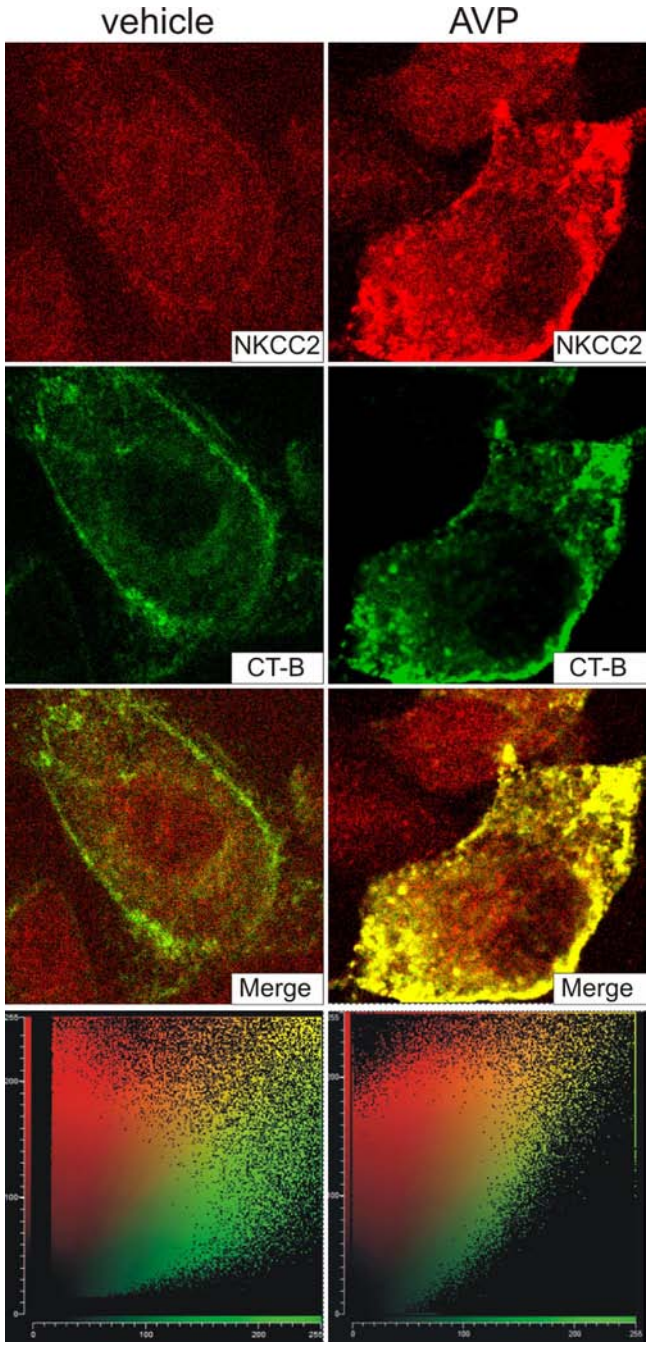

Fig. 8. Short-term AVP administration increases copatching of NKCC2 with the LR component, ganglioside GM1, in rbTAL cells. Confocal analysis shows the effects of short-term vehicle vs. AVP administration (1×10^{-7} M; 1 h) on the degree of coincident fluorescence of immunostained NKCC2 and the choleratoxin-B (CT-B)-labeled ganglioside GM1. Diagrams at *bottom* indicate the degree of merged signals between CT-B plotted on the *X*-axis and NKCC2 on the *Y*-axis, indicating copatching.

In the rbTAL model, Western blot analyses from the floating assays showed that two-step CD induced significant shifts of NKCC2 along with flotillin from lower to higher density fractions, reflecting similar data from elsewhere (20, 28, 55). The histochemical findings further elucidate that LR and their association with NKCC2 in plasma membrane as well as cytoplasmic vesicles were strongly reduced after CD. Studying *X. laevis* oocytes, which have been widely used by us and others as a robust heterologous expression system of rat NKCC2 (13, 15, 27, 39), we have obtained important functional insights into NKCC2 function in conjunction with cholesterol availability. The prominent, highly reproducible decreases in NKCC2-induced $^{86}Rb^{+}$ uptake upon CD by MβCD in a time course of up to 3 h were suggestive of a major role for the integrity of a cholesterol-enriched membrane environment in transporter functioning. Previous analyses of other LR-associated transporters have provided divergent results with respect to their lipid environment (21, 28); for instance, CD failed to affect transepithelial Na^{+} channel activity or expression of ENaC (20, 49). However, CD-induced effects may plausibly diverge among transporters and channels, since the N(K)CC family of proteins differs substantially from ENaC subunits with respect to molecular structure and functional requirements (13, 20). Alterations in membrane fluidity may have affected NKCC2 activity in the oocytes upon MβCD, as shown for a cation-conducting acetylcholine receptor (45). Since the typical distribution of LR in the plasma membrane of TAL cells probably agrees with the original concept of integral proteins distributed in LR or in non-raft membrane domains (25, 50), an equilibrium of silent vs. functional pools of NKCC2 might be effectively adjusted by changes in lipid composition, depending on their LR association (45). Our oocyte results may well resemble the in vivo membrane condition with its particular LR characteristics, since raft properties also have been established in the oocyte cell membrane (26).

Trafficking and polar delivery of NKCC2 on AVP is LR dependent. Our second major point was to investigate the involvement of LR in vesicular trafficking and apical delivery of NKCC2. Short-term exposure to AVP, a potent stimulus not only for water channel and NKA activation in collecting duct (8) but also for transepithelial NaCl reabsorption across TAL (1, 18, 27, 55) was therefore chosen to test our hypothesis. Established parameters for the activation of NKCC2 by short-term AVP application, such as V2R signaling and the particular effects of cAMP, PKA, and intactness of the actin cytoskeleton, have been demonstrated successfully, proving viability of the rbTAL cell line in this respect (1, 18, 29, 54, 55).

Short-term AVP treatment in the present setting produced two per se fundamentally different effects. One was related to changes in NKCC2 abundance and the other to LR-associated trafficking of the transporter. We earlier showed that cellular NKCC2 abundances in Brattleboro DI rats lacking endogenous AVP and in rbTAL cells were increased nearly twofold as early as after 30 min (29), and the present 1-h exposures to AVP produced similar results. As discussed previously (29), these findings are at variance with previous data raised in mice in which comparable, moderately supraphysiological concentrations of AVP after 1 h had failed to produce changes in NKCC2 abundance (14); increases in NKCC2 protein abundance have formerly been reported only from prolonged treatment periods (23). However, DI rats in our hands served as a suitable model for an induction of NKCC2 unbiased by endogenous AVP levels (29), and comparative setups with control rats also produced similar, albeit less drastic, results (unpublished data). Corresponding increases in NKCC2 abundance in rbTAL cells were highly reproducible and were further con-

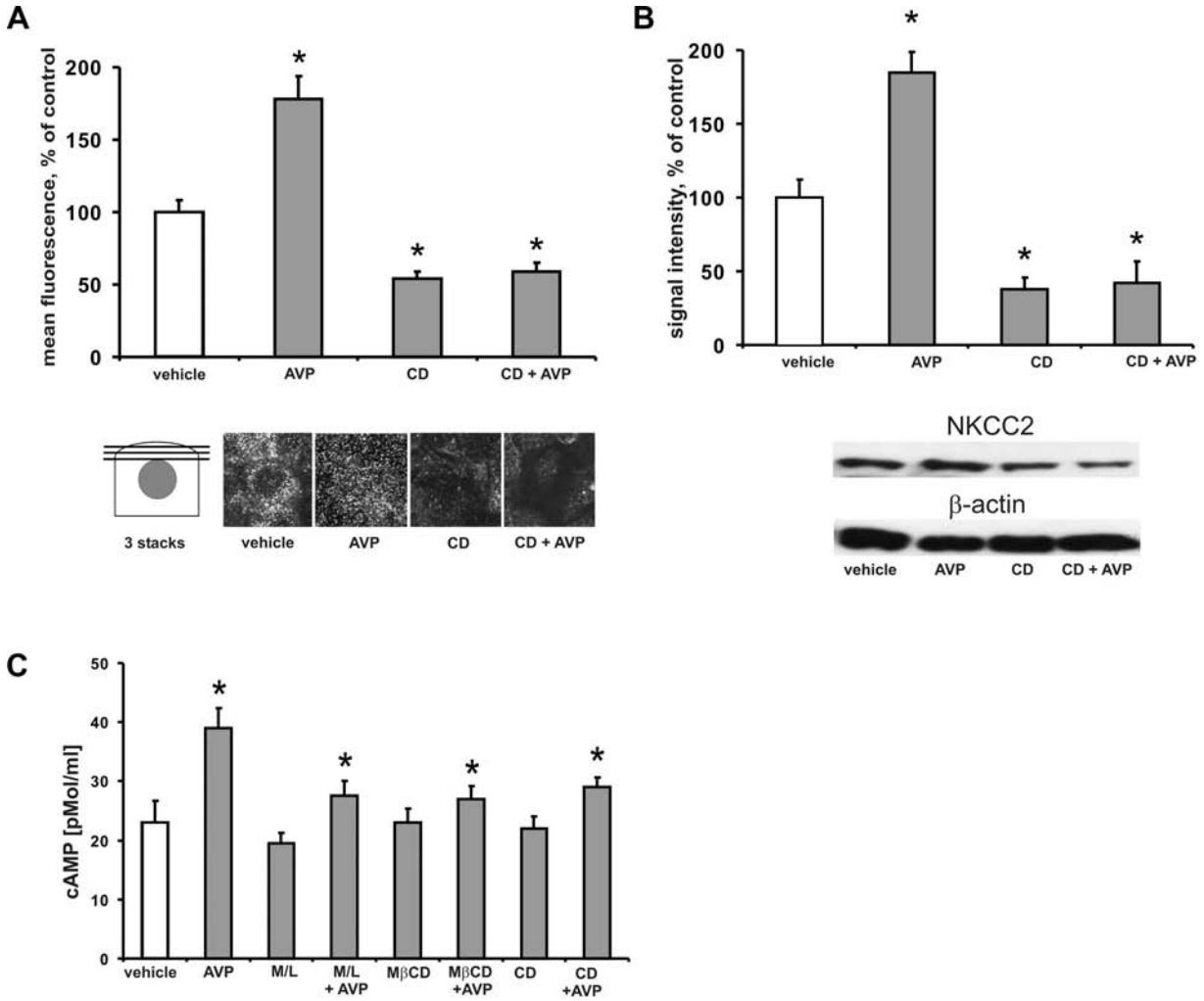

Fig. 9. AVP-induced changes of NKCC2 in rbTAL cells are cholesterol-dependent. *A*: confocal analysis shows the effects of AVP (1×10^{-7} M; 1 h) with and without CD by combined mevalonate-lovastatin (M/L)/MβCD treatment on NKCC2 surface expression. Values indicate quantification of the apical fluorescence intensity from 3 pooled apical confocal stacks with the vehicle control set at 100%. Representative confocal images are shown at *bottom*. *B*: representative Western blots from rbTAL cell extracts show specific bands for NKCC2 and densitometric evaluation with intensity values normalized for β-actin. *C*: ELISA measurements of cAMP accumulation in rbTAL cells incubated for 1 h with vehicle or AVP, combined with CD induced by M/L, MβCD, or a combination of M/L and MβCD. Results are from 3 (*A*), 4 (*B*), and 4 independent experiments (*C*), respectively. *$P < 0.05$ compared with vehicle.

firmed by parallel histochemical evaluation. Changes in NKCC2 mRNA were absent, which could be expected regarding its delayed induction (29, 40). Accordingly, inhibition of translation by cycloheximide was without effect on NKCC2 abundance after 1 h of AVP but blunted its effect after 4 h. Therefore, the observed effects were obviously unrelated to de novo protein biosynthesis. Conceivably, the V2R-cAMP-PKA signal cascade at some point may interfere with NKCC2 stability or so far unrecognized protein degradative mechanisms in TAL.

AVP-induced recruitment of NKCC2 to LR and trafficking were cholesterol-dependent as shown by *1*) shifting of NKCC2 toward the lower density fractions from DI rat kidney and rbTAL cell extracts, *2*) enhanced copatching of NKCC2 and CT-B in rbTAL and primary cultured TAL cells along with apical delivery, and *3*) increased surface biotinylation of NKCC2. Short-term AVP treatment produced more than twofold increases in both surface-expressed and total plasma membrane NKCC2 in rbTAL cells. Changes were dependent on cholesterol availability. The response showed a quick onset with 15 min. For comparison, GPI-anchored proteins typically also appear at the apical membrane within 15 min of leaving the Golgi in Madin-Darby canine kidney cells (48). Conversely, abundance of NKCC2 was significantly diminished upon CD chiefly in the apical cell pole or plasma membrane, but not in intracellular fractions, as depicted in Figs. 9 and 10. Along the same line, decreased apical NKCC2-immunoreactive signals under CD probably reflected disaggregation of LR and diminished apical delivery, since the CT-B-positive sites were also obviously reduced in parallel. These observations suggest that LR substantially interfere not only with trafficking but probably also with stability of NKCC2 at the apical cell pole. The failure to enhance trafficking and luminal insertion of the transporter upon AVP treatment in the absence of LR underscores this interpretation, suggesting that the cholesterol environment of the transporter molecules or the structure of LR proper are required for the maintenance of a

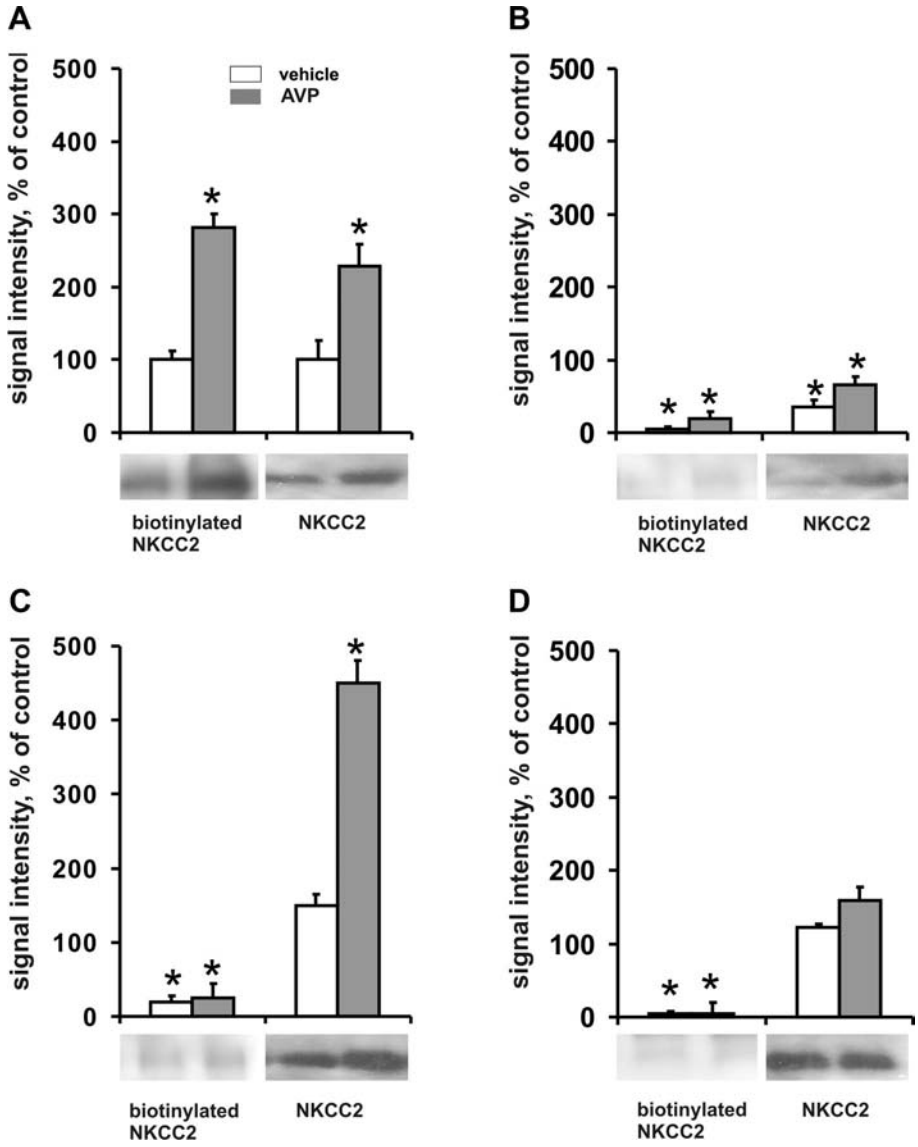

Fig. 10. Biotinylation assays show the amount of surface-expressed NKCC2 is increased upon AVP stimulation of rbTAL cells in a cholesterol-dependent manner. Plasma membrane fractions (*A* and *B*) and intracellular fractions (*C* and *D*) from rbTAL cells pretreated with vehicle (PBS; *A* and *C*) or M/L/MβCD for CD (*B* and *D*) were analyzed for their responses to short-term AVP treatment (1 h). The cell monolayers were surface-biotinylated and lysed, and membrane as well as intracellular fractions were immunoprecipitated with anti-NKCC2 antibody. SDS-PAGE and Western blots were performed with the eluates. In *A–D*, columns at *left* show the biotinylated fraction of NKCC2 as detected by streptavidin-horseradish peroxidase (HRP), whereas columns at *right* show the level of immunoreactive NKCC2 as detected by anti-NKCC2 antibody. Densitometric analysis of the blots from 3 independent experiments were evaluated; the controls are the vehicle bars in *A* of the respective streptavidin-HRP-detected or the anti-NKCC2-detected values, which are set at 100%, respectively. Representative blot images are shown at *bottom*; all documented blot samples were run in parallel in the selected experiment. In each lane, a concentration of 20 μg of protein was run on the gel. $*P < 0.05$ compared with the respective vehicle in *A*.

sufficiently large apical pool of NKCC2 and appropriate trafficking to the plasma membrane. This interpretation is further in line with results on intestinal NHE3 (28) and renal ENaC (49), highlighting a role for LR specifically in apical trafficking of these proteins.

The effects of CD on AVP-dependent increases in NKCC2 abundance and translocation might be questioned regarding the obvious distribution of a pool of V2R itself in LR. V2R themselves could therefore be affected by the CD protocol, possibly resulting in changes in binding as shown for another receptor (41) or in downstream signaling effects. Monitoring intracellular cAMP levels, we accordingly found that AVP application under various conditions of CD caused diminished cAMP accumulation in rbTAL cells; however, albeit reduced, the AVP-induced changes were still significant, thus validating our observations.

Collectively, our results from rat tissue, *X. laevis* oocytes, and TAL cell culture experiments support the hypothesis that NKCC2 distributes in LR both intracellularly and on the cell surface and that cholesterol availability is required for its activity, AVP-induced trafficking, and delivery to the cell membrane. In the plane of the luminal membrane, LR could act as platforms that modulate NKCC2 activity by accumulating active pools of the transporter. We therefore suggest that LR are an essential component in NKCC2 biology and therefore play an important role in the function of renal volume regulation. New aspects for studying lipid effects on ion transporter function have thus been presented. Future investigation must define the nature of protein-lipid interactions of NKCC2 and clarify how LR may determine trafficking, function, and turnover of NKCC2 in mammalian TAL.

ACKNOWLEDGMENTS

We acknowledge the methodological help of J.-H. Frühauf, M. Fromm, and D. Günzel; the gifts of rbTAL cells by R. Kinne (Bochum), NCC antibody by D. H. Ellison, and V2R antibody by W. Müller-Esterl; and the skillful technical assistance of F. Serowka, K. Riskowsky, and P. Landmann.

GRANTS

This study was supported by Deutsche Forschungsgemeinschaft Grant DFG-FOR667 (to S. Bachmann), National Institute of Diabetes and Digestive

and Kidney Diseases Grant DK-64635 (to G. Gamba), and BMBF Grant 0313694A (to H. Schlüter).

REFERENCES

1. **Amlal H, Legoff C, Vernimmen C, Paillard M, Bichara M.** Na^+-$K^+(NH_4^+)$-$2Cl^-$ cotransport in medullary thick ascending limb: control by PKA, PKC, and 20-HETE. *Am J Physiol Cell Physiol* 271: C455–C463, 1996.
2. **Bock J, Gulbins E.** The transmembranous domain of CD40 determines CD40 partitioning into lipid rafts. *FEBS Lett* 534: 169–174, 2003.
3. **Breton S, Lisanti MP, Tyszkowski R, McLaughlin M, Brown D.** Basolateral distribution of caveolin-1 in the kidney. Absence from H^+-ATPase-coated endocytic vesicles in intercalated cells. *J Histochem Cytochem* 46: 205–214, 1998.
4. **Brown DA.** Lipid rafts, detergent-resistant membranes, and raft targeting signals. *Physiology* 21: 430–439, 2006.
5. **Cavallone D, Malagolini N, Serafini-Cessi F.** Mechanism of release of urinary Tamm-Horsfall glycoprotein from the kidney GPI-anchored counterpart. *Biochem Biophys Res Commun* 280: 110–114, 2001.
6. **Crossthwaite AJ, Seebacher T, Masada N, Ciruela A, Dufraux K, Schultz JE, Cooper DMF.** The cytosolic domains of Ca^{2+}-sensitive adenylyl cyclases dictate their targeting to plasma membrane lipid rafts. *J Biol Chem* 280: 6380–6391, 2005.
7. **Danielsen EM, Hansen GH.** Lipid rafts in epithelial brush borders: atypical membrane microdomains with specialized functions. *Biochim Biophys Acta* 1617: 1–9, 2003.
8. **Djelidi S, Beggah A, Courtois-Coutry N, Fay M, Cluzeaud F, Vienghchareun S, Bonvalet JP, Farman N, Blot-Chabaud M.** Basolateral translocation by vasopressin of the aldosterone-induced pool of latent Na-K-ATPases is accompanied by alpha1 subunit dephosphorylation: study in a new aldosterone-sensitive rat cortical collecting duct cell line. *J Am Soc Nephrol* 12: 1805–1818, 2001.
9. **Drab M, Verkade P, Elger M, Kasper M, Lohn M, Lauterbach B, Menne J, Lindschau C, Mende F, Luft FC, Schedl A, Haller H, Kurzchalia TV.** Loss of caveolae, vascular dysfunction, and pulmonary defects in caveolin-1 gene-disrupted mice. *Science* 293: 2449–2452, 2001.
10. **Ehehalt R, Keller P, Haass C, Thiele C, Simons K.** Amyloidogenic processing of the Alzheimer beta-amyloid precursor protein depends on lipid rafts. *J Cell Biol* 160: 113–123, 2003.
11. **Field KA, Holowka D, Baird B.** Structural aspects of the association of Fc-epsilonRI with detergent-resistant membranes. *J Biol Chem* 274: 1753–1758, 1999.
12. **Gamba G, Miyanoshita A, Lombardi M, Lytton J, Lee WS, Hediger MA, Hebert SC.** Molecular cloning, primary structure, and characterization of two members of the mammalian electroneutral sodium-(potassium)-chloride cotransporter family expressed in kidney. *J Biol Chem* 269: 17713–17722, 1994.
13. **Gamba G.** Physiology and pathophysiology of electroneutral cation-chloride cotransporters. *Physiol Rev* 85: 423–493, 2005.
14. **Giménez I, Forbush B.** Short-term stimulation of the renal Na-K-Cl cotransporter (NKCC2) by vasopressin involves phosphorylation and membrane translocation of the protein. *J Biol Chem* 278: 26946–26951, 2003.
15. **Gimenez I, Forbush B.** Regulatory phosphorylation sites in the NH_2 terminus of the renal Na-K-Cl cotransporter (NKCC2). *Am J Physiol Renal Physiol* 289: F1341–F1345, 2005.
16. **Greger R.** Ion transport mechanisms in thick ascending limb of Henle's loop of mammalian nephron. *Physiol Rev* 65: 760–797, 1985.
17. **Hansen GH, Dalskov SM, Rasmussen CR, Immerdal L, Niels-Christiansen LL, Danielsen EM.** Cholera toxin entry into pig enterocytes occurs via a lipid raft- and clathrin-dependent mechanism. *Biochemistry* 44: 873–882, 2005.
18. **Hebert SC, Andreoli TE.** NaCl transport in mouse medullary thick ascending limbs. III. Modulation of the ADH effect by peritubular osmolality. *Am J Physiol Renal Fluid Electrolyte Physiol* 241: F412–F431, 1981.
19. **Hill WG, An B, Johnson JP.** Endogenously expressed epithelial sodium channel is present in lipid rafts in A6 cells. *J Biol Chem* 277: 33541–33544, 2002.
20. **Hill WG, Butterworth MB, Edinger RS, Ovaa H, Burg D, Johnson JP, Frizzell RA.** The deubiquitinating enzyme, UCH-L3 regulates the apical membrane recycling of the epithelial sodium channel (ENaC). *J Biol Chem* 282: 37402–37411, 2007.
21. **Inoue M, Digman MA, Cheng M, Breusegem SY, Halaihel N, Sorribas V, Mantulin WM, Gratton E, Barry NP, Levi M.** Partitioning of NaP_i cotransporter in cholesterol-, sphingomyelin-, and glycosphingolipid-enriched membrane domains modulates NaP_i protein diffusion, clustering, and activity. *J Biol Chem* 279: 49160–49171, 2004.
22. **Kenworthy AK, Nichols BJ, Remmert CL, Hendrix GM, Kumar M, Zimmerberg J, Lippincott-Schwartz J.** Dynamics of putative raft-associated proteins at the cell surface. *J Cell Biol* 165: 735–746, 2004.
23. **Kim GH, Ecelbarger CA, Mitchell C, Packer RK, Wade JB, Knepper MA.** Vasopressin increases Na-K-2Cl cotransporter expression in thick ascending limb of Henle's loop. *Am J Physiol Renal Physiol* 276: F96–F103, 1999.
24. **Li C, Wang W, Summer SN, Cadnapaphornchai MA, Falk S, Umenishi F, Schrier RW.** Hyperosmolality in vivo upregulates aquaporin 2 water channel and Na-K-2Cl co-transporter in Brattleboro rats. *J Am Soc Nephrol* 17: 1657–1664, 2006.
25. **Lillemeier BF, Pfeiffer JR, Surviladze Z, Wilson BS, Davis MM.** Plasma membrane-associated proteins are clustered into islands attached to the cytoskeleton. *Proc Natl Acad Sci USA* 103: 18992–18997, 2006.
26. **Luria A, Vegelyte-Avery V, Stith B, Tsvetkova NM, Wolkers WF, Crowe JH, Tablin F, Nuccitelli R.** Detergent-free domain isolated from *Xenopus* egg plasma membrane with properties similar to those of detergent-resistant membranes. *Biochemistry* 41: 13189–13197, 2002.
27. **Meade P, Hoover RS, Plata C, Vázquez N, Bobadilla NA, Gamba G, Hebert SC.** cAMP-dependent activation of the renal-specific Na^+-K^+-$2Cl^-$ cotransporter is mediated by regulation of cotransporter trafficking. *Am J Physiol Renal Physiol* 284: F1145–F1154, 2003.
28. **Murtazina R, Kovbasnjuk O, Donowitz M, Li S.** Na^+/H^+ exchanger NHE3 activity and trafficking are lipid raft-dependent. *J Biol Chem* 281: 17845–17855, 2006.
29. **Mutig K, Paliege A, Kahl T, Jöns T, Müller-Esterl WP, Bachmann S.** Vasopressin V2 receptor expression along rat, mouse, and human renal epithelia with focus on TAL. *Am J Physiol Renal Physiol* 293: F1166–F1177, 2007.
30. **Nichols BJ, Kenworthy AK, Polishchuk RS, Lodge R, Roberts TH, Hirschberg K, Phair RD, Lippincott-Schwartz J.** Rapid cycling of lipid raft markers between the cell surface and Golgi complex. *J Cell Biol* 153: 529–541, 2001.
31. **Nielsen S, Maunsbach AB, Ecelbarger CA, Knepper MA.** Ultrastructural localization of Na-K-2Cl cotransporter in thick ascending limb and macula densa of rat kidney. *Am J Physiol Renal Physiol* 275: F885–F893, 1998.
32. **Obermüller N, Kunchaparty S, Ellison DH, Bachmann S.** Expression of the Na-K-2Cl-cotransporter by macula densa and thick ascending limb cells of rat and rabbit nephron. *J Clin Invest* 98: 635–640, 1996.
33. **Oppermann M, Mizel D, Huang G, Li C, Deng C, Theilig F, Bachmann S, Briggs J, Schnermann J, Castrop H.** Macula densa control of renin secretion and preglomerular resistance in mice with selective deletion of the B isoform of the Na-K-2Cl co-transporter. *J Am Soc Nephrol* 17: 2143–2152, 2006.
34. **Ortiz PA.** cAMP increases surface expression of NKCC2 in rat thick ascending limbs: role of VAMP. *Am J Physiol Renal Physiol* 290: F608–F616, 2006.
35. **Plata C, Mount DB, Rubio V, Hebert SC, Gamba G.** Isoforms of the Na-K-2Cl cotransporter in murine TAL. II. Functional characterization and activation by cAMP. *Am J Physiol Renal Physiol* 276: F359–F366, 1999.
36. **Polishchuk R, Di Pentima A, Lippincott-Schwartz J.** Delivery of raft-associated, GPI-anchored proteins to the apical surface of polarized MDCK cells by a transcytotic pathway. *Nat Cell Biol* 6: 297–307, 2004.
37. **Reinalter SC, Jeck N, Peters M, Seyberth HW.** Pharmacotyping of hypokalaemic salt-losing tubular disorders. *Acta Physiol Scand* 181: 513–521, 2004.
38. **Ren X, Ostermeyer AG, Ramcharan LT, Zeng Y, Lublin DM, Brown DA.** Conformational defects slow Golgi exit, block oligomerization, and reduce raft affinity of caveolin-1 mutant proteins. *Mol Biol Cell* 15: 4556–4567, 2004.
39. **Rinehart J, Kahle KT, de Los Heros P, Vázquez N, Meade P, Wilson FH, Hebert SC, Gimenez I, Gamba G, Lifton RP.** WNK3 kinase is a positive regulator of NKCC2 and NCC, renal cation-Cl^- cotransporters required for normal blood pressure homeostasis. *Proc Natl Acad Sci USA* 102: 16777–16782, 2005.
40. **Robert-Nicoud M, Flahaut M, Elalouf JM, Nicod M, Salinas M, Bens M, Doucet A, Wincker P, Artiguenave F, Horisberger JD, Vandewalle A, Rossier BC, Firsov D.** Transcriptome of a mouse kidney cortical

collecting duct cell line: effects of aldosterone and vasopressin. *Proc Natl Acad Sci USA* 98: 2712–2716, 2001.
41. **Roepstorff K, Thomsen P, Sandvig K, van Deurs B.** Sequestration of epidermal growth factor receptors in non-caveolar lipid rafts inhibits ligand binding. *J Biol Chem* 277: 18954–18960, 2002.
42. **Rybin VO, Xu X, Lisanti MP, Steinberg SF.** Differential targeting of beta-adrenergic receptor subtypes and adenylyl cyclase to cardiomyocyte caveolae. A mechanism to functionally regulate the cAMP signaling pathway. *J Biol Chem* 275: 41447–41457, 2000.
43. **Sadler SE, Jacobs ND.** Stimulation of *Xenopus laevis* oocyte maturation by methyl-β-cyclodextrin. *Biol Reprod* 70: 1685–1692, 2004.
44. **Santamaria A, Castellanos E, Gomez V, Benedit P, Renau-Piqueras J, Morote J, Reventós J, Thomson TM, Paciucci R.** PTOV1 enables the nuclear translocation and mitogenic activity of flotillin-1, a major protein of lipid rafts. *Mol Cell Biol* 25: 1900–1911, 2005.
45. **Santiago J, Guzmàn GR, Rojas LV, Marti R, Asmar-Rovira GA, Santana LF, McNamee M, Lasalde-Dominicci JA.** Probing the effects of membrane cholesterol in the *Torpedo californica* acetylcholine receptor and the novel lipid-exposed mutation alpha C418W in *Xenopus* oocytes. *J Biol Chem* 276: 46523–46532, 2001.
46. **Schmitt R, Klussmann E, Kahl T, Ellison DH, Bachmann S.** Renal expression of sodium transporters and aquaporin-2 in hypothyroid rats. *Am J Physiol Renal Physiol* 284: F1097–F1104, 2003.
47. **Schnermann J.** Juxtaglomerular cell complex in the regulation of renal salt excretion. *Am J Physiol Regul Integr Comp Physiol* 274: R263–R279, 1998.
48. **Schuck S, Simons K.** Controversy fuels trafficking of GPI-anchored proteins. *J Cell Biol* 172: 963–965, 2006.
49. **Shlyonsky VG, Mies F, Sariban-Sohraby S.** Epithelial sodium channel activity in detergent-resistant membrane microdomains. *Am J Physiol Renal Physiol* 284: F182–F188, 2003.
50. **Simons K, Vaz WL.** Model systems, lipid rafts, and cell membranes. *Annu Rev Biophys Biomol Struct* 33: 269–295, 2004.
51. **Slimane TA, Trugnan G, van Ijzendoorn SC, Hoekstra D.** Raft-mediated trafficking of apical resident proteins occurs in both direct and transcytotic pathways in polarized hepatic cells: role of distinct lipid microdomains. *Mol Biol Cell* 14: 611–624, 2003.
52. **Takahashi N, Chernavvsky DR, Gomez RA, Igarashi P, Gitelman HJ, Smithies O.** Uncompensated polyuria in a mouse model of Bartter's syndrome. *Proc Natl Acad Sci USA* 97: 5434–5439, 2000.
53. **Vereb G, Szollosi J, Matko J, Nagy P, Farkas T, Vigh L, Matyus L, Waldmann TA, Damjanovich S.** Dynamic, yet structured: the cell membrane three decades after the Singer-Nicolson model. *Proc Natl Acad Sci USA* 100: 8053–8058, 2003.
54. **Verrey F, Groscurth P, Bolliger U.** Cytoskeletal disruption in A6 kidney cells: impact on endo/exocytosis and NaCl transport regulation by antidiuretic hormone. *J Membr Biol* 145: 193–204, 1995.
55. **Welker P, Geist B, Frühauf JH, Salanova M, Groneberg DA, Krause E, Bachmann S.** Role of lipid rafts in membrane delivery of renal epithelial Na^+,K^+-ATPase, thick ascending limb. *Am J Physiol Regul Integr Comp Physiol* 292: R1328–R1337, 2007.

Am J Physiol Renal Physiol 295: F1199–F1206, 2008.
First published August 13, 2008; doi:10.1152/ajprenal.90396.2008.

WNK3 and WNK4 amino-terminal domain defines their effect on the renal Na^+-Cl^- cotransporter

Pedro San-Cristobal, José Ponce-Coria, Norma Vázquez, Norma A. Bobadilla, and Gerardo Gamba

Molecular Physiology Unit, Instituto de Investigaciones Biomédicas, Universidad Nacional Autónoma de México, and Instituto Nacional de Ciencias Médicas y Nutrición Salvador Zubirán, Tlalpan, Mexico City, Mexico

Submitted 7 July 2008; accepted in final form 12 August 2008

San-Cristobal P, Ponce-Coria J, Vázquez N, Bobadilla NA, Gamba G. WNK3 and WNK4 amino-terminal domain defines their effect on the renal Na^+-Cl^- cotransporter. *Am J Physiol Renal Physiol* 295: F1199–F1206, 2008. First published August 13, 2008; doi:10.1152/ajprenal.90396.2008.—Loss of physiological regulation of the renal thiazide-sensitive Na^+-Cl^- cotransporter (NCC) by mutant WNK1 or WNK4 results in pseudohypoaldosteronism type II (PHAII) characterized by arterial hypertension and hyperkalemia. WNK4 normally inhibits NCC, but this effect is lost by eliminating WNK4 catalytic activity or through PHAII-type mutations. In contrast, another member of the WNK family, WNK3, activates NCC. The positive effect of WNK3 on NCC also requires its catalytic activity. Because the opposite effects of WNK3 and WNK4 on NCC were observed in the same expression system, sequences within the WNKs should endow these kinases with their activating or inhibiting properties. To gain insight into the structure-function relationships between the WNKs and NCC, we used a chimera approach between WNK3 and WNK4 to elucidate the domain of the WNKs responsible for the effects on NCC. Chimeras were constructed by swapping the amino or carboxyl terminus domains, which flank the central kinase domain, between WNK3 and WNK4. Our results show that the effect of chimeras toward NCC follows the amino-terminal domain. Thus the amino terminus of the WNKs contains the sequences that are required for their activating or inhibiting properties on NCC.

distal convoluted tubule; diuretics; hypertension; kinase

THE WNKS [with no lysine (K)] are a subfamily of serine/threonine kinases that lack the conserved lysine (substituted by cysteine), which in all other serine/threonine kinases is located in the β-strand 3 of kinase subdomain II of the catalytic domain (35). A total of four genes encoding WNK isoforms are present in the human genome: WNK1, WNK2, WNK3, and WNK4, located in chromosomes 12, 9, X, and 17, respectively. The degree of identity among WNKs is >80% in the kinase domain and <17% in the flanking amino- or carboxy-terminal domains. Mutations in WNK1 and WNK4 are the cause of pseudohypoaldosteronism type II (PHAII) (33), an inherited disease that features arterial hypertension, hyperkalemia, and metabolic acidosis. PHAII patients are highly sensitive to thiazide diuretics (18). Clinically, PHAII is the mirror image of Gitelman's disease, an inherited illness characterized by arterial hypotension, hipokalemia, and metabolic alkalosis due to inactivating mutations of the *SLC12A3* gene that encodes the thiazide-sensitive Na^+-Cl^- cotransporter NCC (28). Thus PHAII seems to be the consequence of overactivity of NCC due to a loss of physiological regulation by the WNKs (15, 34, 41). This hypothesis is supported by recent studies in *Xenopus laevis* oocytes (11, 34, 37), culture cells (2), and transgenic mice harboring WNK4 with PHAII-type mutations (15, 41). It is not surprising that the WNKs have emerged as powerful regulators not only of NCC but also of all the members of the cation-coupled chloride cotransporter family (SLC12) (9, 14).

The SLC12 family of membrane transporters is composed of seven members that are divided into two branches. The Na^+-driven branch that includes *SLC12A3* encodes NCC and two other genes: *SLC12A1* (encoding the kidney-specific Na^+-K^+-$2Cl^-$ cotransporter NKCC2) and *SLC12A2* (encoding the ubiquitously expressed Na^+-K^+-$2Cl^-$ cotransporter NKCC1). The K^+-driven branch is composed of four genes, *SLC12A4* to *SLC12A7*, which encode K^+-Cl^- cotransporters KCC1 to KCC4, respectively. Studies from several laboratories have shown that phosphorylation activates Na^+-driven and inactivates K^+-driven cotransporters, whereas dephosphorylation has the opposite effect (for review, see Refs. 1, 5, 6, 9, 12, 16). With the use of *X. laevis* oocytes as a heterologous expression system, it has been observed that WNK4 is a negative regulator of NCC (11, 34, 37) and all four KCCs (7, 10). The effect on both NCC (2, 11, 34) and KCCs (10) is eliminated by the D318A substitution, which renders WNK4 catalytically inactive, proving that the catalytic activity of WNK4 is required. In addition, PHAII-type missense mutations of WNK4 in a conserved acidic region of the carboxy-terminal domain prevent the negative effect of WNK4 on NCC (2, 34). WNK3 is also a powerful regulator of all members of the SLC12 family. However, WNK3 activates NCC, NKCC1, and NKCC2 (13, 27) while inhibiting all four KCCs (3). Interestingly, eliminating WNK3 catalytic activity by the D294A mutation not only prevents it from acting on the cotransporters but also inverts the kinase effect. In other words, WNK3-D294A becomes a powerful inhibitor of NCC, NKCC1, and NKCC2 (13, 27) and an activator of all KCCs (3), regardless of the cell volume changes that are usually required to activate or inhibit these transporters.

All these studies together demonstrate that, with the same expression system of *X. laevis* oocytes, the effect of WNK3 and WNK4 on NCC is opposite, whereas their effect on KCCs is similar. Thus it is reasonable to propose that sequences within WNK3 and WNK4 endow these kinases with the ability to activate or inhibit NCC, respectively. In the present study we undertook a chimeric approach between WNK3 and WNK4 to begin to define structure-function relationships between WNKs and NCC. Our results show that information required for being a positive or a negative regulator of NCC in WNK3 and WNK4 is located within the short amino terminal domain.

Address for reprint requests and other correspondence: G. Gamba, Molecular Physiology Unit, Vasco de Quiroga no. 15, Tlalpan 14000, Mexico City, Mexico (e-mail: gamba@biomedicas.unam.mx or gamba@quetzal.innsz.mx).

The costs of publication of this article were defrayed in part by the payment of page charges. The article must therefore be hereby marked "*advertisement*" in accordance with 18 U.S.C. Section 1734 solely to indicate this fact.

MATERIAL AND METHODS

The cDNAs of rat NCC, mouse WNK4, human WNK3, and human KCC2 have been described previously and are the clones that were used in the studies that demonstrated the effects of WNK3 or WNK4 on NCC or KCC2 (8, 27, 29, 34). Chimeric clones were constructed between WNK3 and WNK4 by swapping the amino- or the carboxy-terminal domain. To this end, unique silent *Kpn*I and *Nsi*I sites were introduced by site-directed mutagenesis (QuickChange; Stratagene) at the beginning and at the end, respectively, of the kinase domain of both WNK3 and WNK4. Amino- and carboxy-terminal domains were then swapped by cutting and pasting cDNA fragments to construct the chimeric proteins shown in Fig. 1. Restriction analysis and sequencing were used to corroborate the appropriate creation of silent sites and to rule out unwanted mutations. In addition, all experiments were performed using the constructs of wild-type WNK3 and WNK4 in which the *Kpn*I and *Nsi*I sites were introduced.

Assessment of the Na^+-Cl^- and K^+-Cl^- cotransporter function. NCC and KCC2 activity was assessed by functional expression in *X. laevis* oocytes following previously described protocols (3, 8, 20, 24, 29). Briefly, oocytes were surgically harvested from adult female *X. laevis* frogs (Nasco) under tricaine anesthesia (0.17%) and incubated in frog Ringer ND96 (in mM: 96 NaCl, 2 KCl, 1.8 $CaCl_2$, 1 MgCl, and 5 HEPES/Tris, pH 7.4) in the presence of collagenase B (2 mg/ml) for 1 h. Oocytes were washed four times in ND96, defolliculated, and incubated overnight at 18°C in ND96 supplemented with 2.5 mM sodium pyruvate and 5 mg/100 ml gentamicin. The next day, mature oocytes were injected with 50 nl of water alone or containing cRNA at 0.2 μg/μl NCC or KCC2 cRNA alone or together with a wild-type, mutant, or chimeric WNK cRNA. After injection, oocytes were maintained for 3 days in frog Ringer.

For NCC influx experiments 2 h before uptake, oocytes were incubated in a Cl^--free isotonic medium (in mM: 96 Na^+ isethionate, 2 K^+-gluconate, 1.8 Ca^{2+}-gluconate, 1.0 Mg^{2+}-gluconate, and 5 HEPES, pH 7.4). Tracer $^{22}Na^+$ uptake (New England Nuclear) was then assessed in groups of 10–15 oocytes exposed to isotonicity using our usual isotonic uptake solution [in mM: 40 NaCl, 56 *N*-methyl-D-glucamine (NMDG)-Cl, 1.8 $CaCl_2$, 1.0 $MgCl_2$, and 5.0 HEPES, pH 7.4; 210 mosmol/kgH_2O] containing 1 mM ouabain, 0.1 mM amiloride, and 0.1 mM bumetanide plus 2 μCi/ml $^{22}Na^+$. To determine the $^{22}Na^+$ uptake due to NCC, we exposed parallel groups to the same uptake solution but in the presence of 100 μM metolazone.

For KCC2 influx experiments, we assessed tracer $^{86}Rb^+$ uptake (New England Nuclear) in experimental groups of 10–15 oocytes. $^{86}Rb^+$ influx was measured in two different osmolar conditions. For hypotonic conditions, oocytes were incubated for 30 min in hypotonic K^+- and Cl^--free medium (in mM: 50 NMDG-gluconate, 4.6 Ca^{2+}-gluconate, 1.0 Mg^{2+}-gluconate, and 5 HEPES/Tris, pH 7.4; 110 mosmol/kgH_2O) with 1 mM ouabain, followed by 60 min in hypotonic Na^+-free medium containing 10 mM KCl, 40 mM NMDG-Cl, 1.8 mM $CaCl_2$, 1 mM $MgCl_2$, and 5 mM HEPES, pH 7.4, and supplemented with 1 mM ouabain and 2.0 μCi/ml $^{86}Rb^+$. Parallel groups of oocytes were exposed to Cl^--free uptake solution in which Cl^- was substituted with gluconate. For uptake in isotonic conditions, the same solutions were used but supplemented with 3.5 g/100 ml sucrose to reach picomolar conditions for oocytes (~210 mosmol/kgH_2O).

In all experiments, tracer activity was determined for each oocyte dissolved in 10% SDS by beta-scintillation counting. All results presented are based on a minimum of three different experiments with at least 10 oocytes per group in each experiment. Statistical significance is defined as two-tailed, with $P < 0.05$, and the results are presented as means ± SE. The significance of the differences between groups was tested by one-way ANOVA with multiple comparisons using Bonferroni correction.

RT-PCR of WNKs in X. laevis oocytes. X. laevis genome data bases were analyzed with BLAST using protein sequences of the carboxy-terminal domain of human WNK1, WNK2, WNK3, and WNK4 as bait. EST sequences with significant identity to each WNK were found. The percentages of identity of sequences from accession nos. EG575770, CA983538, BF048601, and BJ067481 were 75, 68, 76, and 84 with WNK1, WNK2, WNK3, and WNK4 carboxy-terminal domain, respectively. We then designed primer pairs from each sequence to amplify a fragment of each WNK from the oocytes' mRNA by RT-PCR. Total RNA from *X. laevis* oocytes was isolated using the Tripure system (Roche) following the manufacturer's recommendations and treated with DNase I for 1 h to eliminate possible contamination with genomic DNA. Reverse transcription was carried out using 2.5 μg of total RNA extracted from oocytes at 37°C for 60 min in a total volume of 20 μl using 200 units of the Moloney murine leukemia virus reverse transcriptase (Invitrogen). Simultaneous PCR for each WNK was carried out in the absence of reverse transcription to rule out the possibility of DNA genomic contamination. The cDNA fragments obtained from PCR were resolved in 5% acrylamide gels. Fragments from WNK3 and WNK4 were also resolved in agarose gel, excised, and sequenced by automatic DNA sequencing.

RESULTS

As shown in Fig. 1, WNKs can be divided into three structurally defined domains. The first is a short amino-terminal domain that, in WNK3 and WNK4, is made up of 146 and 173 amino acid residues, respectively. This is followed by the serine/threonine kinase domain of 274 amino acid residues in all WNKs and a long carboxy-terminal domain of 1,380 and 796 amino acid residues in WNK3 and WNK4, respectively. To analyze the role of the amino- and carboxy-terminal domains on NCC regulation, we constructed four chimeras between WNK3 and WNK4 by swapping their amino- or carboxy-terminal domains. To this end, silent restriction sites for *Kpn*I and *Nsi*I were introduced by site-directed mutagenesis at the beginning and end of the kinase domain. Figure 1*B* shows the chimeras denoted by three numbers corresponding to the amino-, kinase, and carboxy-terminal domains, respectively. The numbers 3 and 4 represent the origin of each domain. Thus chimeras 344 and 433 contain the amino-terminal domain of WNK3 and WNK4, respectively, fused into the kinase and carboxy-terminal domains of the other WNK. Chimeras 334 and 443 were made by swapping the carboxy-terminal domain of WNK3 or WNK4, respectively, into the amino-terminal and kinase domains of the other WNK. All chimeric constructs were corroborated by a restriction map and sequencing. The effect of each chimera on NCC and KCC2 activity was then assessed in control experiments that used wild-type WNK3 or WNK4 harboring the silent *Kpn*I and *Nsi*I sites (see MATERIALS AND METHODS).

Effect of WNK3 or WNK4 on NCC follows the amino-terminal domain. Figure 2 depicts the compiled results of three different experiments in which *X. laevis* oocytes were injected with NCC cRNA alone or together with wild-type or chimeric cRNAs. As we had previously shown (27), coinjection with NCC cRNA and wild-type WNK3 cRNA resulted in increased NCC activity. Figure 2*A* shows that activation induced by WNK3 increased $^{22}Na^+$ uptake by NCC from 4,006 ± 464 pmol·oocyte^{-1}·h^{-1} in oocytes injected with NCC cRNA alone to 12,925 ± 1,651 pmol·oocyte^{-1}·h^{-1} in oocytes coinjected with NCC and wild-type WNK3 cRNA ($P < 0.01$). Interestingly, coinjection with the chimera 344 cRNA resulted in a similar extent of NCC activation that reached 13,956 ± 1,520 pmol·oocyte^{-1}·h^{-1} ($P < 0.01$ vs. NCC alone). The chimera

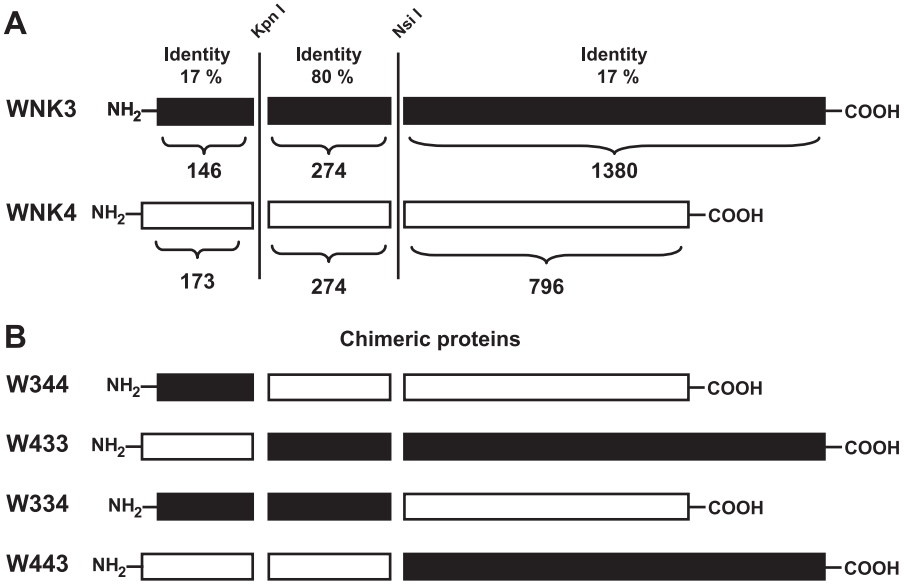

Fig. 1. Identity degree and chimeric proteins between WNK3 and WNK4. *A*: identity degree between WNK3 (black) and WNK4 (white) divided by the amino-terminal, kinase, and carboxy-terminal domains. Vertical lines indicate the regions in which silent restriction sites for *Kpn*I and *Nsi*I were introduced. Numbers above WNKs represent the percentage of identity for each segment. Numbers below WNKs represent the number of amino acid residues of each domain. *B*: chimeric constructs obtained between WNK3 (black) and WNK4 (white) by swapping the amino- or carboxy-terminal domains.

334 cRNA also induced a significant increase in NCC activity to 8,449 ± 1,010·oocyte^{-1}·h^{-1} ($P < 0.05$ vs. NCC alone). Therefore, chimeras containing the amino-terminal domain of WNK3 were able to increase NCC activity.

The opposite results were observed with chimeras containing the WNK4 amino-terminal domain (Fig. 2*B*). As we had previously shown (34), coinjection of NCC cRNA with WNK4 cRNA resulted in a significant reduction of NCC-induced $^{22}Na^+$ uptake (Fig. 2*B*) from 4,562 ± 348 pmol·oocyte^{-1}·h^{-1} in NCC oocytes to 1,456 ± 109 pmol·oocyte^{-1}·h^{-1} in oocytes coinjected with NCC and wild-type WNK4 cRNA ($P < 0.01$). Chimeras 433 and 443 also induced a significant reduction of NCC activity to 2,747 ± 296 and 1,058 ± 75 pmol·oocyte^{-1}·h^{-1}, respectively. Thus data shown in Fig. 2 suggest that WNK3 activating effects and WNK4 inhibiting effects on NCC correspond to the WNKs' amino-terminal domain. Interestingly, the inhibitory effect of chimera 433 was significantly lower than that observed in wild-type WNK4 or chimera 443, suggesting that activity and/or stability of this chimera in these experiments was lower than that of wild-type WNK4 or chimera 443 or that the catalytic domain of WNK3 still exerted some positive effect that somehow competes with the negative effect of the amino terminus. The first possibility is most likely, since in the series of experiments done in Fig. 5 (see below) the inhibitory effect of chimera 433 and wild-type WNK4 was similar.

All chimeras are powerful inhibitors of K^+-Cl^- cotransporter KCC2. It has been shown previously that both wild-type WNK3 and WNK4 are potent inhibitors of K^+-Cl^- cotransporters KCC1 to KCC4. Catalytically inactive forms of WNK3 and WNK4 not only lose their inhibitory effect but also become powerful activators of K^+-Cl^- cotransporters (3, 7, 10). We thus reasoned that if the WNK3 and WNK4 chimeras conserved their catalytic activity, then it would follow that they were able to inhibit K^+-Cl^- cotransporter expression, since this is the effect of both wild-type WNK3 and WNK4. Thus we assessed the effect of wild-type WNK3 and all four chimeras on the activity of KCC2 in hypotonic conditions, in which this cotransporter is maximally active (Fig. 3, *A* and *B*). Oocytes were injected with KCC2 cRNA alone or together with each of the chimeras' cRNA. Three days later, the activity of KCC2 was assessed in hypotonic conditions by measuring the Na^+-independent and Cl^--dependent $^{86}Rb^+$ influx. As we had previously shown (27, 29), injection of oocytes with KCC2 cRNA resulted in a remarkable increase in $^{86}Rb^+$ uptake during cell swelling (Fig. 3, *A* and *B*). When KCC2 was coinjected with wild-type WNK3 or any one of the four chimeras, regardless of their effect on NCC, $^{86}Rb^+$ uptake in these groups was similar to that of water-injected oocytes (Fig. 3, *A* and *B*). This finding implies that all cRNAs induced a complete inhibition of KCC2 activity. Because catalytic activity of WNK3 and WNK4 is required for the inhibition of K^+-Cl^- cotransporters (10, 27), these observations strongly suggest that all four chimeras are functional.

Effect of chimeras 344 and 433 on NCC and KCC2 requires their catalytic activity. We have previously shown that the elimination of catalytic activity in wild type WNK3 (WNK3-D294A) not only prevents its activating effect on NCC but also turns kinase-dead WNK3 into an NCC inhibitor (27). Thus, to further study the chimera 344 properties, we introduced the mutation D294A into this chimera to render it catalytically inactive (344-DA). We then assessed the effect of wild-type WNK3, WNK3-D294A, the chimera 344, and the kinase-dead chimera 344-D294A on NCC activity (Fig. 4). We observed that $^{22}Na^+$ uptake in oocytes injected with NCC cRNA alone was 3,830 ± 444 pmol·oocyte^{-1}·h^{-1}. However, in those coinjected with NCC and either WNK3 or chimera 344 cRNA, the tracer uptake increased to 10,826 ± 1,364 and 7,296 ± 1,114 pmol·oocyte^{-1}·h^{-1}, respectively ($P < 0.01$ vs. NCC alone). In contrast, uptake in oocytes coinjected with NCC and kinase-dead WNK3 or kinase-dead chimera 344 cRNA was significantly reduced. Na^+ uptake in NCC plus WNK3-D294A was 631 ± 120, and in oocytes injected with NCC plus 344-DA, it was 1,772 ± 103 pmol·oocyte^{-1}·h^{-1} ($P < 0.01$ vs. NCC alone). Thus, similar to WNK3-D294A (27), chimera 344-DA lost the activating effect on NCC and became an inhibitor of this cotransporter. This observation, together with results shown in Fig. 3, implies that increased activity of NCC by the chimera 344 requires its catalytic activity.

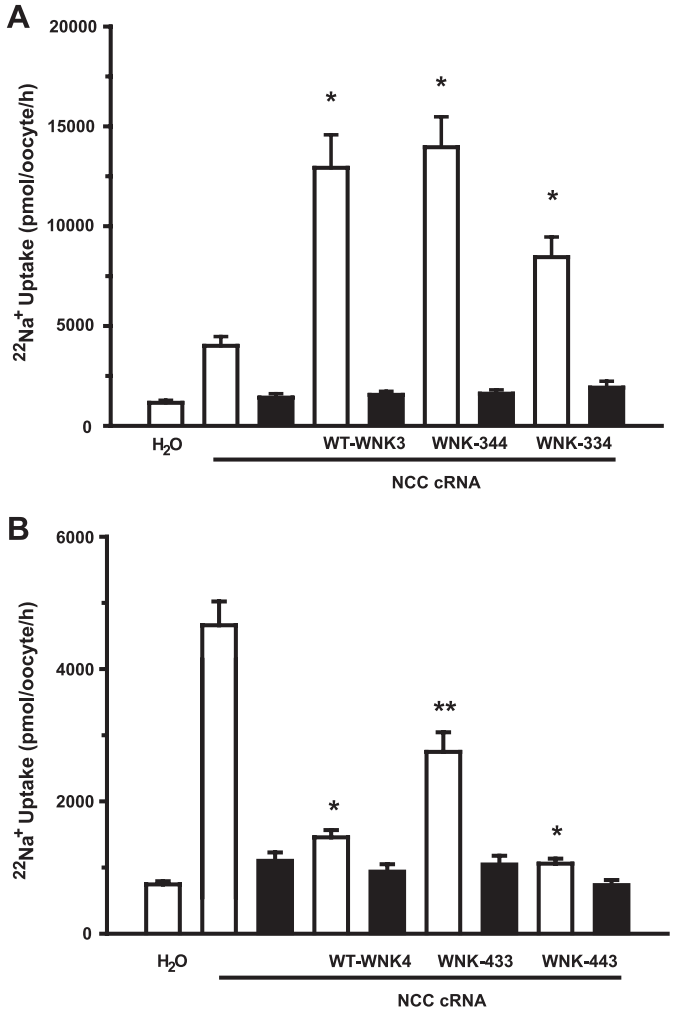

Fig. 2. Effect of WNK3, WNK4, and chimeras on the renal thiazide-sensitive Na+-2Cl^- cotransporter (NCC) activity. *A*: *Xenopus laevis* oocytes were injected with water or NCC cRNA alone or together with WNK3, chimera 344, or chimera 334 cRNAs, as indicated. *B*: oocytes were injected with water or NCC cRNA alone or together with WNK4, chimera 433, or chimera 443 cRNAs, as indicated. $^{22}Na^+$ uptake was assessed in isotonic medium 3 days later in the absence (open bars) or presence (filled bars) of 100 μM metolazone. *Significantly different from the uptake observed in oocytes injected with NCC cRNA alone. **Significantly different from the uptake observed in oocytes injected with NCC cRNA alone or NCC + wild-type WNK4 or 443 chimera.

We and others (2, 11, 34) have shown that the WNK4 inhibitory effect on NCC requires its catalytic activity. Therefore, to further analyze the functional properties of chimera 433, we assessed the effect of wild-type WNK4, the kinase-dead WNK4-D318A, chimera 433, and the kinase-dead chimera 433-D318A (433-DA) on NCC activity. As shown in Fig. 5, the NCC-induced basal $^{22}Na^+$ uptake of 7,225 ± 658 pmol·oocyte^{-1}·h^{-1} was reduced to 4,483 ± 832 and 3,138 ± 855 pmol·oocyte^{-1}·h^{-1} by WNK4 and chimera 433, respectively. In contrast, no significant reduction of NCC activity was induced by WNK4-D318A or chimera 433-DA. Therefore, as in the case of the catalytically inactive WNK4-D318A, eliminating the catalytic activity of chimera 433 prevented its inhibition of NCC. This observation, together with results shown in Fig. 2, also implies that to inhibit NCC, the 433 chimera requires catalytic activity.

Elimination of catalytic activity in both WNK3 and WNK4 also results in interesting effects on the K^+-Cl^- cotransporters. The mutant WNK3-D294A and WNK4-D318A not only lost their inhibitory effect on the K^+-Cl^- cotransporters expressed in oocytes under hypotonic conditions but also became powerful activators of these cotransporters under isotonic conditions (3, 10). Thus we also tested the effect of kinase-dead chimeras 344-D294A and 433-D318A on KCC2 activity under both hypotonic and isotonic conditions. As shown in Fig. 6, oocytes injected with KCC2 cRNA alone exhibited a remarkable increase in $^{86}Rb^+$ uptake. The level of $^{86}Rb^+$ uptake was not affected by coinjection with the catalytically inactive chimeras 344-D294A and 433-D318A. We showed in Fig. 2 that all chimeras were able to inhibit KCC2 activity under hypotonic conditions. Thus kinase-dead chimeras lost their inhibitory properties on KCC2.

When expressed in oocytes and exposed to isotonic conditions during the uptake, KCC2 was minimally active (Fig. 6).

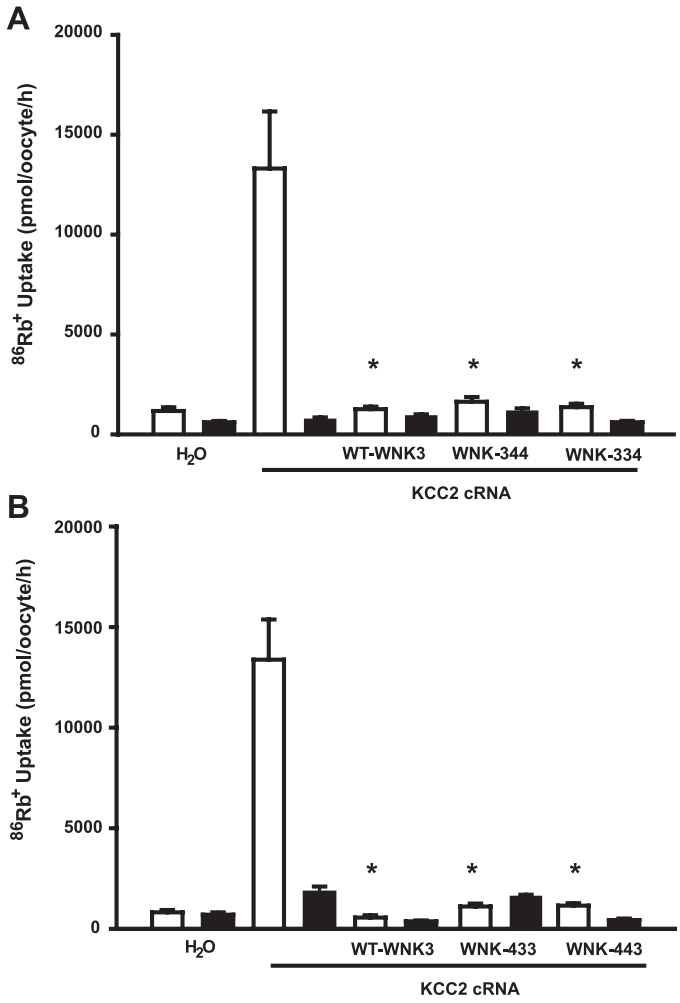

Fig. 3. Effect of WNK3 and chimeras on K^+-Cl^- cotransporter KCC2. *A*: oocytes were injected with water or KCC2 cRNA alone or together with WNK3, chimera 344, or chimera 334 cRNAs, as indicated. *B*: oocytes were injected with water or KCC2 cRNA alone or together with WNK3, chimera 433, or chimera 443 cRNAs, as indicated. $^{86}Rb^+$ uptake was assessed in hypotonic medium 3 days later in the presence (open bars) or absence (filled bars) of extracellular Cl^-. *Significantly different from the uptake observed in oocytes injected with KCC2 cRNA alone.

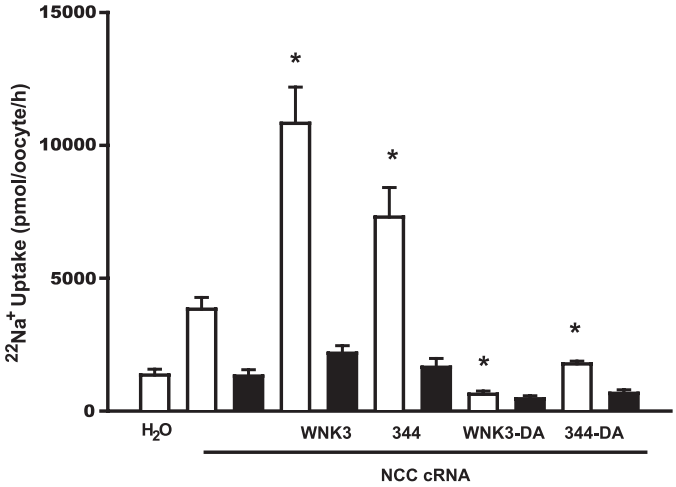

Fig. 4. Effect of aspartic acid substitution in wild-type WNK3 and chimera 344 on NCC activity. Oocytes were injected with NCC cRNA alone or together with wild-type WNK3, WNK3-D294A, chimera 344, or chimera 344-D294A cRNA. Three days later, $^{22}Na^+$ uptake was assessed in the absence (open bars) or presence (filled bars) of 100 μM metolazone. *Significantly different from the uptake observed in oocytes injected with NCC cRNA alone.

Coinjection with catalytically inactive chimeras 344-DA and 433-DA cRNA resulted in a significant activation of KCC2. The observation that D294A or D318A mutations in 344 and 433 chimeras, respectively, as in wild-type WNK3 or WNK4, prevented the inhibitory effect of these chimeras on KCC2 activity in hypotonic conditions (Fig. 3 vs. Fig. 6) is also strong evidence that chimeras 344 and 433 possess catalytic activity. In addition, similar to what we observed for WNK3 (3) and WNK4 (10), the activating effect on KCC2 under isotonic conditions is generated in chimeras 344 or 433 by eliminating their catalytic activity.

DISCUSSION

WNK kinases have emerged as powerful regulators of several transport pathways including transporters, channels, and

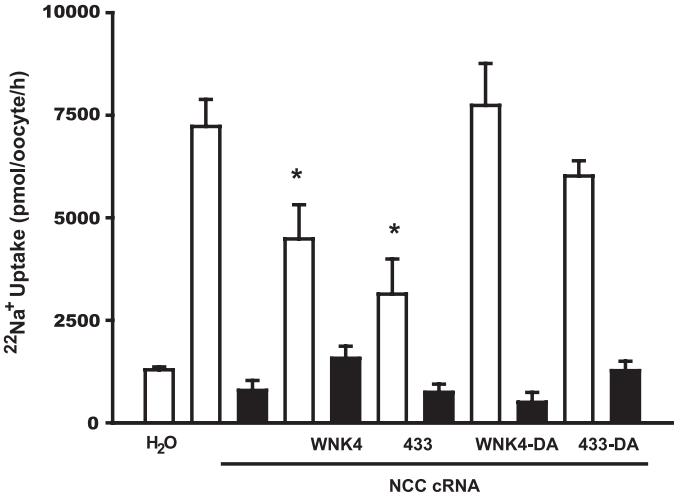

Fig. 5. Effect of aspartic acid substitution in wild-type WNK4 and chimera 433 on NCC activity. Oocytes were injected with NCC cRNA alone or together with wild-type WNK4, WNK4-D318A, chimera 433, or chimera 433-D318A cRNA. Three days later, $^{22}Na^+$ uptake was assessed in the absence (open bars) or presence (filled bars) of 100 μM metolazone. *Significantly different from the uptake observed in oocytes injected with NCC cRNA alone.

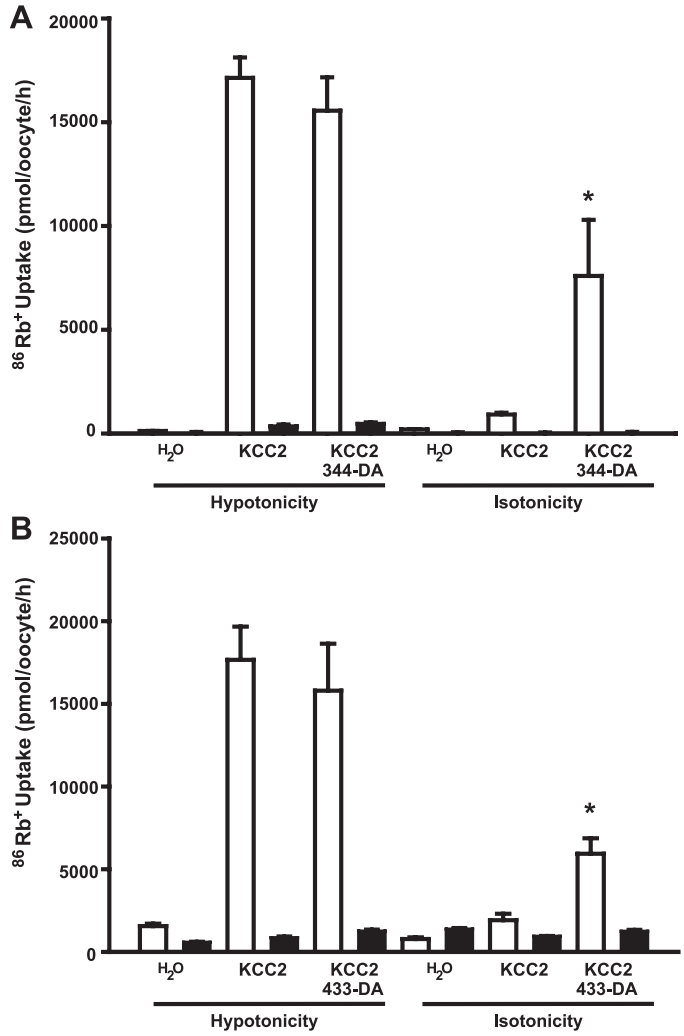

Fig. 6. Effect of chimeras 344-D294A and 433-D318A on KCC2 activity under hypotonic and isotonic conditions. *A*: oocytes were injected with KCC2 cRNA alone or together with 344-D294A cRNA. *B*: oocytes were injected with KCC2 cRNA alone or together with 433-D318A. Three days later, tracer $^{86}Rb^+$ uptake was assessed exposing oocytes to hypotonic or isotonic uptake medium in the presence (open bars) or absence (filled bars) of extracellular Cl^-. *Significantly different from the uptake observed in oocytes injected with KCC2 cRNA alone.

paracellular proteins (for recent review, see Refs. 14 and 25). NCC is one of the most important targets, because impairing its regulation by WNK1 or WNK4 mutations results in the arterial hypertension observed in PHAII patients (15, 18, 41). However, little is known regarding the critical domains within WNKs that endow these kinases with the ability to activate or inhibit NCC. In the present study, we took advantage of the fact that in the same expression system, WNK3 and WNK4 have opposite effects on NCC. WNK3 is an activator (27), whereas WNK4 is an inhibitor of this cotransporter (34). In contrast, both kinases are inhibitors of K^+-Cl^- cotransporters (3, 10). Thus unique sequences within WNK3 and WNK4 should be critical in defining their effects on NCC. WNK3 and WNK4 exhibit a very high degree of identity within the serine/threonine kinase domain but a very low degree of identity in the amino- and carboxy-terminal domains. Therefore, we constructed chimeric proteins by interchanging these

two domains and tested their effects on NCC and KCC2. Our experiments showed that chimeras containing the amino-terminal domain of WNK3 (344 and 334) increased the activity of NCC, whereas chimeras containing the amino-terminal domain of WNK4 (433 and 443) inhibited NCC (Fig. 2). Similar to wild-type WNK3 and WNK4, these effects were lost with DA mutations that render the WNKs kinase-dead (Figs. 4 and 5). Furthermore, all chimeras were able to inhibit KCC2 activity under hypotonic conditions (Fig. 3) in which we had previously shown that catalytic activity is required for such effects of WNK3 or WNK4 (3, 10). In addition, kinase-dead chimeras 344-DA or 433-DA also became KCC activators (Fig. 6). Taking all these observations together, we conclude that behavior of chimeras toward NCC follows the amino-terminal domain and that chimeras are catalytically active.

Two previous studies have suggested that essential sequences for NCC regulation in WNK4 and WNK3 are located within the carboxy-terminal domain. Yang et al. (40) analyzed the effect of coinjecting *X. laevis* oocytes with cRNA from NCC and different fragments of WNK4. Constructs from the amino-terminal and kinase domains (WNK4 1–444) were not able to inhibit NCC, whereas those containing the carboxy-terminal domain, with or without the kinase domain (WNK4 168–1222 or 445–1222), reduced NCC activity with efficacy similar to full-length WNK4. More recently, Yang et al. (39) confirmed our previous observations (27) that wild-type WNK3 activates NCC and that catalytically inactive WNK3-D294A becomes an inhibitor. Nevertheless, they observed that injecting oocytes with a construct containing only the WNK3 carboxy-terminal domain (WNK3 421–1743), without the associated kinase domain, resulted in increased NCC activity. Thus, although catalytic activity in WNK3 is required for activating NCC (34, 39), the authors observed that the carboxy-terminal domain by itself contains the information required for the WNK3 effects on NCC and proposed that WNK3 and WNK4 interact each other for NCC regulation (19). The active site or motif for such regulation was not elucidated. However, these studies did not rule out the possibility of a dominant negative effect induced by fragments of WNKs, particularly since transcripts corresponding to all four WNKs are expressed in *X. laevis* oocytes. As shown in Supplemental Fig. 1 (supplemental data for this article is available online at the *American Journal of Physiology-Renal Physiology* website), a fragment of the expected size for each WNK was amplified from oocytes total RNA, using primers that were designed based on *est* sequences from *X. laevis* that showed a high degree of identity with the carboxy-terminal domain of each mammalian WNK. No fragments were amplified in the absence of reverse transcription. The DNA sequence of excised bands corresponding to WNK3 and WNK4 exhibit a 75 and 82% identity with the corresponding fragment of mammalian WNK3 or WNK4, respectively.

It has been shown that WNKs can interact between each other physically and/or through phosphorylation processes (17, 30, 36, 39). One important example is seen in the WNK1 regulation of WNK4-NCC activity. WNK1 can interact with, and inhibit the effect of, WNK4 on NCC (38, 40). Under physiological conditions, this effect is not observed because the *PRKWNK1* gene produces an alternative spliced variant (S-WNK1), which is expressed exclusively in the distal convoluted tubule (DCT) and the connecting tubule (CNT) of the nephron (22, 23). S-WNK1 lacks the entire amino-terminal and kinase domains and prevents the WNK1-WNK4 interaction by hijacking the long form of WNK1 through protein-protein interaction (30). In PHAII patients, because of the intronic deletion of WNK1, the expression of the long WNK1 isoform is increased, diminishing the ratio of S-WNK1 to L-WNK1 in DCT/CNT. This allows WNK1 to interact with WNK4, preventing its inhibitory effect on NCC (30). These studies show that fragments of WNKs can affect cotransporters through dominant negative action on other WNKs, and this mechanism seems to occur in vivo, since expression of the S-WNK1 protein occurs naturally in DCT and CNT (4, 23). In contrast, there is no evidence for the existence of spliced truncated variants of WNK3 or WNK4 in DCT. Since WNKs are expressed in oocytes, it is possible that the carboxy terminus of WNK3 or WNK4 interacting with endogenous WNK3 or WNK4 prevents their respective effect on NCC. Thus, although the effect of wild-type WNK3 or WNK4 on NCC can be emulated by the carboxy-terminal domain of WNKs in oocytes, there is no implication for a shared mechanism.

The above proposal might explain why the inhibitory effect of WNK4 on NCC has been shown to be kinase dependent by three groups (2, 11, 34) as well as the present study, but not by another group (40). An important difference between these studies could be the WNK4 construct that was used. Wilson et al. (34), Golbang et al. (11), Cai et al. (2), and the present study were performed using the complete WNK4 (1–1222 residues), with or without the D318A mutation that eliminates catalytic activity. In contrast, Yang et al. (40) used a truncated form of WNK4 lacking the first 168 residues of the amino-terminal domain (168–1222 residues). Because WNK3 and WNK4 fragments can interact at the protein level (39) and *X. laevis* oocytes express all four WNKs, it is possible that the truncated WNK4 (168–1222) has a dominant negative effect on endogenous WNK3 or WNK4 resulting in NCC inhibition that is not expected to be kinase dependent.

The extent of identity between WNK3 and WNK4 amino-terminal domains is very low (17%). In essence, the two domains are extremely different. It is not known how WNK3 or WNK4 affects the activity of NCC. This could be due to direct interaction and phosphorylation between WNK and NCC, or alternatively, WNKs could interact with other proteins that in turn define the type of effect on NCC. Supporting the first possibility, it has been shown that WNK4 and NCC form a protein complex that is not affected by the kinase activity (31) or by PHAII type mutations (15), suggesting that at least WNK4 and NCC interact directly. Supporting the second possibility, several studies have shown that WNK1 and WNK4 interact with STE-20 kinases such as SPAK and OSR1 and that this interaction is critical for the effect of WNKs on NKCC1 (7, 21, 31). In this regard, we have shown that SPAK is expressed in *X. laevis* oocytes (10) and that interaction between WNK3 and SPAK is required for WNK3-induced activation of NKCC2 (26). Finally, we also have provided evidences that protein phosphatases are involved in the effect of WNK3 and its catalytically inactive form on the K^+-Cl^- cotransporters (3). Thus it is possible that information that allows WNK3 or WNK4 to activate or inhibit NCC contained within the WNKs' amino-terminal domain endows the kinase with the capacity to associate with NCC or other intermediary proteins (SPAK, protein phosphatases, or others). However, no particular pro-

tein patterns or motifs are found when both WNK3 and WNK4 amino-terminal domains are analyzed using multiple database algorithm sites. Interestingly, WNK3 and WNK4 amino-terminal domains drastically differ in the number of proline residues, 7 of 146 for WNK3 (4.7%) and 32 of 173 for WNK4 (18.4%), suggesting a different structural conformation for each domain. In this regard, a recent report clearly shows that an amino-terminal proline-rich domain of WNK1 is necessary and sufficient for inhibition of ROMK1 by this kinase (32). The identity degree of the amino-terminal domain of WNK1 with WNK3 or WNK4 is, however, also below 15%. Thus further investigation is required to define the motif or active site within the WNK3 or WNK4 amino-terminal domain responsible for their activating or inhibiting properties.

In summary, our data using WNK3/WNK4 chimeras strongly suggest that the activating effect of WNK3 and the inhibitory effect of WNK4 on NCC follow the amino-terminal domain.

GRANTS

This work was supported by National Institute of Diabetes and Digestive and Kidney Diseases Grant DK-64635 and Consejo Nacional de Ciencia y Tecnologia Grant 59992 (to G. Gamba) and by a grant from the Foundation Leducq for the Transatlantic Network on Hypertension-Renal Salt Handling in the Control of Blood Pressure.

REFERENCES

1. **Adragna NC, Fulvio MD, Lauf PK.** Regulation of K-Cl cotransport: from function to genes. *J Membr Biol* 201: 109–137, 2004.
2. **Cai H, Cebotaru V, Wang YH, Zhang XM, Cebotaru L, Guggino SE, Guggino WB.** WNK4 kinase regulates surface expression of the human sodium chloride cotransporter in mammalian cells. *Kidney Int* 69: 2162–2170, 2006.
3. **De Los Heros P, Kahle KT, Rinehart J, Bobadilla NA, Vazquez N, San Cristobal P, Mount DB, Lifton RP, Hebert SC, Gamba G.** WNK3 bypasses the tonicity requirement for K-Cl cotransporter activation via a phosphatase-dependent pathway. *Proc Natl Acad Sci USA* 103: 1976–1981, 2006.
4. **Delaloy C, Lu J, Houot AM, Disse-Nicodeme S, Gasc JM, Corvol P, Jeunemaitre X.** Multiple promoters in the WNK1 gene: one controls expression of a kidney-specific kinase-defective isoform. *Mol Cell Biol* 23: 9208–9221, 2003.
5. **Flatman PW.** Regulation of Na-K-2Cl cotransport by phosphorylation and protein-protein interactions. *Biochim Biophys Acta* 1566: 140–151, 2002.
6. **Flatman PW.** Cotransporters, WNKs and hypertension: important leads from the study of monogenetic disorders of blood pressure regulation. *Clin Sci (Lond)* 112: 203–216, 2007.
7. **Gagnon KB, England R, Delpire E.** Volume sensitivity of cation-Cl^- cotransporters is modulated by the interaction of two kinases: Ste20-related proline-alanine-rich kinase and WNK4. *Am J Physiol Cell Physiol* 290: C134–C142, 2006.
8. **Gamba G, Miyanoshita A, Lombardi M, Lytton J, Lee WS, Hediger MA, Hebert SC.** Molecular cloning, primary structure and characterization of two members of the mammalian electroneutral sodium-(potassium)-chloride cotransporter family expressed in kidney. *J Biol Chem* 269: 17713–17722, 1994.
9. **Gamba G.** Molecular physiology and pathophysiology of the electroneutral cation-chloride cotransporters. *Physiol Rev* 85: 423–493, 2005.
10. **Garzon-Muvdi T, Pacheco-Alvarez D, Gagnon KB, Vazquez N, Ponce-Coria J, Moreno E, Delpire E, Gamba G.** WNK4 kinase is a negative regulator of K^+-Cl^- cotransporters. *Am J Physiol Renal Physiol* 292: F1197–F1207, 2007.
11. **Golbang AP, Cope G, Hamad A, Murthy M, Liu CH, Cuthbert AW, O'Shaughnessy KM.** Regulation of the expression of the Na/Cl cotransporter (NCCT) by WNK4 and WNK1: evidence that accelerated dynamin-dependent endocytosis is not involved. *Am J Physiol Renal Physiol* 291: F1369–F1376, 2006.
12. **Hebert SC, Mount DB, Gamba G.** Molecular physiology of cation-coupled Cl^- cotransport: the SLC12 family. *Pflügers Arch* 447: 580–593, 2004.
13. **Kahle KT, Rinehart J, De Los HP, Louvi A, Meade P, Vazquez N, Hebert SC, Gamba G, Gimenez I, Lifton RP.** WNK3 modulates transport of Cl^- in and out of cells: Implications for control of cell volume and neuronal excitability. *Proc Natl Acad Sci USA* 102: 16783–16788, 2005.
14. **Kahle KT, Rinehart J, Ring A, Gimenez I, Gamba G, Hebert SC, Lifton RP.** WNK protein kinases modulate cellular Cl^- flux by altering the phosphorylation state of the Na-K-Cl and K-Cl cotransporters. *Physiology (Bethesda)* 21: 326–335, 2006.
15. **Lalioti MD, Zhang J, Volkman HM, Kahle KT, Hoffmann KE, Toka HR, Nelson-Williams C, Ellison DH, Flavell R, Booth CJ, Lu Y, Geller DS, Lifton RP.** Wnk4 controls blood pressure and potassium homeostasis via regulation of mass and activity of the distal convoluted tubule. *Nat Genet* 38: 1124–1132, 2006.
16. **Lauf PK, Adragna NC.** K-Cl cotransport: properties and molecular mechanism. *Cell Physiol Biochem* 10: 341–354, 2000.
17. **Lenertz LY, Lee BH, Min X, Xu BE, Wedin K, Earnest S, Goldsmith EJ, Cobb MH.** Properties of WNK1 and implications for other family members. *J Biol Chem* 280: 26653–26658, 2005.
18. **Mayan H, Vered I, Mouallem M, Tzadok-Witkon M, Pauzner R, Farfel Z.** Pseudohypoaldosteronism type II: marked sensitivity to thiazides, hypercalciuria, normomagnesemia, and low bone mineral density. *J Clin Endocrinol Metab* 87: 3248–3254, 2002.
19. **McCormick JA, Yang CL, Ellison DH.** WNK kinases and renal sodium transport in health and disease. An integrated view. *Hypertension* 51: 588–596, 2008.
20. **Moreno E, San Cristobal P, Rivera M, Vazquez N, Bobadilla NA, Gamba G.** Affinity defining domains in the Na-Cl cotransporter: different location for Cl^- and thiazide binding. *J Biol Chem* 281: 17266–17275, 2006.
21. **Moriguchi T, Urushiyama S, Hisamoto N, Iemura S, Uchida S, Natsume T, Matsumoto K, Shibuya H.** WNK1 regulates phosphorylation of cation-chloride-coupled cotransporters via the STE20-related kinases, SPAK and OSR1. *J Biol Chem* 280: 42685–42693, 2005.
22. **O'Reilly M, Marshall E, Macgillivray T, Mittal M, Xue W, Kenyon CJ, Brown RW.** Dietary electrolyte-driven responses in the renal WNK kinase pathway in vivo. *J Am Soc Nephrol* 17: 2402–2413, 2006.
23. **O'Reilly M, Marshall E, Speirs HJ, Brown RW.** WNK1, a gene within a novel blood pressure control pathway, tissue-specifically generates radically different isoforms with and without a kinase domain. *J Am Soc Nephrol* 14: 2447–2456, 2003.
24. **Pacheco-Alvarez D, San Cristobal P, Meade P, Moreno E, Vazquez N, Munoz E, Diaz A, Juarez ME, Gimenez I, Gamba G.** The Na-Cl cotransporter is activated and phosphorylated at the amino terminal domain upon intracellular chloride depletion. *J Biol Chem* 281: 28755–28763, 2006.
25. **Peng JB, Warnock DG.** WNK4-mediated regulation of renal ion transport proteins. *Am J Physiol Renal Physiol* 293: F961–F973, 2007.
26. **Ponce-Coria J, San Cristobal P, Kahle KT, Vazquez N, Pacheco-Alvarez D, De Los HP, Juarez P, Munoz E, Michel G, Bobadilla NA, Gimenez I, Lifton RP, Hebert SC, Gamba G.** Regulation of NKCC2 by a chloride-sensing mechanism involving the WNK3 and SPAK kinases. *Proc Natl Acad Sci USA* 105: 8458–8463, 2008.
27. **Rinehart J, Kahle KT, De Los HP, Vazquez N, Meade P, Wilson FH, Hebert SC, Gimenez I, Gamba G, Lifton RP.** WNK3 kinase is a positive regulator of NKCC2 and NCC, renal cation-Cl^- cotransporters required for normal blood pressure homeostasis. *Proc Natl Acad Sci USA* 102: 16777–16782, 2005.
28. **Simon DB, Nelson-Williams C, Johnson-Bia M, Ellison D, Karet FE, Morey-Molina A, Vaara I, Iwata F, Cushner HM, Koolen M, Gainza FJ, Gitelman HJ, Lifton RP.** Gitelman's variant of Bartter's syndrome, inherited hypokalaemic alkalosis, is caused by mutations in the thiazide-sensitive Na-Cl cotransporter. *Nat Genet* 12: 24–30, 1996.
29. **Song L, Mercado A, Vazquez N, Xie Q, Desai R, George AL, Gamba G, Mount DB.** Molecular, functional, and genomic characterization of human KCC2, the neuronal K-Cl cotransporter. *Brain Res Mol Brain Res* 103: 91–105, 2002.
30. **Subramanya AR, Yang CL, Zhu X, Ellison DH.** Dominant-negative regulation of WNK1 by its kidney-specific kinase-defective isoform. *Am J Physiol Renal Physiol* 290: F619–F624, 2006.
31. **Vitari AC, Deak M, Morrice NA, Alessi DR.** The WNK1 and WNK4 protein kinases that are mutated in Gordon's hypertension syndrome, phosphorylate and active SPAK and OSR1 protein kinases. *Biochem J* 391: 17–24, 2005.
32. **Wang HR, Liu Z, Huang CL.** Domains of WNK1 kinase in the regulation of ROMK1. *Am J Physiol Renal Physiol* 295: F438–F445, 2008.
33. **Wilson FH, Disse-Nicodeme S, Choate KA, Ishikawa K, Nelson-Williams C, Desitter I, Gunel M, Milford DV, Lipkin GW, Achard**

JM, Feely MP, Dussol B, Berland Y, Unwin RJ, Mayan H, Simon DB, Farfel Z, Jeunemaitre X, Lifton RP. Human hypertension caused by mutations in WNK kinases. *Science* 293: 1107–1112, 2001.

34. **Wilson FH, Kahle KT, Sabath E, Lalioti MD, Rapson AK, Hoover RS, Hebert SC, Gamba G, Lifton RP.** Molecular pathogenesis of inherited hypertension with hyperkalemia: the Na-Cl cotransporter is inhibited by wild-type but not mutant WNK4. *Proc Natl Acad Sci USA* 100: 680–684, 2003.
35. **Xu B, English JM, Wilsbacher JL, Stippec S, Goldsmith EJ, Cobb MH.** WNK1, a novel mammalian serine/threonine protein kinase lacking the catalytic lysine in subdomain II. *J Biol Chem* 275: 16795–16801, 2000.
36. **Xu BE, Min X, Stippec S, Lee BH, Goldsmith EJ, Cobb MH.** Regulation of WNK1 by an autoinhibitory domain and autophosphorylation. *J Biol Chem* 277: 48456–48462, 2002.
37. **Yang CL, Angell J, Mitchell R, Ellison DH.** WNK kinases regulate thiazide-sensitive Na-Cl cotransport. *J Clin Invest* 111: 1039–1045, 2003.
38. **Yang CL, Ellison DH.** WNK1 interacts physically with WNK4. *J Am Soc Nephrol* 14: 77A, 2003.
39. **Yang CL, Zhu X, Ellison DH.** The thiazide-sensitive Na-Cl cotransporter is regulated by a WNK kinase signaling complex. *J Clin Invest* 117: 3403–3411, 2007.
40. **Yang CL, Zhu X, Wang Z, Subramanya AR, Ellison DH.** Mechanisms of WNK1 and WNK4 interaction in the regulation of thiazide-sensitive NaCl cotransport. *J Clin Invest* 115: 1379–1387, 2005.
41. **Yang SS, Morimoto T, Rai T, Chiga M, Sohara E, Ohno M, Uchida K, Lin SH, Moriguchi T, Shibuya H, Kondo Y, Sasaki S, Uchida S.** Molecular pathogenesis of pseudohypoaldosteronism type II: generation and analysis of a Wnk4(D561A/+) knockin mouse model. *Cell Metab* 5: 331–344, 2007.

Kidney and beyond – Review Article

American Journal of Nephrology

Am J Nephrol 2008;28:860–870
DOI: 10.1159/000139639

Received: March 10, 2008
Accepted: March 31, 2008
Published online: June 12, 2008

WNK Kinases, Renal Ion Transport and Hypertension

Pedro San-Cristobal[a] Paola de los Heros[a] José Ponce-Coria[a] Erika Moreno[a, b] Gerardo Gamba[a]

[a]Molecular Physiology Unit, Instituto Nacional de Ciencias Médicas y Nutrición Salvador Zubirán and Instituto de Investigaciones Biomédicas, Universidad Nacional Autónoma de México, Mexico City, and [b]Universidad Autónoma del Estado de Hidalgo, Pachuca, México

Key Words
Diuretics · Distal convoluted tubule · Salt transport · Potassium excretion · Phosphorylation

Abstract
Two members of a recently discovered family of protein kinases are the cause of an inherited disease known as pseudohypoaldosteronism type II (PHAII). These patients exhibit arterial hypertension together with hyperkalemia and metabolic acidosis. This is a mirror image of Gitelman disease that is due to inactivating mutations of the *SLC12A3* gene that encodes the thiazide-sensitive Na^+:Cl^- cotransporter. The uncovered genes causing PHAII encode for serine/threonine kinases known as WNK1 and WNK4. Physiological and biochemical studies have revealed that WNK1 and WNK4 modulate the activity of several transport pathways of the aldosterone-sensitive distal nephron, thus increasing our understanding of how diverse renal ion transport proteins are coordinated to regulate normal blood pressure levels. Observations discussed in the present work place WNK1 and WNK4 as genes involved in the genesis of essential hypertension and as potential targets for the development of antihypertensive drugs.

Arterial hypertension is one of the most common diseases affecting more than one billion people worldwide. Most of the affected patients belong to a category known as essential hypertension, which means the origin of their disease is unknown. Unfortunately, most of the time increased blood pressure is not associated with any particular symptom, but induces a remarkable increase in the risk of fatal illnesses such as heart attack, aneurysm or stroke, due to increased pressure on the arterial wall accelerating the processes of atherosclerosis. Arterial hypertension is a prototype of what is currently known as polygenic disease, in which it is postulated that normal variation throughout the genome, due to changes at the single-base level, known as single-nucleotide polymorphisms (SNPs), predispose individuals to an increased susceptibility to environmental factors (i.e. sugar consumption and diabetes mellitus, or salt intake and arterial pressure) to produce the disease. SNPs can also be the reason for the well-known variation in the type or magnitude of response to antihypertensive drugs observed within the population (pharmacogenomics). While the origins of hypertension are unknown, several lines of evidence demonstrate that pressure natriuresis in the kidney plays a key role in the long-term regulation of arterial pressure and that arterial hypertension only occurs when the pressure natriuresis relationship in the kidney

KARGER

Fax +41 61 306 12 34
E-Mail karger@karger.ch
www.karger.com

Accessible online at:
www.karger.com/ajn

Gerardo Gamba, MD, PhD
Molecular Physiology Unit, Vasco de Quiroga No. 15
Tlalpan 14000, México City (México)
Tel. +52 55 5513 3868, Fax +52 55 5655 0382
E-Mail gamba@biomedicas.unam.mx or gamba@quetzal.innsz.mx

is switched to the right (guytonian hypothesis) [1]. That is, increased arterial blood pressure is required in order to achieve normal salt urinary output.

Because arterial hypertension is polygenic, in order to understand the mechanisms of the disease, it is important to identify genes involved in blood pressure regulation. A very successful approach used over the last decade has been unmasking genes causing monogenic diseases that exhibit high or low blood pressure levels under the assumption that if altered function of a single gene is enough to produce an abnormal change in blood pressure, it is highly likely that the gene could be involved in the genesis of essential hypertension. More than 15 genes have been identified following this strategy [2]. Supporting the guytonian hypothesis, all recognized genes are involved in the maintenance of renal salt balance. Good examples of genes discovered by this strategy that have increased our understanding of hypertension mechanisms are the serine/threonine kinases of the WNK family.

WNK Kinases and Genetic Hypertension

Identification of WNK Kinases as Proteins Involved in the Regulation of Arterial Blood Pressure

Two monogenic diseases resulting in abnormal variations in blood pressure exhibit mirror images in their clinical features. On the one hand, Gitelman disease (OMIM No. 263800) is an autosomal recessive disorder associated with arterial hypotension, together with hypokalemic metabolic alkalosis and hypocalciuria. This monogenic disease is due to mutations in the *SLC12A3* gene located in the human chromosome 16 that encodes for the thiazide-sensitive Na^+:Cl^- cotransporter (NCC) that is expressed in the apical membrane of the distal convoluted tubule (DCT) [3–5] (table 1). The mutations are of the 'loss of function' type resulting in inactivation of the cotransporter [9–11]. The absence of NCC activity decreases salt reabsorption in the DCT, resulting in dehydration and arterial hypotension. The consequential increase in salt delivery to the connecting tubule (CNT) and collecting duct (CD) induces increased potassium and hydrogen secretion producing the hypokalemic metabolic alkalosis. On the other hand, a disease known by several names such as Gordon's disease, familial hyperkalemic hypertension or pseudohypoaldosteronism type II (PHAII; OMIM No. 145260) exhibits a mode of inheritance that is compatible with autosomal dominant transmission and features arterial hypertension that is accompanied by hyperkalemic metabolic acidosis and hypercalciuria. This phenotype is Cl^- dependent and is corrected with low doses of thiazide-type diuretics [12]. Thus, PHAII is a mirror image of Gitelman disease, strongly suggesting that increased activity of the NCC must be implicated. However, initial genomic analysis demonstrated no significant linkage of kindred with PHAII to the *SLC12A3* gene on chromosome 16 in patients with PHAII [13], making it unlikely that the cause of PHAII is activating mutations of the NCC. Later, locus heterogeneity of PHAII was identified by Mansfield et al. [14] when positive linkage analysis was observed in two loci: one located in chromosome 1q31–q42 and another in chromosome 17p11–q21 (table 1). The evidence of genetic heterogeneity of PHAII was increased by Disse-Nicodeme et al. [15, 16], who observed in French kindreds a positive linkage to chromosome 12p13.3 and in another family no linkage to the *SLC12A3* gene or to chromosomes 1, 12 and 17. Thus, at least 4 genes are capable of producing the same disease independently (table 1).

Table 1. Genetic defects in PHAII and Gitelman disease

Disease	Location	Gene	Defect	Reference
PHAII1	12p13.3	*PRKWNK1*	intronic deletion	12
PHAII2	17q21	*PRKWNK4*	missense mutations	11
PHAII3	1q31–42	unknown	unknown	11
PHAII4	unknown	unknown	unknown	13
Gitelman	16q13	*SLC12A3*	mutations	3–5

At about the time heterogeneity of PHAII was observed, in their effort to clone novel members of the mitogen-activated protein/extracellular signal-regulated protein kinases from brain tissue, the Cobb group in Texas [17] identified a new type of serine/threonine kinase that lacks the canonical lysine observed in all serine/threonine kinases in the subdomain II of the kinase domain. Due to the absence of this lysine, the new kinase was named WNK1 for 'with no lysine (K)'. This report would probably have passed unnoticed by the renal community if not for a study months later in which the Lifton group from Yale, following the positional cloning strategy [8], identified that the cause of PHAII in families with positive linkage to chromosome 12 was due to deletion of a fragment of intron 1 in the *PRKWNK1* gene, encoding WNK1.

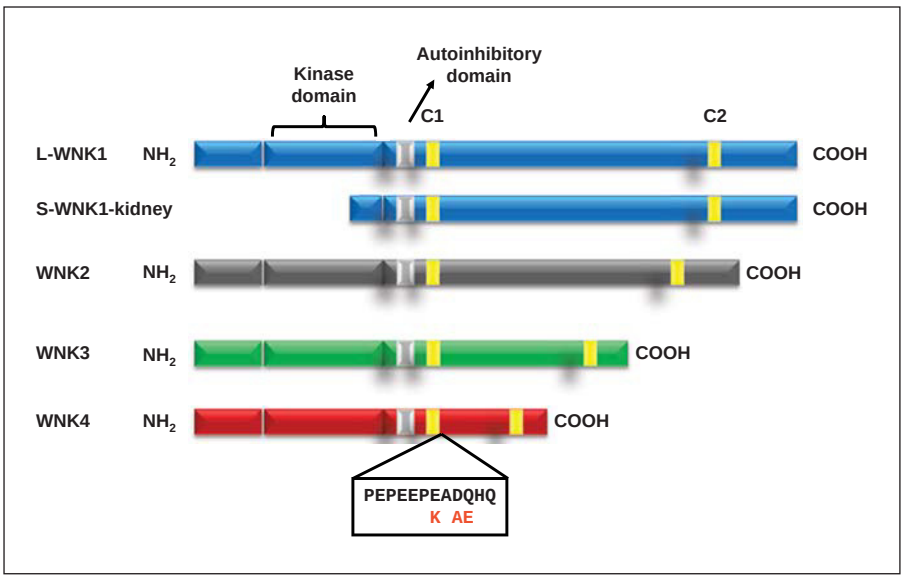

Fig. 1. Proposed model of WNK proteins. The central kinase domain is shown by a bracket. The autoinhibitory domain and the coiled-coil domains are highlighted. Locations of the negatively charged residues in which WNK4 mutations occur are shown below WNK4.

Two Forms of PHAII Are due to Mutations in WNK Kinases

Wilson et al. [8] uncovered 2 genes causing PHAII. They first observed that 2 kindreds with significant linkage to chromosome 12p13 cosegregated with a 41- or 21-kb deletion, respectively, within the first large intron of *PRKWNK1*. No mutations or deletions within the WNK1-coding sequence were detected in these families. The expression of WNK1 mRNA in leukocytes in affected individuals was observed to be 5-fold higher than in nonaffected members of the family. Thus, genomic deletions of the first intron of WNK1 increase the expression of an otherwise normal WNK1 kinase. Supporting this hypothesis, Delaloy et al. [18] later revealed that the region that goes from –2,500 to –1,200 of the human *PRKWNK1* promoter represses transcription of the gene. To date, these are the only 2 PHAII kindreds in which deletion of *PRKWNK1* genes have been reported.

The other form of PHAII that is due to mutations in WNK kinases is the one in which positive linkage was observed with human chromosome 17. Four independent missense mutations in the *PRKWNK4* gene were observed by Wilson et al. [8] in these families. Interestingly, 3 out of 4 missense mutations occur within a highly conserved acidic region that is located within the carboxyl-terminal domain, just after the first coiled-coil domain (fig. 1). This negatively charged region contains 10 amino acid residues that are 100% identical between WNK1, WNK2 and WNK4, and 70% with WNK3. Six out of 10 amino acid residues in this region of WNK4 are charged. The 3 missense mutations that occur in this region change or eliminate the charge of a residue (E562K, D564A and Q565E mutations). Golbang et al. [19] later reported another PHAII kindred in which asparagine 564 is mutated to histidine (D564H). In addition, Wilson et al. [8] also observed that mutation R1185C cosegregates with PHAII in another family. This mutation, although outside the acidic domain, also changes the charge of an amino acid residue. Thus, the PHAII that cosegregates with the *PRKWNK4* gene is due to point mutations that change 1 charged amino acid residue. It is believed that this alteration probably affects the way in which WNK4 interacts with other proteins or charged molecules, resulting in modification of the effect of WNK4 upon transport systems.

The WNK Family Is Composed of Four Members

After the cloning and identification of WNK1 from the rat kidney [17], it was soon observed that the WNK family is composed of 4 members that were named WNK1, WNK2, WNK3 and WNK4 (fig. 1). The corresponding genes *PRKWNK1*, *PRKWNK2*, *PRKWNK3* and *PRKWNK4* are located in human chromosomes 12, 9, X and 17, respectively. As shown in figure 1, WNK kinases are composed of 3 domains. A serine/threonine kinase domain of 274 residues is flanked by a short amino-terminal domain of 146–220 amino acid residues and a large carboxyl-terminal domain of 786–1,888 residues containing an autoinhibitory domain and 2 coiled-coil domains that could be important for protein-protein in-

teraction. The degree of identity among the 4 WNKs at the amino- and carboxyl-terminal domains is below 20%, whereas at the serine/threonine kinase it is above 80%. The WNK1 kinase domain crystal structure was resolved at 1.8 Å demonstrating that the catalytic lysine is located in the β-strand 2, rather than strand 3 as in other serine/threonine kinases [20]. Several in vitro studies have shown that WNK kinases can interact amongst each other at the protein-protein level [21–23] or by phosphorylation processes [24], as well as with many other kinase proteins including mitogen-activated protein kinases [6, 25], transforming growth factor β signaling pathway kinases [26], synaptotagmin [27] and STE-20-related kinases like serine-proline-alanine-rich kinase (SPAK) or oxidative stress response kinase 1 (OSR1) [7, 28–31].

WNK1 is a ubiquitously expressed kinase with predominant expression in the kidney, heart, muscle and testis in the rat [17], mouse [32] and human [33]. In most tissues, it is predominantly expressed in polarized epithelial cells. In the kidney it is expressed along the entire nephron [32, 34]. By RT-PCR analysis it has been observed that WNK3 transcripts are present in all tissues [35], and by immunohistochemistry WNK3 protein was shown to be expressed in all nephron segments, as well as in epithelial cells of several organs such as the pancreas, biliary duct, stomach and intestine [36]. In contrast to WNK1 and WNK4, WNK3 protein is highly expressed in the central nervous system in which it is present in cell bodies of neurons expressing ionotropic γ-aminobutyric acid A receptors [36]. WNK4 is mainly expressed in the aldosterone-sensitive distal nephron. At the protein level it has been shown to be present in the DCT and CD [8, 34], and at the mRNA level, by single-nephron RT-PCR, WNK4 transcripts have been shown to be expressed also in the thick ascending limb of Henle's loop [34]. In addition, Kahle et al. [37] observed that WNK4 transcript and protein are present in several epithelial tissues, in which expression is more prominent in tight junctions. Interestingly, all epithelia expressing WNKs are heavily involved in Cl^- transport.

The molecular diversity of the WNK family has been shown to be increased by expression of several alternative splicing variants described in WNK1 and WNK3. Two independent groups [18, 38] observed by Northern blot analysis 2 WNK1 transcripts, 9.0 and 10.5 kb in size, that differ in the length of the 3′ untranslated region. These transcripts are present in all tested tissues and are known as L-WNK1. In addition, there is an approximately 8.0-kb transcript expressed only in the kidney that is due to alternative splicing of exons 1–4. The transcription of this isoform is under control of an intron 4 alternative promoter and contains sequences from an extra exon located between exons 4 and 5 which has been designed as exon 4a. As shown in figure 1, at the protein level the consequence of this splicing mechanism is a shorter WNK1 isoform that lacks the first 437 amino acid residues, including almost the entire kinase domain. This shorter, truncated isoform is known as S-WNK1. By in situ hybridization it has been demonstrated that within the kidney, L-WNK1 isoforms are present all along the entire nephron, whereas S-WNK1 is only present in the aldosterone-sensitive distal nephron, particularly abundant in the DCT and CNT. These locations are very important to understand the mechanism by which overexpression of L-WNK1 produces activation of the NCC (see below). For WNK1 another 5 different transcripts have been detected due to splicing of exons 9, 11 and 12, either separately or in combination. The functional consequences of all these isoforms are unknown. Finally, human WNK3 exhibits at least 2 alternative variants. One is due to usage of an alternative splice donor into exon 18 that introduces 47 amino acid residues, and the other is due to splicing of exon 22 [35]. The functional consequences of these splicing isoforms are unknown.

Modulation of Renal Ion Transport Systems by WNKs

Several lines of evidence suggested that WNKs would be critical regulators of renal ion transport systems: (1) WNK1 and WNK4 are predominantly expressed in the aldosterone-sensitive distal nephron; (2) in addition to hypertension, PHAII patients exhibit hyperkalemia, metabolic acidosis and hypercalciuria consistent with impairment of the normal renal excretion of these ions; (3) PHAII is the mirror image of Gitelman disease that is due to inactivating mutations of the NCC; (4) the PHAII clinical picture is easily reverted by very low doses of thiazide-type diuretics [12].

Effects of WNK4 upon Distal Nephron Transport Systems

Due to the mirror image between Gitelman disease and PHAII, and the exquisite sensitivity of this latter disease to thiazides, the first transport system that was studied was the NCC, which is the major salt transport pathway in the DCT (fig. 2). The effect of WNK4 upon NCC activity was assessed using the heterologous expression system of *Xenopus laevis* oocytes, which was used to clone these and other transporters [39, 40], and in which

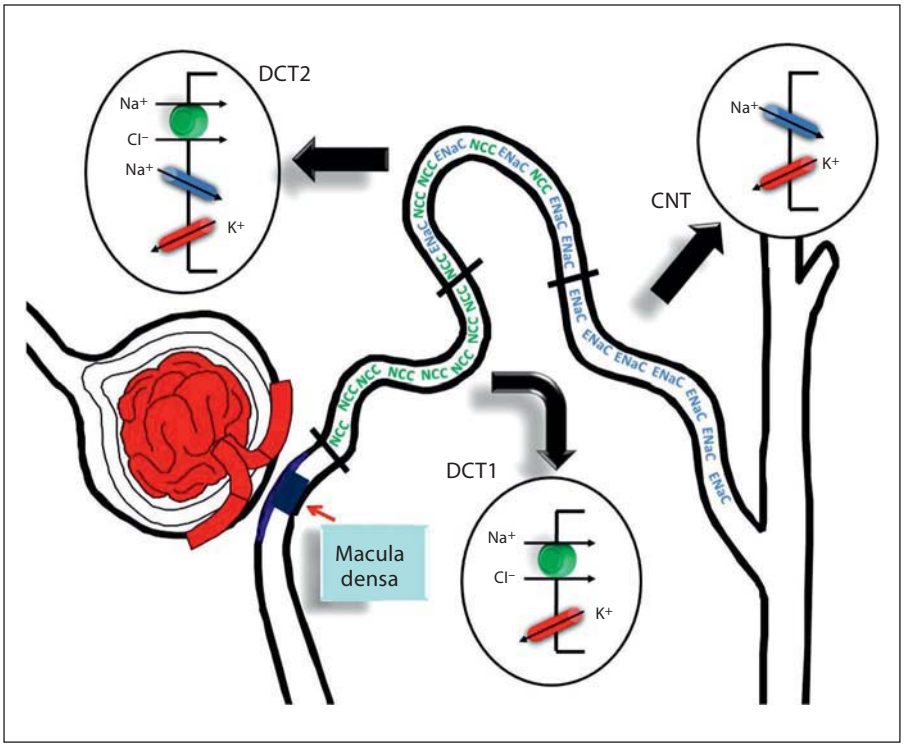

Fig. 2. Salt and potassium transport systems in the DCT and CNT. The DCT begins few cells after the macula densa; it is divided into 2 portions, the DCT1 in which the salt reabsorption pathway is the NCC and the DCT2 in which salt reabsorption takes place through both, the NCC and ENaC. Then, the ENaC is the major salt reabsorption pathway in the CNT and downstream in the CD. In all these segments, the ROMK is the major potassium-secretory pathway. As discussed in the text, L-WNK1, S-WNK1 and WNK4 are heavily expressed in these nephron segments.

most of the functional properties of the NCC have been analyzed [41]. Two independent groups obtained comparable results simultaneously [42, 43]. When coexpressed in oocytes, WNK4 reduces the activity of NCC by decreasing the amount of the cotransporter present on the cell surface. This negative effect upon the NCC was dependent on the WNK4 kinase activity and was also eliminated by introducing the PHAII mutation Q562E (mouse sequence; table 2). These observations were later corroborated by other groups using culture cells as expression systems [19, 44, 45] and, also, added the evidence that decreased expression of NCC on the cell surface is not associated with increased dynamin-induced vesicle internalization but is rather due to increased lysosomal degradation of NCC protein.

PHAII is associated with hyperkalemia and potassium excretion in the nephron that predominantly occurs in the aldosterone-sensitive distal nephron. Thus, another obvious target for WNK4 regulation was the renal outer medullary potassium channel (ROMK) that is the major renal potassium-secretory pathway in the apical membrane of the distal nephron (fig. 2). Similar to NCC, WNK4 is a negative regulator of the ROMK [46]. However, there are important differences between WNK4 effects upon the NCC than upon the ROMK (table 2). First, WNK4 catalytic activity is not required for ROMK inhibition. Second, the mechanism is due to a WNK4-induced increased internalization of the ROMK via clathrin-coated pits. These observations performed originally in *Xenopus* oocytes have been confirmed in mammalian cells [47], in which it has been observed that WNK4 interacts with a protein known as intersectin that is in-

Table 2. Modulation of renal ion transport systems by WNKs

	WNK4	PHAII WNK4	S1169D WNK4	WNK1
NCC	↓	↑	↓	–
ROMK	↓	↓↓	↑	↓
ENaC	↓	↑	↑	↑
Claudin 4	↑	↑↑	n.d.	↑
KCCs	↓	↓	n.d.	n.d.

ROMK = Renal outer medullary potassium channel; ENaC = epithelial Na channel; KCC = K-Cl cotransporter; n.d. = not determined.

volved in the clathrin-induced endocytosis. Additionally, treatment of HEK-293 cells with siRNA against WNK1 and WNK4 resulted in increased activity of the ROMK, indicating that, indeed, basal activity of the channel is modulated by both kinases [48]. Third, while for the NCC PHAII type mutations in WNK4 prevented the dominant negative effect, for ROMK they resulted in increased inhibition. This observation can explain the hyperkalemia in PHAII patients since inhibition of the ROMK is increased by mutant WNK4.

A third candidate target for WNK4 is the apical epithelial sodium channel (ENaC) that in the distal nephron is an important pathway for sodium reabsorption (fig. 2). In addition, activity of the ENaC is required for ROMK potassium excretion since the luminal negative potential that is generated by sodium translocation is required for potassium to be secreted. Ring et al. [49] demonstrated that WNK4 reduces the activity of the ENaC. This effect does not require WNK4 catalytic activity and is lost by elimination of the PPXY motif of the ENaC β- or γ-subunit, indicating that, similar to ROMK, it is due to clathrin-mediated endocytosis. Interestingly, PHAII type mutations in WNK4 prevent the inhibitory effect of WNK4 upon the ENaC (table 2).

The fourth identified targets for WNK4 are the proteins mediating parecellular Cl^- flux in the distal nephron known as claudins. Two independent groups [50, 51] observed simultaneously in MDCKII cells that WNK4 increases the paracellular transport of Cl^- but not that of Na^+. This effect requires WNK4 catalytic activity and is associated with phosphorylation of claudin 4 in its carboxyl-terminal domain. In addition, PHAII-type mutations in WNK4 are associated with a further increase in Cl^- permeability and phosphorylation of claudin 4 (table 2). Finally, WNK4 also inhibits the activity of the K-Cl cotransporters KCC1, KCC3 and KCC4 [52], which in the distal nephron are critical for potassium secretion in the DCT [53] and acid secretion in the CD [54]. KCC4 knockout mice feature metabolic acidosis. The WNK4 inhibitory effect is kinase dependent but was not affected by PHAII-type mutations (table 2).

Effects of WNK1 upon Distal Nephron Transport Systems

The effect of WNK1 upon distal transport systems is probably more complex than WNK4 since it has been demonstrated that WNK1 is a regulator of other WNKs by phosphorylation processes [55] or by WNK-to-WNK interactions at the protein level [21, 22]. For instance, Yang et al. [43] observed that WNK1 has no direct effect upon the NCC, but prevents the WNK4-induced inhibition of the NCC. That is, when the NCC and WNK4 were coexpressed together in *X. laevis* oocytes, WNK4 induced inhibition of NCC activity. However, when WNK1 was added to the coexpression cocktail, the WNK4 inhibitory effect of the NCC was lost. Later on, Subramanya et al. [56] analyzed the effect of the L-WNK1 and S-WNK1 variants of WNK1 upon the NCC and its WNK4 regulation. Their observations are very important to understand the mechanism by which increased expression of a normal L-WNK1 in PHAII patients produces increased activity of the NCC. These authors demonstrated that while L-WNK1 prevented the WNK4-induced inhibition of the NCC, S-WNK1 by interacting with L-WNK1 in a dominant negative fashion eliminated the L-WNK1-induced inhibition of WNK4. As was discussed above, while L-WNK1 is present in several epithelial cells and along the entire nephron, S-WNK1 is mainly expressed in the DCT and CNT [34, 38]. Thus, it is proposed that in normal subjects the ratio of S-WNK1/L-WNK1 expression in the DCT and CNT is in favor of S-WNK1, and thus, the shorter isoform by highjacking L-WNK1 prevents its inhibitory effect upon WNK4, allowing WNK4 to keep the NCC inhibited. In PHAII patients due to intronic deletions of the *PRKWNK1* gene that increases expression of L-WNK1, the ratio S-WNK1/L-WNK1 is reduced. As a consequence, L-WNK1 is able to inhibit WNK4 and thus, NCC activity is increased, augmenting salt reabsorption in the DCT and thus arterial pressure. Similarly, it has been demonstrated that S-WNK1 and L-WNK1 interact with each other regulating ROMK activity. Lazrak et al. [48] observed in HEK cells transfected with ROMK that L-WNK1 decreased the activity of the channel. This effect of L-WNK1 requires the L-WNK1 catalytic activity and can be prevented by coexpression of S-WNK1. In the same study it was observed that exposing rats to a K^+-deficient diet was associated with increased expression of L-WNK1 and decreased expression of S-WNK1, consistent with a situation in which ROMK activity is decreased since K^+ secretion is maximally reduced. Consistent with these findings, O'Reilly et al. [34] also observed that the ratio S-WNK1/L-WNK1 and the expression of WNK4 at the mRNA level are modulated by low- and high-potassium diets.

WNK1 is also a modulator of ENaC activity. In a very interesting study, Xu et al. [57] demonstrated that ENaC can be regulated by WNK1, via another kinase known as serum glucocorticoid kinase (SGK). WNK1 induces a phosphorylation of SGK which in turn phosphorylates and inhibits a protein named Need4 that is known to re-

duce ENaC activity by promoting its endocytosis via a clathrin-dependent mechanism. Therefore, ENaC activity is enhanced. Interestingly, SGK is known to be a key kinase through which aldosterone achieves its effects upon distal nephron transport mechanisms. Finally, similar to WNK4, WNK1 also increases paracellular Cl^- fluxes, an effect that was associated with increased phosphorylation of claudin 4 (table 2).

WNKs Lie Upstream of Kinases Involved in the Regulation of Ion Transporters

Biochemical and functional analysis revealed that WNK kinases and the cation-coupled chloride cotransporter (SLC12 family) interact with each other and with another family of serine/threonine kinases known as SPAK and OSR1 that belong to the STE-20 family. On the one hand, Piechota et al. [28, 58] observed that some members of the SLC12 family, such as the K^+-Cl^- cotransporter KCC3 and the basolateral isoform of the Na^+:K^+:$2Cl^-$ cotransporter, NKCC1, interact with SPAK in a 2-hybrid yeast system. They observed that these interactions occurred through an 'SPAK-binding domain' [RFx(V/I)] present in the cotransporter sequence. Simultaneously, it was demonstrated by Dowd and Forbush [59] that modulation of NKCC1 activity by intracellular chloride concentration involved the activity of this kinase. On the other hand, Vitari et al. [29] observed that immunoprecipitation of WNK1 or WNK4 brought SPAK as an interacting protein. In this study they observed in an in vitro phosphorylation assay using the amino-terminal domain of NKCC1 that the presence of WNK1, WNK4, SPAK or OSR1 alone was not enough to achieve NKCC1 phosphorylation. Only when WNK1 or WNK4 was added together with SPAK or OSR1, did NKCC1 become phosphorylated. This effect disappeared when catalytically inactive kinases were used. The conclusion of the study was that WNK1 or WNK4 is able to induce phosphorylation of NKCC1 only when SPAK or OSR1 is present. Similar observations were obtained by Moriguchi et al. [31] for NKCC1, and also for the apical isoform of the Na^+:K^+:$2Cl^-$ cotransporter, NKCC2, and for the NCC. These observations are supported by the observations of Gagnon et al. [7] at the functional level. These authors observed in *X. laevis* oocytes that injecting WNK4 cRNA had no effect upon the NKCC1 cotransporter, unless SPAK cRNA was added to the injecting cocktail. They observed that injecting cRNA of both kinases resulted in a significant activation of NKCC1. Interestingly, this interaction does not seem to be required for WNK4-induced inhibition of the K^+-Cl^- cotransporters [52]. Finally, detailed definitions of the interacting domains between WNK4 and SPAK were informed [30, 60]. Thus, it is currently believed that at least for some cotransporters, WNK1 or WNK4 lie upstream of SPAK/OSR1 kinases.

In vivo Mouse Models of PHAII

All the above observations regarding modulation of renal ion transport systems by WNKs were done in heterologous expression systems of either amphibian or mammalian origin. Thus, it was necessary to demonstrate that the proposed mechanisms by which PAHII-type mutations in WNKs produce the disease actually occur in an in vivo model. Regarding WNK1 the only study in which genetic manipulation of WNK1 has been performed is in the WNK1 knockout mice produced by Zambrowicz et al. [61]. Mice homozygous for WNK1 deletion died before day 13 of gestation, indicating that WNK1 is an important protein for embryogenesis. However, WNK1 heterozygous mice survived to adulthood and displayed a significant reduction in arterial blood pressure, indicating that WNK1 plays a key role in maintaining normal blood pressure.

Two groups have produced transgenic mice overexpressing WNK4 containing a PHAII-type mutation. First, Lalioti et al. [62] generated bacterial artificial chromosome transgenic mice overexpressing either wild-type *WNK4* or a *WNK4* gene containing one of the PHAII-type mutations (Q562E). Interesting observations were done in this study: when compared with control mice, PHAII-WNK4 transgenic mice were hypertensive, whereas wild-type WNK4 transgenic mice were hypotensive. When exposed to a low-K^+ diet, PHAII-WNK4 transgenic mice were hyperkalemic (approx. 5.3 mM) and when exposed to a high-K^+ diet, these animals developed a dramatic increase in serum K^+ to values over 8.0 mM. In contrast, wild-type WNK4 transgenic mice were hypokalemic (approx. 3.7 mM). Furthermore, PHAII-WNK4 transgenic mice exhibited metabolic acidosis and were hypercalciuric. Within the histological analysis, the observations were more impressive: wild-type WNK4 transgenic mice exhibited a significant reduction in the number and size of DCTs. In contrast, PHAII-WNK4 transgenic mice exhibited a remarkable increase in the number and size of distal tubules, that is DCT hypertrophy and hyperplasia. Therefore, overexpression of PHAII-WNK4 recapitulated the PHAII phenotype, and interestingly, overexpression of wild-type WNK4 recapitulated a phenotype that is similar to Gitelman disease, in which NCC activity is absent. Finally, to find out to what extent the

effects of WNK4 were due to modulation of NCC activity, the PHAII-WNK4 transgenic mice were crossed with NCC knockout mice. The PHAII phenotype disappeared in the new colony. Renal histology was normal, with no changes in the DCT when compared with normal controls. Arterial blood pressure and all other parameters were corrected. Even the hyperkalemia during the high-K^+ diet was prevented, implicating NCC as a key protein, not only for the development of hypertension, but also for hyperkalemia. In the same study, treating PHAII-WNK4 transgenic mice with thiazides also corrected the phenotype. A second transgenic model that has been formed is a knockin of a PHAII mutation (D561A) that was introduced into the endogenous WNK4 locus [63]. In this study it was also observed that knockin mice reproduced the phenotype of the disease with hypertension, hyperkalemia and metabolic acidosis. At the molecular level it was shown that NCC, ENaC and BK K^+ channel expression was increased, with no change in WNK4 and the ROMK. Increased phosphorylation of SPAK/OSR1 was observed in the knockin mice supporting the hypothesis that WNK4 affects the activity of NCC by interacting with, and/or phosphorylation of, STE-20 kinases. In addition, it was also observed that PHAII-WNK4 induced phosphorylation of the NCC at serine 71 where it was previously shown that its phosphorylation was associated with the activity of the NCC [64]. These studies strongly suggest that, as predicted in the heterologous expression systems, wild-type WNK4 is a potent inhibitor of NCC, and PHAII-type mutations eliminate this WNK4 property releasing the NCC from a tonic inhibition by this kinase. However, the consequences of transgenic wild-type WNK4 or PHAII-type WNK4 upon transport systems such as the ROMK, ENaC or paracelin were not reported in detail, and thus, the WNK4 in vitro effects upon this transport system still need to be confirmed in vivo.

Implications of WNK4 for Renal Physiology

The effects of WNK4 upon renal transport systems shown in table 2 reveal that WNK4 exists in at least 3 different states of function. One is the wild-type WNK4 that inhibits NCC, ROMK and ENaC, with slight stimulation of paracellular Cl^- flux. One can think of this as an equilibrium state. A second clearly identified state is the one resulting from PHAII mutations. In this state, WNK4 no longer inhibits the NCC and ENaC resulting in increased activity of these pathways, and increased inhibition of the ROMK. Simultaneously, paracellular Cl^- flux is also enhanced. A third state involves the effect of WNK4 phosphorylation by SGK kinase. WNK4 contains a canonical SGK phosphorylation site at serine 1169. Ring et al. [65] first showed that WNK4 is phosphorylated at this site by SGK. Then they observed that mutation of S1169 for alanine, which eliminates the possibility that WNK4 becomes phosphorylated at this site, had no effect upon WNK4-induced inhibition of the ROMK or ENaC. In contrast, mutation of serine 1169 for aspartic acid (S1169D) that mimics the phosphorylation state of this serine resulted in a WNK4 kinase that lost the inhibitory effect upon the ENaC or ROMK, resulting in increased activity of these channels [65]. However, this mutation S1169D has no effect upon the WNK4-induced inhibition of the NCC [Gamba G., unpubl. observations]. The differential functional properties of WNK4 revealed by these different states, together with observations in PHAII patients and transgenic mice, place WNK4 as the potential kinase and the key molecular switch that explains how the kidney handles the effect of aldosterone as a salt-retaining and K^+-losing hormone. In physiological conditions, losing fluid volume increases aldosterone levels, which in turn activates salt-retaining mechanisms, without affecting the normal urinary potassium excretion. This is achieved by activating the NCC, ENaC and paracellular Cl^- flux, without changing or even reducing the ROMK. As discussed above, WNK4 harboring a PHAII-type mutation mimics this situation. In contrast, another stimulus for aldosterone secretion is hyperkalemia. In this situation, aldosterone release is associated with increased K^+ excretion, without affecting salt retention. This is achieved by increasing ENaC and ROMK activity, without affecting the NCC. Thus, salt reabsorption is not increased in the DCT1 allowing enough sodium to be delivered to the DCT2 and CNT, in which the increased activity of the ENaC and ROMK promotes potassium secretion into the lumen (fig. 2).

Future Research for WNKs, Renal Ion Transport and Human Hypertension

Observations from PHAII patients, transgenic animals and in vitro transfection models together strongly suggest that WNKs and several ion transport systems in the kidney work together to maintain salt and potassium homeostasis and, as a consequence, arterial blood pressure homeostasis. Alterations in the activity of WNKs and/or transport systems are clearly associated with human diseases featuring arterial hypertension or hypotension [2]. One important area that is currently being stud-

ied is defining the role that WNKs can have upon the most common forms of hypertension, particularly since a considerable proportion of patients with essential hypertension exhibit low plasma renin activity, suggesting that increased blood pressure in these patients is due to salt retention. In this regard, the *WNK4* gene in chromosome 17 is just 1 Mb from the locus *D17S1299* that has shown the strongest linkage with hypertension in the Framingham Heart Study population [66], and recent studies suggest the association of SNPs or variants of *PRKWNK1* or *PRKWNK4* with arterial hypertension [67, 68]. It is equally important to define drug development against WNK kinases. The facts that mice heterozygous for WNK1 deletion exhibit a significantly lower blood pressure than normal mice and that PHAII-WNK4 transgenic or knockin mice are hypertensive suggest that drugs affecting the functional properties of WNK1 or WNK4 could play a potential role in the treatment of arterial hypertension.

Acknowledgments

The work performed in our laboratory has been possible thanks to the support from the Consejo Nacional de Ciencia y Tecnología (CONACYT No. 59992) and National Institutes of Health grants DK-064635 to G.G.

References

1 Guyton AC: Blood pressure control – special role of the kidneys and body fluids. Science 1991;252:1813–1816.
2 Lifton RP, Gharavi AG, Geller DS: Molecular mechanisms of human hypertension. Cell 2001;104:545–556.
3 Simon DB, Nelson-Williams C, Johnson-Bia M, Ellison D, Karet FE, Morey-Molina A, Vaara I, Iwata F, Cushner HM, Koolen M, Gainza FJ, Gitelman HJ, Lifton RP: Gitelman's variant of Bartter's syndrome, inherited hypokalaemic alkalosis, is caused by mutations in the thiazide-sensitive Na-Cl cotransporter. Nat Genet 1996;12:24–30.
4 Lemmink HH, van den Heuvel LP, van Dijk HA, Merkx GF, Smilde TJ, Taschner PE, Monnens LA, Hebert SC, Knoers NV: Linkage of Gitelman syndrome to the thiazide-sensitive sodium-chloride cotransporter gene with identification of mutations in Dutch families. Pediatr Nephrol 1996;10:403–407.
5 Mastroianni N, Bettinelli A, Bianchetti M, Colussi G, de Fusco M, Sereni F, Ballabio A, Casari G: Novel molecular variants of the Na-Cl cotransporter gene are responsible for Gitelman syndrome. Am J Hum Genet 1996;59:1019–1026.
6 Kunchaparty S, Palcso M, Berkman J, Zquez H, Desir GV, Bernstein P, Reilly RF, Ellison DH: Defective processing and expression of thiazide-sensitive Na-Cl cotransporter as a cause of Gitelman's syndrome. Am J Physiol 1999;277:F643–F649.
7 De Jong JC, Van der Vliet WA, van den Heuvel LP, Willems PH, Knoers NV, Bindels RJ: Functional expression of mutations in the human NaCl cotransporter: evidence for impaired routing mechanisms in Gitelman's syndrome. J Am Soc Nephrol 2002;13:1442–1448.
8 Sabath E, Meade P, Berkman J, de los Heros P, Moreno E, Bobadilla NA, Vazquez N, Ellison DH, Gamba G: Pathophysiology of functional mutations of the thiazide-sensitive Na-Cl cotransporter in Gitelman disease. Am J Physiol Renal Physiol 2004;287:F195–F203.
9 Mayan H, Vered I, Mouallem M, Tzadok-Witkon M, Pauzner R, Farfel Z: Pseudohypoaldosteronism type II: marked sensitivity to thiazides, hypercalciuria, normomagnesemia, and low bone mineral density. J Clin Endocrinol Metab 2002;87:3248–3254.
10 Simon DB, Farfel Z, Ellison D, Bia M, Tucci J, Lifton RP: Examination of the thiazide-sensitive Na-Cl cotransporter as a candidate gene in Gordon's syndrome. 1995, p 632.
11 Mansfield TA, Simon DB, Farfel Z, Bia M, Tucci JR, Lebel M, Gutkin M, Vialettes B, Christofilis MA, Kauppinen-Makelin R, Mayan H, Risch N, Lifton RP: Multilocus linkage of familial hyperkalaemia and hypertension, pseudohypoaldosteronism type II, to chromosomes 1q31–42 and 17p11–q21. Nat Genet 1997;16:202–205.
12 Disse-Nicodeme S, Achard JM, Desitter I, Houot AM, Fournier A, Corvol P, Jeunemaitre X: A new locus on chromosome 12p13.3 for pseudohypoaldosteronism type II, an autosomal dominant form of hypertension. Am J Hum Genet 2000;67:302–310.
13 Disse-Nicodeme S, Desitter I, Fiquet-Kempf B, Houot AM, Stern N, Delahousse M, Potier J, Ader JL, Jeunemaitre X: Genetic heterogeneity of familial hyperkalaemic hypertension. J Hypertens 2001;19:1957–1964.
14 Xu B, English JM, Wilsbacher JL, Stippec S, Goldsmith EJ, Cobb MH: WNK1, a novel mammalian serine/threonine protein kinase lacking the catalytic lysine in subdomain II. J Biol Chem 2000;275:16795–16801.
15 Wilson FH, Disse-Nicodeme S, Choate KA, Ishikawa K, Nelson-Williams C, Desitter I, Gunel M, Milford DV, Lipkin GW, Achard JM, Feely MP, Dussol B, Berland Y, Unwin RJ, Mayan H, Simon DB, Farfel Z, Jeunemaitre X, Lifton RP: Human hypertension caused by mutations in WNK kinases. Science 2001;293:1107–1112.
16 Delaloy C, Lu J, Houot AM, Disse-Nicodeme S, Gasc JM, Corvol P, Jeunemaitre X: Multiple promoters in the WNK1 gene: one controls expression of a kidney-specific kinase-defective isoform. Mol Cell Biol 2003;23:9208–9221.
17 Golbang AP, Murthy M, Hamad A, Liu CH, Cope G, Hoff WV, Cuthbert A, O'Shaughnessy KM: A new kindred with pseudohypoaldosteronism type II and a novel mutation (564D→H) in the acidic motif of the *WNK4* gene. Hypertension 2005;46:295–300.
18 Min X, Lee BH, Cobb MH, Goldsmith EJ: Crystal structure of the kinase domain of WNK1, a kinase that causes a hereditary form of hypertension. Structure (Camb) 2004;12:1303–1311.
19 Yang CL, Ellison DH: WNK1 interacts physically with WNK4. J Am Soc Nephrol 2003;14:77A.
20 Yang CL, Zhu X, Wang Z, Subramanya AR, Ellison DH: Mechanisms of WNK1 and WNK4 interaction in the regulation of thiazide-sensitive NaCl cotransport. J Clin Invest 2005;115:1379–1387.
21 Yang CL, Zhu X, Ellison DH: The thiazide-sensitive Na-Cl cotransporter is regulated by a WNK kinase signaling complex. J Clin Invest 2007;117:3403–3411.
22 Xu BE, Min X, Stippec S, Lee BH, Goldsmith EJ, Cobb MH: Regulation of WNK1 by an autoinhibitory domain and autophosphorylation. J Biol Chem 2002;277:48456–48462.

23 Xu BE, Stippec S, Lenertz L, Lee BH, Zhang W, Lee YK, Cobb MH: WNK1 activates ERK5 by an MEKK2/3-dependent mechanism. J Biol Chem 2004;279:7826–7831.
24 Moniz S, Verissimo F, Matos P, Brazao R, Silva E, Kotevelets L, Chastre E, Gespach C, Jordan P: Protein kinase WNK2 inhibits cell proliferation by negatively modulating the activation of MEK1/ERK1/2. Oncogene 2007;26:6071–6081.
25 Lee BH, Chen W, Stippec S, Cobb MH: Biological cross-talk between WNK1 and the transforming growth factor beta-Smad signaling pathway. J Biol Chem 2007;282:17985–17996.
26 Lee BH, Min X, Heise CJ, Xu BE, Chen S, Shu H, Luby-Phelps K, Goldsmith EJ, Cobb MH: WNK1 phosphorylates synaptotagmin 2 and modulates its membrane binding. Mol Cell 2004;15:741–751.
27 Piechotta K, Lu J, Delpire E: Cation chloride cotransporters interact with the stress-related kinases Ste20-related proline-alanine-rich kinase (SPAK) and oxidative stress response 1 (OSR1). J Biol Chem 2002;277:50812–50819.
28 Gagnon KB, England R, Delpire E: Volume sensitivity of cation-Cl^- cotransporters is modulated by the interaction of two kinases: Ste20-related proline-alanine-rich kinase and WNK4. Am J Physiol Cell Physiol 2006;290:C134–C142.
29 Vitari AC, Deak M, Morrice NA, Alessi DR: The WNK1 and WNK4 protein kinases that are mutated in Gordon's hypertension syndrome, phosphorylate and active SPAK and OSR1 protein kinases. Biochem J 2005;391:17–24.
30 Vitari AC, Thastrup J, Rafiqi FH, Deak M, Morrice NA, Karlsson HK, Alessi DR: Functional interactions of the SPAK/OSR1 kinases with their upstream activator WNK1 and downstream substrate NKCC1. Biochem J 2006;397:223–231.
31 Moriguchi T, Urushiyama S, Hisamoto N, Iemura S, Uchida S, Natsume T, Matsumoto K, Shibuya H: WNK1 regulates phosphorylation of cation-chloride-coupled cotransporters via the STE20-related kinases, SPAK and OSR1. J Biol Chem 2005;280:42685–42693.
32 Choate KA, Kahle KT, Wilson FH, Nelson-Williams C, Lifton RP: WNK1, a kinase mutated in inherited hypertension with hyperkalemia, localizes to diverse Cl^--transporting epithelia. Proc Natl Acad Sci USA 2003;100:663–668.
33 Verissimo F, Jordan P: WNK kinases, a novel protein kinase subfamily in multi-cellular organisms. Oncogene 2001;20:5562–5569.
34 O'Reilly M, Marshall E, Macgillivray T, Mittal M, Xue W, Kenyon CJ, Brown RW: Dietary electrolyte-driven responses in the renal WNK kinase pathway in vivo. J Am Soc Nephrol 2006;17:2402–2413.
35 Holden S, Cox J, Raymond FL: Cloning, genomic organization, alternative splicing and expression analysis of the human gene WNK3 (PRKWNK3). Gene 2004;335:109–119.
36 Kahle KT, Rinehart J, de los Heros P, Louvi A, Meade P, Vazquez N, Hebert SC, Gamba G, Gimenez I, Lifton RP: WNK3 modulates transport of Cl^- in and out of cells: implications for control of cell volume and neuronal excitability. Proc Natl Acad Sci USA 2005;102:16783–16788.
37 Kahle KT, Gimenez I, Hassan H, Wilson FH, Wong RD, Forbush B, Aronson PS, Lifton RP: WNK4 regulates apical and basolateral Cl^- flux in extrarenal epithelia. Proc Natl Acad Sci USA 2004;101:2064–2069.
38 O'Reilly M, Marshall E, Speirs HJ, Brown RW: WNK1, a gene within a novel blood pressure control pathway, tissue-specifically generates radically different isoforms with and without a kinase domain. J Am Soc Nephrol 2003;14:2447–2456.
39 Gamba G, Saltzberg SN, Lombardi M, Miyanoshita A, Lytton J, Hediger MA, Brenner BM, Hebert SC: Primary structure and functional expression of a cDNA encoding the thiazide-sensitive, electroneutral sodium-chloride cotransporter. Proc Natl Acad Sci USA 1993;90:2749–2753.
40 Brown DD: A tribute to the *Xenopus laevis* oocyte and egg. J Biol Chem 2004;279:45291–45299.
41 Gamba G: Molecular physiology and pathophysiology of the electroneutral cation-chloride cotransporters. Physiol Rev 2005;85:423–493.
42 Wilson FH, Kahle KT, Sabath E, Lalioti MD, Rapson AK, Hoover RS, Hebert SC, Gamba G, Lifton RP: Molecular pathogenesis of inherited hypertension with hyperkalemia: the Na-Cl cotransporter is inhibited by wild-type but not mutant WNK4. Proc Natl Acad Sci USA 2003;100:680–684.
43 Yang CL, Angell J, Mitchell R, Ellison DH: WNK kinases regulate thiazide-sensitive Na-Cl cotransport. J Clin Invest 2003;111:1039–1045.
44 Golbang AP, Cope G, Hamad A, Murthy M, Liu CH, Cuthbert AW, O'Shaughnessy KM: Regulation of the expression of the Na/Cl cotransporter (NCCT) by WNK4 and WNK1: evidence that accelerated dynamin-dependent endocytosis is not involved. Am J Physiol Renal Physiol 2006;291:F1369–F1376.
45 Cai H, Cebotaru V, Wang YH, Zhang XM, Cebotaru L, Guggino SE, Guggino WB: WNK4 kinase regulates surface expression of the human sodium chloride cotransporter in mammalian cells. Kidney Int 2006;69:2162–2170.
46 Kahle KT, Wilson FH, Lifton RP: Regulation of diverse ion transport pathways by WNK4 kinase: a novel molecular switch. Trends Endocrinol Metab 2005;16:98–103.
47 He G, Wang HR, Huang SK, Huang CL: Intersectin links WNK kinases to endocytosis of ROMK1. J Clin Invest 2007;117:1078–1087.
48 Lazrak A, Liu Z, Huang CL: Antagonistic regulation of ROMK by long and kidney-specific WNK1 isoforms. Proc Natl Acad Sci USA 2006;103:1615–1620.
49 Ring AM, Cheng SX, Leng Q, Kahle KT, Rinehart J, Lalioti MD, Volkman HM, Wilson FH, Hebert SC, Lifton RP: WNK4 regulates activity of the epithelial Na^+ channel in vitro and in vivo. Proc Natl Acad Sci USA 2007;104:4020–4024.
50 Yamauchi K, Rai T, Kobayashi K, Sohara E, Suzuki T, Itoh T, Suda S, Hayama A, Sasaki S, Uchida S: Disease-causing mutant WNK4 increases paracellular chloride permeability and phosphorylates claudins. Proc Natl Acad Sci USA 2004;101:4690–4694.
51 Kahle KT, MacGregor GG, Wilson FH, Van Hoek AN, Brown D, Ardito T, Kashgarian M, Giebisch G, Hebert SC, Boulpaep EL, Lifton RP: Paracellular Cl^- permeability is regulated by WNK4 kinase: insight into normal physiology and hypertension. Proc Natl Acad Sci USA 2004;101:14877–14882.
52 Garzon-Muvdi T, Pacheco-Alvarez D, Gagnon KB, Vazquez N, Ponce-Coria J, Moreno E, Delpire E, Gamba G: WNK4 kinase is a negative regulator of K^+-Cl^- cotransporters. Am J Physiol Renal Physiol 2007;292:F1197–F1207.
53 Amorim JB, Bailey MA, Musa-Aziz R, Giebisch G, Malnic G: Role of luminal anion and pH in distal tubule potassium secretion. Am J Physiol Renal Physiol 2003;284:F381–F388.
54 Boettger T, Hubner CA, Maier H, Rust MB, Beck FX, Jentsch TJ: Deafness and renal tubular acidosis in mice lacking the K-Cl co-transporter KCC4. Nature 2002;416:874–878.
55 Lenertz LY, Lee BH, Min X, Xu BE, Wedin K, Earnest S, Goldsmith EJ, Cobb MH: Properties of WNK1 and implications for other family members. J Biol Chem 2005;280:26653–26658.
56 Subramanya AR, Yang CL, Zhu X, Ellison DH: Dominant-negative regulation of WNK1 by its kidney-specific kinase-defective isoform. Am J Physiol Renal Physiol 2006;290:F619–F624.
57 Xu BE, Stippec S, Chu PY, Lazrak A, Li XJ, Lee BH, English JM, Ortega B, Huang CL, Cobb MH: WNK1 activates SGK1 to regulate the epithelial sodium channel. Proc Natl Acad Sci USA 2005;102:10315–10320.
58 Piechotta K, Garbarini N, England R, Delpire E: Characterization of the interaction of the stress kinase SPAK with the Na^+-K^+-$2Cl^-$ cotransporter in the nervous system: evidence for a scaffolding role of the kinase. J Biol Chem 2003;278:52848–52856.

59 Dowd BF, Forbush B: PASK (proline-alanine-rich STE20-related kinase), a regulatory kinase of the Na-K-Cl cotransporter (NKCC1). J Biol Chem 2003;278:27347–27353.
60 Villa F, Goebel J, Rafiqi FH, Deak M, Thastrup J, Alessi DR, van Aalten DM: Structural insights into the recognition of substrates and activators by the OSR1 kinase. EMBO Rep 2007;8:839–845.
61 Zambrowicz BP, Abuin A, Ramirez-Solis R, Richter LJ, Piggott J, Beltrandel Rio H, Buxton EC, Edwards J, Finch RA, Friddle CJ, Gupta A, Hansen G, Hu Y, Huang W, Jaing C, Key BW Jr, Kipp P, Kohlhauff B, Ma ZQ, Markesich D, Payne R, Potter DG, Qian N, Shaw J, Schrick J, Shi ZZ, Sparks MJ, Van Sligtenhorst I, Vogel P, Walke W, Xu N, Zhu Q, Person C, Sands AT: Wnk1 kinase deficiency lowers blood pressure in mice: a gene-trap screen to identify potential targets for therapeutic intervention. Proc Natl Acad Sci USA 2003;100:14109–14114.
62 Lalioti MD, Zhang J, Volkman HM, Kahle KT, Hoffmann KE, Toka HR, Nelson-Williams C, Ellison DH, Flavell R, Booth CJ, Lu Y, Geller DS, Lifton RP: Wnk4 controls blood pressure and potassium homeostasis via regulation of mass and activity of the distal convoluted tubule. Nat Genet 2006;38:1124–1132.
63 Yang SS, Morimoto T, Rai T, Chiga M, Sohara E, Ohno M, Uchida K, Lin SH, Moriguchi T, Shibuya H, Kondo Y, Sasaki S, Uchida S: Molecular pathogenesis of pseudohypoaldosteronism type II: generation and analysis of a Wnk4(D561A/+) knockin mouse model. Cell Metab 2007;5:331–344.
64 Pacheco-Alvarez D, San Cristobal P, Meade P, Moreno E, Vazquez N, Munoz E, Diaz A, Juarez ME, Gimenez I, Gamba G: The Na-Cl cotransporter is activated and phosphorylated at the amino terminal domain upon intracellular chloride depletion. J Biol Chem 2006;281:28755–28763.
65 Ring AM, Leng Q, Rinehart J, Wilson FH, Kahle KT, Hebert SC, Lifton RP: An SGK1 site in WNK4 regulates Na^+ channel and K^+ channel activity and has implications for aldosterone signaling and K^+ homeostasis. Proc Natl Acad Sci USA 2007;104:4025–4029.
66 Levy D, De Stefano AL, Larson MG, O'Donnell CJ, Lifton RP, Gavras H, Cupples LA, Myers RH: Evidence for a gene influencing blood pressure on chromosome 17: genome scan linkage results for longitudinal blood pressure phenotypes in subjects from the Framingham Heart Study. Hypertension 2000;36:477–483.
67 Newhouse SJ, Wallace C, Dobson R, Mein C, Pembroke J, Farrall M, Clayton D, Brown M, Samani N, Dominiczak A, Connell JM, Webster J, Lathrop GM, Caulfield M, Munroe PB: Haplotypes of the WNK1 gene associate with blood pressure variation in a severely hypertensive population from the British Genetics of Hypertension Study. Hum Mol Genet 2005;14:1805–1814.
68 Tobin MD, Raleigh SM, Newhouse S, Braund P, Bodycote C, Ogleby J, Cross D, Gracey J, Hayes S, Smith T, Ridge C, Caulfield M, Sheehan NA, Munroe PB, Burton PR, Samani NJ: Association of WNK1 gene polymorphisms and haplotypes with ambulatory blood pressure in the general population. Circulation 2005;112:3423–3429.

REFERENCIAS

(1) Guyton AC. Textbook of medical physiology.

(2) Boron WF, Boulpaep EL. Medical physiologya cellular and molecular approach. 2009;2nd ed.

(3) Thrasher TN. Arterial baroreceptor input contributes to long-term control of blood pressure. Curr Hypertens Rep 2006 June;8(3):249-54.

(4) Woodard GE, Rosado JA. Natriuretic peptides in vascular physiology and pathology. Int Rev Cell Mol Biol 2008;268:59-93.

(5) de Sa DD, Chen HH. The role of natriuretic peptides in heart failure. Curr Cardiol Rep 2008 May;10(3):182-9.

(6) Tom B, Dendorfer A, Danser AH. Bradykinin, angiotensin-(1-7), and ACE inhibitors: how do they interact? Int J Biochem Cell Biol 2003 June;35(6):792-801.

(7) Tom B, Dendorfer A, de VR, Saxena PR, Jan Danser AH. Bradykinin potentiation by ACE inhibitors: a matter of metabolism. Br J Pharmacol 2002 September;137(2):276-84.

(8) Gkaliagkousi E, Douma S, Zamboulis C, Ferro A. Nitric oxide dysfunction in vascular endothelium and platelets: role in essential hypertension. J Hypertens 2009 December;27(12):2310-20.

(9) Bian K, Murad F. Nitric oxide (NO)--biogeneration, regulation, and relevance to human diseases. Front Biosci 2003 January 1;8:d264-d278.

(10) Bian K, Doursout MF, Murad F. Vascular system: role of nitric oxide in cardiovascular diseases. J Clin Hypertens (Greenwich) 2008 April;10(4):304-10.

(11) Barton M, Yanagisawa M. Endothelin: 20 years from discovery to therapy. Can J Physiol Pharmacol 2008 August;86(8):485-98.

(12) Barton M, Mullins JJ, Bailey MA, Kretzler M. Role of endothelin receptors for renal protection and survival in hypertension: waiting for clinical trials. Hypertension 2006 November;48(5):834-7.

(13) Peart WS. C. The renin-angiotensin system. A history and review of the renin-angiotensin system. Proc R Soc Lond B Biol Sci 1969 July 1;173(32):317-25.

(14) Peart WS. Renin-Angiotensin system. Q J Exp Physiol 1982 July;67(3):401-6.

(15) Re R N. The renin angiotensin system. Med Clin North Am 1987;71:877.

(16) Schrier RW. Body water homeostasis: clinical disorders of urinary dilution and concentration. J Am Soc Nephrol 2006 July;17(7):1820-32.

(17) Bedogni G, Borghi A, Battistini N. Body water distribution and disease. Acta Diabetol 2003 October;40 Suppl 1:S200-S202.

(18) Fried W. Erythropoietin and erythropoiesis. Exp Hematol 2009 September;37(9):1007-15.

(19) Rosen JF, Chesney RW. Circulating calcitriol concentrations in health and disease. J Pediatr 1983 July;103(1):1-17.

(20) Brenner BM, Rector FC. Brenner & Rector's the kidney. 2008;8th ed.

(21) O'Callaghan CA, Brenner BM. The kidney at a glance. 2000.

(22) Lee A, Dawson PA, Markovich D. NaSi-1 and Sat-1: structure, function and transcriptional regulation of two genes encoding renal proximal tubular sulfate transporters. Int J Biochem Cell Biol 2005 July;37(7):1350-6.

(23) Wright EM. Renal Na(+)-glucose cotransporters. Am J Physiol Renal Physiol 2001 January;280(1):F10-F18.

(24) Bobulescu IA, Moe OW. Luminal Na(+)/H (+) exchange in the proximal tubule. Pflugers Arch 2009 May;458(1):5-21.

(25) Donowitz M, Mohan S, Zhu CX, Chen TE, Lin R, Cha B, Zachos NC, Murtazina R, Sarker R, Li X. NHE3 regulatory complexes. J Exp Biol 2009 June;212(Pt 11):1638-46.

(26) Hebert SC, Reeves WB, Molony DA, Andreoli TE. The medullary thick limb: function and modulation of the single-effect multiplier. Kidney Int 1987 February;31(2):580-9.

(27) Hebert SC, Andreoli TE. Control of NaCl transport in the thick ascending limb. Am J Physiol 1984 June;246(6 Pt 2):F745-F756.

(28) Hebert SC, Gamba G. Molecular cloning and characterization of the renal diuretic-sensitive electroneutral sodium-(potassium)-chloride cotransporters. Clin Investig 1994 September;72(9):692-4.

(29) Gamba G, Miyanoshita A, Lombardi M, Lytton J, Lee WS, Hediger MA, Hebert SC. Molecular cloning, primary structure, and characterization of two members of the mammalian electroneutral sodium-(potassium)-chloride cotransporter family expressed in kidney. J Biol Chem 1994 July 1;269(26):17713-22.

(30) Ko B, Hoover RS. Molecular physiology of the thiazide-sensitive sodium-chloride cotransporter. Curr Opin Nephrol Hypertens 2009 September;18(5):421-7.

(31) Hamm LL, Feng Z, Hering-Smith KS. Regulation of sodium transport by ENaC in the kidney. Curr Opin Nephrol Hypertens 2010 January;19(1):98-105.

(32) Guyton AC. The surprising kidney-fluid mechanism for pressure control--its infinite gain! Hypertension 1990 December;16(6):725-30.

(33) Guyton AC. Dominant role of the kidneys and accessory role of whole-body autoregulation in the pathogenesis of hypertension. Am J Hypertens 1989 July;2(7):575-85.

(34) Guyton AC. Kidneys and fluids in pressure regulation. Small volume but large pressure changes. Hypertension 1992 January;19(1 Suppl):I2-I8.

(35) Guyton AC. Long-term arterial pressure control: an analysis from animal experiments and computer and graphic models. Am J Physiol 1990 November;259(5 Pt 2):R865-R877.

(36) Guyton AC. Blood pressure control--special role of the kidneys and body fluids. Science 1991 June 28;252(5014):1813-6.

(37) Strange K. Cellular volume homeostasis. Adv Physiol Educ 2004 December;28(1-4):155-9.

(38) Guyton AC, Manning RD, Jr., Hall JE, Norman RA, Jr., Young DB, Pan YJ. The pathogenic role of the kidney. J Cardiovasc Pharmacol 1984;6 Suppl 1:S151-S161.

(39) Karet FE, Lifton RP. Mutations contributing to human blood pressure variation. Recent Prog Horm Res 1997;52:263-76.

(40) Lifton RP. Molecular genetics of human blood pressure variation. Science 1996 May 3;272(5262):676-80.

(41) Lifton RP, Gharavi AG, Geller DS. Molecular mechanisms of human hypertension. Cell 2001 February 23;104(4):545-56.

(42) Lifton RP. Genetic determinants of human hypertension. Proc Natl Acad Sci U S A 1995 September 12;92(19):8545-51.

(43) Lifton RP, Jeunemaitre X. Finding genes that cause human hypertension. J Hypertens 1993 March;11(3):231-6.

(44) Skott O, Briggs JP. Direct demonstration of macula densa-mediated renin secretion. Science 1987 September 25;237(4822):1618-20.

(45) Dendorfer A, Raasch W, Tempel K, Dominiak P. Interactions between the renin-angiotensin system (RAS) and the sympathetic system. Basic Res Cardiol 1998;93 Suppl 2:24-9.

(46) Itoh S, Carretero O A. Role of the macula densa in renin release. Hypertension 1986;7 (Suppl. I):I23.

(47) Peart WS. Renin release. Gen Pharmacol 1978;9(2):65-72.

(48) Peart WS. Renin-angiotensin system. N Engl J Med 1975 February 6;292(6):302-6.

(49) Rosse C, Linch M, Kermorgant S, Cameron AJ, Boeckeler K, Parker PJ. PKC and the control of localized signal dynamics. Nat Rev Mol Cell Biol 2010 February;11(2):103-12.

(50) Catt KJ, Mendelsohn FA, Millan MA, Aguilera G. The role of angiotensin II receptors in vascular regulation. J Cardiovasc Pharmacol 1984;6 Suppl 4:S575-S586.

(51) Mouw D, Bonjour JP, Malvin RL, Vander A. Central action of angiotensin in stimulating ADH release. Am J Physiol 1971 January;220(1):239-42.

(52) Bonjour JP, Malvin RL. Stimulation of ADH release by the renin-angiotensin system. Am J Physiol 1970 June;218(6):1555-9.

(53) Catt KJ, Aguilera G, Capponi A, Fujita K, Schirar A, Fakunding J. Angiotensin II receptors and aldosterone secretion. J Endocrinol 1979 May;81(2):37P-48P.

(54) Ausiello DA, Skorecki KL, Verkman AS, Bonventre JV. Vasopressin signaling in kidney cells. Kidney Int 1987 February;31(2):521-9.

(55) Takata K, Matsuzaki T, Tajika Y, Ablimit A, Hasegawa T. Localization and trafficking of aquaporin 2 in the kidney. Histochem Cell Biol 2008 August;130(2):197-209.

(56) Tajika Y, Matsuzaki T, Suzuki T, Aoki T, Hagiwara H, Kuwahara M, Sasaki S, Takata K. Aquaporin-2 is retrieved to the apical storage compartment via early endosomes and phosphatidylinositol 3-kinase-dependent pathway. Endocrinology 2004 September;145(9):4375-83.

(57) Katsura T, Gustafson CE, Ausiello DA, Brown D. Protein kinase A phosphorylation is involved in regulated exocytosis of aquaporin-2 in transfected LLC-PK1 cells. Am J Physiol 1997 June;272(6 Pt 2):F817-F822.

(58) Garty H. Molecular properties of epithelial, amiloride-blockable Na+ channels. FASEB J 1994 May;8(8):522-8.

(59) Gimenez I, Forbush B. Short-term stimulation of the renal Na-K-Cl cotransporter (NKCC2) by vasopressin involves phosphorylation and membrane translocation of the protein. J Biol Chem 2003 July 18;278(29):26946-51.

(60) Ortiz PA. cAMP increases surface expression of NKCC2 in rat thick ascending limbs: role of VAMP. Am J Physiol Renal Physiol 2006 March;290(3):F608-F616.

(61) Mutig K, Saritas T, Uchida S, Kahl T, Borowski T, Paliege A, Bohlick A, Bleich M, Shan Q, Bachmann S. Short-term stimulation of the thiazide-sensitive Na+-Cl- cotransporter by vasopressin involves phosphorylation and membrane translocation. Am J Physiol Renal Physiol 2010 March;298(3):F502-F509.

(62) Canessa CM, Schild L, Buell G, Thorens B, Gautschi I, Horisberger JD, Rossier BC. Amiloride-sensitive epithelial Na+ channel is made of three homologous subunits. Nature 1994 February 3;367(6462):463-7.

(63) Bugaj V, Pochynyuk O, Stockand JD. Activation of the epithelial Na+ channel in the collecting duct by vasopressin contributes to water reabsorption. Am J Physiol Renal Physiol 2009 November;297(5):F1411-F1418.

(64) Horisberger JD, Rossier BC. Aldosterone regulation of gene transcription leading to control of ion transport. Hypertension 1992 March;19(3):221-7.

(65) Chen SY, Bhargava A, Mastroberardino L, Meijer OC, Wang J, Buse P, Firestone GL, Verrey F, Pearce D. Epithelial sodium channel regulated by aldosterone-induced protein sgk. Proc Natl Acad Sci U S A 1999 March 2;96(5):2514-9.

(66) Kobayashi T, Cohen P. Activation of serum- and glucocorticoid-regulated protein kinase by agonists that activate phosphatidylinositide 3-kinase is mediated by 3-phosphoinositide-dependent protein kinase-1 (PDK1) and PDK2. Biochem J 1999 April 15;339 (Pt 2):319-28.

(67) Xu BE, Stippec S, Lazrak A, Huang CL, Cobb MH. WNK1 activates SGK1 by a phosphatidylinositol 3-kinase-dependent and non-catalytic mechanism. J Biol Chem 2005 October 7;280(40):34218-23.

(68) Ring AM, Leng Q, Rinehart J, Wilson FH, Kahle KT, Hebert SC, Lifton RP. An SGK1 site in WNK4 regulates Na+ channel and K+ channel activity and has implications for aldosterone signaling and K+ homeostasis. Proc Natl Acad Sci U S A 2007 March 6;104(10):4025-9.

(69) Yoo D, Kim BY, Campo C, Nance L, King A, Maouyo D, Welling PA. Cell surface expression of the ROMK (Kir 1.1) channel is regulated by the aldosterone-induced kinase, SGK-1, and protein kinase A. J Biol Chem 2003 June 20;278(25):23066-75.

(70) Garty H. Regulation of the epithelial Na+ channel by aldosterone: open questions and emerging answers. Kidney Int 2000 April;57(4):1270-6.

(71) Shigaev A, Asher C, Latter H, Garty H, Reuveny E. Regulation of sgk by aldosterone and its effects on the epithelial Na(+) channel. Am J Physiol Renal Physiol 2000 April;278(4):F613-F619.

(72) Zhou R, Snyder PM. Nedd4-2 phosphorylation induces serum and glucocorticoid-regulated kinase (SGK) ubiquitination and degradation. J Biol Chem 2005 February 11;280(6):4518-23.

(73) Snyder PM, Olson DR, Kabra R, Zhou R, Steines JC. cAMP and serum and glucocorticoid-inducible kinase (SGK) regulate the epithelial Na(+) channel through convergent phosphorylation of Nedd4-2. J Biol Chem 2004 October 29;279(44):45753-8.

(74) Talati G, Ohta A, Rai T, Sohara E, Naito S, Vandewalle A, Sasaki S, Uchida S. Effect of angiotensin II on the WNK-OSR1/SPAK-NCC phosphorylation cascade in cultured mpkDCT cells and in vivo mouse kidney. Biochem Biophys Res Commun 2010 March 19;393(4):844-8.

(75) Uchida S. Pathophysiological roles of WNK kinases in the kidney. Pflugers Arch 2010 May 21.

(76) Burt VL, Whelton P, Roccella EJ, Brown C, Cutler JA, Higgins M, Horan MJ, Labarthe D. Prevalence of hypertension in the US adult population. Results from the Third National Health and Nutrition Examination Survey, 1988-1991. Hypertension 1995 March;25(3):305-13.

(77) Chobanian AV, Bakris GL, Black HR, Cushman WC, Green LA, Izzo JL, Jr., Jones DW, Materson BJ, Oparil S, Wright JT, Jr., Roccella EJ. The Seventh Report of the Joint National Committee on Prevention, Detection, Evaluation, and Treatment of High Blood Pressure: the JNC 7 report. JAMA 2003 May 21;289(19):2560-72.

(78) Cuddy ML. Treatment of hypertension: guidelines from JNC 7 (the seventh report of the Joint National Committee on Prevention, Detection, Evaluation, and Treatment of High Blood Pressure 1). J Pract Nurs 2005;55(4):17-21.

(79) Hajjar I, Kotchen JM, Kotchen TA. Hypertension: trends in prevalence, incidence, and control. Annu Rev Public Health 2006;27:465-90.

(80) Weir MR. Hypertension and the kidney: perspectives on the relationship of kidney disease and cardiovascular disease. Clin J Am Soc Nephrol 2009 December;4(12):2045-50.

(81) Stanton JL, Braitman LE, Riley AM, Jr., Khoo CS, Smith JL. Demographic, dietary, life style, and anthropometric correlates of blood pressure. Hypertension 1982 September;4(5 Pt 2):III135-III142.

(82) Merikangas KR, Risch N. Genomic priorities and public health. Science 2003 October 24;302(5645):599-601.

(83) Weir MR. Beta-blockers in the treatment of hypertension: are there clinically relevant differences? Postgrad Med 2009 May;121(3):90-8.

(84) Weir MR. Appropriate use of calcium antagonists in hypertension. Hosp Pract (Minneap) 2001 September 15;36(9):47-5.

(85) Hanes DS, Weir MR. The beta blockers: are they as protective in hypertension as in other cardiovascular conditions? J Clin Hypertens (Greenwich) 2001 July;3(4):236-43.

(86) Neutel JM, Weir MR, Moser M, Harris S, Edwards D, Michelson EL, Wang R, ACTION S, I. The Effects of Candesartan Cilexetil in Isolated Systolic Hypertension: A Clinical Experience Trial. J Clin Hypertens (Greenwich) 2000 May;2(3):181-6.

(87) Weir MR. The Role of Multiple Drug Therapy for Controlling Hypertension in African Americans. J Clin Hypertens (Greenwich) 2000 March;2(2):99-108.

(88) Prisant LM, Neutel JM, Papademetriou V, DeQuattro V, Hall WD, Weir MR. Low-dose combination treatment for hypertension versus single-drug treatment-bisoprolol/hydrochlorothiazide versus amlodipine, enalapril, and placebo: combined analysis of comparative studies. Am J Ther 1998 September;5(5):313-21.

(89) Reisin E, Weir MR, Falkner B, Hutchinson HG, Anzalone DA, Tuck ML. Lisinopril versus hydrochlorothiazide in obese hypertensive patients: a multicenter placebo-controlled trial. Treatment in Obese Patients With Hypertension (TROPHY) Study Group. Hypertension 1997 July;30(1 Pt 1):140-5.

(90) Prisant LM, Weir MR, Papademetriou V, Weber MA, Adegbile IA, Alemayehu D, Lefkowitz MP, Carr AA. Low-dose drug combination therapy: an alternative first-line approach to hypertension treatment. Am Heart J 1995 August;130(2):359-66.

(91) Houston MC, Weir M, Gray J, Ginsberg D, Szeto C, Kaihlenen PM, Sugimoto D, Runde M, Lefkowitz M. The effects of nonsteroidal anti-inflammatory drugs on blood pressures of patients with hypertension controlled by verapamil. Arch Intern Med 1995 May 22;155(10):1049-54.

(92) Lifton RP, Gharavi AG, Geller DS. Molecular mechanisms of human hypertension. Cell 2001 February 23;104(4):545-56.

(93) Lifton RP, Gharavi AG, Geller DS. Molecular mechanisms of human hypertension. Cell 2001 February 23;104(4):545-56.

(94) Arriza JL, Weinberger C, Cerelli G, Glaser TM, Handelin BL, Housman DE, Evans RM. Cloning of human mineralocorticoid receptor complementary DNA: structural and functional kinship with the glucocorticoid receptor. Science 1987 July 17;237(4812):268-75.

(95) Funder JW, Pearce PT, Smith R, Smith AI. Mineralocorticoid action: target tissue specificity is enzyme, not receptor, mediated. Science 1988 October 28;242(4878):583-5.

(96) Geller DS, Farhi A, Pinkerton N, Fradley M, Moritz M, Spitzer A, Meinke G, Tsai FT, Sigler PB, Lifton RP. Activating mineralocorticoid receptor mutation in hypertension exacerbated by pregnancy. Science 2000 July 7;289(5476):119-23.

(97) Geller DS. A mineralocorticoid receptor mutation causing human hypertension. Curr Opin Nephrol Hypertens 2001 September;10(5):661-5.

(98) Chrousos GP, Vingerhoeds A, Brandon D, Eil C, Pugeat M, DeVroede M, Loriaux DL, Lipsett MB. Primary cortisol resistance in man. A glucocorticoid receptor-mediated disease. J Clin Invest 1982 June;69(6):1261-9.

(99) Karl M, Lamberts SW, Detera-Wadleigh SD, Encio IJ, Stratakis CA, Hurley DM, Accili D, Chrousos GP. Familial glucocorticoid resistance caused by a splice site deletion in the human glucocorticoid receptor gene. J Clin Endocrinol Metab 1993 March;76(3):683-9.

(100) Sutherland DJ, Ruse JL, Laidlaw JC. Hypertension, increased aldosterone secretion and low plasma renin activity relieved by dexamethasone. Can Med Assoc J 1966 November 26;95(22):1109-19.

(101) Lifton RP, Dluhy RG, Powers M, Rich GM, Cook S, Ulick S, Lalouel JM. A chimaeric 11 beta-hydroxylase/aldosterone synthase gene causes glucocorticoid-remediable aldosteronism and human hypertension. Nature 1992 January 16;355(6357):262-5.

(102) Lifton RP, Dluhy RG, Powers M, Ulick S, Lalouel JM. The molecular basis of glucocorticoid-remediable aldosteronism, a Mendelian cause of human hypertension. Trans Assoc Am Physicians 1992;105:64-71.

(103) Pascoe L, Curnow KM, Slutsker L, Connell JM, Speiser PW, New MI, White PC. Glucocorticoid-suppressible hyperaldosteronism results from hybrid genes created by unequal crossovers between CYP11B1 and CYP11B2. Proc Natl Acad Sci U S A 1992 September 1;89(17):8327-31.

(104) Chemaitilly W, Wilson RC, New MI. Hypertension and adrenal disorders. Curr Hypertens Rep 2003 December;5(6):498-504.

(105) Carey RM, Douglas JG, Schweikert JR, Liddle GW. The syndrome of essential hypertension and suppressed plasma renin activity. Normalization of blood pressure with spironolactone. Arch Intern Med 1972 December;130(6):849-54.

(106) Fishman LM, Kuchel O, Liddle GW, Michelakis AM, Gordon RD, Chick WT. Incidence of primary aldosteronism uncomplicated "essential" hypertension. A prospective study with elevated aldosterone secretion and suppressed plasma renin activity used as diagnostic criteria. JAMA 1968 August 12;205(7):497-502.

(107) Furuhashi M, Kitamura K, Adachi M, Miyoshi T, Wakida N, Ura N, Shikano Y, Shinshi Y, Sakamoto K, Hayashi M, Satoh N, Nishitani T, Tomita K, Shimamoto K. Liddle's syndrome caused by a novel mutation in the proline-rich PY motif of the epithelial sodium channel beta-subunit. J Clin Endocrinol Metab 2005 January;90(1):340-4.

(108) Snyder PM. Liddle's syndrome mutations disrupt cAMP-mediated translocation of the epithelial Na(+) channel to the cell surface. J Clin Invest 2000 January;105(1):45-53.

(109) Anantharam A, Palmer LG. Determination of epithelial Na+ channel subunit stoichiometry from single-channel conductances. J Gen Physiol 2007 July;130(1):55-70.

(110) Edelheit O, Hanukoglu I, Shriki Y, Tfilin M, Dascal N, Gillis D, Hanukoglu A. Truncated beta epithelial sodium channel (ENaC) subunits responsible for multi-

system pseudohypoaldosteronism support partial activity of ENaC. J Steroid Biochem Mol Biol 2010 March;119(1-2):84-8.

(111) Schild L, Canessa CM, Shimkets RA, Gautschi I, Lifton RP, Rossier BC. A mutation in the epithelial sodium channel causing Liddle disease increases channel activity in the Xenopus laevis oocyte expression system. Proc Natl Acad Sci U S A 1995 June 6;92(12):5699-703.

(112) Schild L, Lu Y, Gautschi I, Schneeberger E, Lifton RP, Rossier BC. Identification of a PY motif in the epithelial Na channel subunits as a target sequence for mutations causing channel activation found in Liddle syndrome. EMBO J 1996 May 15;15(10):2381-7.

(113) Wiemuth D, Ke Y, Rohlfs M, McDonald FJ. Epithelial sodium channel (ENaC) is multi-ubiquitinated at the cell surface. Biochem J 2007 July 1;405(1):147-55.

(114) Delaloy C, Elvira-Matelot E, Clemessy M, Zhou XO, Imbert-Teboul M, Houot AM, Jeunemaitre X, Hadchouel J. Deletion of WNK1 first intron results in misregulation of both isoforms in renal and extrarenal tissues. Hypertension 2008 December;52(6):1149-54.

(115) Hadchouel J, Delaloy C, Faure S, Achard JM, Jeunemaitre X. Familial hyperkalemic hypertension. J Am Soc Nephrol 2006 January;17(1):208-17.

(116) Wilson FH, Disse-Nicodeme S, Choate KA, Ishikawa K, Nelson-Williams C, Desitter I, Gunel M, Milford DV, Lipkin GW, Achard JM, Feely MP, Dussol B, Berland Y, Unwin RJ, Mayan H, Simon DB, Farfel Z, Jeunemaitre X, Lifton RP. Human hypertension caused by mutations in WNK kinases. Science 2001 August 10;293(5532):1107-12.

(117) Wilson FH, Kahle KT, Sabath E, Lalioti MD, Rapson AK, Hoover RS, Hebert SC, Gamba G, Lifton RP. Molecular pathogenesis of inherited hypertension with hyperkalemia: the Na-Cl cotransporter is inhibited by wild-type but not mutant WNK4. Proc Natl Acad Sci U S A 2003 January 21;100(2):680-4.

(118) Ring AM, Cheng SX, Leng Q, Kahle KT, Rinehart J, Lalioti MD, Volkman HM, Wilson FH, Hebert SC, Lifton RP. WNK4 regulates activity of the epithelial Na+ channel in vitro and in vivo. Proc Natl Acad Sci U S A 2007 March 6;104(10):4020-4.

(119) Liu Z, Wang HR, Huang CL. Regulation of ROMK channel and K+ homeostasis by kidney-specific WNK1 kinase. J Biol Chem 2009 May 1;284(18):12198-206.

(120) Kahle KT, Macgregor GG, Wilson FH, Van Hoek AN, Brown D, Ardito T, Kashgarian M, Giebisch G, Hebert SC, Boulpaep EL, Lifton RP. Paracellular Cl- permeability is regulated by WNK4 kinase: insight into normal physiology and hypertension. Proc Natl Acad Sci U S A 2004 October 12;101(41):14877-82.

(121) Yamauchi K, Rai T, Kobayashi K, Sohara E, Suzuki T, Itoh T, Suda S, Hayama A, Sasaki S, Uchida S. Disease-causing mutant WNK4 increases paracellular chloride permeability and phosphorylates claudins. Proc Natl Acad Sci U S A 2004 March 30;101(13):4690-4.

(122) Gamba G. TRPV4: a new target for the hypertension-related kinases WNK1 and WNK4. Am J Physiol Renal Physiol 2006 June;290(6):F1303-F1304.

(123) Fu Y, Subramanya A, Rozansky D, Cohen DM. WNK kinases influence TRPV4 channel function and localization. Am J Physiol Renal Physiol 2006 June;290(6):F1305-F1314.

(124) Vitari AC, Deak M, Morrice NA, Alessi DR. The WNK1 and WNK4 protein kinases that are mutated in Gordon's hypertension syndrome phosphorylate and activate SPAK and OSR1 protein kinases. Biochem J 2005 October 1;391(Pt 1):17-24.

(125) Tatum R, Zhang Y, Lu Q, Kim K, Jeansonne BG, Chen YH. WNK4 phosphorylates ser(206) of claudin-7 and promotes paracellular Cl(-) permeability. FEBS Lett 2007 August 7;581(20):3887-91.

(126) Yang CL, Angell J, Mitchell R, Ellison DH. WNK kinases regulate thiazide-sensitive Na-Cl cotransport. J Clin Invest 2003 April;111(7):1039-45.

(127) Tobin MD, Raleigh SM, Newhouse S, Braund P, Bodycote C, Ogleby J, Cross D, Gracey J, Hayes S, Smith T, Ridge C, Caulfield M, Sheehan NA, Munroe PB, Burton PR, Samani NJ. Association of WNK1 gene polymorphisms and haplotypes with ambulatory blood pressure in the general population. Circulation 2005 November 29;112(22):3423-9.

(128) Newhouse SJ, Wallace C, Dobson R, Mein C, Pembroke J, Farrall M, Clayton D, Brown M, Samani N, Dominiczak A, Connell JM, Webster J, Lathrop GM, Caulfield M, Munroe PB. Haplotypes of the WNK1 gene associate with blood pressure variation in a severely hypertensive population from the British Genetics of Hypertension study. Hum Mol Genet 2005 July 1;14(13):1805-14.

(129) Zambrowicz BP, Abuin A, Ramirez-Solis R, Richter LJ, Piggott J, BeltrandelRio H, Buxton EC, Edwards J, Finch RA, Friddle CJ, Gupta A, Hansen G, Hu Y, Huang W, Jaing C, Key BW, Jr., Kipp P, Kohlhauff B, Ma ZQ, Markesich D, Payne R, Potter DG, Qian N, Shaw J, Schrick J et al. Wnk1 kinase deficiency lowers blood pressure in mice: a gene-trap screen to identify potential targets for therapeutic intervention. Proc Natl Acad Sci U S A 2003 November 25;100(24):14109-14.

(130) Levy D, DeStefano AL, Larson MG, O'Donnell CJ, Lifton RP, Gavras H, Cupples LA, Myers RH. Evidence for a gene influencing blood pressure on chromosome 17. Genome scan linkage results for longitudinal blood pressure phenotypes in subjects from the framingham heart study. Hypertension 2000 October;36(4):477-83.

(131) Erlich PM, Cui J, Chazaro I, Farrer LA, Baldwin CT, Gavras H, DeStefano AL. Genetic variants of WNK4 in whites and African Americans with hypertension. Hypertension 2003 June;41(6):1191-5.

(132) Kamide K, Takiuchi S, Tanaka C, Miwa Y, Yoshii M, Horio T, Mannami T, Kokubo Y, Tomoike H, Kawano Y, Miyata T. Three novel missense mutations of WNK4, a kinase mutated in inherited hypertension, in Japanese hypertensives: implication of clinical phenotypes. Am J Hypertens 2004 May;17(5 Pt 1):446-9.

(133) Subramanya AR, Liu J, Ellison DH, Wade JB, Welling PA. WNK4 diverts the thiazide-sensitive NaCl cotransporter to the lysosome and stimulates AP-3 interaction. J Biol Chem 2009 July 3;284(27):18471-80.

(134) Subramanya AR, Ellison DH. Sorting out lysosomal trafficking of the thiazide-sensitive Na-Cl Co-transporter. J Am Soc Nephrol 2010 January;21(1):7-9.

(135) Zhou B, Zhuang J, Gu D, Wang H, Cebotaru L, Guggino WB, Cai H. WNK4 enhances the degradation of NCC through a sortilin-mediated lysosomal pathway. J Am Soc Nephrol 2010 January;21(1):82-92.

(136) Lalioti MD, Zhang J, Volkman HM, Kahle KT, Hoffmann KE, Toka HR, Nelson-Williams C, Ellison DH, Flavell R, Booth CJ, Lu Y, Geller DS, Lifton RP. Wnk4 controls blood pressure and potassium homeostasis via regulation of mass and activity of the distal convoluted tubule. Nat Genet 2006 October;38(10):1124-32.

(137) Pascoe L, Curnow KM, Slutsker L, Rosler A, White PC. Mutations in the human CYP11B2 (aldosterone synthase) gene causing corticosterone methyloxidase II deficiency. Proc Natl Acad Sci U S A 1992 June 1;89(11):4996-5000.

(138) Mitsuuchi Y, Kawamoto T, Naiki Y, Miyahara K, Toda K, Kuribayashi I, Orii T, Yasuda K, Miura K, Nakao K, . Congenitally defective aldosterone biosynthesis in humans: the involvement of point mutations of the P-450C18 gene (CYP11B2) in CMO II deficient patients. Biochem Biophys Res Commun 1992 January 31;182(2):974-9.

(139) Chang SS, Grunder S, Hanukoglu A, Rosler A, Mathew PM, Hanukoglu I, Schild L, Lu Y, Shimkets RA, Nelson-Williams C, Rossier BC, Lifton RP. Mutations in subunits of the epithelial sodium channel cause salt wasting with hyperkalaemic acidosis, pseudohypoaldosteronism type 1. Nat Genet 1996 March;12(3):248-53.

(140) Nijenhuis T, Vallon V, van der Kemp AW, Loffing J, Hoenderop JG, Bindels RJ. Enhanced passive Ca2+ reabsorption and reduced Mg2+ channel abundance explains thiazide-induced hypocalciuria and hypomagnesemia. J Clin Invest 2005 June;115(6):1651-8.

(141) Gamba G, Friedman PA. Thick ascending limb: the Na(+):K (+):2Cl (-) co-transporter, NKCC2, and the calcium-sensing receptor, CaSR. Pflugers Arch 2009 May;458(1):61-76.

(142) Sands JM, Layton HE. The physiology of urinary concentration: an update. Semin Nephrol 2009 May;29(3):178-95.

(143) Karim Z, Szutkowska M, Vernimmen C, Bichara M. Recent concepts concerning the renal handling of NH3/NH4+. J Nephrol 2006 March;19 Suppl 9:S27-S32.

(144) Karim Z, Szutkowska M, Vernimmen C, Bichara M. Renal handling of NH3/NH4+: recent concepts. Nephron Physiol 2005;101(4):77-81.

(145) Bourdeau JE, Burg MB. Voltage dependence of calcium transport in the thick ascending limb of Henle's loop. Am J Physiol 1979 April;236(4):F357-F364.

(146) Stechman MJ, Loh NY, Thakker RV. Genetic causes of hypercalciuric nephrolithiasis. Pediatr Nephrol 2009 December;24(12):2321-32.

(147) Brenner BM, Rector FC. Brenner & Rector's the kidney. 2008;8th ed.

(148) Kurtz CL, Karolyi L, Seyberth HW, Koch MC, Vargas R, Feldmann D, Vollmer M, Knoers NV, Madrigal G, Guay-Woodford LM. A common NKCC2 mutation

in Costa Rican Bartter's syndrome patients: evidence for a founder effect. J Am Soc Nephrol 1997 November;8(11):1706-11.

(149) Vargas-Poussou R, Feldmann D, Vollmer M, Konrad M, Kelly L, van den Heuvel LP, Tebourbi L, Brandis M, Karolyi L, Hebert SC, Lemmink HH, Deschenes G, Hildebrandt F, Seyberth HW, Guay-Woodford LM, Knoers NV, Antignac C. Novel molecular variants of the Na-K-2Cl cotransporter gene are responsible for antenatal Bartter syndrome. Am J Hum Genet 1998 June;62(6):1332-40.

(150) Simon DB, Lifton RP. The molecular basis of inherited hypokalemic alkalosis: Bartter's and Gitelman's syndromes. Am J Physiol 1996 November;271(5 Pt 2):F961-F966.

(151) Simon DB, Karet FE, Hamdan JM, DiPietro A, Sanjad SA, Lifton RP. Bartter's syndrome, hypokalaemic alkalosis with hypercalciuria, is caused by mutations in the Na-K-2Cl cotransporter NKCC2. Nat Genet 1996 June;13(2):183-8.

(152) Hebert SC. Bartter syndrome. Curr Opin Nephrol Hypertens 2003 September;12(5):527-32.

(153) BARTTER FC, PRONOVE P, GILL JR, Jr., MACCARDLE RC. Hyperplasia of the juxtaglomerular complex with hyperaldosteronism and hypokalemic alkalosis. A new syndrome. Am J Med 1962 December;33:811-28.

(154) Vollmer M, Koehrer M, Topaloglu R, Strahm B, Omran H, Hildebrandt F. Two novel mutations of the gene for Kir 1.1 (ROMK) in neonatal Bartter syndrome. Pediatr Nephrol 1998 January;12(1):69-71.

(155) Derst C, Wischmeyer E, Preisig-Muller R, Spauschus A, Konrad M, Hensen P, Jeck N, Seyberth HW, Daut J, Karschin A. A hyperprostaglandin E syndrome mutation in Kir1.1 (renal outer medullary potassium) channels reveals a crucial residue for channel function in Kir1.3 channels. J Biol Chem 1998 September 11;273(37):23884-91.

(156) Starremans PG, van der Kemp AW, Knoers NV, van den Heuvel LP, Bindels RJ. Functional implications of mutations in the human renal outer medullary potassium channel (ROMK2) identified in Bartter syndrome. Pflugers Arch 2002 January;443(3):466-72.

(157) Derst C, Konrad M, Kockerling A, Karolyi L, Deschenes G, Daut J, Karschin A, Seyberth HW. Mutations in the ROMK gene in antenatal Bartter syndrome are

associated with impaired K+ channel function. Biochem Biophys Res Commun 1997 January 23;230(3):641-5.

(158) Jeck N, Derst C, Wischmeyer E, Ott H, Weber S, Rudin C, Seyberth HW, Daut J, Karschin A, Konrad M. Functional heterogeneity of ROMK mutations linked to hyperprostaglandin E syndrome. Kidney Int 2001 May;59(5):1803-11.

(159) Schulte U, Hahn H, Konrad M, Jeck N, Derst C, Wild K, Weidemann S, Ruppersberg JP, Fakler B, Ludwig J. pH gating of ROMK (K(ir)1.1) channels: control by an Arg-Lys-Arg triad disrupted in antenatal Bartter syndrome. Proc Natl Acad Sci U S A 1999 December 21;96(26):15298-303.

(160) Simon DB, Karet FE, Rodriguez-Soriano J, Hamdan JH, DiPietro A, Trachtman H, Sanjad SA, Lifton RP. Genetic heterogeneity of Bartter's syndrome revealed by mutations in the K+ channel, ROMK. Nat Genet 1996 October;14(2):152-6.

(161) Wagner CA, Loffing-Cueni D, Yan Q, Schulz N, Fakitsas P, Carrel M, Wang T, Verrey F, Geibel JP, Giebisch G, Hebert SC, Loffing J. Mouse model of type II Bartter's syndrome. II. Altered expression of renal sodium- and water-transporting proteins. Am J Physiol Renal Physiol 2008 June;294(6):F1373-F1380.

(162) Konrad M, Vollmer M, Lemmink HH, van den Heuvel LP, Jeck N, Vargas-Poussou R, Lakings A, Ruf R, Deschenes G, Antignac C, Guay-Woodford L, Knoers NV, Seyberth HW, Feldmann D, Hildebrandt F. Mutations in the chloride channel gene CLCNKB as a cause of classic Bartter syndrome. J Am Soc Nephrol 2000 August;11(8):1449-59.

(163) Birkenhager R, Otto E, Schurmann MJ, Vollmer M, Ruf EM, Maier-Lutz I, Beekmann F, Fekete A, Omran H, Feldmann D, Milford DV, Jeck N, Konrad M, Landau D, Knoers NV, Antignac C, Sudbrak R, Kispert A, Hildebrandt F. Mutation of BSND causes Bartter syndrome with sensorineural deafness and kidney failure. Nat Genet 2001 November;29(3):310-4.

(164) Vargas-Poussou R, Huang C, Hulin P, Houillier P, Jeunemaitre X, Paillard M, Planelles G, Dechaux M, Miller RT, Antignac C. Functional characterization of a calcium-sensing receptor mutation in severe autosomal dominant hypocalcemia with a Bartter-like syndrome. J Am Soc Nephrol 2002 September;13(9):2259-66.

(165) Watanabe S, Fukumoto S, Chang H, Takeuchi Y, Hasegawa Y, Okazaki R, Chikatsu N, Fujita T. Association between activating mutations of calcium-

sensing receptor and Bartter's syndrome. Lancet 2002 August 31;360(9334):692-4.

(166) Peters M, Ermert S, Jeck N, Derst C, Pechmann U, Weber S, Schlingmann KP, Seyberth HW, Waldegger S, Konrad M. Classification and rescue of ROMK mutations underlying hyperprostaglandin E syndrome/antenatal Bartter syndrome. Kidney Int 2003 September;64(3):923-32.

(167) Proesmans W. Bartter syndrome and its neonatal variant. Eur J Pediatr 1997 September;156(9):669-79.

(168) O'Sullivan E, Monga M, Graves W. Bartter's syndrome in pregnancy: a case report and review. Am J Perinatol 1997 January;14(1):55-7.

(169) Hebert SC. Bartter syndrome. Curr Opin Nephrol Hypertens 2003 September;12(5):527-32.

(170) Simon DB, Karet FE, Rodriguez-Soriano J, Hamdan JH, DiPietro A, Trachtman H, Sanjad SA, Lifton RP. Genetic heterogeneity of Bartter's syndrome revealed by mutations in the K+ channel, ROMK. Nat Genet 1996 October;14(2):152-6.

(171) Simon DB, Karet FE, Hamdan JM, DiPietro A, Sanjad SA, Lifton RP. Bartter's syndrome, hypokalaemic alkalosis with hypercalciuria, is caused by mutations in the Na-K-2Cl cotransporter NKCC2. Nat Genet 1996 June;13(2):183-8.

(172) Rodan AR, Huang CL. Distal potassium handling based on flow modulation of maxi-K channel activity. Curr Opin Nephrol Hypertens 2009 July;18(4):350-5.

(173) Bailey MA, Cantone A, Yan Q, MacGregor GG, Leng Q, Amorim JB, Wang T, Hebert SC, Giebisch G, Malnic G. Maxi-K channels contribute to urinary potassium excretion in the ROMK-deficient mouse model of Type II Bartter's syndrome and in adaptation to a high-K diet. Kidney Int 2006 July;70(1):51-9.

(174) Simon DB, Bindra RS, Mansfield TA, Nelson-Williams C, Mendonca E, Stone R, Schurman S, Nayir A, Alpay H, Bakkaloglu A, Rodriguez-Soriano J, Morales JM, Sanjad SA, Taylor CM, Pilz D, Brem A, Trachtman H, Griswold W, Richard GA, John E, Lifton RP. Mutations in the chloride channel gene, CLCNKB, cause Bartter's syndrome type III. Nat Genet 1997 October;17(2):171-8.

(175) Estevez R, Boettger T, Stein V, Birkenhager R, Otto E, Hildebrandt F, Jentsch TJ. Barttin is a Cl- channel beta-subunit crucial for renal Cl- reabsorption and inner ear K+ secretion. Nature 2001 November 29;414(6863):558-61.

(176) Janssen AG, Scholl U, Domeyer C, Nothmann D, Leinenweber A, Fahlke C. Disease-causing dysfunctions of barttin in Bartter syndrome type IV. J Am Soc Nephrol 2009 January;20(1):145-53.

(177) Vollmer M, Jeck N, Lemmink HH, Vargas R, Feldmann D, Konrad M, Beekmann F, van Den Heuvel LP, Deschenes G, Guay-Woodford LM, Antignac C, Seyberth HW, Hildebrandt F, Knoers NV. Antenatal Bartter syndrome with sensorineural deafness: refinement of the locus on chromosome 1p31. Nephrol Dial Transplant 2000 July;15(7):970-4.

(178) Starremans PG, Kersten FF, Van Den Heuvel LP, Knoers NV, Bindels RJ. Dimeric architecture of the human bumetanide-sensitive Na-K-Cl Co-transporter. J Am Soc Nephrol 2003 December;14(12):3039-46.

(179) Paredes A, Plata C, Rivera M, Moreno E, Vazquez N, Munoz-Clares R, Hebert SC, Gamba G. Activity of the renal Na+-K+-2Cl- cotransporter is reduced by mutagenesis of N-glycosylation sites: role for protein surface charge in Cl- transport. Am J Physiol Renal Physiol 2006 May;290(5):F1094-F1102.

(180) Caceres PS, Ares GR, Ortiz PA. cAMP stimulates apical exocytosis of the renal Na(+)-K(+)-2Cl(-) cotransporter NKCC2 in the thick ascending limb: role of protein kinase A. J Biol Chem 2009 September 11;284(37):24965-71.

(181) Rinehart J, Kahle KT, de Los HP, Vazquez N, Meade P, Wilson FH, Hebert SC, Gimenez I, Gamba G, Lifton RP. WNK3 kinase is a positive regulator of NKCC2 and NCC, renal cation-Cl- cotransporters required for normal blood pressure homeostasis. Proc Natl Acad Sci U S A 2005 November 15;102(46):16777-82.

(182) Fraser SA, Gimenez I, Cook N, Jennings I, Katerelos M, Katsis F, Levidiotis V, Kemp BE, Power DA. Regulation of the renal-specific Na+-K+-2Cl- co-transporter NKCC2 by AMP-activated protein kinase (AMPK). Biochem J 2007 July 1;405(1):85-93.

(183) Rinehart J, Kahle KT, de Los HP, Vazquez N, Meade P, Wilson FH, Hebert SC, Gimenez I, Gamba G, Lifton RP. WNK3 kinase is a positive regulator of NKCC2 and NCC, renal cation-Cl- cotransporters required for normal blood pressure homeostasis. Proc Natl Acad Sci U S A 2005 November 15;102(46):16777-82.

(184) Dimke H, Flyvbjerg A, Bourgeois S, Thomsen K, Frokiaer J, Houillier P, Nielsen S, Frische S. Acute growth hormone administration induces antidiuretic

and antinatriuretic effects and increases phosphorylation of NKCC2. Am J Physiol Renal Physiol 2007 February;292(2):F723-F735.

(185) Gimenez I, Forbush B. Regulatory phosphorylation sites in the NH2 terminus of the renal Na-K-Cl cotransporter (NKCC2). Am J Physiol Renal Physiol 2005 December;289(6):F1341-F1345.

(186) Gimenez I, Forbush B. Short-term stimulation of the renal Na-K-Cl cotransporter (NKCC2) by vasopressin involves phosphorylation and membrane translocation of the protein. J Biol Chem 2003 July 18;278(29):26946-51.

(187) Castrop H, Schnermann J. Isoforms of renal Na-K-2Cl cotransporter NKCC2: expression and functional significance. Am J Physiol Renal Physiol 2008 October;295(4):F859-F866.

(188) Hediger MA, Romero MF, Peng JB, Rolfs A, Takanaga H, Bruford EA. The ABCs of solute carriers: physiological, pathological and therapeutic implications of human membrane transport proteinsIntroduction. Pflugers Arch 2004 February;447(5):465-8.

(189) Hebert SC, Mount DB, Gamba G. Molecular physiology of cation-coupled Cl-cotransport: the SLC12 family. Pflugers Arch 2004 February;447(5):580-93.

(190) Liapis H, Nag M, Kaji DM. K-Cl cotransporter expression in the human kidney. Am J Physiol 1998 December;275(6 Pt 1):C1432-C1437.

(191) Gillen CM, Brill S, Payne JA, Forbush B, III. Molecular cloning and functional expression of the K-Cl cotransporter from rabbit, rat, and human. A new member of the cation-chloride cotransporter family. J Biol Chem 1996 July 5;271(27):16237-44.

(192) Viitanen T, Ruusuvuori E, Kaila K, Voipio J. The K+-Cl- Cotransporter KCC2 promotes GABAergic Excitation in the Mature Rat Hippocampus. J Physiol 2010 March 8.

(193) Tanis JE, Bellemer A, Moresco JJ, Forbush B, Koelle MR. The potassium chloride cotransporter KCC-2 coordinates development of inhibitory neurotransmission and synapse structure in Caenorhabditis elegans. J Neurosci 2009 August 12;29(32):9943-54.

(194) Uyanik G, Elcioglu N, Penzien J, Gross C, Yilmaz Y, Olmez A, Demir E, Wahl D, Scheglmann K, Winner B, Bogdahn U, Topaloglu H, Hehr U, Winkler J. Novel truncating and missense mutations of the KCC3 gene associated with Andermann syndrome. Neurology 2006 April 11;66(7):1044-8.

(195) Andermann E, Andermann F, Joubert M, Melancon D, Karpati G, Carpenter S. Three familial midline malformtion syndromes of the central nervous system: agenesis of the corpus callosum and anterior horn-cell disease; agenesis of cerebellar vermis; and atrophy of the cerebellar vermis. Birth Defects Orig Artic Ser 1975;11(2):269-93.

(196) Karadsheh MF, Byun N, Mount DB, Delpire E. Localization of the KCC4 potassium-chloride cotransporter in the nervous system. Neuroscience 2004;123(2):381-91.

(197) Boettger T, Hubner CA, Maier H, Rust MB, Beck FX, Jentsch TJ. Deafness and renal tubular acidosis in mice lacking the K-Cl co-transporter Kcc4. Nature 2002 April 25;416(6883):874-8.

(198) Daigle ND, Carpentier GA, Frenette-Cotton R, Simard MG, Lefoll MH, Noel M, Caron L, Noel J, Isenring P. Molecular characterization of a human cation-Cl- cotransporter (SLC12A8A, CCC9A) that promotes polyamine and amino acid transport. J Cell Physiol 2009 September;220(3):680-9.

(199) Huffmeier U, Lascorz J, Traupe H, Bohm B, Schurmeier-Horst F, Stander M, Kelsch R, Baumann C, Kuster W, Burkhardt H, Reis A. Systematic linkage disequilibrium analysis of SLC12A8 at PSORS5 confirms a role in susceptibility to psoriasis vulgaris. J Invest Dermatol 2005 November;125(5):906-12.

(200) Caron L, Rousseau F, Gagnon E, Isenring P. Cloning and functional characterization of a cation-Cl- cotransporter-interacting protein. J Biol Chem 2000 October 13;275(41):32027-36.

(201) De Los Heros P., Kahle KT, Rinehart J, Bobadilla NA, Vazquez N, San Cristobal P, Mount DB, Lifton RP, Hebert SC, Gamba G. WNK3 bypasses the tonicity requirement for K-Cl cotransporter activation via a phosphatase-dependent pathway. Proc Natl Acad Sci U S A 2006 January 30;103:1976-81.

(202) Lang F, Lepple-Wienhues A, Szabo I, Siemen D, Gulbins E. Cell volume in cell proliferation and apoptotic cell death. Contrib Nephrol 1998;123:158-68.

(203) Lang F, Lepple-Wienhues A, Paulmichl M, Szabo I, Siemen D, Gulbins E. Ion channels, cell volume, and apoptotic cell death. Cell Physiol Biochem 1998;8(6):285-92.

(204) Gimenez I, Forbush B. Regulatory phosphorylation sites in the NH2 terminus of the renal Na-K-Cl cotransporter (NKCC2). Am J Physiol Renal Physiol 2005 December;289(6):F1341-F1345.

(205) Haas M, McBrayer D, Lytle C. [Cl-]i-dependent phosphorylation of the Na-K-Cl cotransport protein of dog tracheal epithelial cells. J Biol Chem 1995 December 1;270(48):28955-61.

(206) de Los HP, Kahle KT, Rinehart J, Bobadilla NA, Vazquez N, San CP, Mount DB, Lifton RP, Hebert SC, Gamba G. WNK3 bypasses the tonicity requirement for K-Cl cotransporter activation via a phosphatase-dependent pathway. Proc Natl Acad Sci U S A 2006 February 7;103(6):1976-81.

(207) Kahle KT, Rinehart J, de Los HP, Louvi A, Meade P, Vazquez N, Hebert SC, Gamba G, Gimenez I, Lifton RP. WNK3 modulates transport of Cl- in and out of cells: implications for control of cell volume and neuronal excitability. Proc Natl Acad Sci U S A 2005 November 15;102(46):16783-8.

(208) Rinehart J, Maksimova YD, Tanis JE, Stone KL, Hodson CA, Zhang J, Risinger M, Pan W, Wu D, Colangelo CM, Forbush B, Joiner CH, Gulcicek EE, Gallagher PG, Lifton RP. Sites of regulated phosphorylation that control K-Cl cotransporter activity. Cell 2009 August 7;138(3):525-36.

(209) San-Cristobal P, de los HP, Ponce-Coria J, Moreno E, Gamba G. WNK kinases, renal ion transport and hypertension. Am J Nephrol 2008;28(5):860-70.

(210) McCormick JA, Yang CL, Ellison DH. WNK kinases and renal sodium transport in health and disease: an integrated view. Hypertension 2008 March;51(3):588-96.

(211) Kahle KT, Ring AM, Lifton RP. Molecular physiology of the WNK kinases. Annu Rev Physiol 2008;70:329-55.

(212) Gamba G. Role of WNK kinases in regulating tubular salt and potassium transport and in the development of hypertension. Am J Physiol Renal Physiol 2005 February;288(2):F245-F252.

(213) Hanks SK, Hunter T. Protein kinases 6. The eukaryotic protein kinase superfamily: kinase (catalytic) domain structure and classification. FASEB J 1995 May;9(8):576-96.

(214) Xu B, English JM, Wilsbacher JL, Stippec S, Goldsmith EJ, Cobb MH. WNK1, a novel mammalian serine/threonine protein kinase lacking the catalytic lysine in subdomain II. J Biol Chem 2000 June 2;275(22):16795-801.

(215) Verissimo F, Jordan P. WNK kinases, a novel protein kinase subfamily in multi-cellular organisms. Oncogene 2001 September 6;20(39):5562-9.

(216) Xu B, English JM, Wilsbacher JL, Stippec S, Goldsmith EJ, Cobb MH. WNK1, a novel mammalian serine/threonine protein kinase lacking the catalytic lysine in subdomain II. J Biol Chem 2000 June 2;275(22):16795-801.

(217) Xu B, English JM, Wilsbacher JL, Stippec S, Goldsmith EJ, Cobb MH. WNK1, a novel mammalian serine/threonine protein kinase lacking the catalytic lysine in subdomain II. J Biol Chem 2000 June 2;275(22):16795-801.

(218) Jun P, Hong C, Lal A, Wong JM, McDermott MW, Bollen AW, Plass C, Held WA, Smiraglia DJ, Costello JF. Epigenetic silencing of the kinase tumor suppressor WNK2 is tumor-type and tumor-grade specific. Neuro Oncol 2009 August;11(4):414-22.

(219) Moniz S, Matos P, Jordan P. WNK2 modulates MEK1 activity through the Rho GTPase pathway. Cell Signal 2008 October;20(10):1762-8.

(220) Moniz S, Verissimo F, Matos P, Brazao R, Silva E, Kotelevets L, Chastre E, Gespach C, Jordan P. Protein kinase WNK2 inhibits cell proliferation by negatively modulating the activation of MEK1/ERK1/2. Oncogene 2007 September 6;26(41):6071-81.

(221) Hong C, Moorefield KS, Jun P, Aldape KD, Kharbanda S, Phillips HS, Costello JF. Epigenome scans and cancer genome sequencing converge on WNK2, a kinase-independent suppressor of cell growth. Proc Natl Acad Sci U S A 2007 June 26;104(26):10974-9.

(222) Glover M, Zuber AM, O'Shaughnessy KM. Renal and brain isoforms of WNK3 have opposite effects on NCCT expression. J Am Soc Nephrol 2009 June;20(6):1314-22.

(223) Holden S, Cox J, Raymond FL. Cloning, genomic organization, alternative splicing and expression analysis of the human gene WNK3 (PRKWNK3). Gene 2004 June 23;335:109-19.

(224) Lalioti MD, Zhang J, Volkman HM, Kahle KT, Hoffmann KE, Toka HR, Nelson-Williams C, Ellison DH, Flavell R, Booth CJ, Lu Y, Geller DS, Lifton RP. Wnk4 controls blood pressure and potassium homeostasis via regulation of mass and activity of the distal convoluted tubule. Nat Genet 2006 October;38(10):1124-32.

(225) Cai H, Cebotaru V, Wang YH, Zhang XM, Cebotaru L, Guggino SE, Guggino WB. WNK4 kinase regulates surface expression of the human sodium chloride cotransporter in mammalian cells. Kidney Int 2006 June;69(12):2162-70.

(226) Yang CL, Zhu X, Wang Z, Subramanya AR, Ellison DH. Mechanisms of WNK1 and WNK4 interaction in the regulation of thiazide-sensitive NaCl cotransport. J Clin Invest 2005 May;115(5):1379-87.

(227) Kahle KT, Wilson FH, Leng Q, Lalioti MD, O'Connell AD, Dong K, Rapson AK, Macgregor GG, Giebisch G, Hebert SC, Lifton RP. WNK4 regulates the balance between renal NaCl reabsorption and K+ secretion. Nat Genet 2003 December;35(4):372-6.

(228) Shekarabi M, Girard N, Riviere JB, Dion P, Houle M, Toulouse A, Lafreniere RG, Vercauteren F, Hince P, Laganiere J, Rochefort D, Faivre L, Samuels M, Rouleau GA. Mutations in the nervous system--specific HSN2 exon of WNK1 cause hereditary sensory neuropathy type II. J Clin Invest 2008 July;118(7):2496-505.

(229) Wilson FH, Disse-Nicodeme S, Choate KA, Ishikawa K, Nelson-Williams C, Desitter I, Gunel M, Milford DV, Lipkin GW, Achard JM, Feely MP, Dussol B, Berland Y, Unwin RJ, Mayan H, Simon DB, Farfel Z, Jeunemaitre X, Lifton RP. Human hypertension caused by mutations in WNK kinases. Science 2001 August 10;293(5532):1107-12.

(230) Delpire E, Gagnon KB. SPAK and OSR1: STE20 kinases involved in the regulation of ion homoeostasis and volume control in mammalian cells. Biochem J 2008 January 15;409(2):321-31.

(231) Gagnon KB, England R, Delpire E. A single binding motif is required for SPAK activation of the Na-K-2Cl cotransporter. Cell Physiol Biochem 2007;20(1-4):131-42.

(232) Gagnon KB, England R, Delpire E. Characterization of SPAK and OSR1, regulatory kinases of the Na-K-2Cl cotransporter. Mol Cell Biol 2006 January;26(2):689-98.

(233) Gagnon KB, England R, Delpire E. Volume sensitivity of cation-Cl- cotransporters is modulated by the interaction of two kinases: Ste20-related proline-alanine-rich kinase and WNK4. Am J Physiol Cell Physiol 2006 January;290(1):C134-C142.

(234) Delpire E, Gagnon KB. SPAK and OSR1, key kinases involved in the regulation of chloride transport. Acta Physiol (Oxf) 2006 May;187(1-2):103-13.

(235) Dan I, Watanabe NM, Kusumi A. The Ste20 group kinases as regulators of MAP kinase cascades. Trends Cell Biol 2001 May;11(5):220-30.

(236) Flemmer AW, Gimenez I, Dowd BF, Darman RB, Forbush B. Activation of the Na-K-Cl cotransporter NKCC1 detected with a phospho-specific antibody. J Biol Chem 2002 October 4;277(40):37551-8.

(237) Piechotta K, Garbarini N, England R, Delpire E. Characterization of the interaction of the stress kinase SPAK with the Na+-K+-2Cl- cotransporter in the nervous system: evidence for a scaffolding role of the kinase. J Biol Chem 2003 December 26;278(52):52848-56.

(238) Piechotta K, Lu J, Delpire E. Cation chloride cotransporters interact with the stress-related kinases Ste20-related proline-alanine-rich kinase (SPAK) and oxidative stress response 1 (OSR1). J Biol Chem 2002 December 27;277(52):50812-9.

(239) Villa F, Goebel J, Rafiqi FH, Deak M, Thastrup J, Alessi DR, van Aalten DM. Structural insights into the recognition of substrates and activators by the OSR1 kinase. EMBO Rep 2007 September;8(9):839-45.

(240) Paredes A, Plata C, Rivera M, Moreno E, Vazquez N, Munoz-Clares R, Hebert SC, Gamba G. Activity of the renal Na+-K+-2Cl- cotransporter is reduced by mutagenesis of N-glycosylation sites: role for protein surface charge in Cl- transport. Am J Physiol Renal Physiol 2006 May;290(5):F1094-F1102.

(241) Meade P, Hoover RS, Plata C, Vazquez N, Bobadilla NA, Gamba G, Hebert SC. cAMP-dependent activation of the renal-specific Na+-K+-2Cl- cotransporter is mediated by regulation of cotransporter trafficking. Am J Physiol Renal Physiol 2003 June;284(6):F1145-F1154.

(242) Plata C, Meade P, Vazquez N, Hebert SC, Gamba G. Functional properties of the apical Na+-K+-2Cl- cotransporter isoforms. J Biol Chem 2002 March 29;277(13):11004-12.

(243) Plata C, Meade P, Hall A, Welch RC, Vazquez N, Hebert SC, Gamba G. Alternatively spliced isoform of apical Na(+)-K(+)-Cl(-) cotransporter gene encodes a furosemide-sensitive Na(+)-Cl(-)cotransporter. Am J Physiol Renal Physiol 2001 April;280(4):F574-F582.

(244) Monroy A, Plata C, Hebert SC, Gamba G. Characterization of the thiazide-sensitive Na(+)-Cl(-) cotransporter: a new model for ions and diuretics interaction. Am J Physiol Renal Physiol 2000 July;279(1):F161-F169.

(245) Plata C, Mount DB, Rubio V, Hebert SC, Gamba G. Isoforms of the Na-K-2Cl cotransporter in murine TAL II. Functional characterization and activation by cAMP. Am J Physiol 1999 March;276(3 Pt 2):F359-F366.